Physics – Uspekhi **43** (10) 991 – 1053 (2000)

REVIEWS OF TOPICAL PROBLEMS PACS numbers: **01.70.+w**, 02.40.Dr, **03.30.+p**, 87.19.St

Spatio-temporal problems of locomotion control

V V Smolyaninov

DOI: 10.1070/PU2000v043n10ABEH000796

Contents

Abstract. The problem of the spatio-temporal construction of legged movements involves structural freedoms due to the multi-link structure of the extremities, kinematic freedoms of the stepping cycle, and interextremity coordination freedoms, whose purposive organization is established by means of appropriate synergies, i.e. additional functional links the brain's control system forms. The main focus of attention in this work is on the kinematic and coordination synergies of the legged movements of humans and animals. The comparative historical analysis of experimental data and modelling metaphors concentrates on obtaining a unified description, whereas the ultimate mathematical metaphor reduces to space-time geometry, with base step synergies as its invariants. Thus, the concept of a synergetic organization for biomechanical movement freedoms is transformed to the geochronometry concept, actually a modification of Minkowskian geometry. To determine the spectrum of possible geochronometries, the consequences of a generalized 'postulate of a constant speed of light' are studied and different models of wave chronometers compared.

V V Smolyaninov A A Blagonravov Mechanical Engineering Research Institute, Russian Academy of Sciences
117334 Moscow, ul. Bardina 4, Russian Federation
Tel. (7-095) 135 55 23. Fax (7-095) 135 61 11
E-mail: smolian@iitp.ru

Received 25 May 2000
Uspekhi Fizicheskikh Nauk **170** (10) 1063 – 1128 (2000)
Translated by Yu V Morozov; edited by A Radzig

1. Introduction

Generally speaking, the Anglo-French term *locomotion* refers to the translational displacements of arbitrary mechanical objects in space. In a more narrow sense, however, it is typically applied to biomechanical objects. For example, it is common to speak of locomotion of single-celled organisms, animals, and man, but such word combinations as locomotion of an automobile or airplane may sound strange. The term 'locomotion' was first introduced into wide use in biomechanics by Marey [37]:

"The most characteristic form of motion in animals is doubtless locomotion. It is important to point out the laws which are common for all forms and manifestations of locomotion. But we do not know a task more difficult than the assimilation of acts as different as flying and creeping, the running of a horse and swimming of a fish."

The resolution of the difficult problem aimed at 'assimilating acts' of various forms of locomotion is a separate interesting topic relating to evolutionary biomechanics. In the present paper, however, we confine ourselves to 'the assimilation of acts' of a single variety of locomotion, namely stepping movements, which is very 'popular' in the animal kingdom, from arthropods to anthropoids.

If universal mechanisms of stepping movements are to be elucidated, e.g. those shared by the cockroach and man, a special research strategy needs to be applied in accordance with the principles considered in Section 2. To this effect, different metaphors of stepping movement organization are compared, which lead to different modes of gait description and, therefore, to different research strategies.

The use of dissimilar metaphors of stepping movement organization offers different ways of formulating kinematic control problems. However, we preferred the geochronometric approach. The theoretical aspects of this approach is discussed in Sections 3 and 4 focused on two versions of geochronometry: fundamental ('postulate-based') and constructive ('procedure-based'). The names of the versions are borrowed from A Einstein.

The subject-matter of Sections 3 and 4 may be of independent interest to physicists since geochronometric justification of locomotion synergies involves the discussion of the conceptual basis of relativistic kinematics which is traditionally referred to as the *special theory of relativity* (STR).

The notion of the system of base invariants is extensively used in definitions of geochronogeometries; the relationship of this notion with the Kleinian concept of geometric invariants is discussed in the Appendix.

2. Synergetics of stepping movements

> *Each science is approaching a mathematical precision which it will sooner or later achieve. The mind knows no rest till it creates a theory to explain known facts.*
> E Marey

This section is largely devoted to kinematic rules of stepping movements in man and animals (from bipeds to myriapods). There has been a long-standing interest in this subject. Suffice it to say that already Aristotle [1] called attention to the possibility of a general 'diagonal' organization of the gait in animals having different numbers of legs and the existence of different types of gaits, namely, the diagonal gait and amble, in tetrapods:

''Among terrestrial animals some fly, others move overground either by walking or crawling; aquatic animals either swim or walk. Quadrupeds and myriapods move with diagonal gaits. The lion and the camel amble.''

This excerpt suggests that the verbal mode of defining gaits in animals with synphased and counterphased leg pairs may be the oldest one. In the context of our paper, it is essential that this approach distinguishes the simplest coordination synergies of locomotory movements even though these synergies do not exhaust the entire stock of coordination rules for the construction of locomotory acts; rather, they form only a minor part of this stock.

It is evident from the mechanical point of view that spatial displacements (translational, vibrational, rotational) require certain degrees of freedom. This general thesis of mechanics equally refers to biomechanical systems and is supplemented by cybernetic considerations concerning the number of potential and indispensable freedoms for controlling locomotory acts.

The construction of living organisms and their locomotory systems during the course of evolution was characterized by so to say *libernetic altruism* manifested as redundant freedoms of functional self-organization of vital activity. The accomplishment of this task required organization of movements including locomotory ones. There is little doubt that the *redundant degrees of freedom* (RDFs) in motor end organs is only the visible part of the 'freedoms iceberg' of any living system, from a single cell (amoeba) to a man. A key principle of biological evolution appears to consist for all time in providing significantly more freedoms for all organisms than they are able to utilize throughout their lifespan.

On the other hand, from the cybernetic standpoint a free system is the uncontrollable system incapable of any goal-seeking activity such as locomotory or manipulation movements. The essence of any control [50] is in active overcoming of various RDFs intrinsic, in particular, to motive (locomotor) systems and program-algorithmic support (including both the 'hardware' and 'software' components). This essence also makes itself evident in the creation of means of autonomous automation in the form of skills, stereotypes, habits, and *synergies*.

2.1 Step kinematics

The very first systematic instrumental studies of locomotion in man and horses, designed to elucidate its biomechanical mechanisms, were undertaken by E Marey over 100 years ago [37]. These studies were carried out with the use of pneumatic sensors, accelerometers, and recording equipment (portable multichannel mechanical recorders) specially invented by the author for the purpose.

The pioneering experimental techniques proposed by Marey, which were later supplemented with chronophotography, cyclography and cinematography, created the basis for further laboratory research and yielded a large volume of comparative data on locomotion in a good few animals (see Refs [7, 15, 61, 75 – 86]). For all that, the research programme proposed by Marey with a view to elucidating the *laws* of locomotory movements (similar to Kepler's laws of planetary motion) has never been fully implemented for the lack of an adequate mathematical formulation.

Our research programme is likewise oriented to the deducing of the laws of locomotory movements and, in this sense, can be regarded as a continuation of the Marey programme. There are, however, important methodological and metaphorical differences.

We think that Marey's programme is impossible to complete in principle using only the notograms and support patterns, very popular in the locomotor systematics of quadrupedal gaits [15, 61]. It will be demonstrated below that the programme of locomotion studies as formulated by Marey can be fully implemented only if the following conditions are met:

— the spatio-temporal approach is used, taking into consideration both temporal and spatial characteristics of stepping movements, and

— a synergetic view of the organization of movement coordination is adopted with regard for the freedoms of constructing locomotory movements.

2.1.1 What is 'synergy'? According to the current semantic content of the term 'synergy', all laws of biomechanical movements are obscured in synergies. However, such a generalized view of synergetics of locomotory and other movements in different organisms has taken long time to develop.

The notion of synergy was first introduced into physiology by Charles Sherrington in the early 20th century to define cooperative interaction between different groups of muscles contributing to the realization of a whole locomotory act (see Ref. [10]). Later on, N A Bernshteĭn [10] suggested a more accurate formulation of the motor coordination problem; he reduced it to overcoming the SDFs of a motor organ and proposed distinguishing muscular synergies as major components of motor skills. Then, I M Gel'fand, V S Gurfinkel', M L Tsetlin, and I M Shik [17] introduced an expanded

interpretation of synergies as modes of movement control, which "decrease the number of independent parameters of a system under control". In this way, basic notions of *biosynergetics* came into being and underwent the initial semantic development in the framework of neurophysiological interpretation of biomechanical problems related to movement construction and formation of motor skills.

Locomotory movements are *highly automated synergies* — that is, the number of RDFs of locomotory acts is minimal (in fact, there are no 'redundant' freedoms). Therefore, the notion of RDFs of locomotory acts may be very fruitful for theoretical reasoning but is highly indeterminate as far as the experimental identification and analysis of latent and virtual freedoms are concerned.

2.1.2 Partition of problems. From the very beginning, Marey avoided simplification of the problems pertaining to the examination of locomotory acts and tried to understand all the components of stepping movements [37]:

"Human walk, seemingly so simple at first sight, is in fact very complicated especially if its component motions are considered."

The complexity of kinematic patterns of stepping movements is largely due to the fact that the general kinematic control, say of a step length or period, is effected through multilink extremities. In other words, it involves control of the extremity configuration, i.e. joint angles. Even more complicated is the dynamic control strategy oriented to generating joint forces and moments necessary to form kinematic synergies [8, 65, 67]. Considering it premature to discuss dynamic aspects, we confine ourselves solely to kinematic problems and the simplest dynamic interpretations.

Problems pertaining to the control of multilink leg shapes in the support and swing phases, on the one hand, and those of kinematic step control, on the other hand, can be partitioned and studied separately because they are characterized by different multitudes of freedoms:

(1) configuration freedoms assuring diversity of spatial forms of multilink extremities;

(2) kinematic freedoms which ensure a variety of locomotion velocities and forms (walking, running, jumping).

A complete spatio-temporal representation of stepping movements including consecutive changes in the configuration of a multilink extremity during the step cycle is provided by stick *metachronograms* which are normally recorded in a plane version, i.e. projected onto the vertical (sagittal) plane (Fig. 1a).

N A Bernshteĭn [10] rightfully considered metachronograms to be a notable methodological achievement of Marey. Their principal advantages (compared with photography and cinematography) are maximum compression of space-time information about a locomotor system and fixation of the most important portion necessary for kinematic and dynamic studies (provided relevant data on the inertia properties are available). Bernshteĭn himself and his coworkers markedly improved the metachronogram-based technique. At present, even more sophisticated computerized videosystems are available for three-dimensional recording of biomechanical and other movements which automatically digitize (at a frequency of 100 frames per second or more) the coordinates of the selected points of an object, then construct the corresponding metachronograms, and feed them to a monitor screen.

2.1.3 RRS — road reference system. Figure 1a shows a metachronogram for five marker leg points: *1* — hip joint (HJ), *2* — knee joint, *3* — ankle joint, *4* — heel, and *5* — toe (toe-cap of the foot). The horizontal (x_k) and vertical (z_k) coordinates of the five points $\mathbf{x}_k \equiv (x_k, z_k)', k = 1, \ldots, 5$ have been initially related to the *road reference system* (RRS) connected with the road whereon a man is walking. The instantaneous leg configuration is described by a set of five vectors

$$X_{\text{leg}} \equiv \{\mathbf{x}_1, \mathbf{x}_2, \mathbf{x}_3, \mathbf{x}_4, \mathbf{x}_5\}, \tag{2.1}$$

while the metachronogram is a multitude of configurations $X_{\text{leg}}(t)$ for the discrete sequence of moments with a constant time interval Δt. A metachronogram obtained with respect to the RRS is called *transit* because it represents a passage ('transit') of the legs and the body with respect to the supporting substrate.

Because the whole step or *locomotor cycle* (LC) is divided into two distinct periods (a support phase and a swing phase), the general characteristics of the LC (the step length L and period T) include the corresponding parts T_- and T_+ (support and swing durations, respectively), while L_- and L_+ are the support and swing components of the step length. The graphical representation of these step length components using a metachronogram is shown in Fig. 1a.

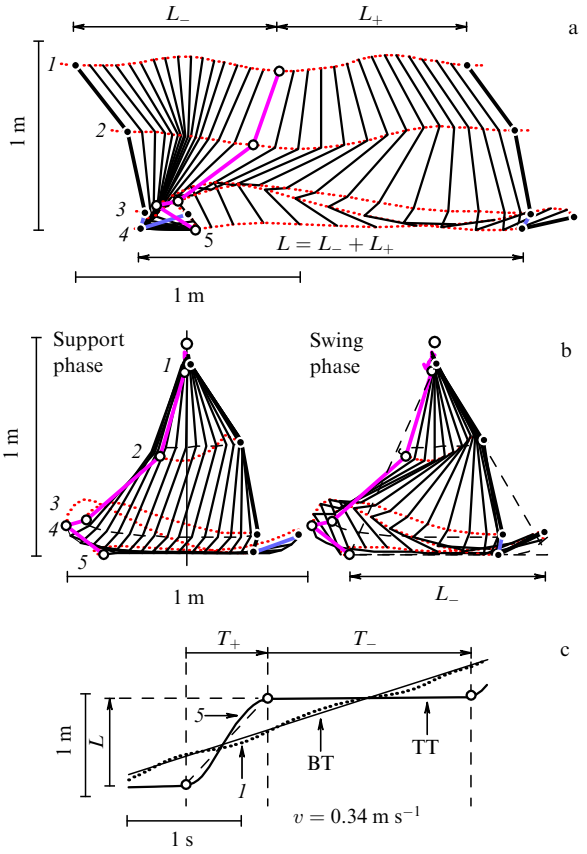

Figure 1. Transit (a) and pendulum (b) metachronograms of one human step — computer processing of videorecords obtained with a specialized system (*Elite*, BTS, Italy); (c) space-time trajectories of horizontal displacements of two marker leg points (*1* — hip joint, *5* — toe), TT — target trajectory, BT — basal trajectory (linear approximation of point *1* trajectory).

When the foot in contact with the soil during a T_--long support phase is fixed, the basal point travels at a constant locomotion speed v and covers the distance $L_- \equiv vT_-$; throughout a T_+-long swing phase, the distance covered is $L_+ \equiv vT_+$. Evidently, the sum of these two distances is equivalent to the step length, i.e. the distance covered by the body during period T:

$$L = L_- + L_+ = v(T_- + T_+) \equiv vT\,. \tag{2.2}$$

But the same distance L is covered by the foot during a shorter swing phase, that is for time $T_+ = T - T_-$ (Fig. 1a, c), because in this phase the foot is moving faster than the body, namely at a speed of $U = u + v$, where u is the foot velocity with respect to the body. Hence, the step length may be defined as

$$L = UT_+ = uT_+ + vT_+ \equiv L_- + L_+\,. \tag{2.3}$$

Using this and Eqn (2.2), there are two ways to determine the support length:

$$L_- = uT_+ = vT_-\,. \tag{2.4}$$

Stepping movements of human legs resemble those of a pendulum, especially in the swing phase. However, two types of pendulum, normal and inverted, are conceivable in the RRS for different step phases, i.e. the swing and the support. The pendulum of the former type is suspended from an upper suspension point in HJ (in swing phase), while the latter has the lower pivot (in support phase).

2.1.4 LRS — locomotor reference system. Even in the case of steady-state locomotion at a certain speed v, no individual point of the body including the center of mass moves at a constant speed equal to v. Therefore, an 'inertial' reference system, hereinafter referred to as the *locomotor reference system* (LRS), can be obtained by the artificial introduction of a '*basal*' point moving with a velocity of locomotion and taken to be the origin of LRS. For all practical purposes, the basal point for steady-state locomotion is found by means of a linear approximation to the HJ coordinates $x_1(t)$ and $z_1(t)$. The transition from RRS (2.1) to LRS:

$$\begin{aligned}\mathbf{x}_k(t) &\equiv \big(x_k(t), z_k(t)\big)' \\ &\to \big(x_k(t) - vt,\, z_k(t)\big)' = \big(y_k(t),\, z_k(t)\big)' \equiv \mathbf{y}_k(t)\,,\end{aligned} \tag{2.5}$$

corresponds to a Galilean transformation.

After transition to LRS, the *transit* metachronogram is transformed to a *pendulum* one (Fig. 1b), more adequate to the pendulum interpretation of leg stepping movements. Here, HJ serves as a natural pendulum suspension point in both phases, which undergoes horizontal and vertical oscillations with a relatively low amplitude. The asymmetry of leg oscillations in the support and swing phases is manifested in different sequences of three-link configurations and, according to Eqn (2.4), in different velocities of the foot motion in these phases.

Leg swinging in LRS produces a characteristic figure of a *support triangle* (Fig. 1b) traced out by a straight line which connects the two extreme points of the leg, the hip joint $x_1(t)$ and the toe $x_5(t)$. The length of this line is called the *functional* or *telescopic* leg length. The base of the support triangle is as long as the support length (2.4). In other words, the quantity L_- measures the double amplitude of locomotory leg oscillation.

Time scans of horizontal and vertical displacements of points $\mathbf{x}_k(t)$ can be examined separately, i.e. as time-dependent graphs $x_k(t)$ and $z_k(t)$. A kinematic description of stepping locomotion regardless of leg configuration requires the knowledge of only two trajectories (Fig. 1c): one of HJ, $x_1(t)$ (to determine the current locomotion velocity), and the other of the front tip of the foot (toe) $x_5(t)$ (to determine spatial and temporal stride parameters). When only the horizontal components of the displacements, $\{x_1(t), x_5(t)\}$, are taken into account, the leg is represented as a *horizontal oscillator* rather than a plane pendulum. The parameters used in formulas (2.2)–(2.4) characterize spatio-temporal properties of the toe target trajectory $x_5(t)$.

In the course of evolution, the complicated kinematics and dynamics of spatial motion of multilink extremities have been adapted to the organization of goal-directed movements of distal segments. That distal trajectories are goal-oriented is fairly well evident from manipulation movements [34]. But the *distal targeting principle* is undoubtedly applicable to locomotor movements too. We shall call the locomotor trajectory of the distal portion of human foot (the toe) or animal (both vertebrate and invertebrate) legs by the same name, *target trajectory* (TT), and denote it by the symbol $\boldsymbol{Z}$ as prompted by its zigzag shape.

Thus, the kinematic description of stepping movements, independent of anatomical features of the extremity, is represented by the space-time parameters of TT $\boldsymbol{Z}$.

2.1.5 Ballistic metaphor. Strictly speaking, portions of TT $\boldsymbol{Z}$ corresponding to the swing phase (Fig. 1c) lack linearity. They are roughly approximated by two parabolas. This means that the leg moves under the effect of a more or less constant force as a localized equivalent mass, first uniformly accelerated and then uniformly retarded. Formally, the description of the TT shape in the swing phase can be simplified by means of 'straightening', that is by substituting a linear TT portion for the nonlinear one.

The replacement of the parabolic swing-phase portion by a linear one actually means simplification of the form of dynamic control. In other words, permanent force actions are replaced by impulse ones (theoretically, by δ-impulses) triggered only at the beginning and the end of the swing phase. The initial impulse is necessary to ensure that the leg mass at rest acquires a constant speed $U = u + v$ with respect to the ground, while the final impulse stops the leg's motion.

Simple kinematics of stepping locomotion described by piecewise linear TTs corresponds to a similarly simple dynamic picture of a locomotor system composed of three masses $\{m_0, m_1, m_2\}$, each capable of a horizontal rectilinear displacement. Here, the mass m_0 is taken to conventionally represent the equivalent mass of the human body, while two other masses m_1 and m_2 are equivalent leg masses which, under normal conditions, can be assumed equal, i.e. $m_1 = m_2 = m$ (the 'mass model' of man is also characterized by the condition that the total leg mass is identical to the body mass: $m_1 + m_2 = 2m \approx m_0$).

The horizontal ballistics model. The body is represented by a mass m_0, and the legs by identical masses m, while stepping movements are due to force interaction between the body mass and leg masses.

In the ballistic model, control of stepping movements is reduced, on the one hand, to determining the instants of time

of triggering force impulses responsible for the onset and cessation of the step cycle and, on the other hand, to setting the impulse size which determines the leg swing velocity and thus the step length L. The horizontal ballistics model appears to better describe just walking in which vertical excursions of both the feet and the body are minimal. If the three-mass ballistic model is to be applied to the simplified dynamic representation of running movements, it should be supplemented by vertical components of impulse forces underlying the interaction between 'leg' and 'body' masses.

2.2 Basic parameters

Previous descriptions of stepping movements in man referred to normal conditions of locomotion (a horizontal walkway, even and hard-surfaced, in the absence of an extra load). In the forthcoming discussion, similar conditions for human and animal locomotion are assumed to be fulfilled. Moreover, locomotion will hereinafter be regarded as steady-state (which means that such quantities as locomotion velocity v, step period T, and step length L are not affected by the passage of time), unless stated to the contrary.

2.2.1 Kinematic uniformity principle. A kinematic description of locomotion of an arbitrary N-pody animal is reduced to the parametric definition of a set of TT $Z_N \equiv \{\boldsymbol{Z}_1, \ldots, \boldsymbol{Z}_N\}$, which may be regarded as the determining set of a locomotor system. In the case of steady-state locomotion, all TTs have similar *locomotor cycles* (LC) identical in terms of general characteristics (step length L and period T). Then, each TT $\boldsymbol{Z}_k$, where $k = 1, \ldots, N$, possesses translational symmetry, i.e. it undergoes self-coincidence upon a shift of the same integer number of step lengths and periods. However, the inhomogeneity of the TT system should be taken into consideration if the basic parameters of Z_N are to be identified.

The minimum number of basic parameters of a Z_N system is feasible if and only if it exhibits a maximum number of symmetries, that is when the initial events of LC (viz. steppings on or 'touches-down') give rise to a regular space-time 'Bravais lattice'. In such a case, the set of Z_N may be said to possess 'crystal' organization.

The steady-state condition does not guarantee uniform locomotion, while the number of variants of the nonuniform realization of stepping locomotion depends on the number of legs N.

Vertebrates are known to have either two (*bipedal* birds and man) or four (*quadrupedal* lizards, turtles, dogs, horses, etc.) legs, while invertebrate animals have at least six legs (*hexapedal* cockroaches and other insects); crayfish, crabs, scorpions, and spiders have eight walking legs, and myriapods from 12 to 100 or more legs. A bilateral set of all N legs is naturally categorized into the following groups:

— contralateral pairs (pairs of legs of one body girdle or segment);

— ipsilateral rows (all legs on one body side, right or left).

If n is the number of legs in a single ipsilateral row, then $N = 2n$ is their total number.

Given a large number of legs, at least three different locomotor problems must be evidently partitioned:

(1) generation of LC for each leg;

(2) temporal coordination of LC phases between different legs, and

(3) spatial distribution of support intervals.

Despite anatomic dissimilarities, different legs of one organism are involved in the collective performance of a general locomotor task, that is they ensure the body travel. Maintaining a constant velocity of locomotion, they have similar step lengths and periods. Moreover, there are normally no heterogeneities. In other words, the normal is characterized by:

The kinematic homogeneity principle. The locomotor system $Z_N \equiv \{\boldsymbol{Z}_1, \ldots, \boldsymbol{Z}_N\}$ represented by a set of TTs has the maximum number of symmetries, i.e. all TTs are congruent and show a regular distribution in space and time.

2.2.2 Tracks. Traces left by animals or men on soft soil (or their footprints impressed in hard soil) show evidence of being the simplest and most natural means to record the stepping locomotion. Archeologists and zoologists are interested in studying the tracks of fossil organisms, which they compare with photographed footprints of living species on desert sand. This approach is instrumental in resolving a number of evolutionary problems [61]. It is equally often applied in biomechanical studies in which researchers make small tetrapods leave ink traces on a paper sheet or analyze trails of arthropod footprints on smoked glass. Due to the long-standing interest in tetrapod paces, there is a well-developed classification based on track records. A key to animal paces using this technique is offered in a book by P P Gambaryan [15].

We confine ourselves to the examination of only the simplest regular cases (Fig. 2a, b).

A track left by one leg is a single train of footsteps, each separated from the previous one by a distance equal to the step length L. A bipedal track consists of two trace strings shifted by δ with respect to each other, where $-L/2 < \delta \leqslant L/2$. Tracks of myriapods are characterized by multiple paired shifts of the trace lines.

By definition, a track of bipedal footprints is described by two independent spatial parameters $\{L, \delta\} \equiv \boldsymbol{S}_\mathrm{T}$. Therefore, $\boldsymbol{S}_\mathrm{T}$ is a determining set of bipedal footprints. Synphased limbs leave unshifted tracks ($\delta = 0$), while counterphased ones make footprints shifted by a half-step, with $\delta = L/2$.

Similarly, the description of a quadrupedal track includes, generally speaking, three shifts. However, one may consider only two shifts of trace lines provided the movements of contralateral pairs of legs are in phase with each other (Fig. 2a, b). Then, the determining set of footprints contains three independent parameters

$$\boldsymbol{S}_\mathrm{T} \equiv \{L, \delta_\perp, \delta_\parallel\}\,. \tag{2.6}$$

The lack of an ipsilateral shift (i.e. at $\delta_\parallel = 0$) results in a 'step-to-step' gait at which the hindfoot trace is superimposed exactly on the imprint of the forefoot. In such a case, a quadrupedal track looks like bipedal one. However, the hindlimbs of tetrapods normally make a somewhat wider trail rut than the forelimbs. This explains why the hindfoot does not in fact fall precisely into the imprint of the forefoot but touches the ground very close to it.

Tracks of reptiles on desert sand have been specially studied by V B Sukhanov [61]. The author has demonstrated that most of them have characteristics suggestive of a 'step-to-step' gait. At a low speed of locomotion, the imprints of hindlimbs lie somewhat behind those left by the forelimbs (when $\delta \equiv \delta_\parallel < 0$). Conversely, at a high locomotion velocity, the former are slightly ahead of the latter (when $\delta > 0$). The 'step-to-step' rule is fully realized at a certain intermediate locomotion velocity. V B Sukhanov tabulated quantitative

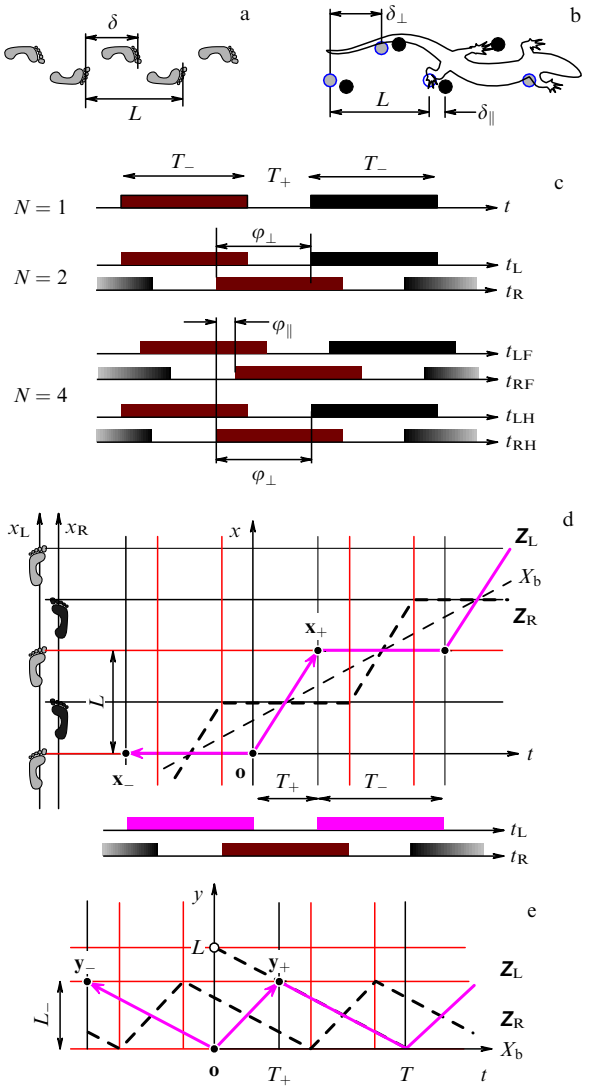

Figure 2. Trace ruts of human (a) and lizard (b) paces; (c) step phase notograms for different leg numbers $N = 1, 2, 4$; (d) synthesis of target trajectories of the right ($\mathbf{Z}_R$) and left ($\mathbf{Z}_L$) legs based on the trace patterns (represented on two space axes x_R and x_L) and notograms (represented on two time axes t_R and t_L), X_b — basal point trajectory; (e) oscillatory nature of target trajectories in the locomotor reference system.

characteristics of the tracks of three reptilian species in his book [61] (an example of the gecko is presented below, see Section 2.6.9).

Earlier, Marey and other authors (see Ref. [37]) showed that equine gaits such as the walk and the trot exemplify an especially close approximation to the 'step-to-step' rule:

"A trotting horse always makes a two-line track, i.e. it places its hindfoot exactly over the imprint of the colateral forefoot. In a short trot, the hindleg strikes the ground slightly behind the foreleg, but if the horse uses the extended and high trot the former is placed in front of the latter. The track of a walking horse resembles that of a trotting one, but the strides are shorter; in an ordinary walk, the step length equals the height of the horse (measured from the ground to the withers)."

Thus, a study of relative track shifts of different leg pairs provides information about phased leg movements and therefore about gaits which are traditionally defined in terms of time-related phase patterns.

What else can be learnt from the analysis of tracks left by animals on a soil? From the pathfinder's standpoint, the following problem can be of interest:

Question 2.1. Is it possible to tell locomotion velocity v from trail characteristics?

The step length may be one of the clews, although the relationship between this parameter and locomotion velocity, $L(v)$, is far from being one-valued when making an identification of the form and regime of locomotion based on tracking records.

Human steps integrated into walking or running are counterphased. Therefore, it is impossible to distinguish between these forms of locomotion based on the arrangement of footprints (their shape can serve as an additional criterion in this case). Analysis of real trains of human footprints must take into consideration the dependence of the step length L on the person's height H. Also, real footprints can be used to find the height dependence of the foot length (L_f). Then, the foot length L_f gives the height H, using a well-known empirical relation $H \approx 6.6L_f$ [67].

The velocity v can be derived from the step length L if the dependence $L(v; H)$ is known (or the dependence $L(v)$ for that matter, if the step length is assumed to be proportional to the person's height). For example, for normal walking (i.e. in the framework of the hypothesis most natural under ordinary conditions), $L(v)$ is a monotone function (Fig. 3b). Hence, it is possible to find the locomotion velocity v from the step length L (provided the above hypothesis is valid).

Let us consider now the case of human footsteps left on railroad sleepers. Evidently, the walking velocity could vary even if the man maintained a constant step length. Therefore, in this case, the locomotion velocity is impossible to estimate. A different regime may prove more suitable for a longer walk. Specifically, the normal walking velocity may be chosen, such that the step length is as large as the sleeper pitch.

Sleeper walking is conceptually different from the *normal walk* (NW) and corresponds to the *isometric walking* (IMW) regime (see Section 2.4.2).

Note 2.1. The author's personal experience indicates that in sleeper walking a subject prefers (for an unclear reason) to maintain his (or her) habitual walking velocity. The stride length in this walking modality being shorter than normal, the gait is adjusted to the habitual velocity by shortening the step period T, that is by increasing the step rate $1/T$. In the mid-1950s, the author, then an undergraduate student at the Moscow Physical-Technical Institute (MFTI) situated in the suburbs, did a good deal of sleeper walking between the Institute and the Dolgoprudnaya railway station. At that time, he developed not only such a walking manner but also the understanding of the underlying relationships which were used years later to formulate the concept of kinematic locomotion regimes [27, 28].

2.2.3 Notograms. Another old method to characterize gaits is based on keeping records of rhythmic leg strokes. Goiffon and Vincent were the first to use musical notation to visually represent gait rhythms as early as 1779 (see Refs [37, 61]). The complexity of step rhythms depends on both the gait mode and the number of legs. When homolateral limbs of a trotting animal move in a 'step-to-step' manner, its diagonal limbs touch the ground more or less simultaneously and only two strikes occur at a time [37]:

"A strictly two-beat variant of the trot is called free trot, whereas split-beat variants are referred to as interrupted trot

in which the hindleg strikes the ground somewhat after the diagonal foreleg.''

As a complement to the musical notation of leg beats, Marey proposed to record support phase durations [37] using pneumopodographic sensors built into footwear soles or horseshoes. Podographic recording converted the musical score method into the *notogram technique* (Fig. 2c) yielding a pulse multitrain portrait of alternating stride phases. A multiline notogram was produced by synchronous recording of pneumograms from all the limbs. The support phases were distinguished by episodes of elevated pressure, the pulse amplitude being a measure of the ground supporting force.

Notogram $\boldsymbol{N}_N$ presents a set of parallel time axes of all N legs showing alternation of the support (dark bars or notes) and swing (blank spaces) phases.

In agreement with the number of supporting-force recording channels, the human gait notogram $\boldsymbol{N}_2$ contains a single pair of lines, while the equine notogram $\boldsymbol{N}_4$ shows two pairs of them; here (see Fig. 2c), the upper pair corresponds to the forelimbs, and the lower one to the hindlimbs.

Note 2.2. The vertical alignment of note lines can be selected in different ways. For example, it may correspond to the sequence of foot contacts LH, LF, RF, RH (Fig. 2b), when the upper and lower line pairs correspond to ipsilateral pairs of legs (such a sequence is advocated in Sukhanov's book [61]). This is at variance with the order preferred by E Marey (LF, RF, LH, RH), in which the upper and lower pairs of lines correspond to contralateral limb pairs (Fig. 2c).

For certainty, the time lags φ between cycles of different limbs are measured between the moments of leg detachment from the ground (Fig. 2c), taking care that the inequalities $-T/2 < \varphi \leqslant T/2$ are satisfied. In the general case, step cycles of two adjacent ipsilateral legs are shifted as much as phase lag $\varphi_{\parallel}$, and those of contralateral legs as much as $\varphi_{\perp}$. The choice of the line sequence in Marey's notograms is dictated by the fact that contralateral leg pairs (in bipeds and other multipedal animals) exhibit fixed phase patterns, i.e. they are either in phase (when $\varphi_{\perp} = 0$) or out of phase (when $\varphi_{\perp} = T/2$) with each other. The dominant diversity of gaits is ensured therewith by a gradual change of ipsilateral time lag $\varphi \equiv \varphi_{\parallel}$. Marey took advantage of gradual variability of ipsilateral phase lags when constructing his synthetic model of gaits (see below).

In the parametric definition of the notogram $\boldsymbol{N}_N$, the phase durations of LC and time-related LC shifts between adjacent leg pairs are used. For this reason, the minimal *determining* set of the notogram contains four parameters

$$S_{\mathrm{N}} = \{T_-, T_+, \varphi_{\parallel}, \varphi_{\perp}\}\,. \tag{2.7}$$

By analogy with the previous discussion, it is appropriate to put the following:

Question 2.2. Is it possible to tell the locomotion velocity v from a notogram?

Unlike a track, a notogram contains additional information about the time structure of LC to which an additional criterion is owed. Suppose that the notogram is given without a scale time mark, which means that the actual phase and period durations are unknown. Then the LC time structure can be deduced from the quantity γ which is equal to the phase duration ratio: $\gamma \equiv T_+/T_-$. A relative notogram allows several individual forms of locomotion to be distinguished, e.g. human walking and running, because the kinematic difference between the *normal walk* (NW) and the *normal run* (NR) is reflected in the support and swing phase duration ratios:

$$\mathrm{NW}: \quad T_- > T_+ \Rightarrow T_{2-} \equiv T_- - T_+ > 0 \Rightarrow \gamma < 1\,, \tag{2.8}$$

$$\mathrm{NR}: \quad T_+ > T_- \Rightarrow T_{2+} \equiv T_+ - T_- > 0 \Rightarrow \gamma > 1\,. \tag{2.9}$$

Note 2.3. These formulas (2.8), (2.9) for interval durations (during a cycle) in a two-phase condition of leg pairs are valid for counterphased cycles ($\varphi = T/2$). In the case of synphased cycles ($\varphi = 0$), one finds $T_{2-} \equiv T_-$ and $T_{2+} \equiv T_+$. Functions $T_{2-}(\varphi)$ and $T_{2+}(\varphi)$ are represented by piecewise linear trapeziform plots. For tetrapods (taking into account the considerable interest in diagonal gaits), a double support period $T_{2\mathrm{D}-}$ for a diagonal limb pair can be introduced (see Ref. [61]). When contralateral limb pairs are out of phase, $T_{2\mathrm{D}-} \equiv T_{2-}(\varphi_{\parallel} + \varphi_{\perp}) = T_{2-}(\varphi + T/2)$.

The absolute locomotion velocity v can be deduced from a relative notogram provided the function $\gamma(v)$ is known. For human walking and running, parameters of the cycle structure γ monotonically increase with increasing velocity v. Therefore, the quantity γ can be used not only to distinguish between the walk and the run but also to measure the speed of locomotion.

2.2.4 Target trajectories. Answers to the above selected questions concerning the locomotion velocity are inevitably ambiguous provided either spatial (trains of footprints) or temporal (notograms) information is available. Conversely, having both spatial and temporal data (i.e. a track and a notogram), one can give unambiguous answers to these questions even if no additional relationships are at hand.

Let us consider a variant of bipedal locomotion taking advantage of a known track and notogram. By reducing and modifying the general definitions (2.6), (2.7) to adjust them to the variant in question, it is possible to represent the determining sets of the track and the notograms, as well as the relationship between them, in the following form

$$S_{\mathrm{T}} = \{L, \delta\} \equiv \{vT, v\varphi_{\perp}\}\,, \qquad S_{\mathrm{N}} = \{T, T_+, \varphi_{\perp}\}\,. \tag{2.10}$$

The spatio-temporal description can be obtained by the union of sets (2.10):

$$S_{\mathrm{T}} \cap S_{\mathrm{N}} = \{T, L, T_+, \varphi_{\perp}\} \equiv S_{\mathrm{TT},2}\,. \tag{2.11}$$

The resultant united set $S_{\mathrm{TT},2}$ contains four parameters for the target trajectory (TT) pair.

Problem 2.1. Let a track and a notogram of bipedal locomotion be given in a graphical form; relevant target trajectories need to be constructed.

Let us introduce a track-related space-time frame of reference $\mathbf{X} \equiv \{\mathbf{x} = (t, x)'\}$, i.e. *road reference system* (RRS). Furthermore, let us map the walking notogram on the time axis. In the coordinate system $\mathbf{X}$, footsteps are represented by horizontal straight lines and interphase boundaries in the notogram by vertical ones (Fig. 2d). If an event $\mathbf{o} \equiv (0, 0)'$ is coincident with the onset of swing, then the stepping event $\mathbf{x}_+ \equiv (T_+, L)'$ falls on its termination. A section of the oblique straight line which connects the events of this pair is actually a TT fragment representing the swing phase. On the other hand, the event $\mathbf{o}$ marks the cessation of the adjacent support phase which starts from the previous stepping event $\mathbf{x}_- = (-T_-, 0)'$; a section of horizontal straight line connecting the events of the latter pair is a TT fragment exhibiting the support phase.

The piecewise linear TT portion incidental to events $\mathbf{X} \equiv (\mathbf{x}_-, \mathbf{x}_+)$ corresponds to a single step, i.e. one locomotor cycle. Let us pick out these events as basic ones; in other words, let us construct a base RRS matrix

$$\mathbf{X} \equiv (\mathbf{x}_-, \mathbf{x}_+) \Leftarrow \mathbf{x}_- = (-T_-, 0)', \quad \mathbf{x}_+ = (T_+, L)'. \quad (2.12)$$

The entire TT $\boldsymbol{Z}$ (an infinite piecewise linear trajectory) is completed by the translation of a base fragment with periods T and L along the time and space axes.

In the case of steady locomotion, all midpoints of the support and swing phases are periodically distributed along one 'basal' straight line X_b with a shift equal to the vector $\mathbf{x}_\mathrm{b} \equiv (\mathbf{x}_+ - \mathbf{x}_-)/2 = (T/2, L/2)'$. In other words, the sequential basic events are counterphased.

The counterphased NN $\boldsymbol{Z}^*$ of a contralateral limb results from the translation of TT $\boldsymbol{Z}$ by a vector $\mathbf{x}_\mathrm{b} = (T/2, L/2)'$. Thus, problem 2.1 is solved. ◆

2.2.5 Parametric degrees of freedom. An obvious advantage of the TT technique consists in the possibility of studying locomotor kinematics in different frames of reference. The *locomotor reference system* (LRS) $\mathbf{Y} \equiv \{\mathbf{y} \equiv (t, y)'\}$ moves with respect to RRS at the speed of locomotion v. In other words, the basal straight line derived in the previous section serves as the time axis of LRS. Systems $\mathbf{X}$ and $\mathbf{Y}$ are related by a Galilean transformation (see Appendix for the notation)

$$\boldsymbol{\Gamma}\colon\ \mathbf{Y} \to \mathbf{X} \Rightarrow \mathbf{x} = \boldsymbol{\Gamma}\mathbf{y} \Leftarrow \boldsymbol{\Gamma} \equiv \mathbf{E} + v\mathbf{E}_{21}\,. \quad (2.13)$$

The base matrix $\mathbf{X}$ (2.12) introduced into RRS undergoes transformation to the base LRS matrix

$$\mathbf{Y} \equiv (\mathbf{y}_-, \mathbf{y}_+) = \boldsymbol{\Gamma}^{-1}\mathbf{X} \Leftarrow \mathbf{y}_- = \boldsymbol{\Gamma}^{-1}\mathbf{x}_- \equiv (-T_-, L_-)', \quad \mathbf{y}_+ = \boldsymbol{\Gamma}^{-1}\mathbf{x}_+ \equiv (T_+, L_-)'. \quad (2.14)$$

In LRS (Fig. 2e), the stepping foot movements represented by TTs $\boldsymbol{Z}$ and $\boldsymbol{Z}^*$ are of a purely oscillatory nature. It follows from Eqn (2.14) that the double amplitude of these asymmetric oscillations is equal to the step length L_- during support. This accounts for the different absolute swing (u) and locomotion (v) velocities due to various phase durations.

The foregoing time-specific criteria of NW (2.8) and NR (2.9) can be supplemented by inequalities for the locomotion velocity, taking into consideration that $u = v/\gamma$:

$$\mathrm{NW}\colon\ T_+ < T_- \Rightarrow u > v, \qquad \mathrm{NR}\colon\ T_+ > T_- \Rightarrow u < v\,. \quad (2.15)$$

The pair of TTs $\{\boldsymbol{Z}, \boldsymbol{Z}^*\}$ totally substitutes the primary reference pair, i.e. the notogram and the track, and combines the kinematic information contained separately in each of them. Therefore, quantity $\varphi_\perp$ in the set (2.11) characterizes in the general case a relative shift of two TTs, $\boldsymbol{Z}$ and $\boldsymbol{Z}^*$, along the basal line. The shape of either TT is unequivocally given by the three parameters contained in the base RRS (2.12) and LRS (2.14) matrices. It differs only in terms of the spatial parameter:

$$S_{\mathrm{TT\,RRS}} = \{T_-, T_+, L\}, \qquad S_{\mathrm{TT\,LRS}} = \{T_-, T_+, L_-\}\,. \quad (2.16)$$

To sum up, we have proved the validity of the following:

Main theorem of step synergetics. *A kinematic definition of the step cycle has three parametric degrees of freedom.*

Doubtless, comparative studies of stepping locomotor movements must take into consideration the existence of three parametric freedoms. The fundamental aspect of this problem consists in the identification of the basic *controlling parameters* of step kinematics, that is distinguishing those basic parameters which are used by the control system (brain) for the solution of kinematic problems, such as the construction of stepping movements.

2.2.6 The problem of basic characteristics. The general description of TT includes eight quantities from the following list:

$$L = \{T, T_-, T_+, L, L_-, L_+, u, v\}\,. \quad (2.17)$$

This is a linguistic set of stride kinematic parameters, which is redundant for the basic TT definition because only three independent parameters (2.16) are actually sufficient for the minimal TT definition. However, the formal choice of the three basic parameters is arbitrary. For example, if the following base set is chosen:

$$B = \{T, T_+, v\}\,, \quad (2.18)$$

then the remaining parameters included in the list (2.17) are expressed via the basic ones:

$$T_- = T - T_+, \qquad L = vT, \qquad L_- = v(T - T_+),$$

$$L_+ = vT_+, \qquad u = \frac{v(T - T_+)}{T_+}\,. \quad (2.19)$$

Formally, it is permissible to assume the existence of an universal basic triple of controlling parameters. However, accounting for the existence of different control levels, it appears more relevant to speak about the identification of basic characteristics.

Definition 2.1. *Basic characteristics* are said to be velocity dependences of basic parameters chosen to serve as determining functions.

A system approach to the identification of basic characteristics proceeds from the comparative evaluation of the variability of an expanded set of *locomotor characteristics*, i.e. dependences of the parameters of set (2.17) on locomotion velocity:

$$L_{(v)} = \big\{T(v), T_-(v), T_+(v), L(v), L_-(v), L_+(v), u(v)\big\}\,. \quad (2.20)$$

Such system approach can be practically realized by means of experimental studies of locomotor movements over a wide range of velocities, designed to identify locomotor characteristics (2.20). It will be shown below that complete 'portraits' of both temporal $\{T(v), T_+(v), T_-(v)\}$ and spatial $\{L(v), L_+(v), L_-(v)\}$ step characteristics are needed to support the rationale for the choice of base synergies.

Definition 2.2. *The kinematic portrait* of locomotion is termed an ensemble of two plot families containing temporal step characteristics, on the one hand, and spatial characteristics of the step, on the other hand.

The graphical representation of locomotor characteristics has sense not only in the context of the assessment of analytical approximations to experimental findings but also for the visualization of the analytical content of traditional metaphors and models.

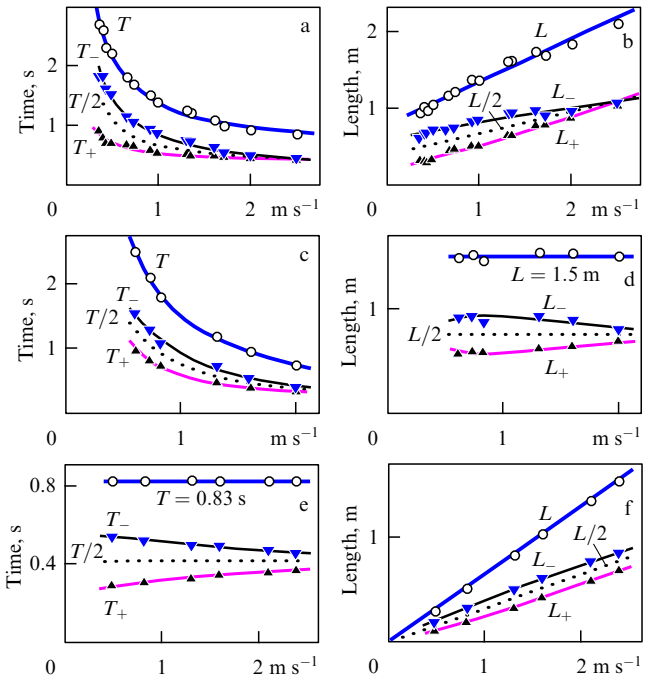

Figure 3. Kinematic portraits of three human walking regimes: (a, b) normal walk; (c, d) isometric walk (step length $L = \text{const}$); (e, f) isorhythmic walk (period $T = \text{const}$); (a, c, e) velocity dependences of temporal step parameters (period T, support T_- and swing T_+ durations); (b, d, f) analogous dependences of spatial step parameters (overall length L, support L_- and swing L_+ components).

A typical kinematic portrait of human NW is shown in Fig. 3a, b. With relevant experimental data for temporal and spatial step characteristics (borrowed in the present case from our earlier work [27]) and the knowledge of linguistic connections between them at our disposal, we encounter the problem of the choice of basic characteristics for the approximation of all kinematic portrait dependences.

2.3 Locomotor metaphors

E Marey believed that "the meddling of mathematicians would be premature" [37] and formulated results of his locomotion surveys in the form of graphic and metaphoric rules. Despite their qualitative character, Marey's metaphors may be successfully translated into analytical language. We consider such a translation to be very helpful for a better understanding of locomotion synergy models.

2.3.1 Stroboscopic metaphor. Although Marey did not directly examine velocity dependences, he noticed a period decrease with increasing speed. At first sight, it may seem strange that the great experimentalist neglected a survey of functional relationships between stride characteristics and locomotion velocity while conducting his own research and posing a question of the existence of biomechanical laws of stepping movements which must be explained, according to his opinion, in quantitative terms. Why?

There are neither mathematical formulas and calculations nor graphic plots in Marey's book [37]. Instead, the author presented numerous specimens of pneumorecorded podograms, schematic notograms, and engravings depicting locomotory postures of a man and horse. Also, much attention in the book was given to the formulation of rules for drawing sequential locomotory postures with the use of notograms and to the methods of animation of such drawings through the stroboscopic viewing. It can therefore be concluded that Marey considered it unnecessary to study velocity dependences of locomotor characteristics, being fully confident of the validity of the following:

Stroboscopic metaphor. Kinematic parameters of real stepping movements appear to depend on locomotion velocity exactly as they do in the case of observing a given sequence of locomotory postures with a stroboscopic device, when only the frame rate for the individual postures can be varied.

An analogue of the stroboscopic metaphor is the cinematographic metaphor which easily allows a corresponding kinematic model to be constructed. Suppose, there is a certain cinematographic record of a steady human (or equine) travel and the possibility to see the film with different frame rates.

Question 2.3. What kinematic laws govern cinematographic animation of locomotor movements?

With varied animation rate, only temporal parameters are likely to change, whereas the spatial dimensions of the locomotor apparatus (including the stride length) remain unaltered. In steady locomotion, the step length is equal to the distance $L = vT$ covered by a subject during the period. Hence, from the condition of constant animation step length it follows that the period is inversely proportional to the velocity:

$$L = \text{const} \;\Rightarrow\; T = \frac{L}{v}\,. \tag{2.21}$$

The walking regime with a varied speed and fixed step length is called an *isometric walk* (IMW). Step length constancy serves as a kinematic synergy ('invariant') of the walk with different speeds. The inversely proportional dependence of the walking period on the velocity ensues from a step length invariance.

An additional consequence of the stroboscopic metaphor is a constant support length and a constant swing length (L_- and $L_+ \equiv L - L_-$, respectively). Hence, it can be concluded by analogy with Eqn (2.21) that the durations of the support and swing phases (similar to the period duration) must vary inversely proportional to the locomotion velocity:

$$L_- = \text{const} \;\Rightarrow\; T_- = \frac{L_-}{v}\,, \tag{2.22}$$

$$L_+ = \text{const} \;\Rightarrow\; T_+ = \frac{L_+}{v}\,. \tag{2.23}$$

To summarize, Marey's stroboscopic (cinematographic) metaphor corresponds to the isometric locomotion regime, the kinematic portrait of which is described by formulas (2.21)–(2.23). It is easy to see from a comparison with a similar NW portrait (Fig. 3a, b) that real normal locomotion is not consistent with Marey's metaphor.

We shall see later that the real isometric locomotion is inconsistent with Marey's metaphor as well.

2.3.3 Anthropomorphic metaphor. When pursuing his research, Marey viewed locomotor movements of legs as periodic oscillations and therefore reduced the definition of the gait to that of phase shifts of such oscillations. Marey's studies were considerably simplified by the following (see Ref. [37]):

Anthropomorphic metaphor. The locomotion of fore- and hindlimb pairs in horses may be compared with a

simultaneous walk of two people following each other in the manner of circus clowns mocking 'a horse' or two subjects carrying 'a log of wood'.

The main corollaries to this metaphor were formulated by Marey as

Gait synthesis rules:

(1) the kinematic characteristics of fore- and hindlimb steps are identical;

(2) the phasings of contralateral limb pairs are identical and constant;

(3) the ipsilateral limb phasing may change independently.

In this context, phasing is taken to mean a phase ratio $\psi \equiv \varphi/T$ expressed in fractions of the period. For example, the counterphase ratio has the form $\psi_\perp \equiv \varphi_\perp/T = 1/2$.

Proceeding from the gait synthesis rules, Marey illustrated the diversity of equine gaits with the help of the following 'synthetic model': counterphase (or synphase) notograms of fore- and hindlimbs were depicted on two parallel strips of wood. The strips were then shifted in parallel to obtain an integrated notogram of a concrete gait. Using this method, Marey demonstrated that equine gaits may be reproduced by pushing in parallel paired notograms of fore- and hindlimbs.

In accordance with the synthetic model, the determining conditions of a gait are represented by the phasing constancy conditions which are actually invariants of the stroboscopic metaphor. Taking into account Corollaries (2.21)–(2.23) of this metaphor either, it is possible to identify the determining conditions of Marey's kinematic model:

$$\mathrm{DC} = \{L = \mathrm{const},\ L_- = \mathrm{const},\ \psi_\parallel = \mathrm{const},\ \psi_\perp = \mathrm{const}\}\,. \tag{2.24}$$

The paramount role of the gait synthesis rule (1) is apparent only when one takes into consideration forms of locomotion differing in the structure of locomotor cycles (2.8) and (2.9). Contralateral phasings also give rise only to bimodal diversity, when $\psi_\perp = 0$ or $\psi_\perp = 1/2$. In fact, gait diversity is first and foremost due to the gradual variation of ipsilateral phasings, $\psi \equiv \psi_\parallel \in (-1/2, 1/2]$.

Note 2.4. The gait synthesis rule (1) permits the choice of one of the two locomotion varieties: either walking, with $T_- > T_+$, or running, when $T_- < T_+$. A synthetic model for tetrapods can be constructed as two staves of four identical lines each, one for the walk, the other for the run. Rule (2) allows the formation, for each staff, of paired notograms of fore- and hindlimbs of one of the two types, counterphased or synphased. The notograms of the pairs of fore- and hindlimbs of the same type being obtained, the synthesis of a concrete gait is completed by applying rule (3), that is by a shift of the paired notograms as large as an arbitrary duration of the ipsilateral phase $\varphi \in (-T/2, T/2]$. An example of this approach to the construction of notograms of quadrupedal locomotion for two conjugate forms of the cycle structure is illustrated in Fig. 2.

The synthetic gait model admits of a *continuous* change of ipsilateral phase $\varphi \in (-T/2, T/2]$. Initially, Marey did not mention the advisability of discrete gait ranking in terms of additional intervals of ipsilateral phase variation. Discrete ranking of ipsilateral gait variants emerged from the combination of notogram and support pattern techniques. The synthetic gait model was first updated by Goubaux and Barrier [19], Marey's disciples. The final version of the combined application of notograms and support patterns was proposed by V B Sukhanov [61].

2.3.4 Support metaphor. The sequential support pattern method for the characterization of quadrupedal gaits was first introduced in the late 19th century by Muybridge who pioneered the use of instantaneous photography in biomechanical studies. Both the simplicity and possibility of visual demonstration earned the method widespread popularity among researchers engaged in comparative evolutionary studies of motor end organs in tetrapods (see Refs [15, 61, 86]). Support sequences represent one more metaphor of discrete gait classification which is different from the sequential beat metaphor (see above) in that it takes into consideration two phases of the *locomotor cycle* (LC). The power of a set of support sequences and the number of gaits they identify depend on the number of legs N.

$N = 1$. Let us introduce a binary representation of the leg's phase states: 1 for the support, and 0 for the swing. A set of phase states in unipedal locomotion is $S_1 = \{(0), (1)\}$. The alternation of phase states can be described by a graph $\boldsymbol{G}_1$ with two vertices and edges depicting transitions from one state of set S_1 to the other (Fig. 4a, $N = 1$).

$N = 2$. Figure 4a also shows notograms of bipedal locomotion for four phase state values $\psi = 0,\ 1/8,\ 1/4,\ 3/8$. The digits 0, 1, and 2 under the notograms stand for the number of support limbs during the time interval shown by vertical bars. At $\psi = 0$, both legs are first in contact with the substrate (support phase) as indicated by the number 2. Thereafter, they convert to the swing phase (0). Thus, this

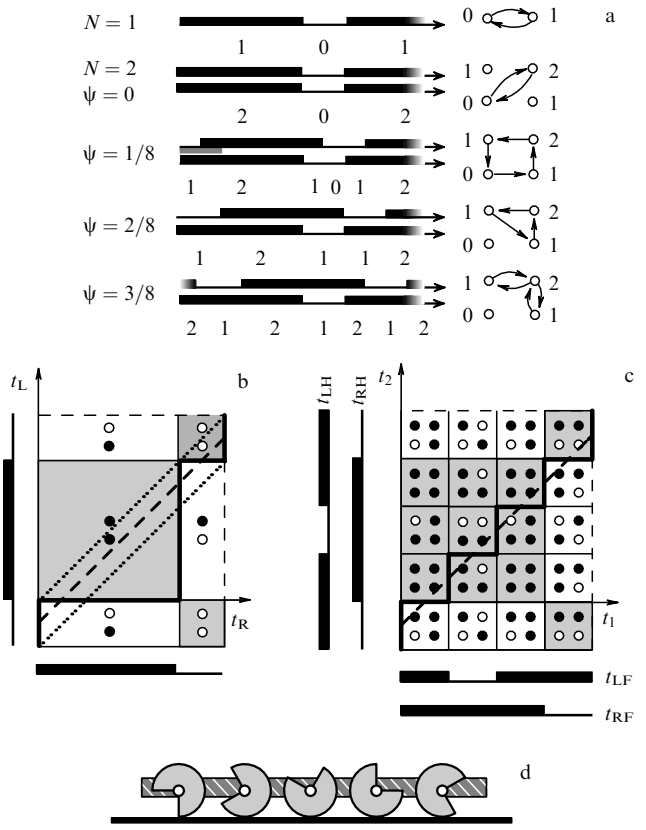

Figure 4. Support sequences and patterns: (a) notogram-based definition of support sequences (right: support cycle graphs); (b) support diagram of bipedal support patterns (paired circles show positions of the right (R — lower circle) and left (L — upper circle) legs; (c) analogous support diagram for tetrapods (LF — left forefoot, RF — right forefoot, LH — left hindfoot, RH — right hindfoot); (d) schematic representation of a cart with sectorial wheels.

notogram of synphased cycles describes the gait $G_2(0) = 2|0$. The same line of reasoning leads to the inference that other notograms (Fig. 4a) are in correspondence with the following support formulas

$$G_2\left(\frac{1}{8}\right) = 1|2|1|0\,, \qquad G_2\left(\frac{1}{4}\right) = 1|2|1\,, \qquad G_2\left(\frac{3}{8}\right) = 2|1|2|1\,. \tag{2.25}$$

The two-place representation is especially convenient for distinguishing phase states of different limbs. For example, notation $(1,0)$ indicates that the first leg is in the support phase, while the second is in the swing, etc. A complete set of phase states is $S_2 = \{(0,0),(1,0),(0,1),(1,1)\}$. The transition graph $\boldsymbol{G}_2$ can be represented as a square with vertices having coordinates of the S_2-set states (Fig. 4a, $N = 2$). In this case, the *gait* is designated a closed path $P_2(\psi)$ in graph $\boldsymbol{G}_2$. For instance (see Fig. 4a), the path $P_2(1/8)$ traverses all the four vertices, while the path $P_2(1/4)$ traverses only three of them.

If a phasing ψ belongs to an open interval of values $(0, 1/4)$, i.e. $0 < \psi < 1/4$, then all the paths $P_2(\psi)$ are isomorphic. In other words, there is a continuous interval of phasing values $\psi \in (0, 1/4)$ within which one and the same gait represented by a sequence of four phase states is realized. The equivalent gait interval in the notogram $\psi = 1/8$ is shaded (Fig. 4a). Apart from 'interval gaits', there are 'point gaits' corresponding to a single phasing, e.g. $P_2(0)$, $P_2(1/4)$, etc. The path length $|P_2(\psi)| = 4$ is a discrete sign of interval gaits, whereas $|P_2(\psi)| < 4$ is inherent in point gaits. Support formulas (2.25) possess analogous properties and thus they are of the order of $|G_2(\psi)| = 4$ for interval gaits, and $|G_2(\psi)| < 4$ for point gaits.

When $N = 2$, it is easy to sort out all the variants of different gaits, using either paired notograms or paths in the graph $\boldsymbol{G}_2$. A more economic method of scrutinizing all the variants of bipedal gaits is based on the use of 2-dimensional notograms (Fig. 4b).

For this purpose, a rectangular coordinate system with two time axes (t_1, t_2) needs to be introduced. A notogram of the first limb is given along one axis, while that of the second limb parallels the other one. The straight lines show the phase boundaries of LC and divide the plane into the phase state zones of bipedal locomotion. This procedure results in the division of the LC rectangle, inside which $t_1, t_2 \in [0, T)$, into four zones. Elements of the set S_2 are used to mark the zones of the diagram thus obtained. The straight line with a unit slope $\boldsymbol{L}(\psi)$ intersects the ordinate at the phase shift point ψ of the second leg. In this diagram, the gait $P_2(\psi)$ is designated the list of zones traversed by the straight line $\boldsymbol{L}(\psi)$. The oblique dashed line in Fig. 4b is the straight line $\boldsymbol{L}(1/8)$. The dotted lines denote 'point gaits' and borders of 'interval gaits', respectively; they are drawn through the vertices of phase state zones.

$N = 4$. The total list of support sequences inherent in tetrapod locomotion is very large and will not be detailed here. The interested reader is referred to the comprehensive coverage in the lists and diagrams elaborated by P P Gambaryan and V B Sukhanov in their respective books (see Refs [15] and [61]). Suffice it to note the most common formal features of support gaits in tetrapods.

The complete set of four-place phase states

$$S_4 = \big\{(0,0,0,0),(1,0,0,0),\ldots,(1,1,1,1)\big\}$$

contains $2^4 = 16$ elements which can be represented as vertices of a 4-dimensional cube. Then, the gaits are defined at these vertices by the transition graph $\boldsymbol{G}_4$. Such a multidimensional metaphor facilitates the understanding of a large stock of support gait variants represented either by the support formulas $G_4(\psi)$ or by the closed paths $P_4(\psi)$. For tetrapods, the discrete traits of interval gaits are given by equalities

$$\big|G_4(\psi)\big| = \big|P_4(\psi)\big| = 8\,,$$

while the inequality

$$|G_4(\psi)| = |P_4(\psi)| < 8$$

holds for point gaits.

A two-dimensional diagram of all support gaits inherent in tetrapods is constructed in the following way. The paired notogram of the forelimbs is placed on the horizontal axis and that of the hindlimbs on the vertical. Figure 4c is constructed to illustrate counterphased steps of each pair and the case when the support duration T_- is greater than the swing duration T_+ (here, $T_-/T_+ = 3$). The straight lines showing LC phase boundaries also divide the plane into phase state zones. Because paired notograms are divided into four segments each, the LC rectangle contains 16 zones. For the sake of clarity, the zones of the diagram thus obtained are marked proceeding from the traditional support patterns instead of using elements of the set S_4. Then, in each quartet of points, the solid circles denote the supporting limbs, while the open ones stand for the swinging limbs. The solid oblique line in Fig. 4c is the straight line $\boldsymbol{L}(1/8)$ to which the interval gait $P_4(1/8)$ and the support formula

$$G_4\left(\frac{1}{8}\right) = 4|3|2|3|4|3|2|3 \tag{2.26}$$

correspond. Based on this diagram, all other gaits are easy to describe. All told, it is valid for four interval and four point gaits.

To complete the picture, we will point out inverted diagrams of support gaits, constructed from inverted notograms, for instance, the inverted variant of the support formula (2.26):

$$G_4^*\left(\frac{1}{8}\right) = 0|1|2|1|0|1|2|1\,. \tag{2.27}$$

N o t e 2.5. If synphased notograms of fore- and hindlimbs are considered (to model gallops) instead of counterphased ones, the diagram of quadrupedal support gaits (Fig. 4c) takes the structure of the bipedal diagram shown in Fig. 4b.

$N > 4$. The above formal methods of gait construction are easy to extend to the general case of an arbitrarily large leg number, however we are led to sacrifice therewith graphic methods and to use nothing but algebraic means. Support gaits at $N > 4$ may be of greatest practical interest for six-legged stepping apparatus (see, for instance, Ref. [86]). For multipedal organisms including hexapods, the support metaphor is of little value because ipsilateral coordination in arthropods better satisfies another metaphor, namely, the wave metaphor.

2.3.5 Wave metaphor. It follows from a quotation cited in the beginning of this section that even at the time Aristotle knew

that the 'diagonal' gait is widely used by multipedal walkers having $N > 4$. As this takes place, hexapods form the so-called:

Alternating tripod. In these animals, the first and last limbs on one side of the body step synchronously with the mid-limb (i.e. diagonal leg) on the other side.

Arguments in favor of the static stability of tripod support have long been used to account for the selection of diagonal coordination between limbs throughout the course of evolution. Considered sufficient, this coordination modality was believed to be the only one feasible in the animal kingdom. G Hughes [80] was the first to cast doubt upon the universal nature of the 'tripod metaphor' as applied to hexapodal gaits. In a study designed to carefully examine a variety of gaits in cockroaches after selective amputation of legs, Hughes made a pioneering discovery of *metachronal* (i.e. happened in waves) swing of ipsilateral legs.

The popularity of Hughes' wave metaphor was further promoted by the cybernetic interpretation of neurophysiological mechanisms of locomotor coordination proposed by D Wilson [91]. The polyanthropomorphic metaphor of Marey was thus replaced by the concept of coupled neuronal 'locomotor generators' which Wilson compared with generators of electrical oscillations for radioengineering.

In order to better illustrate the applicability of the wave metaphor, D Wilson also developed a notogram-based version of the 'symbolic gait model'. However, symbolic notogram images will not be used in the forthcoming discussion because the kinematic rules formulated by Wilson, somewhat differing from the analogous rules (2.24) proposed by Marey, appear to be more relevant to the purpose.

Wilson's kinematic rules:

(1) the period T is inversely proportional to locomotion velocity v;

(2) the swing phase duration is constant: $T_+ = \text{const}$;

(3) the lag-period between consecutive ipsilateral LCs is constant: $\varphi_{\parallel} = \text{const}$;

(4) contralateral LCs are counterphased: $\psi_{\perp} = \text{const} = 1/2$.

It is worthwhile to note that rule (1) has much in common with Marey's stroboscopic metaphor, whereas rule (2) is at variance with it. Therefore, rule (1) contradicts rule (2) because it implies a decrease of the period to an infinitely small value with increasing velocity of locomotion, which is impossible since $T \equiv T_- + T_+ > T_+ = \text{const}$. On the other hand, it appears from Wilson's notogram illustrations that, at a fixed swing phase duration, the period is shortened because the support phase duration decreases. It seems very likely that, when proposing rule (1), Wilson had in mind the support duration T_- rather than the entire T period. Hence, the first rule reads as

(1*) the support duration T_- is inversely proportional to locomotion velocity v.

The most important consequence of the modified rule (1*) is a constancy of the support step length, $L_- = \text{const}$, i.e. the double amplitude of a leg swinging. Therefore, the *determining conditions* (DC) of Wilson's kinematic model can be written in the following form:

$$\text{DC} = \left\{ T_+ = \text{const}\,,\ L_- = \text{const}\,,\ \varphi_{\parallel} = \text{const}\,,\ \psi_{\perp} = \frac{1}{2} \right\}. \tag{2.28}$$

The kinematic portrait of this model can be obtained distinguishing formulas of temporal and spatial characteristics:

$$T = T_+ + \frac{L_-}{v}\,, \qquad T_- = \frac{L_-}{v}\,, \qquad T_+ = \text{const}\,; \tag{2.29a}$$

$$L = L_- + vT_+\,, \qquad L_- = \text{const}\,, \qquad L_+ = vT_+\,. \tag{2.29b}$$

An additional consequence of DC (2.28) is a constancy of the leg swing speed

$$u \equiv \frac{L_-}{T_+} = \text{const}\,. \tag{2.30}$$

Moreover, rule (3) which postulates a constant delay between consecutive ipsilateral LCs can be reformulated in terms of wavy locomotion making use of the notion of *metachronal wave* (MW) velocity

$$w \equiv \frac{d}{\varphi}\,, \tag{2.31}$$

where d is the distance between adjacent support intervals (Fig. 7a, b), while the metachronal delay is $\varphi \equiv \varphi_{\parallel}$. Bearing in mind that the distance d is constant, Wilson's model may be characterized by the condition of constant MW velocity:

$$w = \text{const}\,. \tag{2.32}$$

The condition of constant ipsilateral time lag is satisfied by the constant MW velocity which is independent of the speed of locomotion.

2.3.6 Wheel metaphor. Let us bring Marey's gait model into correspondence with the wave metaphor. A simple mechanical construction may be used for the purpose as proposed elsewhere [30] for the illustration of the kinematic invariant technique.

Let us consider a 'multiwheel cart' with many parallel axles to which pairs of 'contralateral' sectorial wheels are firmly attached. The wheels are not usual disks but made in the form of solid sectors of angle $\alpha_- < 2\pi$ with blank spaces (Fig. 4d). For steady movement of the cart, all the wheels rotate without slip, with constant and equal angular velocities. The rolling of a solid disk sector over the road surface from one radius to the other corresponds to the support phase, and that of a blank to the swing phase. By analogy with the human gait, the rolling of the solid sector may be considered to imitate the rolling of the foot from heel to toe. If r is the radius of the circle, the 'step' length of the wheel as well as support and swing 'step' lengths can be found in the following way:

$$L = 2\pi r\,, \quad L_- = \alpha_- r\,, \quad L_+ = \alpha_+ r \Leftarrow \alpha_- + \alpha_+ \equiv 2\pi\,.$$

Thus, all the spatial characteristics of the step length are fixed constructively and are independent of the locomotion velocity v. This accounts for the inverse relationship between all temporal characteristics (period, support and swing phase durations) and locomotion velocity. In other words, the cart's kinematics are consistent with the stroboscopic metaphor, and

$$u \equiv \frac{L_-}{T_+} = \frac{v}{\gamma} \Leftarrow \gamma = \frac{\alpha_+}{\alpha_-} = \frac{T_+}{T_-} = \frac{L_+}{L_-}\,; \tag{2.33}$$

the swing velocity is proportional to the speed of locomotion because the cycle structure parameter γ is unchanged in the model under consideration.

The relative phasings of 'step' cycles depend on the initial angular position of the sectors. If, for instance, the contralateral wheel sectors have been set out of phase with one another, the midpoint of the arc enclosing solid sector of one wheel coincides with the bisectrix of the blank angle in the contralateral wheel. Uniform phasing of ipsilateral wheels is given by the angle β having the same sign as that of metachrony. The phase delay between adjacent ipsilateral cycles, $\varphi = \beta r/v$, is inversely proportional to the velocity of locomotion, while the relative phasing $\psi \equiv \varphi/T = \beta r/L = \text{const}$ is the same regardless of locomotion velocity, just because the condition $L = \text{const}$ is fulfilled. It is known, however, that the condition $\psi = \text{const}$ determines the gait (in agreement with Marey's model). Therefore, there is a simple relation between Marey's definition of the gait and the wave approach taking advantage of the dependence $w(v) \equiv d/\varphi$:

$$\psi = \text{const} \Rightarrow w = kv. \tag{2.34}$$

In other words, there is a correspondence between the condition of constancy of ipsilateral phasing and the linear MW velocity dependence on locomotion velocity, where $k = d/(\psi L) = d/(\beta r)$ is the constant coefficient, and d is the constant distance between adjacent axles.

To conclude, the model of the cart with sectorial wheels is kinematically adequate to the locomotor model proposed by Marey, and both functions, $u(v)$ and $w(v)$, are directly proportional to the velocity of locomotion.

2.4 Cycle synergy

In order to justify the resultant canonical model of stepping movement synergies, we shall have to investigate variability of different interparametric relations with special reference to different *regimes* of locomotion.

2.4.1 Levels of kinematic control. To begin with, one needs to distinguish between three levels of kinematic control.

The choice of locomotion modality (walking, running, jumping, etc.) should be regarded as the top level of *strategic* control because, on the one hand, it implies radical coordination restructuring of stepping movements and, on the other hand, each form of locomotion may have different intrinsic regimes, such as normal, isorhythmic or isometric.

Coordinated organization of parametric freedoms, related to the choice of a locomotion regime, constitutes an intermediate level of *tactical* stride cycle control.

Tuning in to the chosen form and regime of locomotion is ensured with the aid of relevant synergies in such a way (see below) that, in the end, only one freedom of operating control is retained. Each regime can be realized at different locomotion velocities; therefore, the choice of velocity in the framework of a given regime constitutes the lower level of *operating* control.

2.4.2 Kinematic portraits. Let us first consider *a priori* kinematic variants of changing the steady walking speed. A subject walking with a constant speed v has a variety of means to control his or her movement, which ensue from the definition of velocity as the step length L to the period T ratio:

$$v = \frac{L}{T}. \tag{2.35}$$

Different variants of control are due to the possibility of separately varying either the step length or the period, or simultaneously changing the two parameters. Let a new step period and length be chosen in accordance with the following rules:

(1) $T = \text{const}$, $L = \text{var}$ — *isorhythmic walk* (IRW);
(2) $T = \text{var}$, $L = \text{const}$ — *isometric walk* (IMW);
(3) $L/T = \text{const}$ — *isovelocity walk* (IVW);

in the latter case, the step length and period vary in proportion.

Each of these cases corresponds to a specific walking regime. In the case of *normal walk* (NW), the principle of direct proportionality necessary to maintain the desired locomotion velocity is replaced by:

The inverse proportionality principle. It implies that the period decreases with increasing step length, while an increase of the period results in a shorter step.

The normal human walk is known to be organized subconsciously, i.e. in the form of *locomotor automation*. We do not usually think of how we are walking, nor are we able to intelligibly describe our movements in response to a sudden question.

Definition 2.3. *Normal locomotion* (walking, running, etc.) is designated the natural realization of locomotor displacements unaffected by additional external factors, influences, and limitations.

Although many kinematic laws of NW slip from the grasp of mind, they do operate. It is easy to see by examining a kinematic portrait containing velocity dependences of major kinematic parameters (Fig. 3a, b): three temporal $\{T, T_-, T_+\}$ and three spatial $\{L, L_-, L_+\}$ ones.

The approximating functions of dependences $T(v)$ and $L(v)$ in the regime

$$\text{NW}: \; T = T_c + \frac{L_c}{v}, \qquad L = L_c + T_c v \tag{2.36}$$

are in agreement with the inverse proportionality principle (for the example illustrated by Fig. 3a, b, values of T_c and L_c constants are given below in Table 1). For the properties of the remaining functions $T_\pm(v)$ and $L_\pm(v)$, see the next section.

Under experimental conditions, a subject having to maintain a given stride length and thus realize the regime

$$\text{IMW}: \; L = \text{const} = L_{\text{fix}} \Rightarrow T = \frac{L_{\text{fix}}}{v} \tag{2.37}$$

is aided by the use of a 'zebra' walkway, i.e. a walkway marked by a series of parallel white stripes stuck to the floor at a half-step distance $L_{\text{fix}}/2$ from one another. The subject is asked to step on the stripes at different steady walking velocities in order to reproduce a wide range of locomotion speeds. The conceptual methodological difference between IMW and NW consists in the possibility and necessity of performing a series of gaits at different fixed step lengths. The kinematic portrait of one IMW series is presented in Fig. 3c, d. As expected, the plots of $T(v)$ and $L(v)$ satisfy the definition (2.37).

In experimental studies, a fixed rhythm of the regime

$$\text{IRW}: \; T = \text{const} = T_{\text{fix}} \Rightarrow L = T_{\text{fix}} v \tag{2.38}$$

is conveniently set using a metronome ticking with a period of $T_{\text{fix}}/2$. A subject walking with larger and lower velocities dictated by the metronome produces a series of IRW realizations for one T_{fix} value. Similar to the IMW regime,

repeat IRW series can be obtained for different fixed step periods. Figure 3e, f demonstrates the kinematic portrait of an IRW series. Here, plots of $T(v)$ and $L(v)$ satisfy definition (2.38).

2.4.3 Kinematic realizability areas. A comparative review of different experimental series of IMW, IRW, and NW is appropriate in the space-time format, either in RRS or LRS (Fig. 2d, e), because the real control of locomotion is executed exactly in this form. Despite the utility of parallel presentation of experimental data obtained in the two frames of reference, we confine ourselves to LRS, it being the kinematic analogue of the intrinsic frame of reference in which the brain exerts proper locomotion control. Formation of cycle synergy is an important function of spatio-temporal control of locomotion.

Definition 2.4. *Cycle synergy* (CS) denotes a functional relationship between step length L and period T.

Figure 5a simultaneously depicts CSs of three regimes, IRW, IMW, and NW, obtained in experiments involving one and the same subject. In accordance with the definitions (2.37), (2.38), the IRW and IMW regimes are presented here by families of vertical and horizontal straight lines, while the NW regime (2.36), as a unique one, is represented by a single hyperbola

$$\text{NW:}\ L = \frac{L_c T}{T - T_c}\,. \tag{2.39}$$

It can be seen that the experimental points $\mathbf{y} = (T, L)'$ of all the regimes collectively cover a finite area $\boldsymbol{Y}_w$ referred to as the *potential* walking area:

$$\boldsymbol{Y}_w \equiv \{\mathbf{y} \,|\, \mathbf{y}_{min} < \mathbf{y} < \mathbf{y}_{max}\}\,. \tag{2.40}$$

The rectangular boundaries of this area are formally given by the 'extreme' boundary points $\mathbf{y}_{min} = (T_{min}, L_{min})'$ and $\mathbf{y}_{max} = (T_{max}, L_{max})'$. However, the *real* walking area $Y_w \subset \boldsymbol{Y}_w$ is not rectangular and is limited by oblique straight lines corresponding to the extreme (maximum and minimum) locomotion velocities; the v_{min} boundary is especially prominent.

Note 2.6. It is well known that locomotor-type movements (walking, running, etc.) may be performed on the spot,

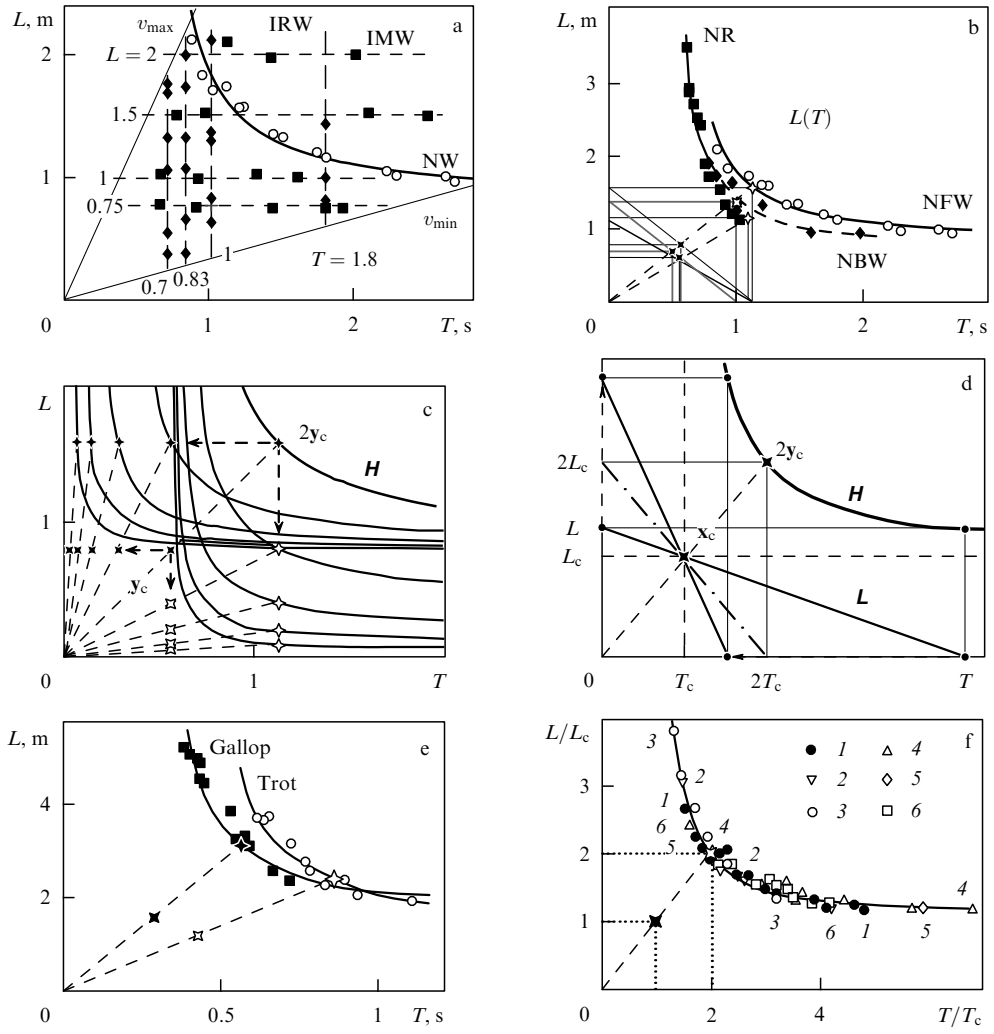

Figure 5. Different variants of cycle synergy changes: (a) three human walking regimes, NW — normal walk, IRW — isorhythmic walk, IMW — isometric walk (all series were obtained in experiments involving one and the same subject); (b) NR — normal running, NFW and NBW — normal forward and backward walking, respectively; (c) consecutive deformations of basal hyperbola following displacements of its centre; (d) reconstruction of basal hyperbola $\boldsymbol{H}$ by rotation of the support straight line $\boldsymbol{L}$ about center $\mathbf{y}_c \equiv (T_c, L_c)'$; (e) two pace varieties of the same horse (based on our cinematographic records); (f) normalized cycle synergies of man (*1*), horse (*2*), dog (*3*), cockroach (*4*), myriapods *Scolopendra* (*5*) and *Julus* (*6*).

that is with a zero step length and therefore at zero locomotion velocity, even though the pace rhythm can be varied as well as the lift of the legs and the height of the jumps. Perhaps, the possibility of such variation has given rise to a view that locomotion can be realized at an arbitrarily low speed. Our own attempts to walk with a minimal speed, starting from stepping on the spot, have led to the discovery of the *low speed paradox* which suggests that it is impossible to walk (or run) at a speed of $v < v_{\min} \approx 0.2\ \mathrm{m\ s^{-1}}$.

It should be emphasized that inner points of area $\boldsymbol{Y}_w$ non-incidental to the NW hyperbola can exist, if at all, only in special IRW and IMW regimes. In other words, when the boundaries of this area are determined from the extreme points on the NW hyperbola, a smaller subarea of $\boldsymbol{Y}_w$ is distinguishable.

2.4.4 Characteristic velocity. Time and length constants (T_c and L_c, respectively) in formulas (2.36) give the coordinates of the center $\mathbf{y}_c \equiv (T_c, L_c)'$ of hyperbola $\boldsymbol{H} \equiv \boldsymbol{H}(\mathbf{y}_c)$, which approximates experimental NW points. Due to this, quantitative evaluation of the constants

$$T_c = 0.575\ \mathrm{s}, \qquad L_c = 0.79\ \mathrm{m} \tag{2.41}$$

yields extremely low minimal values for the step period and length at a normal walking. It follows from the combined graphical representation of CSs for different locomotion modes (Fig. 5a) that walking with a step length $L < L_c$ is realizable only in special IRW and IMW regimes.

From the values presented by estimates (2.41), it is possible to derive a velocity constant

$$v_c \equiv \frac{L_c}{T_c} = 1.37\ \mathrm{m\,s^{-1}} = 82\ \mathrm{m\,min^{-1}}, \tag{2.42}$$

i.e. *characteristic velocity of* NW. This latter value is interesting in that it is close to Ralston's estimate [86, p. 84] of the 'optimal velocity' $v_{opt} \approx 80$ m min^{-1}, which is in agreement with the minimal expenditures of energy for normal walking in humans.

A kinematic criterion for expenditure of energy per step is the product of the period and the step length, $P \equiv TL$. Rewriting parametric functions (2.36) as functions of velocity:

$$\frac{T}{T_c} = \frac{v_c}{v} + 1, \qquad \frac{L}{L_c} = \frac{v}{v_c} + 1, \tag{2.43}$$

results in the following explicit definition of the velocity dependence of product P:

$$P = T_c L_c \left(2 + \frac{v}{v_c} + \frac{v_c}{v}\right), \tag{2.44}$$

while the condition $\mathrm{d}P/\mathrm{d}v = 0$ suggests the minimal $P(v)$ value at a velocity $v = v_c$.

Summarizing the heuristic relationship thus found between kinematics and the expenditure of energy leads to the following:

Heuristic 2.1. In a normal walk, the kinematic minimum of function $P(v) = TL$ coincides with the energy minimum; therefore, the characteristic velocity corresponds to the optimal walking speed.

The substitution of $v = v_c$ into formulas (2.43) yields the 'energetically optimal' step period and length:

$$T_{opt} \equiv 2T_c = 1.15\ \mathrm{s}, \qquad L_{opt} = 2L_c \equiv 1.58\ \mathrm{m}, \tag{2.45}$$

preferred in a prolonged walking.

2.4.5 Transformation of cycle synergy. The versatile role of CS is apparent when NW is compared with other forms and regimes of stepping locomotion. Such a comparison is especially valuable when one and the same subject is tested under identical experimental conditions, because the results give an idea of exactly those properties of functional CS mobility, which arise at the tactical and strategic levels of locomotor movement control (see above). The formal criteria for the characterization of different control levels can be formulated based on the transformation properties of different synergies. This poses the problem of their identification.

Our experiments described in Ref. [27] had the objective of comparing largely three walking regimes (NW, IRW, and IMW). The subjects included in the study were examined under the natural conditions of forward walking (NFW). But one of them had to perform the additional series of locomotor movements, that is a *normal backward walking* (NBW) and *normal running* (NR). Simultaneous representation of cycle synergies for NW, NBW, and NR (Fig. 5b) illustrates two variants of their restructuring.

The NW to NBW conversion can be regarded as a homothety with respect to the origin of coordinates, because these regimes have practically identical characteristic velocities (Table 1). The NW to NR conversion may be estimated as an isorhythmic one, with the T_c reduction being negligibly small (1.06-fold) and L_c undergoing a 1.5-fold decrease; simultaneously, the range of NR velocities is shifted towards higher values, and practically all running episodes have $v > (v_c)_{NR}$.

Table 1. Normal cycle synergies in man.

Locomotion	T_c, s	L_c, m	V_c, m s^{-1}	U_c, m s^{-1}†
NFW	0.57	0.79	1.41	1.91
NBW	0.51	0.70	1.38	2.04
NR	0.54	0.54	1.20	1.04

† Here, U_c is the leg swing velocity at a locomotion speed V_c.

Heuristic 2.2. The alteration of locomotion forms and regimes is underlain with functional CS transformations which formally occur by the displacement of the $\boldsymbol{H}(\mathbf{y}_c)$-hyperbola center $\mathbf{y}_c \equiv (T_c, L_c)'$.

From the formal standpoint, this heuristic looks trivial because the analytical CS description contains only two parameters which are, generally speaking, free and make up the coordinates of the hyperbola center. Hence, there are no other means of functional CS transformation but the shift of the center. In all likelihood, the nontrivial content of the latter heuristic consists in that it implies real requirements of functional CS transformation rather than its formal feasibility and the fulfillment of these requirements in the framework of the same possibilities. An unexpected consequence of heuristic 2.2 lies in the possibility of a similar functional interpretation of IRW and IMW regimes.

2.4.6 The unified model of locomotion regimes. Until now, the NW regime, on the one hand, and the IRW and IMW

regimes, on the other hand, have been understood as conceptually different. Such an understanding is largely based on the fact that NW is a natural and unique regime, while IRW and IMW are artificial and polymodal ones (to put it differently, they allow for the choice of different fixed values of the step length and period). Moreover, analytical definitions of these regimes, viz. formulas (2.36)–(2.38), are also different. However, in-depth comparison of these formulas reveals an inner (parametric) relation between them, formulated in the following:

Lemma 2.1. *Linear cycle synergies of the IRW and IMW regimes can be interpreted as limiting cases of a hyperbolic synergy of the NW cycle*.

Proof. Let us consider a family of isorhythmic transformations: $T_c = \text{const}$, $L_c = \text{var}$. Then, with decreasing L_c (Fig. 5c), the hyperbola $\boldsymbol{H}(\mathbf{y}_c)$ undergoes deformation such that in the $L_c \to 0$ limit it degenerates into the vertical straight line of the IRW cycle synergy. Direct substitution of $T_c = T_{fix}$, $L_c = 0$ values into formulas (2.36) transforms these general parametric formulas of NW to parametric IRW formulas (2.38).

Similar isometric transformations give rise to another family of deformed hyperbolas whose limiting case at $T_c = 0$, $L_c = L_{fix}$ is a horizontal straight line of the IMW cycle synergy (Fig. 5c). Direct substitution of the limiting coordinates of the center, $T_c = 0$, $L_c = L_{fix}$, into formulas (2.36) yields the IMW formulas (2.37).

Thus, continuous parametric transformations NW $\to$ IRW and NW $\to$ IMW are theoretically feasible and correspond to vanishing of one of the center coordinates. ◆

Despite the elementary mathematical content of this lemma, it gives reason, taking into account Heuristic 2.2, to regard isorhythmic and isometric regimes as boundary states of the general cycle synergy control programme rather than specific autonomous programmes ensuring kinematic conditions of stride length and period fixation.

Let us rule out parametrization with respect to velocity in the CS definition (2.43):

$$\left(\frac{T}{T_c} - 1\right)\left(\frac{L}{L_c} - 1\right) = 1 \;\Rightarrow\; TL = T_c L + L_c T\,, \qquad (2.46)$$

and distinguish the canonical equation having the linear-fractional form

$$\frac{T_c}{T} + \frac{L_c}{L} = 1\,. \qquad (2.47)$$

Let us now focus attention on the dual 'linear-hyperbolic' content of this canonical equation:

(1) there is a 'support' straight line in coordinates T_c, L_c:

$$\boldsymbol{L}(\mathbf{y}_T, \mathbf{y}_L)\colon\ \mathbf{y} = (1-\lambda)\mathbf{y}_T + \lambda \mathbf{y}_L \equiv \big((1-\lambda)T, \lambda L\big)'\,, \qquad (2.48)$$

given in segments $\mathbf{y}_T \equiv (T, 0)'$ and $\mathbf{y}_L \equiv (0, L)'$ cut by this straight line on the coordinate axes;

(2) there is hyperbola $\boldsymbol{H}(\mathbf{y}_c)$ in coordinates T, L.

The assessment of optimal values in Eqn (2.45) reveals an important property of the CS hyperbola:

$$2\mathbf{y}_c \in \boldsymbol{H}(\mathbf{y}_c) \;\Leftrightarrow\; \mathbf{o} \in \boldsymbol{H}(\mathbf{y}_c)\,. \qquad (2.49)$$

In other words, the point with double coordinates of the hyperbola center lies on the hyperbola. It is easy to see that the condition $2\mathbf{y}_c \in \boldsymbol{H}$ ensues from the condition $\mathbf{o} \in \boldsymbol{H}$, and vice versa.

That the hyperbola (2.47) passes through the origin of coordinates is not immediately evident because only one of its branches participates in the description of CS, namely, the one which does not cross the origin. However, a complete description of the hyperbola includes two centrally symmetric branches. In the general case, an arbitrary hyperbola, as a 3-parametric second-order curve, does not necessarily pass through the origin of coordinates. Therefore, an additional condition (2.49) distinguishes a special class of 'basal' hyperbolas.

Definition 2.5. A hyperbola is called *basal* if one of its branches passes through the origin of coordinates.

Lemma 2.2. *Basal hyperbola* $\boldsymbol{H}(\mathbf{y}_c)$ *emerges from the rotation of a support straight line* $\boldsymbol{L}(\mathbf{y}_T, \mathbf{y}_L)$ *about the point* $\mathbf{y}_c \in \boldsymbol{L}(\mathbf{y}_T, \mathbf{y}_L)$.

The proof obviously ensues from Fig. 5d. The support straight line (2.48) is the principal diagonal of the coordinate rectangle $\boldsymbol{P} \equiv \{\mathbf{o}, \mathbf{y}_T, \mathbf{y}_L, \mathbf{h}_c\}$ in which the sum vector

$$\mathbf{h}_c \equiv (T, L)' = T\mathbf{e}_1 + L\mathbf{e}_2 \equiv \mathbf{y}_T + \mathbf{y}_L$$

makes up the radial diagonal. If $\mathbf{y}_c$ is the center of rotation of the support straight line (2.48), the assumption of $\mathbf{y} = \mathbf{y}_c$ in Eqn (2.48) gives the equation

$$\mathbf{x}_c = \text{diag}\,(1-\lambda, \lambda)\mathbf{h}_c \;\Rightarrow\; \mathbf{h}_c(\lambda) = \left(\frac{T_c}{1-\lambda}\,,\, \frac{L_c}{\lambda}\right)'\,, \qquad (2.50)$$

i.e. λ-parametric equations of cycle characteristics $T(\lambda)$ and $L(\lambda)$. The exclusion of the parameter λ from these equations gives the scalar equation (2.47), while the replacement of linear λ-parametrization of the support straight line by nonlinear v-parametrization with respect to velocity, $v \equiv L/T$, $\lambda = 1/(1 + v/v_c)$, results in parametric equations (2.36):

$$\mathbf{h}_c(v) = \left(T_c + \frac{L_c}{v}\,,\, L_c + T_c v\right)'\,.$$

Therefore, during rotation of the principal diagonal of the coordinate rectangle, the basal hyperbola is traced out by the radial diagonal vector. ◆

Corollary 2.1.

(1) $\mathbf{y}_c = \mathbf{y}_T \;\Rightarrow\; \boldsymbol{H}(\mathbf{y}_c) = \boldsymbol{L}(\mathbf{y}_T, \mathbf{y}_T + \mathbf{y}_L)$;

(2) $\mathbf{y}_c = \mathbf{y}_L \;\Rightarrow\; \boldsymbol{H}(\mathbf{y}_c) = \boldsymbol{L}(\mathbf{y}_L, \mathbf{y}_T + \mathbf{y}_L)$.

In particular cases, e.g. when the center of rotation lies on one of the coordinate axes, the basal hyperbola degenerates into the corresponding straight line, i.e. CS of NW turns into: (1) CS of IRW; (2) CS of IMW (yielding 'rotational' versions of Lemma 2.1).

2.4.7 Cycle synergies of animals and man. The ability of humans to use different walking regimes (NW, IMW, and IRW) is an important fact which indicates that walking kinematics not only has intrinsic parametric freedoms but that the system of walk control displays a certain locomotor intellect. The latter does not only contribute to the subconscious realization of the NW regime formed in early ontogeny (see Refs [3, 4]) but also controls IRW and IMW regimes which are volitional actions requiring preliminary training. In this sense, animals are not so 'clever', despite having the same kinematic freedoms. Therefore, they are incapable of reali-

zing special locomotor regimes and always tend to keep the regime of normal locomotion.

Assuming that stepping kinematics in man and animals is similarly organized by their controlling systems, then all walkers should be expected to display a certain degree of mathematical similitude, in the first place that of *cycle synergies* (CS). The CS of human NW and NR having the form of basal hyperbola (2.47) (see Table 1), the applicability of such an approximation needs to be checked up as regards experimental data obtained for different animal species.

Our electronic database contains quantitative characteristics of locomotor movements of man and a variety of different animals. Some of the data obtained in our experimental studies were published elsewhere (see Refs [3, 4, 6, 27, 28, 49, 51] for human locomotor kinematics, [5] for the same in dogs, [26, 30] in the centipede *Scolopendra*, and [29, 56] in the millipede *Julus*). Capacious materials obtained by cinematographic recording of locomotor movements in cockroaches, crabs, tortoises, lizards, horses, and other animals remain unpublished. Data concerning equine paces appear to be of special interest in the present context because they were collected using only one horse handled by the same rider who directed him either at a trot or a gallop at different velocities. Differential approximation of experimental data on these two main paces (Fig. 5e) reveals that, in horses, the transition from one pace to the other is induced or accompanied by CS transformations. Compared with analogous 'normal' CS transformations in humans (see Fig. 5b and Table 1), horses exhibit a greater velocity difference:

$$V_{\mathrm{c,trot}} < V_{\mathrm{c,gallop}}\,,$$

evidenced by the same sequence of characteristic length L_{c} increase and characteristic time T_{c} decrease (Table 2).

Table 2. Cycle synergies of equine paces, $h = 0.9$ m.

Pace	T_{c}, s	L_{c}, m	V_{c}, m s^{-1}	U_{c}, m s^{-1}†
Trot	0.42	1.20	2.85	2.48
Gallop	0.28	1.52	5.32	3.69

† Here, U_{c} is the swing velocity at a locomotion speed V_{c}.

Examples of characteristic CS constants for several animal species are given in Table 3 which in addition provide data on the glenoacetobular length h (distance between foot bases). It can be seen that in vertebrates (e.g. tetrapods) $L_{\mathrm{c}} \approx h$, while invertebrates have $L_{\mathrm{c}} \approx 4h$, and the relationship between T_{c} and h in the latter group is less apparent.

Table 3. Characteristics of cycle synergy constants.

Object	T_{c}, s	L_{c}, cm	V_{c}, cm s^{-1}	U_{c}, cm s^{-1}	h, cm
Dog [7]	0.35	35.6	101.2	177.0	45.5
Gecko [61]	0.06	5.3	85.2	105.2	4.2
Cockroach [75]	0.05	1.9	34.8	63.7	0.6
Scolopendra [26]	0.11	3.5	31.2	25.7	0.9
Julus [56]	0.29	0.4	1.3	1.8	0.1

It appears worthwhile to comment on selected data in Table 3.

One of the first in-depth studies on locomotion synergies in dogs was performed by our colleagues Yu I Arshavskiĭ and co-workers. In Ref. [7], these authors used their records to roughly characterize locomotor cycle kinematics in dogs by two conditions corresponding to the Wilson model:

$$T_{+} \approx \mathrm{const} = 0.26\ \mathrm{s}\,,$$

$$L_{-} \approx \mathrm{const} = 0.5\ \mathrm{m}\,.$$

However, additional analysis of graphical data reported in Ref. [7] has demonstrated the relevance of the model treatment procedure being developed in the present work. Specifically, it has been shown that the dog's cycle synergy has the form of a basal hyperbola; this inference was confirmed in Ref. [6].

Comparative studies of overground locomotion in many reptilian species have been performed by V B Sukhanov [61]. This author analyzed temporal characteristics of locomotor cycles, besides tracks. He chose a combination of support patterns and notograms to graphically represent reptilian gaits. In addition, he documented gecko motion patterns by filming under laboratory conditions and constructed plots of their time-specific characteristics versus locomotion velocity. Special attention was given by V B Sukhanov to the velocity dependence of the period, $T(v)$. He demonstrated that in all reptiles included in his studies, this dependence could be analytically approximated by a displaced hyperbola

$$T = T_{\mathrm{c}} + \frac{L_{\mathrm{c}}}{v}$$

(in monograph [61], the T_{c} and L_{c} approximation constants are denoted by other symbols). The author paid little attention to stride length variability. Nevertheless, his approximation of the dependence $T(v)$ implies a linear relationship between the stride length and velocity:

$$L(v) \equiv vT = L_{\mathrm{c}} + T_{\mathrm{c}}v\,,$$

and this result confirms his own data obtained in a track study (see below Fig. 8e). In a word, the findings of V B Sukhanov [61] provide independent evidence that the CS of reptiles are also described by the basal hyperbola.

Qualitative studies of Hughes [80] were followed by a detailed quantitative analysis of cockroach locomotion over a wide velocity range, carried out by F Delcomyn [75]. The latter author questioned the validity of Wilson's model which he considered to be inadequate to the observed phenomena. Our limited cinematographic records of running cockroaches of the same species (*Periplaneta americana*), used in Delcomyn's experiments, confirmed his findings for low and intermediate locomotion velocities. The cockroach data included in Table 3 and discussed below have been borrowed from the work of F Delcomyn.

The cinematographic characteristics of two myriapod species, *Scolopendra* and *Julus*, have been described at length in Refs [26, 56]. Their gaits are briefly discussed below (see Section 2.6.1 and Fig. 7c, d).

In summary, the cycle synergies of various locomoting objects, from man to myriapods, differ only in the value of the constants T_{c} and L_{c}. In other words, they all show spatio-temporal similarity. Choosing constants T_{c} and L_{c} as scale units, one obtains the normalized representation of cycle synergy for humans and animals in the form of a unified hyperbola with the center (Fig. 5f)

$$\mathbf{x} = (1, 1)' \equiv \mathbf{e}\,.$$

2.5 Cycle structure synergy

The above cycle synergy connects spatial and temporal characteristics of the entire cycle, including step length and period. However, an additional synergy, *cycle structure synergy* (CSS), is needed to form the internal structure of the locomotor cycle (support and swing phase durations). The mathematical description of the cycle structure can be reduced to a dimensionless parameter $\gamma(v)$; the knowledge of its analytical form is sufficient for reconstructing the velocity dependences of phase durations $T_{\pm}(v)$, provided the cycle synergy is also known. However, the primary distinction of the parameter γ is inopportune for the further elucidation of geometric properties of CSS because the cycle structure parameter characterizes the relationship between the values of either temporal or spatial structure components alone:

$$\gamma \equiv \frac{T_+}{T_-} \equiv \frac{L_+}{L_-} .$$

For geometric purposes, the swing velocity $u \equiv v/\gamma$ appears to be more suitable because it characterizes the ratio of spatial (support length) to temporal (swing duration) quantities: $u \equiv L_-/T_+$. The primary distinction of the velocity characteristic $u(v)$ simplifies the subsequent geometric construction of CSS in the form of an 'etalon manifold of stepping on events' determined by the functional dependence $L_-(T_+)$.

2.5.1 Symmetry of phase characteristics. Let us now turn back to the kinematic portraits of the three walking regimes (see Fig. 3). The swing phase characteristics $T_+(v)$ or $L_+(v)$ are given together with support phase characteristics $T_-(v)$ or $L_-(v)$ in order to show their symmetric distribution with respect to the median $T(v)/2$ or $L(v)/2$. It can be seen that in terms of shape the paired plots, e.g. those of temporal phases $T_{\pm}(v)$ for the three regimes, depend, on the one hand, on the shape of period $T(v)$ plots and, on the other hand, have their 'own' shapes readily apparent in the IRW regime.

Let us use angle brackets to designate centered components. Then, the property of *bilateral symmetry* of phase components $T_{\pm}(v)$ with respect to the half-period $T(v)/2$ can be analytically written as

$$\left\langle T_-(T)\right\rangle \equiv T_- - \frac{T}{2} = -T_+ + \frac{T}{2} \equiv -\left\langle T_+(T)\right\rangle .$$

The phase components of the stride length $L_{\pm}(v)$ relative to the half-length $L(v)/2$ are described in a similar manner (the preceding formulas should be additionally multiplied by the velocity v).

Furthermore, the calculation of centered dependences $\left\langle T_{\pm}(v; T_{\text{fix}})\right\rangle$ for different values of isorhythmic fixation $T = T_{\text{fix}}$ reveals the multiplicative T_{fix} dependence of centered plots (Fig. 6a), i.e. the longer the fixed period T_{fix}, the farther plots of temporal components $\left\langle T_{\pm}(v; T_{\text{fix}})\right\rangle$ are from the axis of symmetry.

In order to remove this multiplicative dependence, centered dependences should be normalized with respect to the fixed period length. Then, as shown in Fig. 6b, the normalized forms

$$\frac{\left\langle T_{\pm}(v; T_{\text{fix}})\right\rangle}{T_{\text{fix}}} \equiv \frac{T_{\pm}(v; T_{\text{fix}})}{T_{\text{fix}}} - \frac{1}{2}$$

coincide. Because experiments on step length fixation were carried out independently, similar transformations can be made for the stride length phase components of isometric regimes. They demonstrate that both displaced and normalized forms $\langle L_{\pm}(v; L_{\text{fix}})\rangle/L_{\text{fix}}$ also coincide. Moreover, any walking regime can be fictively transformed into an isorhythmic regime of a unit period by normalizing the time-specific phase components $T_{\pm}(v)$ with respect to the period $T(v)$. In a similar way, any walking regime is fictively transformed into an isometric regime of a unit step length by means of normalization of spatial phase components $L_{\pm}(v)$ with respect to the step length $L(v)$. The similarity of phase characteristic properties is summarized in the following:

Heuristic 2.3. There is a canonical form of phase characteristics and, therefore, a canonical form of cycle structure synergy must exist.

This empirical inference needs to be additionally substantiated in theory if the analytical nature of canonical forms is to be understood. The necessary substantiation follows from the possibility of expressing normalized phase durations using parameter γ:

$$\frac{T_+}{T} \equiv \frac{\gamma}{1+\gamma} , \qquad \frac{T_-}{T} \equiv \frac{1}{1+\gamma} .$$

In other words, the normalized phase components of the step length and period can be presented only via the swing u and the locomotion v velocities:

$$\frac{T_+}{T} \equiv \frac{L_+}{L} = \frac{v}{u+v} , \qquad \frac{T_-}{T} \equiv \frac{L_-}{L} = \frac{u}{u+v} . \tag{2.51}$$

Therefore, a simple rationale for the foregoing heuristic concerning the existence of normalized canonical forms of phase characteristics is offered by the new:

Heuristic 2.4. In humans, the velocity characteristic $u(v)$ has a constant form regardless of a walking regime.

Experimental findings (Fig. 6c) confirm this heuristic. Indeed, experimental points of all series for all regimes (NW, IRW, and IMW) are distributed along a certain common line approximately linear in shape:

$$u \approx u_0 + \alpha v .$$

For comparison, Fig. 6c presents a 'data-point' straight line $u = v$; experimental points lie above this line and roughly parallel to it (all the experimental points are linearly approximated using values $u_0 = 0.43$ and $\alpha = 1$). Moreover, the same figure depicts two nonlinear approximations, one (continuous line) for NW points, the other (dashed line) for the sum total of IRW and IMW points (the separate approximation of IRW and IMW points yields closely related curves).

Note 2.7. The assessment of the relevance of linear or other forms of functional relation $u(v)$ depends not only on the accuracy of measurements (e.g. of the step phase duration) but also on the range of recorded velocities v (see Ref. [49] for the statistical evaluation of different approximation variants). It is not always easy to realize a sufficiently wide range of locomotion velocities under experimental conditions. It is understandable that in the case of a narrow range of locomotion velocities one has to apply a linear approximation of the velocity characteristic $u(v)$, the use of which, apart from other advantages, facilitates comparative assessment. For this reason, we used the linear dependence $u(v)$ in our earlier studies to approximate a variety of experimental human walking data including those for

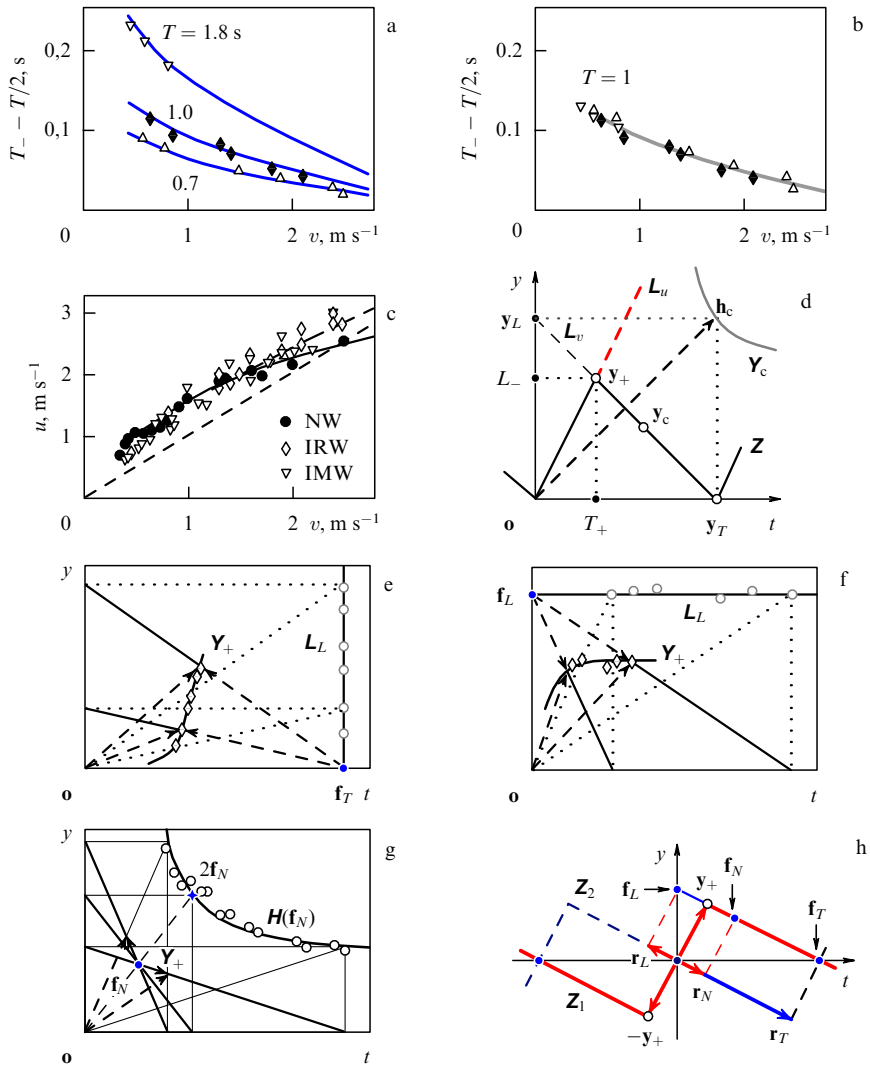

Figure 6. Cycle structure synergy: centered support phase durations for three variants of period fixation before (a) and after (b) normalization with respect to the period; (c) summary representation of velocity characteristics $u(v)$ for three human walking regimes (using the same data as in Fig. 4a); (d) schematic representation of the target stepping on event $\mathbf{y}_+$ as a correspondence between two straight lines $\boldsymbol{L}_u$ and $\boldsymbol{L}_v$; (e–g) examples of the reconstruction of structural etalons $\boldsymbol{Y}_+$ for the three walking regimes; (h) schematic definition of complementary events of the three walking regimes: $\mathbf{r}_T$ — IRW, $\mathbf{r}_L$ — IMW, and $\mathbf{r}_N$ — NW.

children [3, 4], healthy adults [27, 28], disabled subjects [6], etc.

A practically unified velocity characteristic $u(v)$ has also been obtained for two equine paces (not shown here).

2.5.2 Linear-fractional form. Nonlinear approximations to the dependence $u(v)$ are analytically described by the linear-fractional function

$$u = \frac{\alpha_1 + \alpha_2 v}{1 + \alpha_3 v}\,. \tag{2.52}$$

Table 4 shows coefficients of the form (2.52) for those curves which approximate experimental findings in humans (Fig. 6c).

Table 4. Coefficients of linear-fractional form.

Regime	α_1	α_2	α_3
NW	0.14	2.25	0.15
IRW + IMW	0.11	1.74	0.52

Also, coefficients of the linear-fractional form (2.52) can be defined in a different way as

$$u = \frac{a_1 + a_2 v}{a_3 + v} \equiv \mathrm{fr}\,(v; \mathbf{A})\,. \tag{2.53}$$

These variants may be specified in a matrix form as

$$\mathbf{A} = \begin{pmatrix} \alpha_1 & \alpha_2 \\ 1 & \alpha_3 \end{pmatrix} = \begin{pmatrix} a_1 & a_2 \\ a_3 & 1 \end{pmatrix}$$

$$\Leftarrow a_1 = \frac{\alpha_1}{\alpha_3}\,, \quad a_2 = \frac{\alpha_2}{\alpha_3}\,, \quad a_3 = \frac{1}{\alpha_3}\,. \tag{2.54}$$

The former α-coefficients appear to be more suitable to identify cases of small values of the coefficient α_3 (see Table 4), i.e. when the linear-fractional form is close to linear. However, the form (2.53) will be used in the forthcoming theoretical reasoning as more convenient for the purpose.

There is a third way to determine the coefficients of the hyperbolic linear-fractional form, which takes into consideration the algebraic relation between this form and a double ratio or wurf (see Section 6.13), due to the fact that the wurf

contains velocity parameters of asymptotes as etalon constants which are opportunely called *etalon velocities*:

$$u = \mathrm{fr}\,(v;\mathbf{A}) \Leftrightarrow \mathrm{w}\,(v_1, v_2; c_1, c_2) = -q\,. \tag{2.55}$$

Simple wurf transformations produce a linear-fractional form

$$u = \frac{c_1 c_2 + (q_1 c_2 + q_2 c_1)v}{q_1 c_1 + q_2 c_2 + v}\,. \tag{2.56}$$

Here, $v_1 = -v$, $v_2 = u$, $q \equiv -s_1/s_2$ is the anharmonicity constant, and c_1, c_2 are etalon velocities; in addition one obtains

$$q_1 \equiv \frac{1}{1+q}\,, \quad q_2 \equiv \frac{q}{1+q} \Leftrightarrow q_1 + q_2 = 1\,, \quad \frac{q_2}{q_1} = q\,. \tag{2.57}$$

From Eqns (2.56) and (2.53), it follows that

$$2a \equiv a_2 + a_3 = c_1 + c_2\,,$$

i.e. c_1, c_2 are the roots of the quadratic equation

$$c^2 - 2ac + a_1 = 0 \Rightarrow c_{1,2} = a \pm (a^2 - a_1)^{1/2}\,.$$

The anharmonicity constant q is computed according to the formula

$$q = \frac{a_2 - c_2}{c_1 - a_2} = \frac{a_3 - c_1}{c_2 - a_3}\,.$$

Using the above empirically estimated α-coefficients (see Table 4) and taking into consideration subsequent substitutions (2.54), it is possible to find etalon velocities and an anharmonicity constant for walking regimes in humans (Table 5).

Table 5. Etalon constants in man.

Regime	c_1, m s^{-1}	c_2, m s^{-1}	$-q$
NW	0.043	6.21	0.44
IRW + IMW	0.041	11.83	0.57

Analogous estimates of etalon constants for a few animal species are collected in Table 6.

Table 6. Etalon constants in animals.

Object	c_1	c_2	$-q$	$[c]$
Horse	0.099	14.1	0.850	m s^{-1}
Dog	0.046	4.3	0.307	m s^{-1}
Cockroach	0.910	292.5	0.469	cm s^{-1}
Scolopendra	1.648	323.2	1.150	cm s^{-1}
Julus	0.987	274.6	0.783	mm s^{-1}

The common properties of etalon constants (see Tables 5 and 6) can be listed as follows:

(1°) etalon velocities have the same sign (unidirectionality);

(2°) the velocity c_2 is much higher than c_1, $c_2/c_1 \geqslant 100$ (anisotropy);

(3°) the constant q differs from 1 (anharmonicity).

If property (2°) is strengthened and the second etalon velocity c_2 is assumed to be infinitely high, then the linear-fractional form is substituted by the linear one:

$$c_2 \to \infty \Rightarrow u = u_0 + \alpha v\,,$$

where $u_0 = c_1/q_2$, and $\alpha = q_1/q_2 = 1/q$. If the first etalon velocity c_1 is in addition assumed to be infinitely low, the simplest variant of a linear relationship between swing and locomotion velocities has the form

$$c_2 \to \infty\,, \quad c_1 \to 0 \Rightarrow u = \frac{v}{q}\,.$$

Thus, in compliance with the wave interpretation of coefficients of the linear-fractional form (2.53), the use of a linear approximation to the velocity characteristic $u(v)$ does not mean the choice of another chronometric model. Instead, it means the choice of a particular variant in which the second etalon velocity may be assumed to be very high.

Note 2.8. It follows from the determining conditions (2.24) of the Marey locomotor model that the cycle structure parameter is constant, viz.

$$\gamma \equiv \frac{T_+}{T_-} \equiv \frac{L_+}{L_-} = \mathrm{const}\,.$$

Hence, the linear relation between swing and locomotion velocities is resulted in the form

$$u \equiv \frac{L_-}{T_+} = \frac{v}{\gamma}\,.$$

Comparison of this relation with formula (2.56) brings about the conclusion that Marey's model corresponds to the linear version of the velocity characteristic $u(v) = v/q$, whose etalon velocities have extreme values $\{c_1 = 0,\ c_2 = \infty\}$, while the anharmonicity constant equals the cycle structure constant, $q = \gamma$.

2.5.3 Event control metaphor. The ballistic metaphor of stepping movements reduces a cycle structure control to the evaluation of two pulsed dynamic events, namely, the foot lift in the late support phase and the foot touch-down at the end of the swing phase. Although the ballistic metaphor considerably simplifies the real mechanism of locomotion control (for example, it ignores the multipulse character of muscle force generation), the distinguished events are crucial for the complicated system of control over the motion of multilink extremities. Restricting ourselves to the consideration of only two key events, the foot lift and touch-down, we shall nevertheless have to elucidate their coordination in the course of the entire stride cycle. In what is forthcoming we shall need the notion of a target event. It may be conjectured that the role of the target event in walking is played by the foot touch-down. This hypothesis is supported by the following observations;

IMW. When a man tries to step on the stripes stuck to the floor, he is consciously solving the problem of foot placement precisely in the expected position and at the correct time. In this case, the touch-down may be considered to be the *target* event. The contralateral limb plays therewith the role of a coordinating referent with respect to which the target task is accomplished;

IRW. The subject of the study preliminarily adjusts his or her gait to the given walking rhythm on the spot and thereafter maintains it throughout the trial using touch-

down events as a clew. Therefore, in this case too, the touch-down is the target event. Also, the contralateral leg serves as a rhythmic referent; in other words, the subject adjusts the rhythm of 'half-steps' to accomplish the task;

NW. Phase alternation occurs subconsciously, but if the subject has to control it under certain constraints, he (or she) usually does it by correcting touch-down events.

The universally accepted view of a spatio-temporal organization of walking locomotion is expressed as the following:

Target principle of locomotor event control. Stepping movements are organized by the brain so that the current control and adjustment of each step cycle during the walk are performed in relation to the target event of touch-down. The purpose is to place the foot in the right place and at a certain instant of time.

It is only natural that the brain uses LRS as its intrinsic frame of reference. This must be kept in mind when synthesizing the space-time geometry of the processes involved in gait control by the 'locomotor intellect'. The brain may be supposed to use two 'in-built' maps: the body map which serves as the LRS, and the map of the surroundings acting as RRS. Therefore, the brain has to measure space-time parameters by comparing the intrinsic body map with the incessantly varying map of the surroundings. It is well known that, in the absence of locomotion, visual perception of the environment is characterized by the property of 'constancy'. In contrast, very little is known about the travel of space visual image during locomotion.

2.5.4 Target etalons. Let us turn back to the spatio-temporal image of *target trajectory* (TT) $\boldsymbol{Z}$. The synergetic approach gains advantage from the family of $\boldsymbol{Z}(v)$ inherent in any locomotion regime rather than from individual TTs.

Let the origin of LRS $\mathbf{Y} \equiv \{\mathbf{y} = (t, y)'\}$ be coincident with the foot lift event (Fig. 2e); then, the next target event (touch-down of the same limb) is $\mathbf{y}_+ \equiv (T_+, L_-)'$, and the lift event that follows is $\mathbf{y}_T \equiv T\mathbf{e}_1$. Let us draw the support straight line $\boldsymbol{L}_v \equiv \boldsymbol{L}(\mathbf{y}_T, \mathbf{y}_L)$ [see Eqn (2.48)] which is incidental to the support phase portion of $\boldsymbol{Z}$ and intersects the space axis at the point $\mathbf{y}_L \equiv L\mathbf{e}_2$. Let us single out, in addition, another straight line $\boldsymbol{L}_u \equiv \boldsymbol{L}(\mathbf{o}, \mathbf{y}_+)$ incidental to the swing phase portion of $\boldsymbol{Z}$. The target event is defined as the point of intersection of the support and swing straight lines:

$$\mathbf{y}_+ \equiv \boldsymbol{L}_u \cap \boldsymbol{L}_v \,. \tag{2.58}$$

In other words, the target event is equivalent to that of the correspondence of two bundles of straight lines:

$$\boldsymbol{B}(u; \mathbf{o}) \equiv \{\boldsymbol{L}_u\}\,, \qquad \boldsymbol{B}(v; \mathbf{y}_c) \equiv \{\boldsymbol{L}_v\}\,,$$

which, firstly, have different centers $\mathbf{o}$ and $\mathbf{y}_c$, and, secondly, are parametrized with respect to velocities u and v. Well then, the velocity characteristic $u(v)$, i.e. *cycle structure synergy* (CSS), serves as the analytical expression of this correspondence.

It has been shown in a previous section that *cycle synergies* (CS) of all the three walking regimes (NW, IRW, and IMW) are formed in a similar way, namely, by means of rotation of the support straight line [see Lemma (2.2) and Corollary (2.1)]. When the velocity v changes, the 'cycle cessation' event $\mathbf{h}_c(v)$ traces out, in the general case, the etalon line of cycle $\boldsymbol{Y}_c$, the shape of which depends on the walking regime which is in turn geometrically determined by the choice of the support bundle center:

$$\begin{aligned}
&\text{IRW:} \quad \mathbf{y}_c = \mathbf{f}_T \;\Rightarrow\; \boldsymbol{Y}_c = \boldsymbol{L}_T \equiv \boldsymbol{L}(\mathbf{f}_T, \mathbf{y}_L)\,,\\
&\text{IMW:} \quad \mathbf{y}_c = \mathbf{f}_L \;\Rightarrow\; \boldsymbol{Y}_c = \boldsymbol{L}_L \equiv \boldsymbol{L}(\mathbf{y}_T, \mathbf{f}_L)\,,\\
&\text{NW:} \quad \mathbf{y}_c = \mathbf{f}_N \;\Rightarrow\; \boldsymbol{Y}_c = \boldsymbol{H}(\mathbf{f}_N)\,,
\end{aligned}$$

where $\mathbf{f}_T$ and $\mathbf{f}_L$ are the axial vectors of fixed events, and $\boldsymbol{H}(\mathbf{f}_N)$ is the basal hyperbola, the center of which is the fixed event of norm $\mathbf{f}_N \in \boldsymbol{L}_v \equiv \boldsymbol{L}(\mathbf{y}_T, \mathbf{y}_L)$.

Now, in analogy to the geometric model of the formation of cycle $\boldsymbol{Y}_c$ etalon, one may conclude that under changes of the locomotion velocity v the target event $\mathbf{y}_+(v)$ also depicts a certain curve $\boldsymbol{Y}_+$ (target etalon), the shape of which is likewise a function of the walking regime.

An example of graphical reconstruction of IRW etalons is presented in Fig. 6e. Here, the support straight line $\boldsymbol{L}_v$ rotates about a point on the time axis $\mathbf{f}_T \equiv T\mathbf{e}_1$ ($T = 0.83$ s), while the total cycle vector

$$\mathbf{h}_c \equiv \mathbf{f}_T + \mathbf{y}_L \in \boldsymbol{L}_T$$

'slides' along the vertical straight line of the cycle etalon and the target vector $\mathbf{y}_+$ traces out therewith the target etalon curve $\boldsymbol{Y}_+$.

A similar graphical reconstruction of IMW etalons is illustrated in Fig. 6f. Here, the support straight line $\boldsymbol{L}_v$ rotates about a point on the space axis $\mathbf{f}_L \equiv L\mathbf{e}_2$ ($L = 1.5$ m), and the cycle vector $\mathbf{h}_c \equiv \mathbf{y}_T + \mathbf{f}_L \in \boldsymbol{L}_L$ traces out the horizontal straight line of the cycle etalon, while the target vector $\mathbf{y}_+$ traces out another target etalon curve $\boldsymbol{Y}_+$.

Finally, a similar approach is employed to construct graphic images of the hyperbolic etalon $\boldsymbol{H}$ and the target etalon $\boldsymbol{Y}_+$ in the NW case (Fig. 6g), when the rotation center of the support straight line falls on the center of the hyperbola $\boldsymbol{H}(\mathbf{f}_N)$.

To conclude, the geometric rules for the construction of cycle and target etalons appear fairly obvious and uniform if the support straight line rotation model is used.

2.5.5 Complementary bases. To wind up the discussion of cycle structure synergy, it is necessary to obtain algebraic descriptions of target etalons, i.e. those $\boldsymbol{Y}_+$ curves which approximate experimental points $\mathbf{y}_+ \equiv (T_+, L_-)'$ in Fig. 6e–g. The algebraic identification of a target etalon is facilitated by the system approach in which a target event $\mathbf{y}_+$ is considered concurrently with a reference event $\mathbf{y}_-$. This pair of events forms the TT basis represented by matrix $\mathbf{Y} \equiv (\mathbf{y}_-, \mathbf{y}_+)$ [see Eqn (2.14)]. The basis vectors have corresponding etalons $\boldsymbol{Y}_-$ and $\boldsymbol{Y}_+$ that form a system of base invariants of locomotion chronogeometry.

Problem 2.2. Find the form of target ($\boldsymbol{Y}_+$) and reference ($\boldsymbol{Y}_-$) etalons for three walking regimes NW, IRW, and IMW.

It seems appropriate to consider a pair of TT, $\boldsymbol{Z}$ and $\boldsymbol{Z}^*$, rather than a single TT, for two contralateral legs stepping out of phase. Such TTs intersect at the phase midpoints, i.e. when one leg is in the swing mid-phase and the other is in the support mid-phase (Fig. 2e). In this case, it is more convenient to choose the origin of LRS, $\mathbf{Y} \equiv \{\mathbf{y} = (t, y)'\}$, at the point of intersection of the two TTs with respect to which touch-down and lift events incident to both legs are distributed centrally symmetrically (Fig. 6h).

Let us first choose a pair of phase switching events as the base one

$$\mathbf{y}_- \equiv \left(\frac{T_-}{2}\,, -\frac{L_-}{2}\right)' \in \boldsymbol{Z}^*\,, \qquad \mathbf{y}_+ \equiv \left(\frac{T_+}{2}\,, \frac{L_-}{2}\right)' \in \boldsymbol{Z}\,. \quad (2.59)$$

The target event $\mathbf{y}_+$ of a leg touch-down is different from the previous definition (2.58) in that it contains an unimportant multiplier $1/2$; similar factors appear in the definitions of axial events of the support straight line $\boldsymbol{L}_v(\mathbf{y}_T, \mathbf{y}_L)$: $\mathbf{y}_T \equiv (T/2)\mathbf{e}_1$, $\mathbf{y}_L \equiv (L/2)\mathbf{e}_2$.

The reference event $\mathbf{y}_-$ of the conjugate leg lift is incidental to the straight line $\boldsymbol{R}_v \equiv \boldsymbol{L}_v(\mathbf{o}, \mathbf{y}_-)$ which is parallel to the support straight line $\boldsymbol{R}_v \parallel \boldsymbol{L}_v$. In other words, the reference straight line shows evidence of being the straight line of the support portion of conjugate TT $\boldsymbol{Z}^*$.

The scalar description of the cycle structure synergy [see Eqn (2.53)] is converted into the vector condition of projective orthogonality:

$$u = \mathrm{fr}\,(v; \mathbf{A}) \;\Rightarrow\; \mathbf{y}_+'\mathbf{M}\mathbf{y}_- = 0\,, \qquad \mathbf{M} = -\mathbf{F}\mathbf{A}\,. \quad (2.60)$$

This locomotor situation differs from the previous one only by the use of the inverted version of the linear-fractional form. This explains why the relationship between the matrix of coefficients $\mathbf{A}$ and metric matrix $\mathbf{M}$ is written down in a different way.

The isorhythmic case turned out to be key for the unified representation of general 'locomotion chronogeometry' because it is under isorhythmic conditions that the naturally distinguished pair of basic events (2.59) acquires a remarkable property of 'sum fixation'. Indeed, summation of vectors (2.59) yields $\mathbf{y}_- + \mathbf{y}_+ = (T/2)\mathbf{e}_1 \equiv \mathbf{y}_T$, while an additional condition $T = T_{\mathrm{fix}}$ connects a fixed IRW event $\mathbf{y}_T = \mathbf{f}_T$ with base vectors $\mathbf{y}_- + \mathbf{y}_+ = \mathbf{f}_T$.

Before passing to IMR and NW, let us introduce:

Definition 2.6. Two events are called *complementary* if their sum equals the fixed event.

The fixed event of IMW being known [$\mathbf{y}_L = (L_{\mathrm{fix}}/2)\mathbf{e}_2 \equiv \mathbf{f}_L$], the complementarity of the IMW basis is ensured by the choice of a new reference event $\mathbf{y}_- = \mathbf{f}_L - \mathbf{y}_+ \equiv \mathbf{r}_L$, while retaining the target event $\mathbf{y}_+$ unaltered. The choice of the IRW reference event (2.59) is denoted in a similar way: $\mathbf{y}_- = \mathbf{f}_T - \mathbf{y}_+ \equiv \mathbf{r}_T$. These definitions are supplemented by the definition of the NW reference event $\mathbf{y}_- = \mathbf{f}_N - \mathbf{y}_+ \equiv \mathbf{r}_N$ (Fig. 6h), where $\mathbf{f}_N$ is the center of the cycle synergy hyperbola (see the previous section).

Thus, if $\mathbf{f}$ is an arbitrary fixed event, the determining relations for the complementary basis can be obtained along with the bilinear form (2.60):

$$\mathbf{y}_+'\mathbf{M}\mathbf{y}_- = 0\,, \qquad \mathbf{y}_- + \mathbf{y}_+ = \mathbf{f}\,. \quad (2.61)$$

As a consequence, the quadratic forms of metric standards may be found:

$$\begin{aligned} &\boldsymbol{Y}_+\!: \quad \mathbf{y}_+'\mathbf{M}\mathbf{y}_+ - \mathbf{y}_+'\mathbf{M}\mathbf{f} = 0\,,\\ &\boldsymbol{Y}_-\!: \quad \mathbf{y}_-'\mathbf{M}\mathbf{y}_- - \mathbf{f}\,'\mathbf{M}\mathbf{y}_- = 0\,. \end{aligned} \quad (2.62)$$

Thus, problem 2.2 is solved. ◆

We have demonstrated the theoretical possibility of a common metric description of different walking regimes in our first summary report [49] and suggested:

The homometricity hypothesis. Target etalons of all three regimes (NW, IMW, and IRW) are represented by metrically identical hyperbolas having the same metric matrix and differing in the positions of a center and diameters.

The method of fixed events used in the present study provides a clear and simple rationale for the hypothesis of homometricity of locomotion chronogeometry. The diameter of the basal hyperbola $\boldsymbol{H}(\mathbf{y}_c)$ depends on the localization of center $\mathbf{y}_c$, and vector $2\mathbf{y}_c$ may be regarded as the principal diameter. This simplifies the homometric description of such hyperbolas due to the fact that their diameter does not make the third independent parameter.

2.6 Wave synergy of gaits

The constant velocity of a *metachronal wave* (MW), resulting from constancy of an ipsilateral delay as proposed by Wilson, is in conflict with the real locomotion situation. On the other hand, proportionality of the MW velocity to the speed of locomotion (as a consequence of constant ipsilateral phasing and Marey's stroboscopic metaphor) is closer to reality because the 'step-to-step' rule characteristic of certain arthropods is a special case of such proportionality.

2.6.1 Metachronal waves in myriapods. Stepping movements of myriapods are of peculiar interest in terms of wave coordination rules. Let us consider first the locomotion of a typical centipede, *Scolopendra sp.*, having $N = 40$ legs and a body length $H = 5-10$ cm [26]. The general property of ipsilateral coordination in this animal is described by:

The 'step-to-step' rule. The choice of a new contact point on the ground is the responsibility of the forelegs, whereas each of the remaining legs on either side of the body is put exactly where the previous one touched the substrate.

In multipedal animals, this walking pattern is readily apparent on instantaneous photographs on which the supporting legs can be seen gathered in bundles converging to contact points (Fig. 7c). The analytical criterion for the 'step-to-step' rule is formulated as

$$w = -v\,. \quad (2.63)$$

In other words, the absolute MW velocity w always equals the walking velocity v, but the wave propagates oppositely to the direction of locomotion (from head to tail). This is the case of *negative* metachrony.

Note 2.9. In this case, the wave to locomotion velocity ratio is constant: $w/v = -1$. It is worthwhile to note that bending waves in fish also progress backward along the body, and their swimming is also characterized by the constant ratio $w/v = k < 1$. This ratio should be expressed as a negative constant were this not in conflict with the common practice (see Ref. [76]). In fish, the constant k is smaller than unity because inevitable slipping of the travelling wave occurs in water. With this in mind, metachrony in *Scolopendra* can be regarded as analogous to fish metachrony with the sole exception that locomotion in *Scolopendra* is realized without slipping.

Another mode of metachronal coordination (see Fig. 7d) is displayed by millipedes of the genus *Julus* [56] which have $N \geqslant 120$ leg pairs (with two contralateral pairs per girdle). A small positive phase shift makes a wave of ipsilateral leg transfer easy to see, while contralateral pairs of legs step in phase with one another. Indeed, several waves simultaneously run from head to tail along a row of ipsilateral legs, their length and velocity being functions of the speed of locomotion.

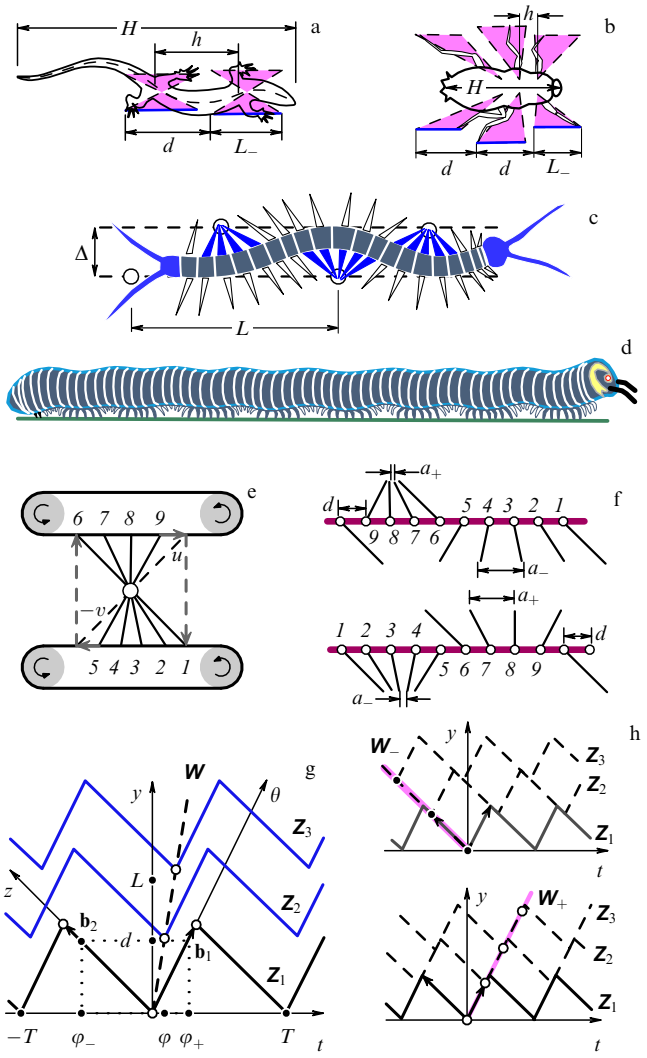

Figure 7. Locomotor postures of a lizard (a), cockroach (b), *Scolopendra* (c), and *Julus* (d) (support leg triangles and distances between foot bases h and triangle bases d are shown for lizard and cockroach); (e) locomotor cycle scheme obtained in experiments on a two-belt treadmill; (f) progressive and reverse spatial scans of the locomotor cycle, represented as a metachronal row; (g) definition of the trajectory frame of reference by a pair of basis vectors $\mathbf{b}_1$ and $\mathbf{b}_2$ for the case of an arbitrary metachronal wave $\boldsymbol{W}$; (h) extreme variants of negative $\boldsymbol{W}_-$ and positive $\boldsymbol{W}_+$ metachronies.

An instantaneous photograph of a locomoting millipede *Julus sp.* (Fig. 7d) shows that legs in the swing phase form bundles within which they come together to one point of the substrate. Such a configuration is a sign of positive metachrony. When the legs to be swung are gathered in such converging bundles, they give rise to a particular mode of inverted 'step-to-step' locomotion in the swing phase [57]. Such a variant of the inverted 'step-to-step' ('wing and wing') rule for the swing phase is termed 'stroke-by-stroke' motion. The *Julus* gait submits to this rule albeit not very strictly (see below).

The kinematic criterion for the 'stroke-by-stroke' gait is analogous to the condition (2.63), with the exception that

$$w = u\,, \qquad (2.64)$$

i.e. the MW velocity is positive and equal to the velocity of legs in the swing phase.

The discovery of the two types of phase-conjugate gaits (2.63) and (2.64) gave rise to a variety of kinematic interpretations of wave coordination and gait characterization techniques (see Refs [57–59]). Considering gaits (2.63) and (2.64) as particular boundary cases of interlimb coordination

$$\text{'step-to-step': } w = -v, \quad \text{'stroke-by-stroke: } w = u, \qquad (2.65)$$

leads to the following theoretical:

Problem 2.3. Propose such a gait definition which will include variants (2.65) as particular cases of the general principle.

The search for the solution of this problem is possible using different gait metaphors. The following three metaphors are considered and compared below: configurational, trace, and relativistic; the latter is formulated as the 'relative metachrony principle'.

2.6.2 Configurational metaphor. The characterization of myriapod gaits in terms of leg bundle shape gives rise to a new coordinative metaphor, the so-called 'configurational' metaphor [57, 58]. A special case of configuration is exemplified by a transit *metachronogram* (MCG) of one leg (Fig. 1a), which combines spatial and temporal scans of the unipedal walking cycle. But the same transit MCG may be interpreted in a purely spatial context as an instantaneous photograph of the collective walking of many people marshalled into a rank. Then, it is appropriate to put:

Question 2.4. What type of collective walking gait is simulated by a transit MCG?

Previously, we have demonstrated the relationship between the transit MCG obtained in RRS and pendulum MCG obtained in LRS. The task of constructing an arbitrary metachronal row ('metarow') can be accomplished in a similar way but using only spatial transformations of pendulum MCG. For the simplicity of graphical representation, we confine ourselves to the one-link 'telescopic' leg model, while pendulum oscillating movements of such a leg in LRS will be presented in the form of rotational ('wheelwise') motion.

Let us consider the two-point leg model containing *basal* and *distal points* (BP and DP, respectively). In LRS, BP is fixed, while DP in the support phase moves backward at a velocity v along the rectangular segment of the support interval of length L_-. The usual pendulum leg motion takes place if DT in the swing phase is assumed to move along the same segment (a slight elevation of DT above the soil may be neglected) and forward, at a velocity u. In order to simulate rotational movements of the leg, the forward movement during the swing phase should be mirrored with respect to the basal line. The replacement of support and swing segments in such a representation by treadmill belts moving in opposite directions (see Fig. 7e) produces:

The two-belt treadmill metaphor. In the support phase, DP moves backward along the lower belt. In the swing phase it moves forward over the upper belt and instantaneously jumps within the phase boundaries from one belt to the other.

In this case, the leg in LRS rotates clockwise, and DP moves along the rectangular phase contour. The two-belt treadmill metaphor clearly demonstrates kinematic equivalence of support and swing phases, which is essential for the configurational and trace gait criteria. For example, we have

a right to speak of ordinary footsteps on the lower belt, and conjugate footsteps on the upper one.

In order to follow the DP motion correctly along the phase contour with a stroboscope, let us divide the target trajectory period into time intervals

$$\Delta t = \frac{T}{n}$$

and transfer the space coordinates of the division points y_i, $i = 0, \ldots, n$ onto the fragments corresponding to the support and swing phases. In this case, similar distances between the adjacent inner DPs of different phases are defined as

$$\Delta a_+ = u\Delta t\,, \qquad \Delta a_- = v\Delta t\,.$$

Suppose that the gating interval is equal to the metachronal delay, $\Delta t = \varphi$. For the construction of an instantaneous metarow image, it is necessary to distinguish the cyclogram of individual leg rotation in LRS and distribute sequential images of the leg cyclogram along the basal line, with each leg image displaced a distance d. Let the leg images on the cyclogram be numbered clockwise. Then, two types of metarow can be obtained by aligning ascending posture numbers either from tail to head (negative metachrony; Fig. 7f, top row) or from head to tail (variant of positive metachrony; Fig. 7f, bottom row). In each of the two cases of negative $(-)$ and positive $(+)$ metachrony, the distances between adjacent DPs in MCG are described by the following formulas

$$a_- = d - \Delta a_- = \left(1 + \frac{v}{w}\right)d\,, \quad a_+ = d + \Delta a_+ = \left(1 - \frac{u}{w}\right)d \Leftarrow w < 0\,, \qquad (-)$$

$$a_- = d + \Delta a_- = \left(1 + \frac{v}{w}\right)d\,, \quad a_+ = d - \Delta a_+ = \left(1 - \frac{u}{w}\right)d \Leftarrow w > 0\,, \qquad (+)$$

which can be substituted, taking into consideration the sign of MW velocity, by two formulas

$$\frac{a_-}{d} = 1 + \frac{v}{w}\,, \qquad \frac{a_+}{d} = 1 - \frac{u}{w}\,. \qquad (2.66)$$

The assumption of $a_- = 0$ in the first formula leads to the 'step-to-step' rule [see Eqn (2.67)]. Similarly, the assumption of $a_+ = 0$ in the second formula yields the 'stroke-by-stroke' dependence. How can a generalized definition of configurational gaits be obtained from formulas (2.66)?

2.6.3 Configurational gaits. When gaits are characterized in terms of the configuration of instantaneous leg positions, the role of characteristic quantities is played by distances (2.66) between adjacent DPs in the support and swing phases. These distances depend on the distance d between adjacent TTs. However, this relationship is lacking in extreme gait variants where the corresponding distances vanish:

$$\text{'step-to-step'}: a_- = 0, \quad \text{'stroke-by-stroke'}: a_+ = 0. \qquad (2.67)$$

Apparently, the general definition of configurational gaits must not explicitly depend on the distance d, in conformity with the 'thinning out' metaphor.

Let both the metachronal delay φ and the distance d be initially small. Then, there appears a rather dense metarow containing a large number of adjacent legs in each of support and swing phases. Let us 'thin out' the initial metarow, e.g. remove every other leg, that is all legs given even (or odd) numbers upon initial natural numbering. In this case, all quantities a_-, a_+, d, and φ will increase two-fold without a change of either MW velocity or ratios a_-/d and a_+/d in formulas (2.66). A similar conclusion is valid with respect to other variants of 'thinning out' metarow, including nonuniform cases.

The reverse transition from a 'thinned out' metarow to the 'intact' one can be described as an inverse operation consisting in the 'insertion' of intermediate legs.

Let us declare that all metarow derived from a certain metarow by means of thinning out and/or insertion are configurationally *equivalent*. Then, the configurational gait may be defined via the condition of constancy of either a_-/d or a_+/d relation in formulas (2.66). Gaits (2.67) present special cases of such a definition.

Note 2.10. In the Marey model (2.24), $w = kv$. Therefore, the first relation in Eqn (2.66) for the support traces is unvaried: $a_-/d = 1 + 1/k = \text{const}$. In Wilson's model, the second relation in Eqn (2.66) for conjugate traces is permanent: $a_+/d = \text{const}$ [according to Eqn (2.28)]. It may be inferred that both the Marey and Wilson models fulfill the criteria for configurational gaits.

Another variant of defining configurational gaits consists in the use of a common criterion instead of one of the two conditions (2.66):

$$\mathsf{Co} \equiv \frac{a_-}{a_+} = \frac{w + v}{w - u}\,. \qquad (2.68)$$

In this approach, an arbitrary configurational gait is defined by the constancy condition for a given criterion: $\mathsf{Co} = \text{const}$. Gaits (2.67) become special cases of one criterion:

$$\text{'step-to-step'}: \mathsf{Co} = 0, \quad \text{'stroke-by-stroke'}: \mathsf{Co} = \infty. \qquad (2.69)$$

The geometric sense of the configurational criterion (2.68) is elucidated below. For more details concerning the configurational approach see Refs [57,58].

2.6.4 Trace gaits. Let us confine ourselves to the comparison of tracks left by myriapods on the upper and lower belts of a two-belt treadmill (Fig. 7e), neglecting the shape of the bundles formed by their legs in the support and swing phases. In this case, the distances between adjacent footsteps should be compared with step lengths rather than basal distances d, taking into account that these step lengths may be different on different belts. Indeed, the common definition

$$L \equiv L^- \equiv vT$$

holds for the lower treadmill belt, and the conjugate one

$$L^+ \equiv uT$$

for the upper belt. With these corrections, the method of gait definition based on track patterns is analogous to the configurational approach, excepting the fact that the former technique uses normalization to the step length. This means that characteristic quantities in the trace gaits are the following simple relations

$$\frac{a_-}{L^-} \equiv \frac{a_-}{vT}\,, \qquad \frac{a_+}{L^+} \equiv \frac{a_+}{uT}\,,$$

while the double ratio (see Ref. [58]) serves as the trace criterion of the gait:

$$\mathsf{Tr} \equiv \frac{a_-/L^-}{a_+/L^+} = \frac{(w+v)/(w-u)}{v/u}\,. \tag{2.70}$$

At first sight, the trace-related criterion Tr is, in principle, indistinguishable from the configurational criterion Co. However, it implies a new possibility and, perhaps, expediency of projective invariance of gait criteria. Indeed, it is easy to discern the wurf structure in the double ratio above. This structure is even more distinct if an additional constant velocity c_0 is introduced, leading to a new projective criterion

$$\mathsf{Pr} \equiv \frac{(v+c_0)/(v+w)}{(u-c_0)/(u-w)} = \mathsf{Pr}\,(c_0)\,. \tag{2.71}$$

Now, it is possible to fix different values of c_0 constant and thus choose from different previous criteria:

$$\mathsf{Pr}\,(0) = \mathsf{Tr}\,, \quad \mathsf{Pr}\,(\infty) = \mathsf{Co}\,.$$

It is concluded that configurational and trace gait metaphors allow for the generalized projective interpretation and, by analogy with special variants, the introduction of the general notion of projective gait satisfying the criterion $\mathsf{Pr} = \text{const}$.

2.6.5 General metachronal scheme. In the general case, if $2n$-pod locomotion is steady and coordinationally uniform, then the *locomotor cycle* (LC) serves as the basic motif for translational definition of the *target trajectory* (TT). In its turn, TT is the basic motif for translational definition of the *locomotor system* or, in other words, of the spatio-temporal 'crystal' containing locomotor kinematics of all legs.

It follows from the MW definition as Eqn (2.31) that $\mathbf{w} \equiv (\varphi, d)'$ is the translation vector of TT for one row of ipsilateral legs. In this case, the initial TT events are aligned along the straight line $\boldsymbol{W}$ which is a formal graphic image of MW.

If both the TT parameters and the spatial shift d are fixed, the potential variability of metachronal delay φ is restricted by values φ_- and φ_+ (Fig. 7g). The TTs do not intersect, and there are no collisions of adjacent legs, when the time interval of kinematic safety $\varphi \in [\varphi_-, \varphi_+]$.

Note 2.11. The existence of 'overlapping' tracks emphasizes the importance of the topical problem of collision of fore- and hindlimbs in tetrapods. This problem has a structural solution: the track of tetrapod hindlimbs is wider than that of forelimbs. In hexapods, the tracks of leg pairs relevant to different body segments are also of different width (Fig. 7a, b). But in myriapods, in particular, *Scolopendra* [26] and *Julus* [56], all leg pairs of different girdles leave similarly spaced tracks (Fig. 7c). This probably explains why the prevention of adjacent leg collision in myriapods is achieved by kinematic means.

Cophasal TTs being consistent with a zero delay $\varphi = 0$ and infinite MW velocity $w = \infty$, the use of gait velocity criteria of the type (2.71) dictates the necessity to distinguish two MWs, positive and negative, which are defined by two velocity intervals of kinematic safety:

$$\boldsymbol{W}_-\colon\ w \in (-\infty, -v]\,, \qquad \boldsymbol{W}_+\colon\ w \in [u, \infty)\,. \tag{2.72}$$

In the graphic spatio-temporal representation, the 'step-to-step' rule (2.65) manifests itself in that the support TT portions of one wave set are incidental to the same support trace straight line $\boldsymbol{W}_-$ (Fig. 7h) which has the negative slope $-v$ in LRS. In other words, the support portions of TT are 'glued' in space-time, while the adjacent feet are standing at one trace point.

The graphic sign of the 'stroke-by-stroke' rule is described in a similar way, i.e. TT portions corresponding to the swing phase of the adjacent legs are incidental to one space-time straight line $\boldsymbol{W}_+$ (Fig. 7h). In other words, the swing portions of TTs are also glued in space-time.

2.6.6 Relative metachrony principle. Let us consider the TT of a single n-pod row, with individual TT $\boldsymbol{Z}_j$ numbered from tail to head ($j = 1, \ldots, n$). It can be seen from Fig. 7g that the first TT $\boldsymbol{Z}_1$ is associated with a trace string network which can be related to the *trajectory reference system* (TRS). For clarity, Fig. 7g shows basis TRS vectors as TT segments:

$$\begin{aligned} \mathbf{b}_1 &= (-T_-, L_-)' = -T_-(1, -v)'\,, \\ \mathbf{b}_2 &= (T_+, L_-)' = L_-(u^{-1}, 1)'\,, \end{aligned} \tag{2.73}$$

but the way to more completely defined **B**-basis remains to be found (see below).

In relation to TRS, the gaits (2.65) are characterized in canonical terms, with MW being coincident with one of the two TRS axes. These extreme cases are generalized by a 'rigorous' connection between MW and TRS axes, being manifested as:

The relative metachrony principle (RMP). The MW velocity is unvaried relative to TRS. This means that relativistic gaits are consistent with such a law governing variation of MW velocity with a change of locomotion speed, at which the MW trajectory has constant slope in TRS.

Let a certain event **y** incidental to MW be distinguished in LRS and **z** be an equivalent event in TRS:

$$\mathbf{y} = \mathbf{B}\mathbf{z} \;\Leftarrow\; \mathbf{y} = \tau(1, w)'\,, \qquad \mathbf{z} = \theta(1, \omega)'\,.$$

The slopes of base axes are given by TT, $v_1 = -v$, $v_2 = u$, while scale characteristics of the **B**-basis are assumed to be arbitrary:

$$\mathbf{B} \equiv (\mathbf{b}_1, \mathbf{b}_2) = \left(\tau_{\mathrm{b}}(1, -v)',\, y_{\mathrm{b}}(u^{-1}, 1)'\right). \tag{2.74}$$

Let us introduce a scale (gauge) velocity $v_{\mathrm{b}} \equiv y_{\mathrm{b}}/\tau_{\mathrm{b}}$ and formulas for direct and inverse *linear-fractional transformations* (LFT) of MW velocity values, which immediately ensue from the linear transformation (2.74):

$$w = \frac{\omega v_{\mathrm{b}} + v}{1 + \omega v_{\mathrm{b}}/u} \;\Leftrightarrow\; \omega = \frac{v_{\mathrm{b}}^{-1}(w+v)}{1 - w/u}\,.$$

Comparison of the second expression with Eqn (2.71) indicates that the RMP-constant ω may serve as a Pr-criterion if the gauge velocity equals

$$v_{\mathrm{b}} = \frac{v + c_0}{1 - c_0/u}\,.$$

Consequently, the RMP is compatible with the above definitions of configurational and trace gaits, which is what we are expecting.

Thus, the theoretical analysis of different versions of a unified explanation concerning the existence of phase-conjugate gaits (2.65) leads to the following conclusion:

the diversity of locomotor coordinations submits to the general principle of projective correspondence of three velocities $\{v, u, w\}$*, namely, the velocity of locomotion, the swing velocity, and the velocity of metachrony*.

The analytical formula of this conclusion may be the double ratio (2.71), i.e. the projective invariant (wurf) of the following general form

$$PI\colon\ \mathbf{w}(-v, u; w, c_0) = s_0\,. \tag{2.75}$$

The previous conceptual reasoning was intended to satisfy the boundary functional conditions (2.65) which impose certain restrictions on the form of functional dependences. In terms of the above criteria, each individual always realizes one and the same gait. Using (2.75) as the determining formula, any gait can be characterized by two constants, s_0 and c_0.

2.6.7 Three-wurf problem. Doubtless, one of the remarkable properties of the wurf (2.75) is that it *a priori* relates independent entities of locomotion control, namely, *locomotor cycle* (LC) and *metachronal wave* (MW) properties.

If the generalized formula (2.75) contains a fixed MW velocity $w = \text{const} = w_0$, the introduction of a new notation for the constants will result in a projective relationship between velocities v and u or the *structural invariant* described in the previous section [see Eqn (2.71)]:

$$SI\colon\ \mathbf{w}(-v, u, c_1, c_2) = q_0\,. \tag{2.76}$$

Alternative fixation of the swing velocity $u = \text{const} = u_0$ in formula (2.75) leads to the *wave invariant*

$$WI\colon\ \mathbf{w}(-v, w, c_1, c_2) = p_0 \tag{2.77}$$

compatible with the general condition (2.75).

It should be understood that, because invariants *SI* and *WI* are compatible with the projective condition *PI*, they can exist regardless of the initial assumptions concerning a constancy either metachronal velocity w or swing velocity u. The invariants *SI* and *WI* being postulated *a priori*, condition (2.75) may be regarded as a corollary to these postulates, expressing the constants in Eqn (2.75) via constants of the conditions (2.76) and (2.77):

$$c_0 = c_2\,, \qquad s_0 = \frac{q_0(p_0 - 1)}{p_0 - q_0}\,.$$

Therefore, RMP is equivalent to *WI* but allows the definition of the wurf constant p_0 to be improved, provided constants s_1, s_2, and ω are known.

2.6.8 Wave gaits in arthropods. The first objects of our locomotion research were myriapods of the genera *Julus* [56] and *Scolopendra* [26]. This made us abandon traditional methods developed largely for the investigation of quadrupedal gaits in favor of a wave description, using a $w(v)$ type dependence. Before demonstrating the efficiency of the wave approach for the description of tetrapod gaits, it is appropriate to consider the locomotion strategy of millipedes (*Julus*) and cockroaches.

The close resemblance between configurational properties of the *Julus* metachronal limb row and the 'stroke-by-stroke' gaits is readily apparent due to the short distance d between the adjacent ipsilateral legs and small metachronal lag φ (Fig. 7d). This similarity greatly facilitates both the observation and the measurement of MW propagation. For example, it appears possible to mark swing-zone boundaries in the course of frame-by-frame analysis of *Julus* locomotion and use this graphic approach to reconstruct space-time tracks of phase zone movements in order to explicitly measure MW velocities. The sketches thus obtained were used in Ref. [56] to relate MW velocities w to the speed of locomotion v. If the notion of wavelength $\lambda_w \equiv wT$ is additionally introduced as well as the notion of its phase components, i.e. $\lambda_\pm \equiv wT_\pm$, these quantities can be approximately estimated on instantaneous photographs by counting the leg number in the support and swing zones. It is understandable that in a 'step-to-step' gait, the wavelength is identical to the stride length as wavelength components are to the stride length components:

$$\lambda_w = L \equiv L^-\,, \qquad \lambda_\pm \equiv L_\pm\,.$$

Whereas conjugate equalities hold for 'stroke-by-stroke' gaits, with

$$\lambda_+ \equiv uT_+ = L_-\,.$$

In studies [26, 56], we used a visual evaluation of wavelength components for the correction of frame-by-frame time-specific measurements on step phase durations.

Figure 8a, b shows the base synergies of the millipede *Julus sp*. It can be seen that the cycle synergy $L(T)$, cycle structure synergy $L_-(T_+)$, and velocity-dependent characteristic $u(v)$ resemble human walk analogues considered earlier in this paper. The approximation parameters for the

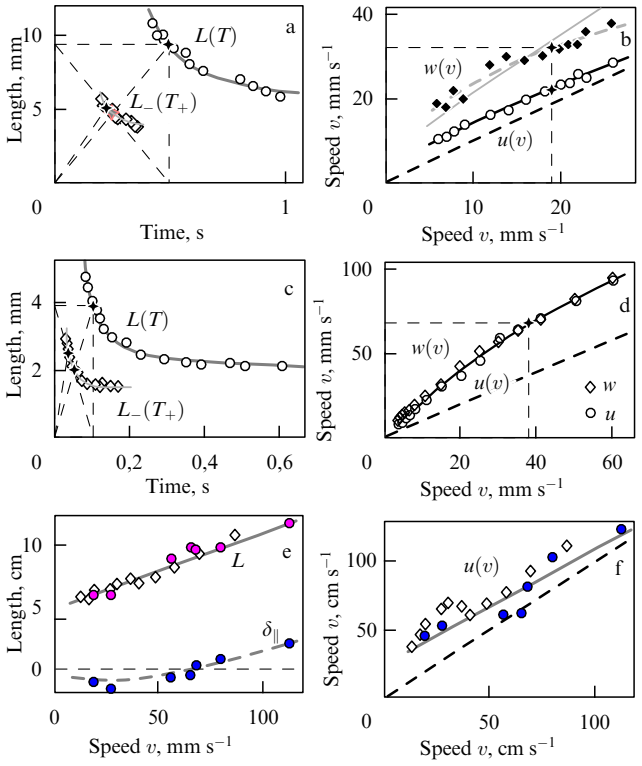

Figure 8. Examples of basic kinematic functions of millipede *Julus sp*. (a, b), cockroach *Periplaneta americana* (c,d), and plate-tailed gecko *Teratoscincus* (e, f).

dependences $L(T)$ and $u(v)$ in *Julus* are presented in Tables 3 and 6, respectively. An additional distinction of the 'synergetic portrait' of human locomotion consists in the appearance of a wave characteristic $w(v)$. In this case, the wave function $w(v)$ does not coincide with the velocity function $u(v)$ as it should be in a 'stroke-by-stroke' gait because the MW velocity is always approximately 1.5-times higher than the swing velocity: $w(v) \approx 1.5u(v)$.

Note 2.12. Special attention has been given to the examination of locomotor movements in decapitate *Julus* preparations (obtained by cutting neural pathways leading into suprapharyngeal ganglia) [29]. In these experiments, locomotor movements of a functionally restrained preparation were either elicited by electrical stimulation of abdominal ganglia or mimicked by means of mechanical stimulation, using a treadmill belt to displace legs. The study has shown that forced locomotion in *Julus* is characterized by kinematic synergies resembling those of normal locomotion.

Let us now turn to the synergetic portrait of cockroach running (Fig. 8c, d), based largely on the experimental data reported by Delcomyn [75]. Evidently, our theory fairly well describes these findings too (see Tables 3 and 6 for relevant approximation parameters). Of independent interest is the property of metachronal coordination in this portrait. Delcomyn criticizes Wilson's model of a constant metachronal delay [see Eqn (2.28)] and provides convincing evidence of a monotonic decrease of this delay with increasing velocity of locomotion. If the metachronal delay data contained in Ref. [75] are to be converted into information on the MW velocity $w \equiv d/\varphi$, knowledge of distance d between the support intervals (Fig. 7a) is indispensable.

Our estimating cinerecords of running locomotion in the cockroach (*Periplaneta americana*) provided a more accurate value of $d \approx 2.5$ cm, on the one hand, and confirmed the closeness of our kinematic measurements (delay φ and step phase duration) at low and moderate locomotion velocities to those of Delcomyn, on the other. Comparison of the resultant $u(v)$ and $w(v)$ plots (Fig. 8d) showed that $w(v) \approx u(v)$. This means that the 'stroke-by-stroke' strategy is realized throughout the entire velocity range of cockroach gaits.

2.6.9 Relay gaits in tetrapods. Generally speaking, the wave metaphor does not require a large number of ipsilateral limbs. When the principle of kinematic homogeneity is obeyed, the properties of wave coordination are determined in the same way for any pair of adjacent ipsilateral legs. Such an approach allows ipsilateral leg pairs in tetrapods to be considered as minimal fragments of the general wave scheme.

Since the publication of an album containing photographs of sequential locomotor postures of man and animals by E Muybridge in the late 19th century [85], many authors of comparative reviews and experimental studies have illustrated locomotor movements with a series of contour drawings based either on Muybridge's photos or their own cinematographic records (see Refs [15, 61, 76]). Muybridge himself was well aware that this approach was cumbersome and inconvenient. To make up for these drawbacks, he introduced the support pattern technique (see Section 2.3.4 above). The reconstruction of interlimb coordination properties from TT graphs is also underlain with the analysis of frame-by-frame sketches of horizontal positions of distal leg ends (as opposed to the whole object's contour). A distinguished record fragment is presented in the form of a *geochronogram* (GCG), i.e. a set of vertically aligned horizontal straight lines, each corresponding to a horizontal space RRS axis on which horizontal coordinates of distal leg ends are depicted by a series of points. The axial straight lines are drawn from bottom to top in ascending order of frame numbers, with a vertical shift Δt (interframe interval). A cinematographic record fragment being thus presented graphically, the GCG of an individual leg is a set of points with coordinates $x_i(j\Delta t)$, where i is the leg number, and j is the frame number. Evidently, since GCGs show discrete images of limb TT, their support phase portions are approximated by vertical straight line fragments, and portions corresponding to swing phases by oblique lines.

In experiments on a steppe tortoise ($H = 17$ cm, $d = 13$ cm), we managed to obtain records of its motion over a broad range of velocities. Frame-by-frame contour sketches obtained as described in the previous paragraph demonstrate that these animals use a *relay* gait, with contralateral legs being out of phase with each other (Fig. 9a). That is to say, the foreleg starts to be swung approximately from the place where the hindleg touches the ground and immediately after the latter stops.

It is clear that the new term 'relay gait' has been coined to denote a specific variant of the stroke-by-stroke gait of tetrapods because in this case the equality $w = u$ is essential.

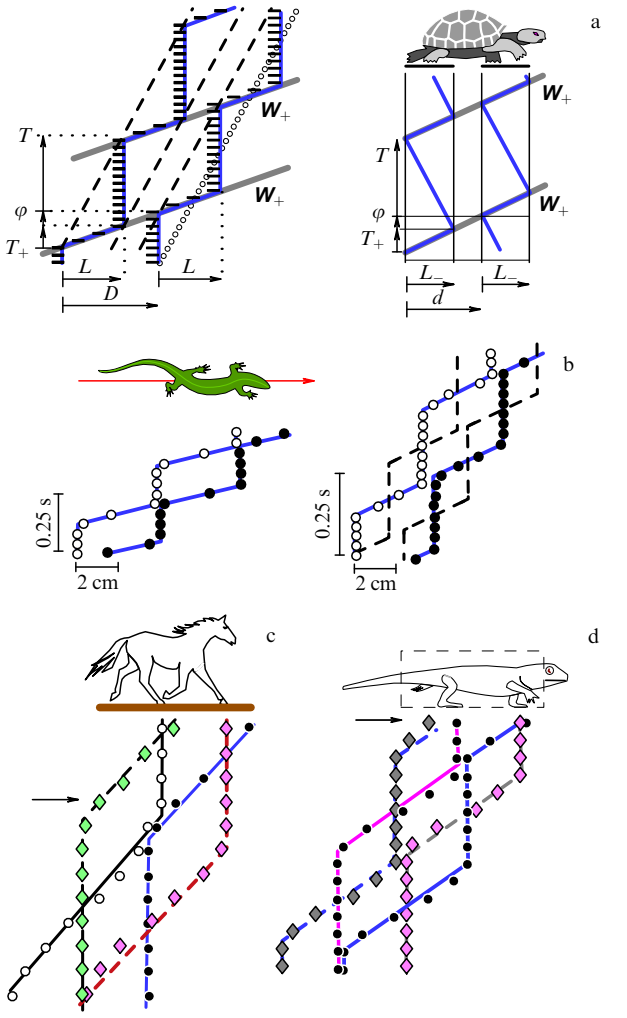

Figure 9. Geochronograms of relay gaits of a tortoise (a), lizard (b), horse (c), and gecko (d).

We have obtained a limited number of cinematographic records relevant to the gait of common lizards ($H = 9$ cm, $d = 2.9$ cm) collected near Moscow. Figure 9b presents two examples of ipsilateral TTs for two locomotion velocities, which suggest that lizards, similarly to tortoises, use the relay gait (their contralateral legs are also out of phase with each other).

Using the same approach, we have constructed GCGs of the horse's trot using contour drawings from the book of P P Gambaryan [15] (Fig. 9c). This figure also reveals a clear-cut tendency toward the relay coordination strategy.

Support diagrams of the dog's gait at 0.83 and 2.22 m s^{-1} in Ref. [7] indicate that it is also best described in terms of relay coordination. Our comparative study of walk kinematics in normal dogs prior to and after damage to the cerebellum [5] has likewise given evidence that such a lesion fails to affect the relay principle of gait organization.

In conclusion, it is worthwhile to discuss the results of reptilian locomotion studies reported by V B Sukhanov [61]. It can be shown that the relay coordination hypothesis allows us to bring into accord two sorts of data obtained independently by track analysis and chronogram-based technique. By way of example, we shall consider the data obtained in experiments on a gecko specimen having a total body length $H = 12.5$ cm and glenoacetobular length $h = 4.2$ cm. The plots of dependences $\delta(v)$ and $L(v)$ are presented in Fig. 8e. It can be seen that the step length increases linearly with increasing locomotion velocity, while the shift of sequential footprints $\delta(v)$ due to the placement of one ipsilateral leg slightly behind or ahead of the other monotonically grows near zero. Given that similar data for a number of geckos of an approximately equal size are available, it is possible to construct the general cycle synergy. Thereafter, the cycle structure parameters γ for different legs (Sukhanov calls the quantity $1/\gamma$ the 'working limb rhythm') are averaged and the swing velocities $u = v/\gamma$ for the points contributing to the cycle synergy graph are computed. This procedure allows the linear approximation $u = 34.5 + 0.83v$ to be used in subsequent descriptions (Fig. 8f).

However, data for the evaluation of MW velocities are lacking from Sukhanov's work. This author characterizes various gaits in terms of diagonal support duration $\varphi_{\mathrm{d}} \equiv T_{2\mathrm{D}-}$ rather than metachronal delay φ. Unfortunately, the quantity φ_{d} is of little value since the relationship between φ_{d} and φ is not varied in a one-to-one manner.

Another theoretical approach to the solution of the inverse gait reconstruction problem consists in the verification of the relay hypothesis, $w(v) = u(v)$. In this case, the calculation of $\varphi = d/u$ leads to the dependence

$$\delta = L - d - \varphi v = L - \left(1 + \frac{v}{u}\right) d$$

for a shift of ipsilateral trails, which fairly well approximates the experimental points (Fig. 8e).

Finally, the book by Sukhanov contains frame-by-frame contour sketches of locomotor postures of the gecko, which can be used to construct geochronograms (Fig. 9d) in support of the relay hypothesis.

2.7 System of locomotion synergies

Before summarizing the foregoing experimental and theoretical considerations, it is appropriate to discuss in brief general methodological questions.

2.7.1 Locomotor paradigms. In the beginning of this section, we mentioned the necessity of completing Marey's programme which initially had the primary objective to elucidate locomotion laws and was finalized by the author himself as far as the stroboscopic metaphor was concerned (see Section 2.3.3). Today, it is clear, however, that this metaphor was inadequate. The search for an adequate metaphor poses a special methodological problem which requires the adoption of an appropriate scientific paradigm to be resolved. In the foregoing sections, we have considered various locomotor metaphors by comparing different ways of the gait definition. Let us now consider different approaches to the elucidation of locomotion laws.

"We call a law a numerical relation between different phenomena. In this sense, there can yet be no well-defined physiological laws... and the meddling of mathematicians would be inopportune till experience and exploration of nature have brought precise observed data which can by itself serve as the starting point for computation. There is no doubting in the existence of numerical relations between vital phenomena, which would be discovered sooner or later, depending on the accuracy of methods adopted for research" [37].

It appears that Marey ascribed the possibility of experimentally discovering a biomechanical law solely to the accuracy of measuring techniques. Such a view is certainly correct, but it is incomplete. One should know, in addition, what and how to measure and for what purpose, too. Indeed, creative work in experimental science begins with answering these questions. It is directed by the conceptual question 'what for?', organized by the model question 'what?', and completed by the methodical questions 'how?'.

Marey started his experimental survey from the classification of various paces ('what for?') and reduced the problem to the description of stride phases relevant to different legs. This required measurement of the time moments at which the legs came in contact with the substrate during locomotions differing in pace patterns ('what?'). Marey's experimental genius led him to the development of podographic and other methods for keeping records of stepping movements. In other words, it prompted him to answer the questions of type 'how?'. In the framework of the pace classification metaphor, Marey successfully solved the problem of interest and created a 'synthetic model' described in the previous Section 2.3.3. However, the 'problem of laws' governing locomotor movements remained unresolved. To be precise, it was not even posed because no possible answers to the main question 'what for?' were offered.

Could Marey answer these questions? Doubtless not, in the context of the stroboscopic metaphor, because this metaphor ignored the problem of 'law-making' activity in 'animal organisms'. It took a century of development of biomechanics and a change of paradigms before such a possibility appeared. A fundamental contribution to the creation of the new biomechanical paradigm proceeding from the 'physiology of activity' concept was made by Bernshteĭn [10] who suggested a hierarchy of the levels of locomotory act control and distinguished a special level of generation of stereotyped locomotor patterns. Also, he coined the term 'synergy' to refer to locomotion control at this level.

The paradigmatic thinking is known to be a form of conceptual reasoning which relies on a certain basis set of semantic referents on which to base the model and the theory

of a given phenomenon. For this reason, a change of paradigms inevitably leads to a change of basic notions. The notion of synergy has become a new referent for the physiology of activity. This notion proved to be both essential and very fruitful. In recent years, it has been extensively exploited to develop a new line of scientific research (synergetics) understood, in general terms, as a science of cooperative phenomena in multicomponent systems.

It is worthwhile noting that a change of metaphors is either analogous to a change of paradigms or constitutes a special case of the latter, with the metaphor taken to mean a concrete model image of the phenomenon under consideration. When referent notions are preserved but the model of their relations changes, it appears more appropriate to speak about a change of metaphors. For example, the kinematic notions of locomotor movements have been borrowed from mechanics and can hardly change though the semantic model of their system organization can.

Our interpretation of the tasks of locomotor movement control as those of synergetic constructions designed to overcome redundant degrees of freedom of motor end organs and locomotory acts has led us to a comparative study of human locomotion regimes [27]. Our question 'what for?' implied the elucidation of the diversity of locomotion synergies, while the ensuing question 'what?' laid emphasis on the identification of spatial and temporal characteristics of locomotor cycles, i.e. interparametric relations constructed by the brain in the form of synergies. We were not actually faced with a separate question 'how?' because we largely used routine methods (with the exception of specialized monitoring of steady locomotion in test subjects). Our first experimental series (see Ref. [27]) had much in common with those of Marey barring the use of electric sensors, instead of pneumatic ones, to improve the accuracy of recording stride phase boundaries. In essence, we used the old method of Marey to solve a new (synergetic) problems. A change of metaphor in the kinematic experiments was prompted by a new understanding of the nature of locomotion laws.

2.7.2 Correspondence: synergy → invariant. Interestingly, Marey's definition of a law is analogous to the definition of synergy. Indeed, the term 'numerical relation' in this definition (see the last quotation) can be understood as a constant ratio, and 'different phenomena' as independent and given by quantitative information, i.e. by a certain set of quantities. Because the number of independent quantities defining a given phenomenon is actually the number of the degrees of freedom of this phenomenon, any constant ratio plays the role of a constant relation which reduces the number of independent quantities, namely, reduces the number of freedoms of the phenomenon's system organization. Taking these semantic modernizations into account leads to the following:

Definition 2.7. *The law of system organization* (of a phenomenon, object, motion, etc.) is designated a constant relation between independent characteristic quantities, which reduces the system's variability freedoms.

In the general case, concrete forms of the laws show an additional dependence on the specific properties of the system (structure, function or mode of control [55]) under study.

In the foregoing, we had an opportunity to examine the properties of variability of leg joint trajectory shapes in RRS and LRS (Fig. 1a, b), for instance, in the case of altered locomotion speed. Thereby, we were able to determine the synergies of such trajectory shapes. However, we chose not to dwell on this extensive subject in order to concentrate on other types of synergies which are directly related to the kinematic control of stepping movements, i.e. to kinematic locomotion laws.

Another distinctive feature of our locomotion research programme consists in that the aim of experimental examination of synergies is set as:

A 'discover the law' task. This task implies the elucidation of invariant functional relationships between independent locomotor cycle characteristics through the comparison of locomotion regimes.

Here, the invariance condition requires that the relation between all kinematic characteristics remain unaltered, firstly with respect to the natural variability of locomotor movements, associated, in particular, with a change of locomotion velocity v, and, secondly, with respect to the 'regime' variability at changing regime fixations and quantities being fixed. It is this artificial approach that enabled us to decouple two synergies: cycle synergy and cycle structure synergy.

Either such synergy is elementary, i.e. it reduces one parametric degree of freedom of the target trajectory. Such a mathematical specification of synergies allows their interpretation as locomotor diversity invariants of target trajectory shapes and consideration as locomotor cycle laws.

2.7.3 The problem of base synergies. The integrated motion of multilink limbs is generated with the contribution from many synergies of, so to say, different levels of control. This dictates the necessity of searching for criteria for the splitting of synergetic control levels. It appears that synergies must be differentiated and classified in terms of the number of relationships between independent variables and parameters that they form, i.e. by the number of reduced motion variability freedoms. In addition, elementary synergies, each reducing a single degree of freedom, should be distinguished.

When distinguishing basic characteristics (see Section 2.2.6), we are guided in the first place by mathematical criteria. However, it would be more in point to be based on the following:

Definition 2.8. *Base synergies* are designated functional relations between independent parameters of a locomotory act, formed by the controlling system, i.e. the brain, in order to ensure goal-oriented control — strategic, tactical, and operating.

This explains why all subsequent attempts to search for base synergies required additional semantic substantiations in the form of such notions as 'target and reference events', 'configurational gaits', and 'relative metachrony principle'.

We are sure that knowledge of biomechanical laws of animal and human locomotion is necessary to be acquainted with those mathematical problems which the brain has to solve when it forms motor synergies. Therefore, the elucidation of biomechanical laws being in essence an intermediate procedure in physiology of motor activity, it is nevertheless a very important operation which determines the direction of a subsequent search for adequate neurophysiological models.

2.7.4 New method — new system. The aforesaid interorganism generality of analytic representations of two synergies, CS and CSS, which can be interpreted geometrically as a *locomotor invariant system* (LIS), provides theoretical evi-

dence of the kinematic similarity of stepping locomotion in all walkers, both vertebrate and invertebrate. The LIS concept being developed in this paper differs from our earlier version (see Refs [27, 28, 30, 49, 59]) in a greater degree of mathematical generality.

An interregime property of the velocity characteristic $u(v)$ was first demonstrated in our work [27]. This empirical finding made us consider $u(v)$ as a *general invariant* (*GI*) of all the three kinematic walking regimes. In such a mathematical context, it is natural to refer to one of the additional conditions, e.g. the condition of period constancy, $T = \text{const}$, or stride length constancy, $L = \text{const}$, as a *concrete invariant* (*CI*) of IRW and IMW, respectively. The introduction of such a 'two-invariant' system for the definition of walking regimes was methodologically justified in the first place by the fact that the formal system approach 'by analogy' raised the problem of specification of an *a priori* unknown concrete invariant of NW.

However, the analogy was at that time sought not only in the subject matter content (the necessity of distinguishing a 'regime invariant') but also in the form (the necessity of searching for a quantity with a property of 'constancy' specific to just the NW regime). The quantity possessed of such a property was first found empirically as a product of swing duration and step length, i.e. $P_+ \equiv T_+ L$. It proved to remain more or less constant throughout the entire range of human walk velocities. For this reason, the first 'productive' LIS model of human walking (see Refs [27, 28]) was formally defined as

$$\text{LIS}\colon \{GI, CI\} \Leftarrow GI = \{u(v)\}\,, \quad CI = \{P_+ = \text{const}, T = \text{const}, L = \text{const}\}\,.$$

Here, *GI* has a monofunctional representation, whereas *CI* has to do with alternative polyfunctional (so to say, switching type) regimes in which the tactical control block can switch to the performance of several (in this case, three) regime-dependent functions. The presence of a special NW function $P_+ = \text{const}$ in this block inevitably led to functional discretization of the regime executive power over human locomotion.

The fixed sum method used in this study appears to be more adequate to the tasks of locomotion control because it offers a unified variant of *CI* specification based on the construction of *cycle synergy* (CS) as described above. The new LIS model in which the role of two invariants *GI* and *CI* is played by CS and CSS provides a formal definition of the new model

$$\text{LIS}\colon \{GI, CI\} = \{L(T), u(v)\}\,.$$

In the general case, this system is incomplete because it does not take into consideration the interlimb coordination properties, but it is sufficient for bipeds in which permanent features of contralateral phasings are taken into account default. When the leg number is $N \geqslant 4$, phase patterns of ipsilateral locomotor cycles need to be identified and characterized. Therefore, the complete LIS version in the case of an implicit condition of constancy and uniformity of contralateral phasings includes three invariants

$$\text{LIS}\colon \{CI, GI, WI\} = \{L(T), u(v), w(v)\}\,, \tag{2.78}$$

where *WI* is the wave invariant.

Rewriting the determining conditions of models (2.24) and (2.28) in the form of formula (2.78):

$$\text{LIS}_{\text{MM}}\colon \left\{L = \text{const}, u = \frac{v}{\gamma}\,, w = kv\right\},$$

$$\text{LIS}_{\text{WM}}\colon \left\{\frac{T_+}{T} + \frac{L_-}{L} = 1, u = \text{const}, w = \text{const}\right\},$$

leads to concrete LIS versions of *the Marey and Wilson models* (MM and WM, respectively) appropriate for comparison with the general model (2.78).

2.7.5 From myriapods to man. The generality of kinematic walking laws for arthropods and humans revealed in our comparative studies naturally provokes thought about the phylogenetic invariance mechanisms of just the kinematic control programmes by virtue of occurrence of substantial differences between mass-inertial properties of locomotor systems in invertebrate and vertebrate walkers. Locomotor movements are known to be highly automated synergies organized by common generating mechanisms. It is therefore possible, as a preliminary version, to assume that the simplicity of structural and functional realization of the locomotor cycle generator may account for phylogenetic universality of kinematic synergies.

Mathematicians (and not infrequently physicists) use the 'simplicity' criterion as a criterion of 'truth'. Mathematics is a linguistic science whose language has been developing in the context of solution of various problems amenable to mathematical formulation. Therefore, the heuristic principle of equivalence of 'simplicity and truth' can really serve as a criterion for the adequacy of 'language and problem'. On the other hand, just the physics oriented to learn laws of nature plays the role of a task-provider and therefore depends on linguistic adequacy. However, progress in physics depends not only on the development of adequate mathematical methods but also on the availability of adequate instruments which meet specific criteria of truth and hence simplicity. There is one more (third) criterion used in biomechanics; we call this adequacy criterion the *algorithmic* criterion. The brain controlling volitional and locomotor movements has its own criteria of 'simplicity'. The method of synergies appears to be one of the principle tools to achieve a 'simplicity' of control.

Myriapods and man occupy the extreme ends of the enormous range of pedal locomotor systems. Since these extremes 'meet' under the umbrella of a unified kinematic theory, there is every reason to assume fundamental generality of the control principles realized by neurophysiological mechanisms (simple variants of neurophysiological models have been described in Refs [49, 53]).

Former metaphors of locomotion synergies can be characterized as declarative, descriptive, and classifying; they contain intuitive and groundless qualitative rules the translation of which into quantitative language reveals their complete or partial inconsistence with the real locomotor laws. The new metaphor proposed by us can be characterized in a somewhat different way. On the one hand, it is a libernetic metaphor because its development proceeds from the specification of virtual freedoms attendant to kinematic diversity of target trajectories. On the other hand, it is a synergetically canonical metaphor because the aim of the theory is to reveal the entire stock of kinematic relations treated as locomotion

control synergies. We do not know yet how kinematic synergies are formed at the neurophysiological level, but we are in the course of understanding which kinds of mathematical problems the brain has to solve to ensure integrated organization of locomotor movements.

3. Chronometric postulates

Relativity theory belongs to the class of fundamental theories.
A Einstein

The locomotion geochronometry described in Section 2 is analogous to the well-known Minkowskian geometry even though the analogy is not immediately obvious. More general models of a special theory of relativity (STR) need to be first considered in order to elicit the similarity. In the present section, we shall use the postulate-based theoretical strategy of A Einstein to first generalize his *postulate of the constant speed of light* (PCSL) and examine the mathematical consequences of such generalization.

Our strategy for the construction of the generalized geochronometric model is based on the geometric method of specification of the *base invariant system* (BIS), described in the Appendix. In geometry, a free group of affine transformations is reduced with the aid of BIS to an 1-parametric group of metric transformations. It has been shown in Section 2 that in locomotion, the virtual diversity of motor coordinations is reduced, using the *locomotor invariant system* (LIS), to an 1-parametric diversity of locomotor realizations called locomotion *regime*. The kinematics of locomotor movements have to do with the space-time characteristics of motor acts. This explains why, from the formal point of view, the problem of LIS identification can be more explicitly interpreted as a BIS problem of that space-time geometry which is formed by the controlling system, i.e. the brain. Therefore, in the framework of this context, it is possible to speak about a definite brain geochronometry and formulate mathematical problems aimed at the description of locomotor movements as problems pertaining to the elucidation of metric properties of locomotion control geochronometry.

Formally speaking, the postulate-based strategy of A Einstein provides the possibility to declare the existence of such 'etalon waves' in the brain, the velocities of which have a property of invariance with respect to the varying locomotion speed. Such a declaration does not extend the sphere of STR action to the low-velocity region of locomotor movements; it only suggests the possibility of other wave processes analogous to the STR light wave in terms of independence of wave velocity from the speed of reference system movement. In this case, etalon wave velocities in the brain are consistent with nerve conduction velocities. That is to say, they are much lower than the speed of light. Such a way of formal interpretation of the *locomotor theory of relativity* (LTR) is analytically correct, but it does not facilitate understanding the neurophysiological nature of locomotor relativism. Therefore, we believe that the formal transition from relativistic mechanics to 'relativistic biomechanics' is irrelevant without the search for a common constructive basis. To avoid the confusion of different approaches, we choose to discuss constructive aspects of geochronometric procedures in Section 4 below.

To sum up, the results of biomechanical studies on kinematic synergies of stepping movements in animals and humans (to be precise, the results of attempts at theoretical spatio-temporal representation of step synergies rather than of experimental studies proper) dictate the necessity to revise the conceptual basis of STR, at least for the purpose of constructing the generalized geochronometric model.

On the whole, the task of generalizing the well-known Einstein version of STR can be solved regardless of the secondary objective of establishing its relationship with LTR. Such an independent approach used in our earlier work [54] is described below and supplemented by a short review of the known methods for the derivation of the Lorentz transformation.

3.1 Types of physical theories

Physicists are well aware that STR is very simple, even elementary, as far as its mathematical structure is concerned. At the same time, the understanding of its physical content is difficult, which gives rise to controversy and a clash of opinions [12, 18, 38, 42]. We believe that a source of these psychological difficulties lies in the declarative mode of STR construction which A Einstein called fundamental.

3.1.1 A Einstein's classification. H Poincaré's widely known refutation of the declarative method for constructing physical theories [42, 43] had no serious consequence. This does not mean that A Einstein, the main progenitor of the declarative or fundamental STR method, did not consider it to be the sole possible approach (see Ref. [69], pp. 247 – 248):

"In physics, a few types of theories are distinguished. Most of them are constructive, i.e. their objective is to build up a picture of complicated phenomena, proceeding from certain relatively simple propositions...

When we say that we understand this or that group of natural phenomena, it means that we have developed a constructive theory embracing the group of phenomena. Apart from this most important class of theories, there are other theories which we shall call fundamental. They use an analytical method instead of a synthetic one. The starting point and the basis of these theories are not hypothetical theses but empirically found general properties of phenomena and principles from which mathematically formulated criteria of universal applicability arise...

The advantages of constructive theories include completeness, flexibility, and lucidity; those of fundamental theories are their logical perfection and reliability of initial propositions. The theory of relativity belongs to the class of fundamental theories. To understand it, one needs to be acquainted with its fundamental principles."

By listing the advantages of each class of theories, A Einstein thus implicitly indicated the main drawback of the fundamental methodology he used in STR — it does not give the understanding of that 'group of natural phenomena' which it embraces. It follows from the above quotation that such understanding cannot be achieved without a constructive theory of relativism. In other words, the inverse thesis would be more to the point for all practical purposes, namely, the understanding of the nature of relativism is an indispensable prerequisite for building up a constructive theory.

It may be concluded that, although A Einstein realized the importance of further clarification of the nature of relativistic concepts and the advisability of transition from fundamental to constructive methodology, there was no experimental foundation for such a transition in his time. It was justly remarked by H Bondi [12] that a new impetus to the revision of relativistic concepts was given by the

progress in radar technology for estimating distances from time measurements.

3.1.2 Variants of generalization. A number of fundamental STR versions initiated by the first work of A Einstein are actually different variants of derivation of Lorentz transformations for the case of isotropic light propagation. We do not share the opinion of H Bondi [12] that knowledge and understanding of the Lorentz transformation is not necessary to understand STR. It will be shown that his approach is incomplete. Moreover, we would like to emphasize that knowledge of the traditional form of the Lorentz transformation is insufficient for understanding STR.

More general analogues of the Lorentz transformation are useful to better understand STR, in particular, those taking into account the anisotropic case of light propagation.

It may be argued that such generalization is not essential for the traditional aspects of practical STR application because real physical space is isotropic. However, generalization of STR is certainly indispensable in the comparative evaluation of procedures for testing light propagation anisotropy in other media.

Question 3.1. Is it possible to generalize STR without taking into account anisotropic light propagation?

It turns out that this question has a positive answer. In addition, it is possible to demonstrate the existence of one more aspect of STR generalization, arising from the anharmonicity of light beams and reference system axes.

In the forthcoming sections, we shall consider an algebraic scheme for the specification of STR invariants and introduce a generalized postulate taking into account not only anisotropic light propagation but also anharmonicity of light rays, in order to obtain a general model of SRT. However, before constructing generalized relativistic models, we deem it appropriate to compare the various methods used to derive Lorentz transformations and thus, on the one hand, to recall the history of development of major notions and, on the other hand, to introduce the necessary algebraic formalism using known examples.

3.2 Reference system algebra

This section is an auxiliary one. It is designed to characterize agreed opinions about the definition of base chronogeometric matrices.

3.2.1 2-dimensional world. Let a fixed standard of length be in the *absolute frame of reference* (AFR), and a mobile one in the *relative frame of reference* (RFR) which travels with respect to the AFR at a constant velocity $v < c$, where c is the speed of light. Moreover, either frame of reference (FR) must contain a fixed and free-going clock, respectively, i.e. an intrinsic time etalon. In this case, it is natural to initially postulate the following:

Condition of etalon inertial equivalence. In AFR and RFR, etalon rods are of the same length $l = 1$, and etalon clocks have equal periods $T = 1$.

However, an unsubstantiated postulate of such 'equality' is to no purpose unless certain procedural and other rules are indicated to support the validity of its length and time etalons.

It is convenient to divorce from the very beginning the problems of physical realizability of certain metric procedures from problems of their mathematical description and geometric representability. For example, the physical solution of the synchronization problem for differently located clocks is possible by different methods which saves us the trouble of repeating the descriptions of H Poincaré and A Einstein (see Refs [42, 43, 69]). Geometrically, this problem is resolved by setting axes of simultaneous events, i.e. straight lines parallel to the space axes of AFR and RFR. Then, the time axis of AFR is the world line of an 'absolutely fixed observer', while the time axis of RFR is the world line of a 'relatively fixed observer', that is one stationary in the RFR and moving with respect to AFR at the constant speed of the RFR's motion.

Note 3.1. It would be natural from the very beginning to consider relativistic problems in a 4-dimensional world (4-world). However, inertial movements are always 1-dimensional movements along a certain space straight line. Therefore, by taking such a straight line as the RFR axis, it is possible to save on writing unessential intercoordinate relations and initially narrow the geometric description to the 2-world, while attaining greater simplicity and better visualization without losing the necessary generality. Such planimetric narrowing is used below.

3.2.2 Base matrices. By analogy with the definitions of SFA and SMA (see Section 6.4), we shall assume that 2-world events in AFR give rise to a certain distinguished flat manifold of events $\mathbf{X} = \{\mathbf{x} = (t, x)' \,|\, \mathbf{E}\}$ containing the 'standpoint of a fixed observer', while 2-world events in RFR form another plane manifold of events $\mathbf{Y} = \{\mathbf{y} = (\tau, y)' \,|\, \mathbf{B}\}$, i.e. the world of the 'standpoints of a moving observer'. Events $\mathbf{x}$ and $\mathbf{y}$ of different FRs are referred to as *equivalent* if they are related by one of the conditions

$$\mathbf{x} = \mathbf{B}\mathbf{y} \Leftrightarrow \mathbf{y} = \mathbf{A}\mathbf{x}\,, \tag{3.1}$$

where $\mathbf{A}$ and $\mathbf{B}$ are mutually inverse RFR bases compatible with AFR: $\mathbf{B} = \mathbf{B}(v)$, $\mathbf{B}(0) = \mathbf{E}$.

The general formal description of RFR bases (3.1) is more convenient to represent kinematically, i.e. in polar coordinates. However, the Cartesian vectors $\mathbf{b}_1 = (t_1, x_1)'$ and $\mathbf{b}_2 = (t_2, x_2)'$ admit different variants of the choice of polar representations:

(1) both axes are assumed to be timelike: $\mathbf{b}_1 = t_1(1, v_1)'$, $\mathbf{b}_2 = t_2(1, v_2)'$;

(2) both axes are assumed to be spacelike: $\mathbf{b}_1 = x_1(1/v_1, 1)'$, $\mathbf{b}_2 = x_2(1/v_2, 1)'$;

(3) the first axis is assumed to be timelike, and the second one spacelike.

In the forthcoming discussion, variant (3) of kinematic definition of AFR and RFR bases is most frequently used (exception is made for the reviews of literature sources where the authors' mathematical notation is preserved if possible). With variant (3) (see Fig. 10a), etalon vectors of the time ($\mathbf{b}_1$) and space ($\mathbf{b}_2$) axes contain gauge coefficients t_b (of 'local time') and x_b ('of local distance'), velocity of travel $v_1 = v$, and parameter v_2 having the sense of velocity:

$$\mathbf{b}_1 = t_\mathrm{b}(1, v_1)' \equiv t_\mathrm{b}\mathbf{v}_1\,, \qquad \mathbf{b}_2 = x_\mathrm{b}\left(\frac{1}{v_2}\,,\, 1\right)' \equiv x_\mathrm{b}\mathbf{v}_2\,.$$

Therefore, in the general matrix definition of basis

$$\mathbf{B} \equiv (\mathbf{b}_1, \mathbf{b}_2) = \mathbf{V}[v_1, v_2]\,\mathbf{D}[t_\mathrm{b}, x_\mathrm{b}] \tag{3.2}$$

it is possible to distinguish matrices of two pairs of independent parameters having different physical content:

$$\mathbf{V}[v_1, v_2] \equiv \mathbf{E} + (v_1\mathbf{e}_2, v_2^{-1}\mathbf{e}_1)\,, \qquad \mathbf{D}[t_\mathrm{b}, x_\mathrm{b}] \equiv \mathrm{diag}(t_\mathrm{b}, x_\mathrm{b})\,.$$

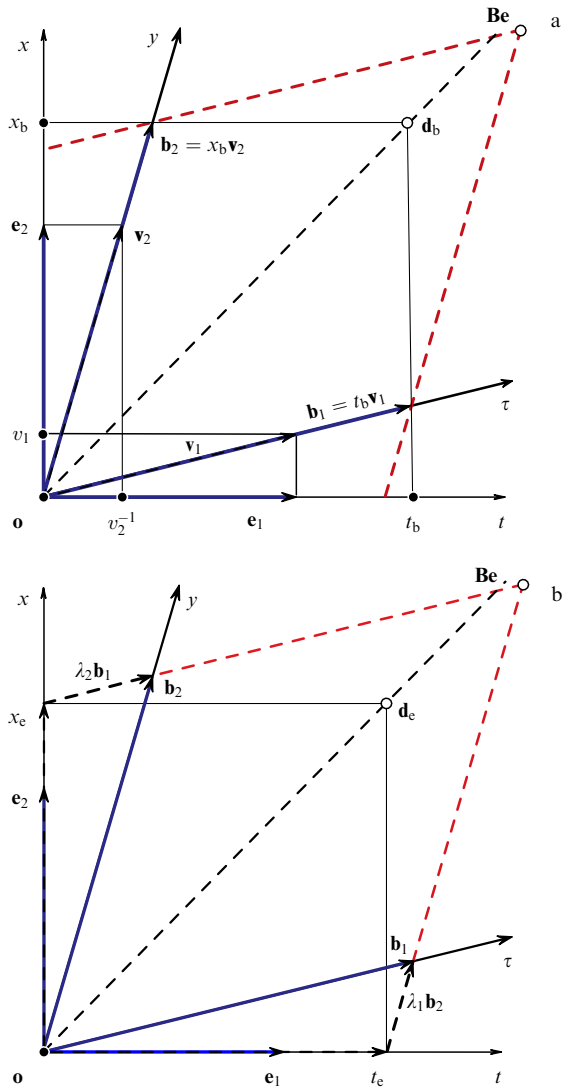

Figure 10. Definition of space-time bases in AFR and RFR: (a) canonical variant, (b) alternative variant of etalon choice.

Distinguishing events of intersection of RFR etalon boundaries with AFR axes, denoted as $t_e\mathbf{e}_1$ and $x_e\mathbf{e}_2$ (Fig. 10b), and solving equations

$$\mathbf{b}_1 = t_e\mathbf{e}_1 + \lambda_1\mathbf{b}_2\,, \qquad \mathbf{b}_2 = \lambda_2\mathbf{b}_1 + x_e\mathbf{e}_2$$

with undetermined multipliers λ_1 and λ_2 brings about $\lambda_1 = v_1/v_b$, $\lambda_2 = v_b/v_2$ and the base matrix

$$\mathbf{B} = |\mathbf{V}|^{-1}\mathbf{D}[t_e, x_e]\,\mathbf{V}\left[\frac{v_1}{v_e}\,, \frac{v_2}{v_e}\right], \tag{3.3}$$

where $v_e \equiv x_e/t_e = v_b \equiv x_b/t_b$. In other words, the gauge velocities are equal, the same as the ratios $t_e/t_b = x_e/x_b = 1 - v_1/v_2 \equiv |\mathbf{V}|$ os scale quantities.

3.2.3 Basis functions. If a certain RFR is given and only its velocity v with respect to the AFR is known, it is understandable that such minimal information allows identification of only the 'angle' of the local time axis, $v_1 = v$, in the description of the **B**-basis. The entire base triple of RFR parameters $\{t_b, x_b, v_2\}$ remains undefined, i.e. free. This means that the libernetic reserve for extension of the definition of RFR is three: $\mathrm{lib}\,(\mathbf{B}) = 3$. In order to reduce the parametric indefiniteness of an arbitrary RFR, it is necessary to use a principle or a postulate, or to proceed from the properties of instrumental procedures.

Therefore, the principle- or postulate-based analytical reconstruction of RFR can be reduced to the identification of a set of three parameters $B = \{t_b, x_b, v_2\}$ defined as basis functions of the inertial velocity v_1, which satisfy conditions of compatibility with the AFR:

$$B = \big\{t_b(v), x_b(v), v_2(v)\,|\,v_1 = v;\ t_b(0) = x_b(0) = 1,\ v_2(0) = \infty\big\}. \tag{3.4}$$

Example 3.1. Let us distinguish basis functions (3.4) and matrix bases they define for three classical metric geometries:

$$\text{GG:}\quad B = \{1, 1, \infty\}\,, \qquad \mathbf{B}(v) = \mathbf{E} + v\mathbf{E}_{21}\,, \tag{3.5a}$$

$$\text{MG:}\quad B = \{\gamma_-, \gamma_-, v^{-1}\}\,, \qquad \mathbf{B}(v) = \gamma_-(\mathbf{E} + v\mathbf{I})\,, \tag{3.5b}$$

$$\text{EG:}\quad B = \{\gamma_+, \gamma_+, -v^{-1}\}\,, \qquad \mathbf{B}(v) = \gamma_+(\mathbf{E} + v\mathbf{J})\,, \tag{3.5c}$$

where $\gamma_\pm^2 = 1/(1 \pm v^2)$. Velocity v-parametrization has a physical sense in Galilean geometry (GG) and Minkowskian geometry (MG) but is not normally used in Euclidean geometry (EG) because the space-time version of the latter is lacking. When EG is defined for spatial coordinates:

$$t \to x_1\,, \quad x \to x_2 \Rightarrow \mathbf{x} \equiv (x_1, x_2)'\,,$$

parametrization in terms of velocity $v = x/t$ has the sense of projective parametrization, $v = x_2/x_1$.

Each of the three models, GG, MG, and EG, admits of an infinite number of parametrizations. It is worthwhile distinguishing *additive* parametrizations, when the multiplication of base matrices is equivalent to the summation of parameters:

$$\mathbf{B}(\alpha_1)\mathbf{B}(\alpha_2) = \mathbf{B}(\alpha_1 + \alpha_2)\,. \tag{3.6}$$

This condition implies the possibility of representing the basis in the form of a matrix exponent. Indeed, all 'good' geometries possess this property [see Eqns (6.8)–(6.10) in Appendix]. However, parametrization with respect to velocity is additive only in Galilean geometry. Therefore, it is possible to speak about 'summation of velocities' only in this geometry. ◆

3.3 Review of known methods

In this section, we compare different methods for the derivation of Lorentz transformations. Before passing to new generalized models of relativism, it is worth considering the merits and demerits of the methods which have stood 'the test of time'.

3.3.1 Procedural method of A Einstein. In his first work published in 1905 [42], A Einstein used the procedural method for the derivation of Lorentz transformations. The method included comparative analysis of elementary events of light reflection from the ends of fixed and moving etalon rods, and the events of return of the reflected beams. In other words, the events of light reflection and return gave rise to a pair of equivalent events necessary to find the RFR basis.

Einstein's procedure. 'A light ray is sent' from the common origin of AFR and RFR in the direction of motion,

to be reflected from the front ends of the rods and come back to the origin.

The test procedure in AFR is depicted in Fig. 11a by a forward light beam $\mathbf{c}_1 = t_1(1, c)'$ (from the initiation event $\mathbf{o}$ to the reflection event $\mathbf{x}_{10}$) and a backward light beam $\mathbf{c}_2 = t_2(1, -c)'$ (from the reflection event $\mathbf{x}_{10}$ to the return event $\mathbf{x}_{20}$). Test events $\mathbf{X}_0 = (\mathbf{x}_{10}, \mathbf{x}_{20})$ are formed with the participation of *boundary* conditions defined by the world lines of the front and back ends of the rod:

$$\boldsymbol{L}_0 : \ \mathbf{x} = t\mathbf{e}_1 , \qquad \boldsymbol{L}_1 : \ \mathbf{x} = t\mathbf{e}_1 + L_0\mathbf{e}_2 .$$

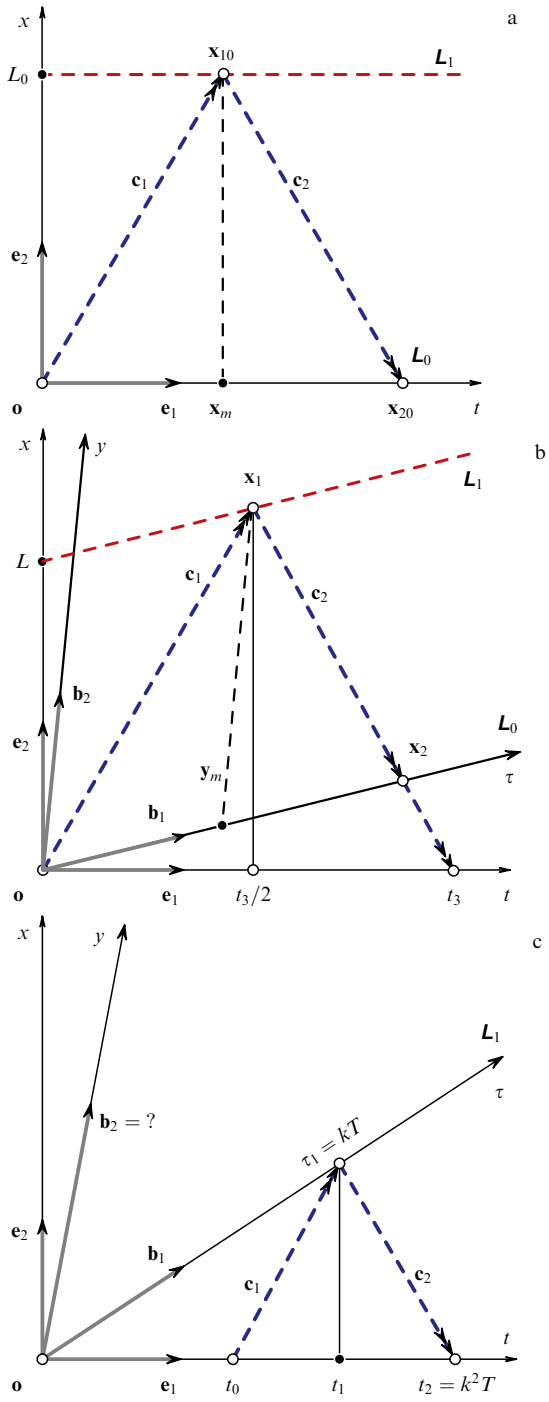

Figure 11. Ray triangles of test procedures of A Einstein (a, b), and H Bondi (c).

The boundary conditions being taken into account, we arrive at the equations

$$\mathbf{x}_{10} = (T_1, L_0)' = \mathbf{c}_1 = (t_1, ct_1)' ,$$
$$\mathbf{x}_{20} = (T_2, 0)' = \mathbf{c}_1 + \mathbf{c}_2 = \big(t_1 + t_2, (t_1 - t_2)c\big)' ,$$

from which the representation of test events in terms of the known quantities only can be found:

$$\mathbf{x}_{10} = \left(\frac{L_0}{c} , L_0\right)' , \qquad \mathbf{x}_{20} = \left(\frac{2L_0}{c} , 0\right)' .$$

In Fig. 11a illustrating this procedure, the forward and backward light beams form an 'isosceles' triangle $X_3^2 = \{\mathbf{o}, \mathbf{x}_{10}, \mathbf{x}_{20}\}$ the midbase of which is coincident with the reflection event. This property of the AFR test was assumed by A Einstein to be the general simultaneity criterion suitable for all inertial FRs.

For an observer in AFR, the main new property of the test performed in RFR is a change of boundary conditions which determine new parallel straight lines

$$\boldsymbol{L}_0 : \ \mathbf{x} = t\mathbf{v} , \qquad \boldsymbol{L}_1 : \ \mathbf{x} = t\mathbf{v} + L\mathbf{e}_2 ,$$

where $\mathbf{v} \equiv (1, v)'$ and L is the *a priori* unknown rod length determined (see Fig. 11b) from the point of intersection of the space ordinate and the straight line $\boldsymbol{L}_1$ (such an intersection can be tentatively interpreted as an 'instantaneous photograph' of a moving rod, taken at the initial instant of time in the AFR). Using the new boundary conditions

$$\mathbf{x}_1 = (T_1, L + cT_1)' = \mathbf{c}_1 = (t_1, ct_1)' ,$$
$$\mathbf{x}_2 = (T_2, vT_1)' = \mathbf{c}_1 + \mathbf{c}_2 = \big(t_1 + t_2, (t_1 - t_2)c\big)' ,$$

it is possible to identify new test events depending on the relative velocity of motion v:

$$\mathbf{x}_1 = L(c - v)^{-1}\mathbf{c} , \qquad \mathbf{x}_2 = 2\gamma^2 Lc^{-1}\mathbf{v} ,$$

where $\mathbf{c} \equiv (1, c)'$, and $\gamma^2 \equiv (1 - v^2/c^2)^{-1}$. PCSL is manifested in the fact that an observer in RFR considers his test to be identical with the AFR test (3.7), $\mathbf{Y} = \mathbf{X}_0 \equiv (\mathbf{x}_{10}, \mathbf{x}_{20})$, while an observer in AFR interprets matrix $\mathbf{Y}$ as matrix $\mathbf{X} \equiv (\mathbf{x}_1, \mathbf{x}_2) = \mathbf{BY}$; hence, one finds

$$\mathbf{B} \equiv \mathbf{XY}^{-1} = \rho\mathbf{L}(v; c) ,$$

where $\mathbf{L}(v; c) \equiv \gamma(\mathbf{E} + v(\mathbf{e}_2, c^{-2}\mathbf{e}_1))$ is the Lorentz matrix, and $\rho \equiv \gamma L/L_0$ is the additional multiplier containing an unknown scale parameter L.

A Einstein resolves the problem of supplementing a definition of the 'redundant' multiplier ρ based on the factor symmetry condition. According to this condition, the multipliers of the direct and inverse transformations must coincide ($\rho = \rho^{-1}$), which is feasible if $\rho = 1$. Then, the basis to be found

$$\mathbf{B}(v) = \mathbf{L}(v; c) , \qquad |\mathbf{B}| = 1 \tag{3.7}$$

is equivalent to the unimodular Lorentz transformation.

Therefore, the mathematical sense of elimination of a 'redundant' multiplier consists in obtaining the unimodular basis. An essential additional property of such a basis is that the scale quantities of length L and time T, apparent to an

observer in AFR (Fig. 11b), prove to be dependent on the RFR velocity:

$$\rho = 1 \Rightarrow L = Tc = \frac{L_0}{\gamma} \equiv L_0\left(1 - \frac{v^2}{c^2}\right)^{1/2}, \qquad (3.8)$$

while the relations between scale parameters in AFR and RFR, $L/T = L_0/T_0 = c$, ensue from formulas (3.3). It follows from formula (3.8) that length L and time T scale quantities decrease with increasing velocity v. These relationships are termed the *effects of relativistic shrinkage of length and time dilation*.

Note 3.2. In the works of H Lorentz [42, pp. 67–87] and H Poincaré [42, pp. 90–93], the initial equations of inter-coordinate transformations also contain an arbitrary multiplier (denoted in the cited works by the letter l) which is further considered to be a unit one by reason of necessary unimodularity.

Conclusion 3.1. The PCSL-based procedural method does not fully determine the RFR basis because a 'redundant' parameter ρ in the form of the common multiplier of Lorentz transformation remains unknown and requires additional considerations to be defined completely.

3.3.2 Invariant ray technique. In a review paper published in 1917 [69, pp. 223–227], Einstein no longer analyzed specific features of the procedural method. He used instead another postulate-based method for the derivation of Lorentz transformations, the so-called *invariant ray technique*.

In this technique, light beams C_1 and C_2 are supposed to emanate from the common origin of the AFR and RFR in the negative and positive directions. In accord with PCSL, these rays have equal ('invariant') velocities $\pm c$ in either FR. In other words, they are described by equations

$$C_1\colon\ x + ct = 0 \Leftrightarrow y + c\tau = 0\,,$$
$$C_2\colon\ x - ct = 0 \Leftrightarrow y - c\tau = 0\,.$$

This means that event $\mathbf{x} \equiv (t, x)'$ incidental to a beam in the AFR is converted, upon transition to the RFR, into an equivalent event $\mathbf{y} \equiv (\tau, y)'$ which remains incidental to the same beam. A Einstein expresses this property of *isotropic beam invariance* in the form of two equalities having two undetermined coefficients μ and λ:

$$x + ct = \mu(y + c\tau)\,, \qquad x - ct = \lambda(y - c\tau)\,. \qquad (3.9)$$

After an introduction of the matrix $\mathbf{C} = (-c\mathbf{Fe}, \mathbf{e})$, $\mathbf{D} = \mathrm{diag}\,(\mu, \lambda)$, these equalities are rewritten as

$$\mathbf{Cx} = \mathbf{DCy}\,.$$

Then, in agreement with the general definition of equivalence, we obtain

$$\mathbf{x} = \mathbf{By}\,, \qquad \mathbf{B} = \mathbf{C}^{-1}\mathbf{DC}\,.$$

Taking into consideration the kinematic representation of basis (3.2), the gauge parameters are found as

$$t_\mathrm{b} = x_\mathrm{b} = d_+ \equiv \frac{\lambda + \mu}{2}\,.$$

Subsequent simple transformations yield the matrix

$$\mathbf{B} = \rho\mathbf{L}(v; c) \Leftarrow \rho = \frac{d_+}{\gamma}\,.$$

In order to solve the problem of the 'redundant' multiplier, A Einstein introduced the 'instantaneous photograph' method analogous to the base representation (3.3) where gauge parameters are substituted by scale axis fragments. A fragment of length $x_\mathrm{e} = \rho\gamma$ is called the *instantaneous photograph* of the RFR etalon rod, taken by an observer in the AFR. However, if a similar 'photo' of the analogous AFR rod is taken by an observer in the RFR, the desired length is $y_\mathrm{e} = \gamma/\rho$. Now, the *relativity principle* is formulated as the equality among relative scales of the standards of length: $x_\mathrm{e} = y_\mathrm{e}$. Then, $\rho = 1$, i.e. the Lorentz basis is again obtained for RFR.

Conclusion 3.2. The invariant ray technique does not fully determine the RFR basis.

3.3.3 *k*-Coefficient method of H Bondi. The k-coefficient method was proposed by H Bondi [12] as an alternative way to expound the STR. It actually reflects one of the properties of Lorentz transformation and represents a variant of parametrization of the RRF timelike axis.

Let us consider the world line of inertial motion $L_1\colon x = vt$ and event $\mathbf{x}_0$ of the initial test signal (e.g. light) emission in AFR with a time delay T. Then, the event $\mathbf{x}_0 = T\mathbf{e}_1$ (Fig. 11b) is the initial point of the beam

$$C_1\colon\ \mathbf{x} = \mathbf{x}_0 + t(1, c)'\,,$$

which traverses the line L_1, on condition $v < c$, at the world point

$$\mathbf{x}_1 \equiv (t_1, x_1)' = C_1 \cap L_1\,.$$

In this case, the two determining conditions of AFR

$$\mathbf{x}_1 \in L_1 \Rightarrow x_1 = vt_1\,, \qquad \mathbf{x}_1 \in C_1 \Rightarrow x_1 = c(t_1 - T)$$

are used to explicitly calculate the time necessary for the test signal to reach the line L_1:

$$t_1 = \frac{T}{1 - v/c}\,. \qquad (3.10)$$

Question 3.2. How the equivalent time of this event in RFR can be determined?

To answer this question, H Bondi proposed using the following simple line of reasoning [12]. Let τ_1 be the desired time at the clock in RFR and $\tau_1 = kT$, where k is an unknown coefficient. If, in addition, the first incidence event is identical with the event of reflection, the backward signal will come back to the AFR origin at the instant of time $t_2 = k^2T$. However, taking into consideration the isotropic conditions of signal propagation and incidence/reflection time, t_1 can be expressed as one-half the sum of the emission time t_0 and recurrence time t_2:

$$t_1 = \frac{t_0 + t_2}{2} = \frac{(1 + k^2)T}{2}\,.$$

Comparison of this result with Eqn (3.10) allows the unknown coefficient to be expressed through the velocity ratio and vice versa:

$$k^2 = \frac{1 + v/c}{1 - v/c} \Leftrightarrow \frac{v}{c} = \frac{k^2 - 1}{k^2 + 1}\,.$$

Hence, the k-coefficient can be used instead of the velocity-dependent parameter to characterize inertial motion.

The etalon vector $\mathbf{b}_1 = (b_{11}, b_{21})'$ of the timelike RFR axis and the incidence/reflection event $\mathbf{x}_1$ are collinear: $\mathbf{x}_1 = kT\mathbf{b}_1$.

This allows, after simple transformations, k-parametrization of this etalon to be performed:

$$\mathbf{b}_1 = \left(\frac{k+k^{-1}}{2}\,,\ \frac{c(k-k^{-1})}{2}\right)'.$$

The introduction of additional α-parametrization opens the possibility to express the etalon vector $\mathbf{b}_1$ through hyperbolic functions of the α-angle :

$$k = \mathbf{e}^{\alpha} \Leftrightarrow \frac{v}{c} = \tanh\alpha \Leftrightarrow \mathbf{b}_1 = (\cosh\alpha, c\sinh\alpha)'.$$

Conclusion 3.3. The k-coefficient method may be used to fully reconstruct the time standard in the RFR but does not resolve the problem of the standard of length; additional ideas are necessary for the purpose.

3.3.4 Invariant quadratic form method. Examining the group properties of Lorentz transformation, H Poincaré distinguishes invariants of this group, the list of which includes, if dynamic problems are considered, different forms of coordinates and velocities (see Ref. [42, pp. 154–156]). However, the primary one is the hyperbolic-type quadratic form ('interval').

The inverse geometric approach of H Minkowski (see Ref. [42, pp. 167–180]) is based on the primary postulate of quadratic form invariance:

$$-t^2 + x^2 = -\tau^2 + y^2 \Rightarrow \mathbf{B}'\mathbf{F}\mathbf{B} = \mathbf{F}\,, \tag{3.11}$$

which ensures a hyperbolic metric of 'unified' space-time or the STR world. In this approach, the Lorentz group is a requisite consequence of invariance of the determining quadratic form (3.11) and the corresponding matrix equation (see A.33). Bearing in mind Minkowskian geometry consistent with this method and described in Appendix (see Section 6.8 and Fig. 18c), it is possible to draw the following:

Conclusion 3.4. The method of invariant quadratic form provides a complete definition of the base invariant system in the RFR.

3.4 Generalized models

The attitudes to various declarative methods for the construction of relativistic kinematics differ significantly. In recent years, some authors have criticized them, while others advocated their use. We think that each method described in the previous sections has its merits and demerits:

- the invariant quadratic form method allows us to directly obtain a complete BIS, hence the fundamental 'space-time unity' concept is framed;
- the procedural method and invariant ray technique provide a 2-stage approach: firstly, the Lorentz basis is determined to within an arbitrary common multiplier; secondly, the definition of the multiplier is extended with the basis unimodularity condition.

Comparison of different methods for the derivation of Lorentz basis has useful corollaries:

Corollary 3.1. *The conditions of common basis reduction, defined by PCSL and the physical principle of relativity (PPR), are procedurally independent and represent different invariants of an equivalent set of BIS*;

Corollary 3.2. *Because PPR is used for the reduction of a single 'redundant' parameter, PCSL implicitly substitutes two invariants, while PPR only one.*

Question 3.3. Which two BIS invariants are implicitly represented by PCSL?

The formulation of PCSL needs generalization if the answer to this question is to be of general character. Evidently, the first step to the generalization should consist in the introduction of anisotropy.

3.4.1 Anisotropic version. In the first method of Einstein and in Bondi's method, the property of isotropic propagation of the test signal is essentially used because the signal reflection time is assessed by dividing in half the total propagation time in the 'forward and backward' directions. An attempt to 'generalize' this method of evaluation of synchronous events to the anisotropic case encounters the question: how can it be done? A simple answer is obtained if two synchronous signals are sent in two different directions at a time, instead of sending one signal (to be subsequently reflected) in one direction. Then, in an isotropic situation, both signals simultaneously reach equally remote boundaries. In the anisotropic case, the distances must be set proportional to the propagation velocities of the signals to ensure that they reach their destinations at the same time. In the present section, we use the invariant ray technique as described by K Lanczos [36], in our modification for the anisotropic case.

Let the equivalent events $\mathbf{x}$ and $\mathbf{y}$, $\mathbf{x} = \mathbf{B}\mathbf{y}$, be incidental to the light rays emanating from the common origin of AFR and RFR. Then, in agreement with PCSL, one finds

$$x = c_i t \Leftrightarrow y = c_i\tau\,, \qquad i = 1, 2\,. \tag{3.12}$$

The substitution of definitions of coordinates x and t from the general base equivalence condition into the first equality (3.12) yields two equations for two rays

$$C_1\colon\ x = c_1 t \to b_{21}\tau + b_{22}y = c_1(b_{11}\tau + b_{12}y)\,,$$
$$C_2\colon\ x = c_2 t \to b_{21}\tau + b_{22}y = c_2(b_{11}\tau + b_{12}y)\,.$$

Taking into account the second equality (3.12) permits us to rewrite these equations in the 'coordinate-free' manner. At the same time, the introduction of matrices

$$\mathbf{C} \equiv (c_1\mathbf{e}_1 + c_2\mathbf{e}_2, -\mathbf{e})\,, \qquad \mathbf{D} = \operatorname{diag}(c_1, c_2)$$

makes it possible to represent the transformed scalar equations as

$$\mathbf{C}\mathbf{b}_1 = -\mathbf{D}\mathbf{C}\mathbf{b}_2 \Leftrightarrow \mathbf{b}_2 = \mathbf{A}\mathbf{b}_1\,, \qquad \mathbf{A} = -\mathbf{C}^{-1}\mathbf{D}^{-1}\mathbf{C}\,.$$

Hence, the base matrix $\mathbf{B}$ has the following structure

$$\mathbf{B} = (\mathbf{b}, \mathbf{A}\mathbf{b}) = t_{\mathrm{b}}(\mathbf{v}, \mathbf{A}\mathbf{v}) = t_{\mathrm{b}}(\mathbf{E} + v\mathbf{A})\,, \tag{3.13}$$

where $\mathbf{A} \equiv (\mathbf{e}_2, -(c_1c_2)^{-1}\mathbf{e}_1 - (c_1^{-1} + c_2^{-1})\mathbf{e}_2)$ is the matrix of linear relation of base vectors, and the base vector $\mathbf{b} = \mathbf{b}_1 \equiv t_{\mathrm{b}}(1, v)' = t_{\mathrm{b}}\mathbf{v}$ contains an arbitrary gauge parameter t_{b} the square of which is found from the unimodularity condition

$$t_{\mathrm{b}}^2 = \frac{1}{(1 - v/c_1)(1 - v/c_2)}\,.$$

With such a normalization, the etalons of base vectors $\mathbf{b}_1$ and $\mathbf{b}_2$ are represented in the forms

$$B_1\colon\ \left(t-\frac{x}{c_1}\right)\left(t-\frac{x}{c_2}\right)=1\,,\qquad B_2\colon\ (c_1t-x)(c_2t-x)=1\,, \tag{3.14}$$

while the axes correspondence condition (or orientational invariant) is

$$OI\colon\ \frac{v_2}{c_2}+\frac{c_1}{v_1}=1+\frac{c_1}{c_2}\,. \tag{3.15}$$

Conclusion 3.5. The invariant ray technique allows us to construct an anisotropic STR model and define a more general system of base invariants.

3.4.2 Generalized postulate. The initial invariant ray technique of Einstein [see Eqn (3.9)] involves only one constant c which characterizes the isotropic velocity of light. In the anisotropic modification of this method [see Eqn (3.12)], there are two constants, c_1 and c_2, giving speeds of light in different 1-dimensional directions. One more generalization of anisotropic relativistic kinematics containing four constants is feasible. Specifically, the speeds of light are represented by constants c_1 and c_2 in AFR, and by s_1 and s_2 in RFR. The physical advisability of taking into consideration such differences can be understood and explained only with the use of the constructive approach (see Section 4.1.3). Here, we simply declare (observing the rules of the fundamental approach):

The Generalized PCSL. In the AFR, light propagates in the negative and positive directions with different velocities c_1 and c_2. In all the RFR, other constant velocities are tested (s_1 and s_2, respectively).

Let us consider the relationship between two ray bases, an AFR ray basis

$$\mathbf{C}\equiv(\mathbf{c}_1,\mathbf{c}_2)=\mathbf{V}[c_1,c_2]\,\mathbf{D}[t_C,x_C]\equiv\mathbf{V}_C\mathbf{D}_C \tag{3.16}$$

and a ray basis $\mathbf{S}$ defined with respect to the RFR basis (3.2) in the form

$$\mathbf{S}\equiv(\mathbf{s}_1,\mathbf{s}_2)=\mathbf{V}[s_1,s_2]\,\mathbf{D}[t_S,x_S]\equiv\mathbf{V}_S\mathbf{D}_S\,. \tag{3.17}$$

Thus, the task of defining the metric RFR basis $\mathbf{B}$ is reduced to the identification of two ray bases $\mathbf{C}$ and $\mathbf{S}$:

$$\mathbf{C}=\mathbf{BS}\ \Rightarrow\ \mathbf{B}=\mathbf{CS}^{-1}=\mathbf{V}_C\mathbf{D}\mathbf{V}_S^{-1}\,. \tag{3.18}$$

In this case, a common diagonal matrix is naturally distinguished as

$$\mathbf{D}\equiv\mathbf{D}_C\mathbf{D}_S^{-1}=\mathbf{D}\left[\frac{t_C}{t_S}\,,\frac{x_C}{x_S}\right]\equiv\mathbf{D}[d_1,d_2]\,. \tag{3.19}$$

Note 3.3. Let us list major variants of polar parametrizations of an arbitrary diagonal 2-matrix $\mathbf{D}\equiv\mathbf{D}[d_1,d_2]$. In all these variants, the 'length' parameter ρ is defined as a module of the product of elements or the 'norm' of determinant, $\rho^2=|d_1d_2|=\|\mathbf{D}\|$:

(1) $\lambda^2=\dfrac{d_2}{d_1}\quad\Rightarrow\ \mathbf{D}=\rho\mathbf{D}[\lambda^{-1},\lambda]\,;$

(2) $\lambda=\mathbf{e}^{\alpha}\quad\Rightarrow\ \mathbf{D}=\rho(\cosh\alpha\,\mathbf{E}+\sinh\alpha\,\mathbf{F})\,;$

(3) $\dfrac{v}{c}=\tanh\alpha\ \Rightarrow\ \mathbf{D}=\rho\gamma\left(\mathbf{E}+\dfrac{v}{c}\,\mathbf{F}\right),\qquad \gamma^{-2}\equiv1-\dfrac{v^2}{c^2}\,;$

(4) $\mathbf{e}^{\alpha}=\mathrm{w}(v,c_0,c_1,c_2)\,.$

Variant (1) is the analogue of Bondi's k-parametrization; with a wurf, variant (4) corresponds to Kleinian projective parametrization; variants (2) and (3) are regular variants of hyperbolic and kinematic parametrizations, respectively.

It is essential that in the general ray representation of the RFR basis (3.18) variable gauge parameters are contained only in the diagonal 2-matrix $\mathbf{D}$. Because gauge parameters of different ray bases enter matrix (3.19) in the form of ratios, explicit partition of their respective contributions is impossible. Therefore, we have proved:

The main STR theorem. *The RFR basis satisfying PCSL has two free parameters, elements of the diagonal matrix* $\mathbf{D}$*, so that*

$$\left\{\mathbf{B}(v_1,v_2,t_b,x_b)\,|\,\mathrm{PCSL}\right\}\ \Rightarrow\ \mathbf{B}=\mathbf{V}_C\mathbf{D}\mathbf{V}_S^{-1}\,. \tag{3.20}$$

Corollary 3.3. *The basis vectors of RFR* (3.20) *are linearly dependent*:

$$\mathbf{b}_2=\mathbf{A}\mathbf{b}_1\,,\qquad \mathbf{A}\equiv-\mathbf{V}_C\mathbf{D}[s_2,s_1]^{-1}\mathbf{V}_C^{-1}\,. \tag{3.21}$$

Proof. Let us distinguish, in the general description of basis vectors

$$\mathbf{b}_1=(1-q)^{-1}\left(d_1-\frac{d_2s_1}{c_2}\,,\,d_1c_1-d_2s_1\right)',$$

$$\mathbf{b}_2=(1-q)^{-1}\left(-\frac{d_1}{s_2}+\frac{d_2}{c_2}\,,\,d_2-\frac{d_1c_1}{s_2}\right)',$$

vector $\mathbf{d}\equiv(d_1,d_2)'$ and matrices $\mathbf{D}_1\equiv\mathbf{D}[1,-s_1]$, $\mathbf{D}_2\equiv\mathbf{D}[-s_2^{-1},1]$:

$$\mathbf{b}_1=|\mathbf{V}_S|^{-1}\mathbf{V}_C\mathbf{D}_1\mathbf{d}\,,\qquad \mathbf{b}_2=|\mathbf{V}_S|^{-1}\mathbf{V}_C\mathbf{D}_2\mathbf{d}\,. \tag{3.22}$$

The exclusion of vector $\mathbf{d}$ yields the linear relation of two base vectors: $\mathbf{b}_2=\mathbf{A}\mathbf{b}_1$. ◆

Corollary 3.4. *The PCSL geometry is the analogue of double number geometry*.

Proof. Let us introduce a hyperbolic parametrization (see Note 3.3) and distinguish the normalized basis

$$\mathbf{B}(\alpha)\mathbf{B}_0^{-1}\equiv\mathbf{X}\,,$$

where $\mathbf{B}_0\equiv\mathbf{B}(0)$. Then, the matrix

$$\mathbf{X}=\frac{\rho}{\rho_0}(\cosh\alpha\,\mathbf{E}+\sinh\alpha\,\mathbf{N}) \tag{3.23}$$

is the matrix representation of a double number $\mathbf{N}\equiv\mathbf{V}_C\mathbf{F}\mathbf{V}_C^{-1}$, $\mathbf{N}^2=\mathbf{E}$. ◆

3.4.3 New system of invariants. Let us rewrite Eqn (3.20) distinguishing the diagonal matrix

$$\mathbf{D}=\mathbf{V}_C^{-1}\mathbf{B}\mathbf{V}_S\,. \tag{3.24}$$

Setting nondiagonal components of the triple product equal to zero in the right-hand side, the two resultant interparametric relations can be represented in the form of two invariants, *the projective invariant* (*PI*) *and the gauge*

invariant (*CI*):

$$PI:\ \frac{(v_1-c_1)/(v_1-c_2)}{(v_2-c_1)/(v_2-c_2)}=\frac{s_1}{s_2}\,, \tag{3.25a}$$

$$CI:\ \frac{s_1v_\mathrm{b}+v_1-c_1}{s_2v_\mathrm{b}+v_1-c_2}=\frac{c_1s_1}{c_2s_2}\,, \tag{3.25b}$$

where $v_\mathrm{b}\equiv x_\mathrm{b}/t_\mathrm{b}$ is the gauge velocity. In accordance with the classical scheme, the transition to the one-parametric basis $\mathbf{B}(v)$ can be effected using a unimodular invariant

$$UI:\ |\mathbf{B}|\equiv t_\mathrm{b}x_\mathrm{b}\left(1-\frac{v_1}{v_2}\right)=1\,. \tag{3.26}$$

Therefore, the PCSL-based generalized version of STR can be characterized as the geometry of projective, gauge, and unimodular invariants:

$$\mathbf{B}(v)=\left\{\mathbf{B}(v_1,v_2,t_\mathrm{b},x_\mathrm{b})\,|\,PI,CI,UI\right\}. \tag{3.27}$$

Let us now compare a BIS variant of Minkowskian geometry (A.36) with the new BIS variant (3.27). It is readily apparent that the two specialized sets of invariants

$$\mathrm{BIS}_1=\{MI_1,MI_2,OI\},\qquad \mathrm{BIS}_2=\{PI,CI,UI\}$$

are different even though they define essentially similar geometries. The BIS_2 set contains no metric invariants, whereas the nonmetric invariant *OI* from BIS_1 is analogous to the projective invariant *PI*.

3.4.4 Ray basis. Let $\overline{\mathbf{B}}$ be the RFR basis assigned with respect to the ray basis $\mathbf{V}_\mathrm{C}$, i.e. $\mathbf{B}=\mathbf{V}_\mathrm{C}\overline{\mathbf{B}}$. Then, the general description of RFR in the ray basis is given by analogy with Eqn (3.2):

$$\overline{\mathbf{B}}\equiv(\bar{\mathbf{b}}_1,\bar{\mathbf{b}}_2)=\mathbf{V}[\bar{v}_1,\bar{v}_2]\,\mathbf{D}[\bar{t}_\mathrm{b},\bar{x}_\mathrm{b}]\,,$$

and the diagonal representation (3.24) is defined in the following way

$$\overline{\mathbf{B}}=\mathbf{V}_\mathrm{C}^{-1}\mathbf{B}=\mathbf{D}\mathbf{V}_\mathrm{S}\ \Rightarrow\ \mathbf{D}=\overline{\mathbf{B}}\mathbf{V}_\mathrm{S}^{-1}\,. \tag{3.28}$$

Hence, for the nondiagonal elements, there are equalities

$$\bar{v}_\mathrm{b}\equiv\frac{\bar{x}_\mathrm{b}}{\bar{t}_\mathrm{b}}=-\frac{\bar{v}_2}{s_2}=-\frac{\bar{v}_1}{s_1}\,.$$

In other words, the projective invariant double ratio (3.25a) in the ray basis is replaced by a simple ratio, and the formula of the gauge invariant (3.25b) is also simplified:

$$PI:\ \frac{\bar{v}_1}{\bar{v}_2}=\frac{s_1}{s_2}\,,\qquad CI:\ \bar{v}_\mathrm{b}=-\frac{\bar{v}_1}{s_1}\,. \tag{3.29}$$

Similarly, the relations between velocities specified in different bases are expressed as simple ratios

$$\bar{v}_1=\frac{v_1-c_1}{1-v_1/c_2}\,,\qquad \bar{v}_2=\frac{1-c_1/v_2}{v_2^{-1}-c_2^{-1}}\,, \tag{3.30}$$

while the diagonal elements of matrix $\mathbf{D}$ are defined as

$$d_1=\bar{t}_\mathrm{b}=\frac{t_\mathrm{b}(1-v_1/c_2)}{1-c_1/c_2}\,,\qquad d_2=\bar{x}_\mathrm{b}=\frac{x_\mathrm{b}(1-c_1/v_2)}{1-c_1/c_2}\,.$$

Note 3.4. RFR bases $\mathbf{B}$ and $\overline{\mathbf{B}}$ coincide in the case of 'exotic' degeneration of signal propagation anisotropy, when $c_1=0$ and $c_2=\infty$, because $\mathbf{V}_\mathrm{C}=\mathbf{V}[0,\infty]=\mathbf{E}$.

In common, invariants (3.29) show the linear relation between base vectors:

$$\bar{\mathbf{b}}_1=\mathbf{D}_\mathrm{S}\bar{\mathbf{b}}_2\,,\qquad \mathbf{D}_\mathrm{S}\equiv\mathbf{D}[s_2,s_1]\,. \tag{3.31}$$

This is an analogue of Corollary (3.3) in the ray basis [cf. Eqn (3.21)].

Note 3.5. Another variant of transition from wurf (3.25a) to the linear relation between base vectors is possible using the transformation (A.61). Comparison of the two variants reveals a quasi-involutive property of matrix $\mathbf{V}_\mathrm{C}\mathbf{F}$, as is readily apparent from the formula $(\mathbf{V}_\mathrm{C}\mathbf{F})^2=|\mathbf{V}_\mathrm{C}|\mathbf{E}$.

Conclusion 3.6. Two scalar invariants (3.25) and (3.29) (projective and gauge) can be represented by one vector condition of the linear relation between base vectors.

3.4.5 Harmonically isotropic world. The above-singled out projective invariant *PI*, i.e. wurf (see Section 6.13)

$$q\equiv\mathrm{w}(v_1,v_2;c_1,c_2)=\frac{s_1}{s_2}\,, \tag{3.32}$$

characterizes the relative positions of four straight lines which form a bundle of two line pairs. The first pair $B=\{v_1,v_2\}$ in the given order of velocity-specific arguments of wurf (3.32) shows evidence of being 'basic', and the second, $C=\{c_1,c_2\}$, is the 'ray' pair. In the general case, two main variants of the B and C relative location are conceivable [65]. Of physical interest is the negative wurf: if $q<0$, pairs B and C separate each other.

A harmonic case of negative wurf $q=-1$ is especially interesting.

From the physical point of view, the harmonicity is remarkable because

$$q=-1\ \Leftrightarrow\ s_1=s\,,\ s_2=-s\,. \tag{3.33}$$

In this case, the 'relative ether' is tested as isotropic, in accordance with Eqn (3.33), even if $c_1/c_2\neq1$ (i.e. if the 'absolute ether' is anisotropic).

A classical variant of STR is represented by the case of ether *harmonic isotropy*, when light propagates at the same speed c in all directions and in all FR:

$$c_1=s_1=c\,,\qquad c_2=s_2=-c\,. \tag{3.34}$$

Then, formulas of the projective and gauge invariants undergo further simplification to

$$PI:\ v_1v_2=c^2\,,\qquad CI:\ v_\mathrm{b}=1\,. \tag{3.35}$$

It is concluded that the formal use of generalized PCSL exposes:

The projective property of RFR in STR. RFR axes and light rays are in projective harmonic correspondence.

Coming back to the anisotropic version of the Lanczos method, it is easy to see that the derived nonmetric *OI* invariant (3.15) is also projective, but only in the case when $s_1=c_1,\ s_2=c_2$. PCSL invariants in this version can be presented as

$$PI:\ \mathrm{w}(v_1,v_2;c_1,c_2)=\frac{c_1}{c_2}\,,\qquad CI:\ v_\mathrm{b}=1-\left(\frac{1}{c_1}+\frac{1}{c_2}\right)v_1. \tag{3.36}$$

Here, generally speaking, the projective invariant is anharmonic: $q = c_1/c_2 \neq -1$, and this case can be referred to as *anharmonicity of anisotropy*.

The well-known review by W Pauli (see Ref. [41, pp. 44, 45]) lists groups of transformations of primary importance for physics. It contains an interesting comment on the projective group, relevant to the subject matter of our discussion:

"It played an important role in early research of mathematicians on non-Euclidean geometry. It is not so important for physicists."

Conclusion 3.7. Analysis of the system of generalized PCSL invariants demonstrates the importance of the projective group for relativistic kinematics.

4. Wave clock

> *When we say that we understand one or another group of natural phenomena, this means that we have built up a constructive theory embracing this group of phenomena.*
> A Einstein

The development of the constructive aspect requires a revision of the traditional clock concept which treats the clock as a 'black box' with a dial. If time-study in different inertial systems is based on etalon movements, e.g. using an optical chronometer (see below), then unification of this procedure allows a chronogeometry to be constructed proceeding from the property of a constant speed of light rather than from a postulate. Moreover, it can be shown that the choice of chronometer predetermines the choice of chronogeometry because the latter is not absolute as H Minkowski thought but relative (or procedure-dependent). The use of a chronometer in which sound, instead of light, plays the role of the etalon wave provides an acoustic model of Minkowski chronogeometry in which the absolute (limiting) velocity c is equal to the speed of sound in a given medium. It is therefore clear, from the standpoint of the constructive methodology, that the 'absolutism' (hence, 'fatalism') of the fundamental method is due to the simple fact that light and electromagnetic waves serve as the principal etalon wave in many physical space-time measurements.

Thus, the constructive theory of relativism does not affect the mathematical structure of the fundamental theory but changes the attitude to relativistic effects by facilitating the understanding of their measuring nature. In other words, our criticism of the fundamental approach implies the denial of the 'global space-time unity' concept declared by H Minkowski in favor of the constructive 'instrumental unity' concept. An essential aspect of such a change of paradigms consists in the possibility of considerably expanding the sphere of applicability of relativistic notions and concurrent increasing the diversity of chronogeometries.

4.1 Langevin's clock

Attempts to rewrite the fundamentals of STR undertaken by certain critically inclined physicists, such as H Bondi, are based on quite correct preconditions [12]:

"Any quantity in physics is defined by that method which is used to measure it. Therefore, time is what is measured with a clock. There is no reason to think that all clocks, regardless of their motion, will show one and the same time."

However, these preconditions have received no further constructive development (see above).

A broad view of the 'clock problem' and its paradoxes would require relativistic analysis of all known types of clocks, such as the sun-dial, sand-glass, clepsydra, as well as pendulum and atomic clocks. However, such comparative analysis is lacking in modern relativistic physics. This explains why the analysis of procedures for the coordination of clocks of different inertial observers is not based on a specific clock type but has to rely on declarations which are in essence consistent with Minkowskian geometry.

It may be argued that the lack of a relativistic theory of the mechanical clock is not a result of omission or neglect on the part of theorists. There is no doubt, however, that the reasons for the absence of such a theory are poorly understood. The thing is that the classical theories of the mechanical clock proceed from the laws of classical mechanics, invariant with respect to the Galilean transformation but not invariant with respect to the Lorentz transformations. It is easy to see considering the simple example of a mathematical pendulum or the even simpler one of a linear oscillator containing only a mass and an ideal spring.

Corollary 4.1. *There can be no universal relativistic theory of the clock. It is therefore irrelevant to speak about an 'arbitrary clock' in the relativistic context.*

We think that a relativistic theory is the theory of another, 'wave', clock, where the emphasis is laid on the propagation of that 'etalon wave' which is used for the purpose of measuring. Indeed, the descriptions of relativistic effects frequently mention special chronometers, e.g. Langevin's clock (see Refs [11, 38, 62]).

Langevin's clock. A one-meter hard rod on the ends of which a pair of mirrors are attached in a parallel arrangement. A light pulse 'ticks' between the mirrors and is alternately reflected (without absorption losses) on either of them.

Langevin's clock is actually a cyclic version of Einstein's chronometric procedure (see Section 3.3.1). For this reason, the 'run' of Langevin's clock must agree with either a fundamental or constructive relativistic theory.

Now, there is an opportunity for 'procedural inversion' of the theory, that is for using Langevin's clock both as a chronometer and a ruler, instead of introducing fundamental postulates. In other words, we may assume that all inertial observers use this device as a navigational aid to ascertain their position.

Question 4.1. What are the consequences of Langevin's clock's submission to Minkowski's chronogeometric laws?

It is evident that, with PCSL and the unimodularity condition accepted from the very beginning, Langevin's clock must be in concert with Minkowskian geometry. And what if Einstein's strategy and PCSL are disregarded from the outset?

Let us consider this opposite situation separately.

4.1.1 Ether hypothesis. When formulating generalized PCSL in a previous section, we did not insist on the expediency of accepting the ether hypothesis (see Section 3.4.2) because in the framework of the fundamental ('postulate-based') relativistic concept it is virtually unessential what is postulated, either an ether which maintains the constant speed of light or only the property of constant speed of light regardless of the ether. The kinematic character of STR allows the propagation of light (electromagnetic) waves to be considered apart from their physical aspects and to analyze the necessary and sufficient conditions for the existence of relativistic effects

from a purely geometric standpoint, as the invariant ray problem. It follows from the comparative review of theoretical methods in Section 3 that the postulate-based methodology predominates in exposition and revision of STR, while the first procedural method of A Einstein chiefly illustrates the possibility to obtain, with this 'experimental' approach, the same results (if we proceed therewith from PCSL) as with nonprocedural methods.

When passing to the constructive concept of relativism, we have no alternatives besides solely procedural methods for which the ether hypothesis is an indispensable component. Denying the primary declaration of PCSL, it is necessary to have a 'material' substitute. Let us partition the major ingredients of PCSL:

(P1) the speed of light is independent of the motion of the source;

(P2) the speed of light is independent of the motion of the detector.

It is proposition (P1) that is at the core of the ether hypothesis, ether being understood as a light-carrying medium. It reflects the materialistic orientation of the classical (nonrelativistic) scientific methodology of physicists who tried to overcome the metaphysical isolation of electromagnetic phenomena on the assumption that many other processes (perhaps with the exception of gravitation) have material carriers (heat, sound, nerve impulse, etc.). Generally speaking, the ether hypothesis looks very natural in the general physical context. But how it is treated is another matter.

Question 4.2. Is it necessary to refuse what it is possible not to refuse? or the best plan to be followed is to refuse what cannot be brought to light?

STR does not necessarily imply negation of the ether hypothesis. On the contrary, it may help to first understand the essence of proposition (P1) and thereafter decide whether the kinematic means are sufficient to 'enter' the ether's frame of reference. To be able to examine constructive options, we accept:

The ether hypothesis. *A homogeneous light-carrying medium does exist*.

Now, proposition (P1) may be interpreted as ensuing from the ether hypothesis. Let us see what other corollaries can be derived from this hypothesis.

4.1.2 Optical chronometer. Both Einstein's procedure and the method of Bondi use asymmetric variants of sending test signals. Meanwhile, it would be more to the point to directly introduce symmetric variants to be able to consider not the triangles of three events but the parallelograms of four events, matching AFR and RFR origins with the middle of the chronometer rod (see below). The advantages of such procedural symmetrization can be accounted for by a known theorem of projective geometry which states that four straight lines incidental to two diagonals and two sides of the parallelogram are in harmonic correspondence.

Corollary 4.2. *The fact of distinguishing a light-beam parallelogram provides direct geometric evidence of projective invariance of RFR bases*.

Had Einstein employed the symmetric variant of the test procedure, he would not have had to introduce an additional assumption that the axis of concurrent events passes through the center of the base of the test event triangle because the diagonals of a parallelogram are known to always intersect at midpoints.

It is desirable to modify the construction of Langevin's clock so that the light rays form a parallelogram, following a single act of emission.

Optical chronometer (OC). A rod as long as $2L_0$ has two mirrors attached to its ends and a pulsed light source and two detectors (two photoelements) in the middle. Each detector receives light pulses reflected on a homolateral arm. A new flash is generated when two reflected signals are recorded simultaneously.

The constructive approach differs from the fundamental one mainly in that it uses the ether hypothesis rather than PCSL as the initial determining condition, because this hypothesis contains the necessary information about velocities of light. In order to calculate OC clock periods, it is sufficient to know the boundary and initial conditions, i.e. the arm length L_0 and the moment $t = 0$ of generation of the first flash (δ-pulse of light).

The initial elementary act of light passage from the OC center to the equally remote mirrors and back forms a ray parallelogram (Fig. 12a, b)

$$\mathbf{P} \equiv \{\mathbf{o}, \mathbf{c}_1, \mathbf{c}_2, \mathbf{c}_1 + \mathbf{c}_2\}\,, \tag{4.1}$$

with vertices **o** (initiation event),

$$\mathbf{c}_1 \equiv (t_1, x_1)' = t_C(1, c_1)', \qquad \mathbf{c}_2 \equiv (t_2, x_2)' = x_C(c_2^{-1}, 1)'$$

(events of reflection from the back and front mirrors), and $\mathbf{c}_1 + \mathbf{c}_2$ (event of synchronous return).

AFR. In the case of isotropic ether ($c_2 = -c_1 = c$), as in Fig. 12a, the light reflection events are concurrent ($t_1 = t_2 = T_0$) and bilaterally symmetrical with respect to the time axis: $x_2 = -x_1 = L_0$. Therefore, the return event falls on the time axis of AFR at moment $2T_0$, while $\mathbf{c}_1 + \mathbf{c}_2 = (2T_0, 0)'$. In such a case, the ray parallelogram (4.1) has a rhombus shape.

In analogy to the foregoing [see Eqn (3.16)], we represent a pair of initial rays as a matrix

$$\mathbf{C} \equiv (\mathbf{c}_1, \mathbf{c}_2) \equiv \mathbf{V}_C \mathbf{D}_C \equiv \mathbf{V}[-c, c]\,\mathbf{D}[t_C, x_C]\,,$$

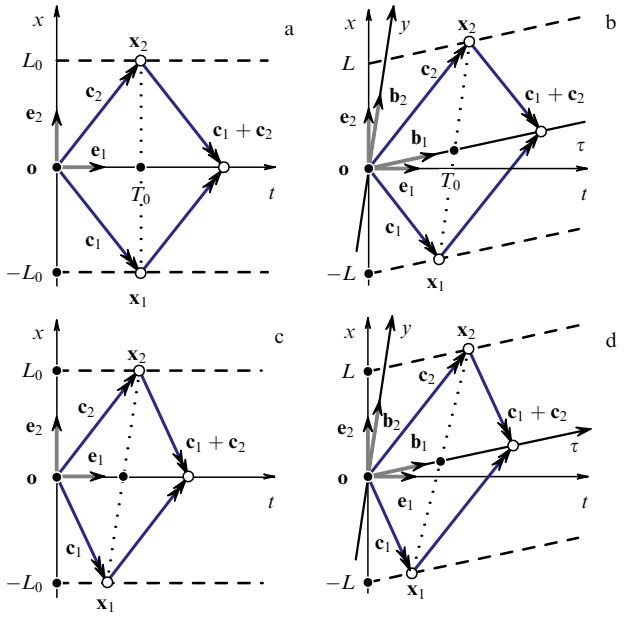

Figure 12. Ray parallelograms of the wave clock in AFR (a, c) and RFR (b, d) in isotropic (a, b) and anisotropic (c, d) media.

and the boundary conditions as a matrix

$$\mathbf{X} \equiv (\mathbf{x}_1, \mathbf{x}_2) = \big((t_1, -L_0)', (t_2, L_0)'\big) .$$

The solution of the boundary-value problem $\mathbf{C} = \mathbf{X}$ yields a gauge matrix $\mathbf{D}_C$:

$$\mathbf{C} = \mathbf{X} \Rightarrow \mathbf{D}_C = \mathrm{diag}\left(\frac{L_0}{c}, L_0\right) . \tag{4.2}$$

In this procedure, unlike that described previously [see Eqn (3.18)], the vectors of half-diagonals of the ray parallelogram first form a 'parallelogram basis' $\mathbf{P}_0 \equiv (\mathbf{p}_{10}, \mathbf{p}_{20})$ which is related to the ray basis in the simple way:

$$\mathbf{c}_1 \equiv \mathbf{p}_{10} - \mathbf{p}_{20} , \qquad \mathbf{c}_2 \equiv \mathbf{p}_{10} + \mathbf{p}_{20} \Rightarrow \mathbf{C} = \mathbf{P}_0\mathbf{S} ,$$

where an additional matrix

$$\mathbf{S} \equiv (\mathbf{s}_1, \mathbf{s}_2) = \mathbf{E} - \mathbf{J}$$

is, on the one hand, the algebraic operator of the additive relation between the ray and diagonal vectors but, on the other hand, we have

$$\mathbf{S} \equiv \mathbf{V}[-1, 1]\,\mathbf{D}[1, 1]$$

or the geometric basis of rays $\mathbf{C}$, defined with respect to the parallelogram basis.

This trivial situation is important for the introduction of matrix symbols because it is a typical one, with the following general cases being described in practically the same way. Simple calculations give

$$\mathbf{P}_0 = \mathbf{C}\mathbf{S}^{-1} = (T_0\mathbf{e}_1, L_0\mathbf{e}_2) , \tag{4.3}$$

where $T_0 = L_0/c$. Thus, in the given simplest case, basis $\mathbf{P}_0$ is collinear with the $\mathbf{E}$-basis of AFR.

RFR. Because the variant with OC placed in the RFR basis is described with respect to AFR, the beam trajectories remain the same, in agreement with the ether hypothesis (Fig. 12b). The altered boundary conditions are represented now by the matrix

$$\mathbf{X} = \big((t_1, -L + vt_1)', (t_2, L + vt_2)'\big) , \tag{4.4}$$

and the solution of a new boundary problem leads to a new gauge matrix

$$\mathbf{C} = \mathbf{X} \Rightarrow \mathbf{D}_C = \mathrm{diag}\left(\frac{L}{c+v}, \frac{L}{1 - v/c}\right) . \tag{4.5}$$

In AFR, an elementary act of light passage from the center of OC to equally remote mirrors and back forms a ray parallelogram which is described, using vector notation, by the above formula (4.1). However, the ray basis changes in agreement with Eqn (4.5). As a result, the parallelogram basis of RFR alters as well:

$$\mathbf{P} \equiv (\mathbf{p}_1, \mathbf{p}_2) = \mathbf{C}\mathbf{S}^{-1} . \tag{4.6}$$

It is worthwhile to note that to an observer in RFR having his own basis $\mathbf{B}$, $\mathbf{P}$ will appear as $\mathbf{P}_0$. The algebraic conversion of the 'RFR-observer's standpoint' into the 'AFR-observer's standpoint' is achieved by the simple substitution of the $\mathbf{B}$-basis for the $\mathbf{E}$-basis. Indeed, the replacement of vectors $\mathbf{e}_1$ and $\mathbf{e}_2$ in matrix (4.3) by vectors $\mathbf{b}_1$ and $\mathbf{b}_2$ provides the description of basis (4.6) with respect to basis $\mathbf{B}$:

$$\begin{aligned}\mathbf{P} &= (T_0\mathbf{b}_1, L_0\mathbf{b}_2) = (T_0\mathbf{B}\mathbf{e}_1, L_0\mathbf{B}\mathbf{e}_2) \\ &= \mathbf{B}(T_0\mathbf{e}_1, L_0\mathbf{e}_2) = \mathbf{B}\mathbf{P}_0 .\end{aligned} \tag{4.7}$$

Therefore, the RFR basis to be found is expressed through the parallelogram bases:

$$\mathbf{B} = \mathbf{P}\mathbf{P}_0^{-1} = \rho\mathbf{L}(v; c) , \tag{4.8}$$

where $\rho = \gamma L/L_0$ is the same 'redundant' multiplier that occurs in the fundamental version of STR as well, and $\mathbf{L}(v; c)$ is the basis of the Lorentz transformation [see Eqn (3.7)]. In other words, we have obtained the old formula by a new method. The most important aspect of this approach is that it does not require PCSL to be applied at the very beginning but is based on the ether hypothesis and symmetric construction of the optochronometer. It therefore provides the possibility of revising the 'space-time unity' problem.

Suppose that many independent inertial observers carry clocks, including personal OCs, which run variously because their constructions differ. Shall we then treat the OC as being essentially different from other types of clocks and the only device that shows 'true time'? We do not think so (see Conclusions).

Conclusion 4.1. Relativistic chronogeometry in a light-carrying medium is a consequence of the choice of the wave clock model.

4.1.3 Procedural isomorphism. The ray parallelogram technique provides an opportunity to visualize psychological problems arising from the transition to the anisotropic ether model. In the fundamental version of STR, these problems are inapparent only when the invariant ray technique is used. This explains why we took advantage of this method when making generalizations. In the construction version, however, procedural methods are most extensively used. Here, the difficulty of understanding is related to the parallelogram basis of AFR, the diagonals of which are not collinear with AFR axes. For this reason, the description of RFR poses the problem of the choice of the principle underlying the construction of the RFR basis. This problem can be resolved by generalizing the procedure for the coordination of the standpoints of different observers to the vector structure of parallelogram bases, described above in connection with the derivation of formula (4.8) from Eqn (4.6). Ray parallelogram is a version of test procedure designed to elucidate the chronogeometric properties of a wave clock. It is in this sense that we formulate the following:

Principle of procedural isomorphism (PPI). An arbitrary RFR is procedurally equivalent to AFR if the spatio-temporal description of the test is geometrically expressed as the replacement of AFR $\mathbf{E}$-basis by $\mathbf{B}$-basis of RFR.

The previous description of OC parallelogram bases through Eqn (4.1) contains vector and matrix formulas which are also valid for an anisotropic ether. The solution of the same boundary problems without an additional isotropy condition brings about

$$\mathbf{C} = \mathbf{X} \Rightarrow \mathbf{D}_C = \mathrm{diag}\left(\frac{L}{c_1 + v}, \frac{L}{1 - v/c_2}\right) . \tag{4.9}$$

Hence, for AFR (Fig. 12c) at $v = 0$, matrix $\mathbf{C}_0$ and matrix

$$\mathbf{P}_0 \equiv \mathbf{C}_0\mathbf{S}^{-1} = (t_+\mathbf{e}_1, t_-\mathbf{e}_1 + L_0\mathbf{e}_2)\,, \tag{4.10}$$

where

$$t_+ = \frac{t_2 + t_1}{2} = \frac{L_0}{c_+}\,, \qquad t_- = \frac{t_2 - t_1}{2} = \frac{L_0}{c_-}\,,$$

$$c_+^{-1} \equiv \frac{c_2^{-1} - c_1^{-1}}{2}\,, \qquad c_-^{-1} \equiv \frac{c_2^{-1} + c_1^{-1}}{2}\,,$$

can be found at first.

Thereafter, matrix $\mathbf{C}$ and matrix

$$\mathbf{P} = \mathbf{C}\mathbf{S}^{-1} = (t_+\mathbf{b}_1, t_-\mathbf{b}_1 + L_0\mathbf{b}_2) = \mathbf{B}\mathbf{P}_0 \tag{4.11}$$

are found for RFR, when $v \neq 0$ (Fig. 12d). Hence, the metric basis of an arbitrary RFR is given by

$$\mathbf{B} \equiv \mathbf{P}\mathbf{P}_0^{-1} = \rho\mathbf{P}_0\mathbf{H}(\alpha)\mathbf{P}_0^{-1}\,. \tag{4.12}$$

The RFR basis thus obtained is the analogue of the anisotropic version of the Lanczos method (see Section 3.4.1).

Conclusion 4.2. We have obtained a procedural-instrumental definition of chronogeometry which is identical to Minkowskian geometry under the unimodularity condition $\rho = 1$. To achieve this goal, we used the ether hypothesis for the determination of ray bases in AFR and RFR, and the principle of procedural isomorphism for the determination of the relationship between parallelogram and metric bases.

4.1.4 Acoustic chronometer. Neither the type of the wave source (e.g. light or sound) nor the type of the medium in which the waves travel (e.g. air, water, etc. for the sound) is actually essential for the described wave clock model (*optical chronometer*, OC). What is really needed is that each clock type associated with a specific wave variety be defined independently and the medium regarded as infinite. Such autonomy is crucial for understanding the necessity of a self-contained definition of wave chronogeometry.

The known contrapositions of physical properties of light and sound are possible only because acoustic wave properties can be investigated based on visual information or by using light and electromagnetic waves, the velocity of which is much higher than that of sound waves. The properties of electromagnetic waves can be characterized only by studying electromagnetic waves themselves. However, a conscious refusal to employ visual criteria and electromagnetic waves in a study of sound properties (that is, to admit the use of only acoustic instruments and techniques) inevitably leads to the concepts of acoustic relativism, specifically to the postulates of a constant speed of sound.

This approach is easier to understand based on the 'model of the development of blind mankind', that is humans enjoying all organs of sense besides vision. What kind of physics would we have in such a situation? Certainly, we would consider sound to be the fastest signal and use acoustic radars instead of modern electromagnetic sensors for the same purpose. In other words, we would use the same principle of spatial orientation to which the blind have to resort. But even for 'mankind with eyes to see', it is useful to have an idea of:

The acoustic chronometer (AC). The AC differs from OC in that it contains a pulsed sound source and acoustic baffles replacing mirrors; it also uses an acoustic medium instead of a 'light-carrying' one.

The AC theory will be described using the same formulas which have been derived above for OC, on the assumption that constants c_1 and c_2 are the velocities of sound for the anisotropic model.

Of course, it is not difficult, with the experience gained in visual studies, to design experiments for examining 'effects of entrainment of air'. For example, a pair of ACs can be placed inside and outside a moving railway carriage or aircraft, or 'ticks' of two ACs can be recorded in synchrony. In such cases, the experimenter knows *a priori* where and how the medium is entrained. However, such experiments performed in isolation fail to reveal 'air entrainment effects'.

It is important to understand that the effects of entrainment of the gas medium are immaterial for the internal geometry of relativism associated with a given type of etalon wave:

if one and the same velocity of the etalon wave is recorded in different RFRs moving relative to each other, it is unessential whether additional inertial movements of the medium due to the 'entrainment effect' occur or not.

Therefore, when the interface between the entrained and stationary media is impossible to create to keep records locally and simultaneously, it is likewise impossible to demonstrate the presence of a medium in kinematic experiments with a single type of etalon wave.

4.1.5 Mechanical chronometer. A formal transition from Minkowskian geometry to *Galilean geometry* (GG) is normally achieved as a limiting transition when the speed of isotropically propagating light infinitely increases. Indeed, if the 'constant speed of light' understood as a formal mathematical parameter grows infinitely, then the Lorentz matrix $\mathbf{L}(v; c)$ [see Eqn (3.7)] undergoes transformation to the Galilean matrix $\mathbf{G}(v)$:

$$\mathbf{L}(v; c)_{c\to\infty} \to \mathbf{G}(v) \equiv \mathbf{E} + v\mathbf{E}_{21}\,. \tag{4.13}$$

From the mathematical point of view, such a limiting transition looks faultless but physically it leads to the interpretation of GG as a chronogeometry of infinitely fast or instantaneous interactions. Proceeding from the physical postulate of the absence of instantaneous interactions, the limiting interpretation of GG (4.13) ranks it as a fictive model of spatio-temporal relationships.

We think it more relevant to define GG based on other characteristics of inertial movements unrelated directly to the wave properties of light propagation. In order to clarify an alternative concept, it is worthwhile to examine:

The mechanical chronometer (MC). A $2L_0$-long rod carries two 'machine guns' mounted on its middle part and firing at 'material points' in positive and negative directions. Ideally elastic screens are attached to the ends of the rod.

We confine ourselves to an isotropic version: the velocities of material points in AFR are $c_2 = -c_1 = c$. Using a test procedure analogous to that for OC, we obtain for a stationary MC version a similar 'ray' parallelogram or parallelogram of material point trajectories described by the matrix equality

$$\mathbf{C}_0 = \mathbf{P}_0\mathbf{S} \Leftarrow \mathbf{C}_0 = \mathbf{V}[-c, c]\,\mathbf{D}\left[\frac{L_0}{c}\,,\, L_0\right],\ \ \mathbf{P}_0 = \mathbf{D}\left[\frac{L_0}{c}\,,\, L_0\right].$$

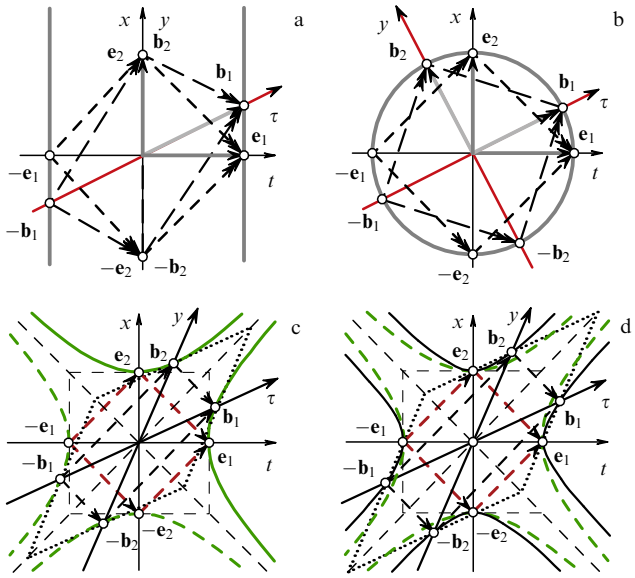

Figure 13. Ray models of Galilean (a), Euclidean (b), and Minkowskian (c) geometries, and the isorhythmometric version (d).

If the MC travels at a velocity v, the material point velocities in negative and positive directions can be determined in the usual way, following known mechanical laws (Fig. 13a):

$$c_1 = -c + v\,, \qquad c_2 = c + v\,. \tag{4.14}$$

Hence, the ray matrix takes the form

$$\mathbf{C} \equiv \mathbf{V}[c_1, c_2]\,\mathbf{D}[t_c, x_c] = \mathbf{V}[c_1, c_2]\,\mathbf{D}\left[\frac{L}{c}\,,\, L + \frac{Lv}{c}\right],$$

in which scale parameters are completely defined by the boundary conditions (4.4). Furthermore, by analogy with Eqn (4.8), the metric basis for RFR of MC is found as

$$\mathbf{B} = \mathbf{P}\mathbf{P}_0^{-1} = \mathbf{C}\mathbf{C}_0^{-1} = \frac{L}{L_0}\,\mathbf{G}(v)\,. \tag{4.15}$$

In other words, an assumption that the velocity of inertial motion has no effect on the MC rod length and the multiplier L/L_0 is unity in all RFR leads to $\mathbf{B} = \mathbf{G}(v)$ as the unimodular GG basis (4.11).

Conclusion 4.3. The definition of Galilean geometry can be obtained based on the wave-type chronometric procedure, using, however, 'corpuscular' rather than wave determining relations (4.14).

Note 4.1. The ray technique can also be employed for the formal definition of Euclidean geometry (Fig. 13b) by choosing the following ray matrix in the equation $\mathbf{C} = \mathbf{BS}$, where

$$\mathbf{C} = (\sin\alpha + \cos\alpha)\mathbf{E} + (\sin\alpha - \cos\alpha)\mathbf{J}\,,$$

and the matrix $\mathbf{S}$ retains the standard form $\mathbf{S} = \mathbf{E} - \mathbf{J}$.

4.1.6 Constant length postulate. In the previous descriptions of wave and corpuscular clocks, an *a priori* arbitrary rod length $L(v)$ has been chosen to be graphically identical with the length of an intercept on the AFR space axis distinguished by the world lines of the OC rod ends (Fig. 12b). When completing a definition of the Galilean basis (4.15), it was assumed that

$$L(v) = \text{const} \equiv L_0\,. \tag{4.16}$$

That is to say, we actually accepted the constant length postulate (CLP) for all RFRs and AFRs.

In the case of the OC, the 'arbitrary choice' of the length function $L(v)$ was associated with the choice of the value of a common multiplier ρ [see Eqns (4.8) and (4.12)] which was considered 'redundant' in Section 3 [see Eqn (3.8)]; in the isotropic variant, it was related to other parameters in the following way

$$\rho^2 = \frac{(L/L_0)^2}{1 - v^2/c^2} = \left(\frac{L}{L_0}\,\gamma\right)^2 = \left(\frac{L}{L_0}\cosh\alpha\right)^2. \tag{4.17}$$

The epithet 'redundant' appeared chiefly because unimodular Minkowskian geometry is consistent with the condition of disappearance of this multiplier:

$$\rho = 1 \;\Rightarrow\; L = \frac{L_0}{\gamma} = L_0\sqrt{1 - \frac{v^2}{c^2}} = \frac{L_0}{\cosh\alpha}\,. \tag{4.18}$$

This, however, gives rise to the relativistic effect of 'shrinkage of length' $L(v)$ with increasing velocity v of inertial motion. It appears from the ray scheme of Minkowskian geometry (Fig. 13c) that, in this case, ray parallelograms are tangential to hyperbolic etalons. For this reason, the lengths of axis segments cut by these tangents decrease with increasing velocity of RFR, in accord with Eqn (4.18).

Question 4.2. Is supplementing of a definition of the 'redundant' multiplier possible based on the constant length postulate?

Indeed, it is possible but such a description leads to a new chronogeometry with hyperbolic etalons and without length-shrinkage and time-dilation effects.

The choice of condition (4.16) instead of (4.18) gives, in agreement with Eqn (4.17), the relationship

$$L = L_0 \;\Rightarrow\; \rho = \left(1 - \frac{v^2}{c^2}\right)^{-1/2} = \cosh\alpha\,. \tag{4.19}$$

Then, the standard matrix of Lorentz basis or hyperbolic rotation acquires an additional multiplier:

$$\mathbf{B} = \rho\mathbf{L}(v; c) = \cosh\alpha\,\mathbf{H}(\alpha)\,,$$

which modifies the basis in the following way

$$\mathbf{B} = \cosh\alpha\,\mathbf{H}(\alpha) = (\cosh\alpha)^2\mathbf{E} + \cosh\alpha\sinh\alpha\,\mathbf{I}$$
$$= \frac{1}{2}\left(\mathbf{E} + \mathbf{H}(2\alpha)\right). \tag{4.20}$$

Taking into account that matrix $\mathbf{H}$ is the solution of the generating equation in Minkowskian geometry [see Eqns (A.33) and (3.11)], the following matrix equation can be written for basis (4.20):

$$(2\mathbf{B} - \mathbf{E})'\,\mathbf{F}(2\mathbf{B} - \mathbf{E}) = \mathbf{F}\,. \tag{4.21}$$

This is the generating equation of the isometric version.

It is easy to see that in this modification of Minkowskian geometry, the isometricity condition (4.19) ensures at the same time the isorhythmicity condition $T = T_0$, the two parameters being related [see Eqn (3.9)] by the condition $L/T = L_0/T_0 = c$. The graphical comparison of unimodular and isometric versions is given in Fig. 13d. Here, the sides of the ray parallelograms in isometric and isorhythmic versions are secants of hyperbolic etalons. When the RFR velocity changes, the sides of the parallelograms 'rotate' about basal points $\pm\mathbf{e}_1$ and $\pm\mathbf{e}_2$, which thereby represent fixed events of all RFRs.

Conclusion 4.4. Chronogeometry may satisfy PCSL in the absence of length-shrinkage and time-dilation effects and be defined in a generalized form by matrix equation (4.21).

4.2 Pascal's procedure

A common element of chronometers considered in previous sections was end mirrors or screens for the reflection of etalon signals which, being reflected, change the direction of motion (of a corpuscle) or propagation (of light and sound). Such clock construction may be referred to as the *mirror metaphor*: the mirrors in AFR and RFR are represented kinematically by straight lines parallel to the time axis, and ray parallelograms by two pairs of vertices. One pair corresponds therewith to the initial emission event and the final event of ray intersection, either being incidental to the time axis. The other pair corresponds to intermediate events of reflection from mirrors which, in an isotropic case, are interpreted as concurrent events determining the spacelike axis.

The chronogeometric interpretation of locomotor synergies proposed in Section 2 is inconsistent with the mirror metaphor and will be tentatively termed the *locomotor metaphor*. In this interpretation, reference events incidental to the support straight line (Figs 5d and 6h) are considered to be analogous to reflection events. Additional hypotheses of instrumental properties of the controlling brain system are needed to explain the formation of hyperbolic etalons of locomotion synergies (Fig. 6e–g).

4.2.1 Wave instrumentation of the brain. In the framework of the control theory well-developed for technological systems, stride invariants may also be explained in terms of feedback circuits. However, we believe the wave control hypothesis to be more adequate for the interpretation of distributed brain media since it allows new concepts of neurophysiological relativism to be generated. The speculative assimilation of this approach is naturally to begin based on the 'etalon wave' postulate. Prior to this, however, it is advantageous to reach an agreement, in an abstract form, on the relationship between external events (e.g. representing the target trajectory of limb motion) and internal processes in the central nervous system. The minimal coordination of real kinematic events and their virtual images requires two assumptions.

Target map hypothesis. *Distributed brain media generate a linearlike image of the limb target trajectory*.

Such a hypothesis allows the same parameters as before to be used (to within linear isomorphism) for the description of the intracentral target trajectory image. Also, it makes it possible to match limb and etalon wave space-time trajectories as kinematic brain map entities. Generally speaking, the brain may be supposed to contain two maps: the *body map* which plays the role of the AFR and is associated with the target trajectory image, and the *environmental map* serving as the RFR during locomotion. The existence of these maps has been confirmed in neurophysiological studies.

With this in mind, kinematic problems of locomotion control can be interpreted as that of the coordination of events on the two maps. Certainly, the problem of coordination of events on the body map and the map of the variable outer world is very important in the context of 'locomotor intellect'. The question arises, what neural instruments and mechanisms are involved in the solution of this problem?

Etalon wave hypothesis. *Measuring procedures for orderly brain map events are realized taking advantage of standard spreading processes, i.e. etalon waves generated by nerve cells*.

Estimates of constants c_1 and c_2 obtained in the descriptions of cycle structure synergy (see Tables 5 and 6) may be interpreted as etalon wave velocities involved in the formation of this synergy. Earlier, we considered the major quantitative characteristics of these velocities (see Section 2.5.2). In terms of unidirectionality, anisotropy, and anharmonicity, etalon waves of the *locomotor theory of relativity* (LTR) are different from their well-known physical analogue — etalon waves of STR.

By virtue of unusual properties of etalon waves, space-time diagrams of LTR are constructed differently from the analogous STR diagrams. Anisotropic and anharmonic versions of STR proposed earlier in this review served to prove the possibility of taking such modifications into account in the framework of the mirror metaphor. However, the property of unidirectionality of etalon waves is inconsistent with the chronometric technique based on this metaphor. New constructive approaches differing in principle from the existing ones are necessary if this property is to be taken into consideration.

4.2.2 Secondary ray reinitiation model. Figure 14a exemplifies a new diagram representing a kinematic-type algorithm for the construction of a target event of swing phase cessation $\mathbf{y}_+ \in \boldsymbol{Z}$ by means of a wave procedure which differs from both the Einstein procedure (Fig. 11a, b) and the OC ray parallelogram (Fig. 12a, b). Here, $\mathbf{o} \in \boldsymbol{Z}$ is a pacemaker event of initiation of two primary rays $\mathbf{c}_1$ and $\mathbf{c}_2$, for which the support portion of the conjugate trajectory $\boldsymbol{Z}^*$ serves as the boundary condition of secondary ray reinitiation ($\mathbf{r}_1$ and $\mathbf{r}_2$ are reinitiation events determined with respect to the point $\mathbf{c}_0$ where trajectories intersect). The secondary rays form a target event $\mathbf{y}_+ = \mathbf{c}_1 + \mathbf{c}_2$ coincident with the fourth vertex of the etalon wave ray parallelogram.

In the kinematic perspective, it is worth noting the projective properties of diagrams with unidirectional etalon waves (Fig. 14a), in which the support straight line has the projective sense of the so-called Pascal's straight line. Consideration of this simple mathematical fact is conducive to the understanding of how a hyperbolic space-time metric can be formed with the participation of etalon waves, based on measuring logical procedures. To further emphasize the projective nature of this diagram, it should be conveniently termed *Pascal's procedure* to distinguish it from the Einstein physical procedure which, from the mathematical point of view, is a modification of Pascal's procedure.

The latter procedure is elementary in the sense that it allows for a hyperbola to be graphically constructed only with the aid of a T-square. But it is this instrumental simplicity that is crucial for understanding the constructive nature of neurochronogeometry (where etalon waves play the role of a T-square).

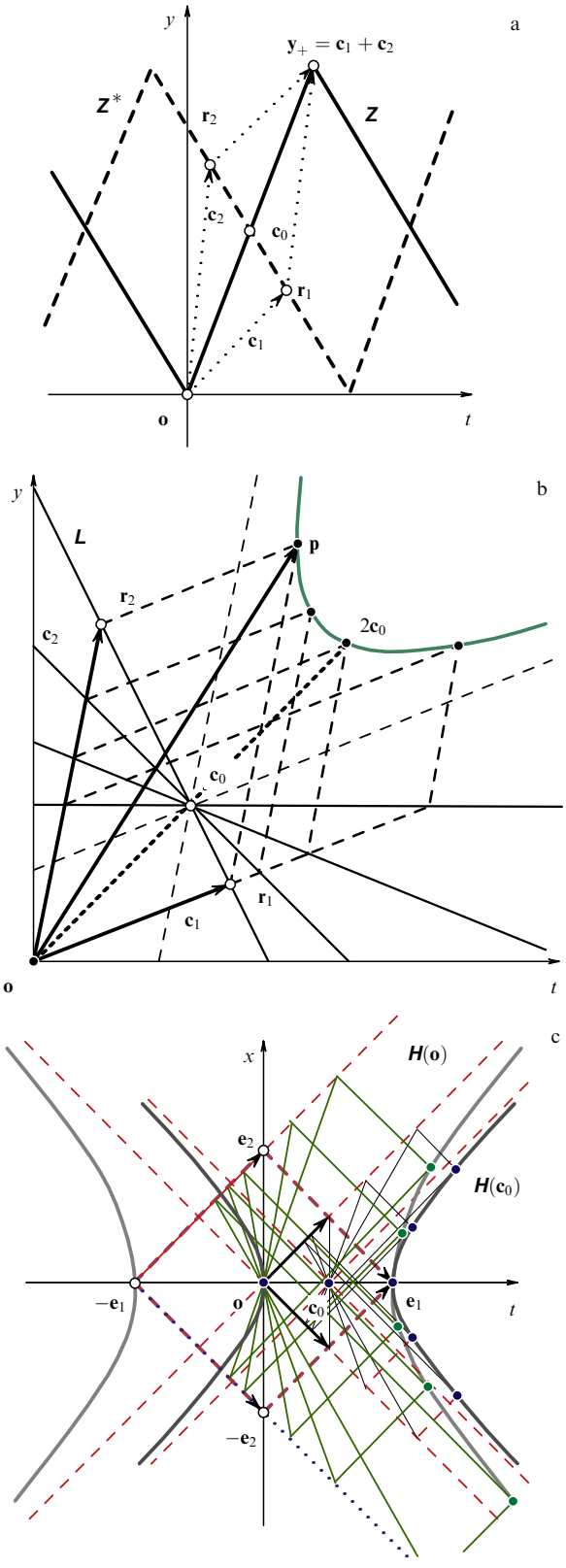

Figure 14. Ray diagram illustrating formation of a target step event (a) used as a synthetic mechanism (Pascal's procedure) for the hyperbolic metric of locomotion control; (b, c) ray method for the construction of canonical hyperbola $\boldsymbol{H}(\mathbf{o})$ in Minkowskian geometry and basal hyperbola $\boldsymbol{H}(\mathbf{c}_0)$ of isorhythmometric geochronometry.

4.2.3 Support straight line method. The previously described general method for the construction of parallelogram basis **P** in the form of Eqn (4.6) may be used to determine base matrix **B** of 'Pascal's clock', but taking into account the new boundary conditions for primary rays. Thereafter, the initial parallelogram $\mathbf{P}_0$ is distinguished and the RFR metric basis **B** determined, the latter being understood as a basis with respect to which an arbitrary parallelogram $\mathbf{P} = \mathbf{B}\mathbf{P}_0$ is presented as the initial parallelogram $\mathbf{P}_0$. In the previous relativistic clock models, the natural criterion for distinguishing the initial AFR parallelogram $\mathbf{P}_0$ was the zero relative velocity condition, $v = 0$. In Pascal's clock, however, such a criterion does not always hold, and its alternative analogue is the condition $v = v_0$, i.e. the choice of characteristic velocity.

In the general matrix definition of parallelogram basis $\mathbf{P} = \mathbf{C}\mathbf{S}^{-1}$, the ray matrix $\mathbf{C} \equiv (\mathbf{c}_1, \mathbf{c}_2)$ is completely defined (Fig. 14b) by the boundary conditions of intersection of the rays and the support straight line $\boldsymbol{L}(\mathbf{r}; \mathbf{c}_0)$, where $\mathbf{r} \equiv (t_r, x_r)' = t_r(1, v)'$ is the direction vector, and $\mathbf{c}_0 \equiv (t_0, x_0)'$ is the center of rotation of the support line. By distinguishing collinear events $\mathbf{r}_1$ and $\mathbf{r}_2 \equiv \lambda\mathbf{r}_1$ on the support straight line, the following boundary conditions can be deduced for initial rays:

$$\mathbf{c}_1 = \mathbf{c}_0 + \mathbf{r}_1\,, \qquad \mathbf{c}_2 = \mathbf{c}_0 + \mathbf{r}_2\,.$$

Passing over to the matrix representation of these conditions

$$\mathbf{C} = \mathbf{X} \equiv (\mathbf{c}_0 + \mathbf{r}_1, \mathbf{c}_0 + \lambda\mathbf{r}_1)\,,$$

we shall take into consideration [see Eqn (3.16)] that the ray matrix is factorizable into a product of two matrices, base and gauge ones, $\mathbf{C} \equiv \mathbf{V}_C\mathbf{D}_C$. This directly enables the diagonal matrix to be distinguished:

$$\mathbf{D}_C = \mathbf{V}_C^{-1}\mathbf{X} \equiv (\bar{\mathbf{c}}_0 + \bar{\mathbf{r}}_1, \bar{\mathbf{c}}_0 + \lambda\bar{\mathbf{r}}_1)\,.$$

Then, the right-hand side of the boundary conditions is the previously defined (see Section 3.3.4) transition to the ray basis (the bar over vector notations indicates the representation of these vectors in the ray basis). The solution of these equations gives $\lambda = \bar{v}/\bar{v}_0$ and the components of the gauge matrix $\mathbf{D}_C$:

$$\bar{t} = \bar{t}_0 + \frac{\bar{x}_0}{\bar{v}}\,, \qquad \bar{x} = \bar{v}\bar{t}_0 + \bar{x}_0\,, \tag{4.22}$$

i.e. elements of vector $\bar{\mathbf{p}} \equiv (\bar{t}, \bar{x})'$ one half of which form the bilaterally symmetric parallelogram basis

$$\overline{\mathbf{P}} \equiv \mathbf{D}_C\mathbf{S}^{-1} = \frac{1}{2}(\bar{\mathbf{p}}, \mathbf{F}\bar{\mathbf{p}})\,.$$

It follows from the parametric equations (4.22) that vector $\bar{\mathbf{p}} \equiv (\bar{t}, \bar{x})'$ is incidental to the equilateral hyperbola $\boldsymbol{H}(\bar{\mathbf{c}}_0)$ the center of which is coincident with the center of rotation of the support straight line (a similar construction has been described above, see Fig. 5d). Basis $\overline{\mathbf{P}}_0 = (\bar{\mathbf{c}}_0, \mathbf{F}\bar{\mathbf{c}}_0)$ corresponding to the characteristic velocity $\bar{v} = \bar{v}_0$ is regarded as an 'initial' one. Therefore, it follows that

$$\overline{\mathbf{B}} \equiv \overline{\mathbf{P}}\,\overline{\mathbf{P}}_0^{-1} = \mathbf{D}\left[\frac{\bar{t}}{\bar{t}_0}\,, \frac{\bar{x}}{\bar{x}_0}\right] = \mathbf{D}\left[1 + \frac{\bar{v}_0}{\bar{v}}\,, 1 + \frac{\bar{v}}{\bar{v}_0}\right]. \tag{4.23}$$

Hence, metric basis will assume the form

$$\mathbf{B} = \mathbf{V}_C\overline{\mathbf{B}}\mathbf{V}_C^{-1} \equiv \mathbf{V}_C\mathbf{D}[d_1, d_2]\,\mathbf{V}_C^{-1}\,. \tag{4.24}$$

When deciphering symbols $d_1 \equiv 1 + \bar{v}_0/\bar{v}$, $d_2 \equiv 1 + \bar{v}/\bar{v}_0$, the velocity ratios defined in the ray basis should be substituted by the following wurf

$$\frac{\bar{v}}{\bar{v}_0} = \mathrm{w}(v, v_0; c_1, c_2)\,; \tag{4.25}$$

the first formula in Eqn (3.30) is sufficient to obtain this wurf.

We now exclude the velocity parameter from the equations and replace them by the quadratic form

$$(\bar{\mathbf{p}} - \bar{\mathbf{c}}_0)'\,\mathbf{I}(\bar{\mathbf{p}} - \bar{\mathbf{c}}_0) = \bar{\mathbf{c}}_0'\,\mathbf{I}\bar{\mathbf{c}}_0$$

$$\Rightarrow\ (\mathbf{p} - \mathbf{c}_0)'\,\mathbf{M}(\mathbf{p} - \mathbf{c}_0) = \mathbf{c}_0'\mathbf{M}\mathbf{c}_0\,, \tag{4.26}$$

where $\mathbf{M} \equiv (\mathbf{V}_\mathrm{C}^{-1})'\,\mathbf{I}\mathbf{V}_\mathrm{C}^{-1} = (\mathbf{C}^{-1})'\,\mathbf{I}\mathbf{C}^{-1}$ because $\mathbf{DID} = |\mathbf{D}|\,\mathbf{I}$, i.e. the target etalon of basis **B** in 'Pascal's clock' makes up basal hyperbola $\boldsymbol{H}(\mathbf{c}_0; \mathbf{C})$ with a center $\mathbf{c}_0$ and asymptotes directed by the vectors of ray matrix **C**. That this hyperbola is basal: $\mathbf{o} \in \boldsymbol{H}(\mathbf{c}_0; \mathbf{C})$, i.e. one of its branches passes through the origin of coordinates (see Definition 2.5), follows from the right-hand side of its quadratic form since the analogous hyperbola of the common place with a distinguished fixed point $\mathbf{p}_1 \in \boldsymbol{H}(\mathbf{c}_0; \mathbf{C})$ is described by a similar form

$$(\mathbf{p} - \mathbf{c}_0)'\,\mathbf{M}(\mathbf{p} - \mathbf{c}_0) = (\mathbf{p}_1 - \mathbf{c}_0)'\,\mathbf{M}(\mathbf{p}_1 - \mathbf{c}_0)\,. \tag{4.27}$$

Corollaries to the requirement of invariance of the general quadratic form with the symmetrical metric matrix have been discussed previously (see Section 2.2.4).

4.2.4 'Pascal's clock' invariants. In terms of the general algebraic structure, the Pascal clock basis (4.24) is a special case of the generalized model (3.20) in which the ray basis is procedurally invariant as follows from the equality $\mathbf{V}_\mathrm{S} = \mathbf{V}_\mathrm{C}$. This accounts for the coincidence of the projective and gauge invariants of basis (4.24) with the invariants of the anisotropic version of Lanczos method (3.36). This inference can be confirmed by applying Corollary 3.3 to basis (4.24). This procedure reveals a linear relation of base vectors $\mathbf{b}_2 = \mathbf{A}\mathbf{b}_1$ and a connection matrix **A** having the form (3.13).

Salient properties of Pascal's clock are manifested in gauge variables (4.22), from which the elements of the diagonal basis (4.23) are formed. Because natural parametrization of the resultant basis (4.24) with respect to velocity results in distinguishing wurf (4.25), the substitution

$$\mathbf{e}^{2\alpha} = \mathrm{w}(v, v_0; c_1, c_2) \tag{4.28}$$

is equivalent to Kleinian projective reparametrization (see Note 3.3) which leads to the standard representation of basal basis

$$\mathbf{B} = \frac{1}{2}\left(\mathbf{E} + \mathbf{H}(2\alpha; c_1, c_2)\right) = \cosh\alpha\,\mathbf{H}(\alpha; c_1, c_2)\,,$$

where $\mathbf{H}(\alpha; c_1, c_2) \equiv \mathbf{e}^{\alpha\mathbf{N}}$ is the matrix of generalized hyperbolic rotation characterized by the generalized structural matrix $\mathbf{N} \equiv \mathbf{V}_\mathrm{C}\mathbf{F}\mathbf{V}_\mathrm{C}^{-1}$, $\mathbf{N}^2 = \mathbf{E}$ [cf. Eqn (3.23)]. Hence, we arrive at the following form of the generalized generating equation of 'Pascal's support chronogeometry':

$$(2\mathbf{B} - \mathbf{E})'\,\mathbf{M}(2\mathbf{B} - \mathbf{E}) = \mathbf{M}\,, \tag{4.29}$$

where $\mathbf{M} = \mathbf{J}\mathbf{N}^{-1}$ is the metric matrix (see Section 6.3). In a special canonical case of the isotropic model, one finds

$$\mathbf{H}(\alpha; -1, 1) \equiv \mathbf{H}(\alpha)\,, \qquad \mathbf{N} = \mathbf{I}\,, \qquad \mathbf{M} = \mathbf{F}\,.$$

This means that in this case Eqn (4.26) undergoes transformation into Eqn (4.21). Support reconstruction of canonical isometric chronogeometry (Fig. 14c) provides a comparative visual demonstration of the constructive properties of Pascal's clock and optochronometer (Fig. 12a).

Equation (4.21) has been initially derived in the framework of the mirror metaphor of chronometry using Einstein's procedure. However, this required an additional condition of constant etalon length (or period). Now, chronogeometry with an identical algebraic structure is obtained using Pascal's procedure without additional isometric or isorhythmic conditions. It is the absence of additional conditions that makes the 'support metaphor' more adequate for the constructive interpretation of isometric properties of chronometry which gives rise to the basal etalons of Eqn (4.26).

Conclusion 4.5. A geochronometry satisfying PCSL and lacking in length-shrinkage and time-dilation effects is constructively defined with the aid of Pascal's procedure.

4.3 Fixed event method

The most difficult area of constructive chronogeometry is the development of the procedural rationale for projective anharmonism which is supposed to be due to the additional properties of projective correspondence between bundles of base axes rather than to the anisotropic propagation of etalon signals. This difficulty can be overcome with the *fixed event method* (FEM) which has been preliminarily described above in connection with analytical substantiation of stride cycle structure synergy (see Section 2.5.5). In the present section, we consider the general geometric properties of FEM as an additional concept ('metaphor') of constructive relativism. Pascal's procedure may be used to construct not only hyperbolas but also other second-order curves. By analogy, FEM may also be used to form nonhyperbolic metric etalons. It is however clear that hyperbolic forms are more suitable for chronogeometric applications.

4.3.1 Two construction problems. Many circle properties are closely related to the notion of perpendicularity (for example, a tangent can be perpendicular to the radius, the same as the diameter across the middle of a chord is perpendicular to this line). The analogue of such *orthogonal* correspondence for the hyperbola is the property of *harmonic* correspondence.

Let $\boldsymbol{C}(\mathbf{x}_\mathrm{c}; \mathbf{x}_1)$ be a circle with the center $\mathbf{x}_\mathrm{c}$ and incidental point $\mathbf{x}_1$. Similarly, let $\boldsymbol{H}(\mathbf{x}_\mathrm{c}; \mathbf{x}_1)$ be a hyperbola for which asymptotic directions defined by constants c_1 and c_2 need to be known besides the center $\mathbf{x}_\mathrm{c}$ and incidental point $\mathbf{x}_1$ (in the forthcoming discussion, the directions of asymptotes will be assumed to be known).

Problem 4.1. A figure (circle or hyperbola) has center $\mathbf{x}_\mathrm{c}$ and point $\mathbf{x}_1$; it is necessary to find another arbitrary point of the figure.

The solution for both figures is offered in Fig. 15a, b. In the case of circle $\boldsymbol{C}(\mathbf{x}_\mathrm{c}; \mathbf{x}_1)$, we draw an arbitrary radial straight line $\boldsymbol{L}_2$, construct bisector $\boldsymbol{L}_3$, and drop a perpendicular on the bisector from point $\mathbf{x}_1$; the perpendicular is extended to intersect the straight line $\boldsymbol{L}_2$ at the desired point $\mathbf{x}_2$. The parallelogram $\boldsymbol{P} \equiv \{\mathbf{x}_\mathrm{c}, \mathbf{x}_1, \mathbf{x}_2, \mathbf{x}_3\}$ formed by vectors $\mathbf{r}_1 \equiv \mathbf{x}_1 - \mathbf{x}_\mathrm{c}$ and $\mathbf{r}_2 \equiv \mathbf{x}_2 - \mathbf{x}_\mathrm{c}$ is rhomboid in shape, and its

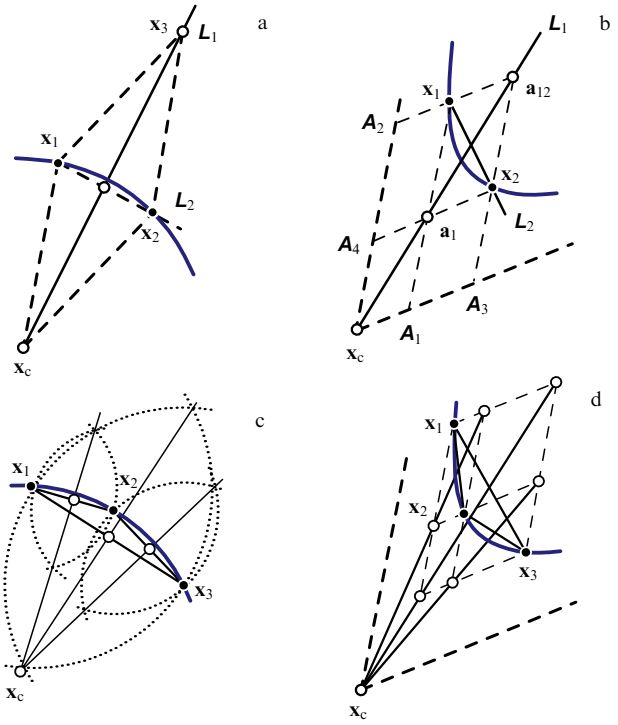

Figure 15. Construction of a circle (a) and a hyperbola (b) with a given center and one point; reverse procedure of the construction of circle (c) and hyperbola (d) centers by three points.

diagonals, i.e. chord $\boldsymbol{L}(\mathbf{x}_1, \mathbf{x}_2)$ and radial $\boldsymbol{L}(\mathbf{x}_c, \mathbf{x}_3)$ straight lines, are mutually perpendicular.

To construct the hyperbola $\boldsymbol{H}(\mathbf{x}_c; \mathbf{x}_1)$, two straight lines $\boldsymbol{A}_1$ and $\boldsymbol{A}_2$ parallel to asymptotes are first drawn through a given point $\mathbf{x}_1$. Then an arbitrary radial straight line $\boldsymbol{L}$ crosses straight lines $\boldsymbol{A}_1$ and $\boldsymbol{A}_2$ at points $\mathbf{a}_1$ and $\mathbf{a}_2$, respectively. Additional straight lines $\boldsymbol{A}_3$ and $\boldsymbol{A}_4$ parallel to the asymptotes are drawn through new auxiliary points $\mathbf{a}_1$ and $\mathbf{a}_2$. Then, the point to be found is $\mathbf{x}_2 \equiv \boldsymbol{A}_3 \cap \boldsymbol{A}_4$. The parallelogram of asymptotes, $\boldsymbol{P} \equiv \{\mathbf{a}_1, \mathbf{x}_1, \mathbf{x}_2, \mathbf{a}_2\}$, has a chordal diagonal $\boldsymbol{L}(\mathbf{x}_1, \mathbf{x}_2)$ and a radial diagonal $\boldsymbol{L}(\mathbf{a}_1, \mathbf{a}_2)$ in harmonic correspondence. The diagonals of the central parallelogram $\boldsymbol{P} \equiv \{\mathbf{x}_c, \mathbf{x}_1, \mathbf{x}_2, \mathbf{x}_3\}$ are collinear with those of the parallelogram of asymptotes. ◆

Problem 4.2. A figure (circle of hyperbola) has three given points $\{\mathbf{x}_1, \mathbf{x}_2, \mathbf{x}_3\}$; one should find the center $\mathbf{x}_c$ of the figure.

The solution for both figures is presented in Fig. 15c, d. The given points are first connected in pairs by chords which form a triangle. Then, perpendicular lines drawn through the middle of the chords intersect at point $\mathbf{x}_c$, thus giving the center of the circumscribed circle $\boldsymbol{C}(\mathbf{x}_c; \mathbf{x}_1)$.

In the case of hyperbola $\boldsymbol{H}(\mathbf{x}_c; \mathbf{x}_1)$, a parallelogram of asymptotes is constructed for each chord. Its radial diagonals intersect at the center $\mathbf{x}_c$. ◆

In the chronogeometric context, parallelograms of asymptotes are equivalent to ray parallelograms. It has been shown earlier in this paper that projective correspondences are easier to represent in the ray basis. If the above two problems for hyperbolas are transformed into the ray basis, the ray parallelograms turn into rectangles with bilaterally symmetrical diagonals. This means that bilateral symmetry of straight lines or vectors is a special (and simplest) case of harmonicity. For brevity and for greater analytical simplicity, FEM is further considered in the ray basis (the bar over the symbol in this basis, its identifier, will be not used any longer).

4.3.2 Linear bundle correspondence. It has been mentioned before that the plane basis $\mathbf{B} = (\mathbf{b}_1(v_1), \mathbf{b}_2(v_2))$ is formed by a pair of coordinate axis bundles having a common center at the origin of coordinates $\mathbf{o}$. The orientational invariant establishes the scalar correspondence of the axes (see Section 6.7), which can be expressed in the vector form. For example, if the axes' correspondence fulfills the bilateral symmetry condition, the axis slopes have different signs:

$$\mathbf{b}_2 = \lambda \mathbf{F} \mathbf{b}_1 \;\Rightarrow\; v_2 = -v_1 \,,$$

i.e. such bundles are in harmonic correspondence. The simplest variant of anharmonic linear correspondence is ensured by continuous additional deformation:

$$\mathbf{b}_2 = \lambda \mathbf{D} \mathbf{F} \mathbf{b}_1 \;\Rightarrow\; v_2 = -q v_1 \,, \tag{4.30}$$

so that $q \equiv d_2/d_1$ is the linear correspondence coefficient if $\mathbf{D} \equiv \mathrm{diag}\,(d_1, d_2)$.

It has been shown above that the projective correspondence between base vectors defined by the generalized PCSL is represented in the ray basis (see Section 3.4.4) in the form of linear relation (4.27). Let us now consider geometric conditions maintaining the linear correspondence of two bundles, $\boldsymbol{B}_1(v_1; \mathbf{x}_1)$ and $\boldsymbol{B}_2(v_2; \mathbf{x}_2)$, having no common center: $\mathbf{x}_1 \neq \mathbf{x}_2$.

An interesting subject is the correspondence between the bundles of hyperbola chords, which is due to three points located on hyperbola $\boldsymbol{H}$. Let us therefore turn back to the three points in Problem 4.2 and suppose that

$$\{\mathbf{x}_1 = \mathbf{f},\ \mathbf{x}_2 = \mathbf{o},\ \mathbf{x}_3 = \mathbf{h}_1\} \in \boldsymbol{H}(\mathbf{x}_c; \mathbf{h}_1) \,.$$

In other words, let us consider the first and the second point to be fixed points of a certain hyperbola $\boldsymbol{H}$, and the third point to be free. Vector $\mathbf{x}_3 - \mathbf{x}_2 = \mathbf{h}_1 - \mathbf{o} = \mathbf{h}_1$ corresponds to the first chord, and vector $\mathbf{x}_3 - \mathbf{x}_1 = \mathbf{h}_1 - \mathbf{f} \equiv -\mathbf{h}_2$ to the second. Therefore, vectors $\mathbf{h}_1 \equiv (t_1, x_1)'$ and $\mathbf{h}_2 \equiv (t_2, x_2)'$ may be considered as vectors emanating from the initial point $\mathbf{o}$ and satisfying the fixed sum condition

$$\mathbf{h}_1 + \mathbf{h}_2 = \mathbf{f} \;\Leftarrow\; \mathbf{h}_1 \equiv \boldsymbol{B}_1(v_1; \mathbf{o}) \cap \boldsymbol{B}_2(v_2; \mathbf{f}) \,. \tag{4.31}$$

To avoid confusion of figure centers and bundle centers, we introduce the following

Definition 4.1. The centers of straight line bundles are termed *foci*.

It is worthwhile to note that this nomenclatural definition is in agreement with the known notions of foci, e.g. of an ellipse or hyperbola, which can also be represented in the ray-specific interpretation as bundle centers (Fig. 16a), while vectors of correspondence points satisfy the condition (4.28).

Theorem 4.1. *If the common point of two bundles and also their centers (foci) lie on a hyperbola, then such bundles are in linear correspondence:*

$$\{\mathbf{o}, \mathbf{h}_1, \mathbf{f}\} \in \boldsymbol{H}(\mathbf{x}_c) \;\Rightarrow\; v_2 = -q v_1 \;\Leftarrow\; q = \frac{v_f}{v_c} \,. \tag{4.32}$$

Proof. Hyperbola $\boldsymbol{H}(\mathbf{x}_c)$ in the ray basis is described by parametric Eqn (4.22) which can be simplified if written in the vector form, namely

$$\mathbf{h}_1 = \mathbf{V}_1 \mathbf{x}_c \,,$$

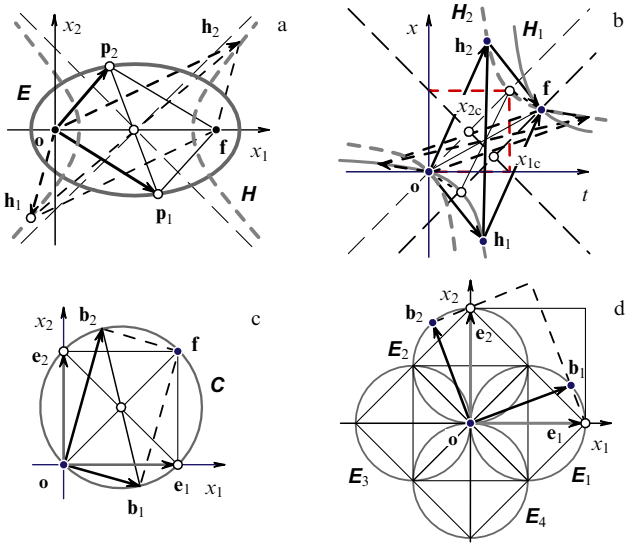

Figure 16. Variants of focal geometries: (a) focal parallelograms of ellipse ***E*** and hyperbola ***H***; (b) hyperbolic etalons of the fixed event method; (c) fixed point **f** of basal ***C***-circle geometry; (d) geometry of two pairs of basal circles.

where $\mathbf{V}_1 \equiv \mathbf{V}[v_1] = \mathbf{E} + (v_1\mathbf{e}_2, v_1^{-1}\mathbf{e}_1)$. By analogy, in accordance with Eqn (4.29), it is possible to write

$$\mathbf{f} = \mathbf{V}_\mathrm{f}\mathbf{x}_\mathrm{c}\,, \qquad \mathbf{o} = \mathbf{V}_0\mathbf{x}_\mathrm{c}\,,$$

where $\mathbf{V}_\mathrm{f} \equiv \mathbf{V}[v_\mathrm{f}]$ and $\mathbf{V}_0 \equiv \mathbf{V}[v_0]$, i.e. $v_0 = -v_\mathrm{c}$. For a complementary vector $\mathbf{h}_2$,the equation

$$\mathbf{h}_2 = \mathbf{f} - \mathbf{h}_1 = (\mathbf{V}_\mathrm{f} - \mathbf{V}_1)\mathbf{x}_\mathrm{c}$$

implies that $v_2 = -v_1 v_\mathrm{f}/v_\mathrm{c}$. ◆

The constructive meaning of the proved theorem consists not only in the relation of fixed and free events to the hyperbola but also in the elucidation of the geometric sense of the anharmonicity coefficient. The quantity v_c being a characteristic velocity, harmonic case takes place at $\mathbf{f} = 2\mathbf{x}_\mathrm{c}$, i.e. when the fixed event is characteristic, and then $q = 1$. In the opposite situation, fixed and characteristic events do not coincide. An example of graphical representation is given in Fig. 16b.

Conclusion 4.6. Anharmonic correspondence reflects the degree of displacement of a fixed event **f** with respect to the characteristic event $2\mathbf{x}_\mathrm{c}$.

4.3.3 Chord basis. Vectors $\mathbf{h}_1$ and $\mathbf{h}_2$ introduced above may be considered separately as vectors that form the chord basis $\mathbf{H} = (\mathbf{h}_1, \mathbf{h}_2)$.

Theorem 4.2. *In the case of anharmonic correspondence between axes, the hyperbolic chord basis is bifocal and bicentral: metric etalons of different axes are represented by hyperbolas that pass through foci and have different centers*:

$$\mathbf{H} \equiv (\mathbf{h}_1, \mathbf{h}_2) = (\mathbf{V}_1\mathbf{x}_{\mathrm{c}1}, \mathbf{V}_2\mathbf{x}_{\mathrm{c}2})\,. \tag{4.33}$$

Proof. Assuming that anharmonicity of correspondence between axes of chord basis is given by quantity q, the above scalar relation $q = v_\mathrm{f}/v_\mathrm{c}$ can be used to determine the relationship between focal and central vectors:

$$t_\mathrm{c} = q_1 t_\mathrm{f}\,, \qquad x_\mathrm{c} = q_2 x_\mathrm{f} \;\Rightarrow\; \mathbf{x}_\mathrm{c} = \mathbf{D}\mathbf{f}\,, \tag{4.34}$$

where $\mathbf{D} \equiv \mathrm{diag}\,(q_1, q_2)$. Coefficients q_1, q_2 of this vector relation form the diagonal matrix and are expressed through the parameter q as follows

$$q_1 \equiv \frac{q}{1+q}\,, \qquad q_2 \equiv \frac{1}{1+q}\,, \tag{4.35}$$

and hence $q_1 + q_2 = 1$, $q_1/q_2 = q$.

On the assumption that $\mathbf{x}_\mathrm{c} \equiv \mathbf{x}_{\mathrm{c}1}$ and $\mathbf{D}_1 \equiv \mathbf{D}$, the equation for a base vector $\mathbf{h}_1$ can be substituted in the following way

$$\mathbf{h}_1 = \mathbf{V}_1\mathbf{x}_{\mathrm{c}1} \;\Leftarrow\; \mathbf{x}_{\mathrm{c}1} = \mathbf{D}_1\mathbf{f}\,. \tag{4.36}$$

Furthermore, in accord with the initial definition one has

$$\mathbf{h}_2 = \mathbf{f} - \mathbf{h}_1 = (\mathbf{E} - \mathbf{V}_1\mathbf{D}_1)\,\mathbf{f} = \mathbf{V}_2\mathbf{D}_2\mathbf{f}\,,$$

where $\mathbf{D}_2 \equiv \mathbf{I}\mathbf{D}_1\mathbf{I}$; then vector $\mathbf{h}_2$ is defined by the following parametric equation

$$\mathbf{h}_2 = \mathbf{V}_2\mathbf{x}_{\mathrm{c}2} \;\Leftarrow\; \mathbf{x}_{\mathrm{c}2} = \mathbf{D}_2\mathbf{f} \tag{4.37}$$

and forms a hyperbola, the center of which, $\mathbf{x}_{\mathrm{c}2}$, does not coincide with the center $\mathbf{x}_{\mathrm{c}1}$ if matrices $\mathbf{D}_1$ and $\mathbf{D}_2$ are different. Only in the particular case of harmonic correspondence when

$$q = 1\colon\ \ \mathbf{D}_1 = \mathbf{D}_2 = \frac{\mathbf{E}}{2} \Rightarrow\ \mathbf{x}_{\mathrm{c}1} = \mathbf{x}_{\mathrm{c}2} = \frac{\mathbf{f}}{2}\,,$$

the centers of branches $\mathbf{h}_1$ and $\mathbf{h}_2$ coincide, one has $v_2 = -v_1 = -v$, and the effect of displacement of the origin **o** with respect to the center of the hyperbola $\mathbf{H} = (\mathbf{V}(v)\,\mathbf{f}/2,\, \mathbf{V}(-v)\,\mathbf{f}/2)$ is preserved. ◆

4.3.4 Inverse problem. Inversion of the previous problem implies that bundle centers do not initially lie on a certain hyperbola. Assume that the initial condition is presented by the condition of linear correspondence

$$v_2 = -qv_1 \tag{4.38}$$

for two arbitrary bundles $\boldsymbol{B}_1(v_1; \mathbf{x}_1)$, $\boldsymbol{B}_2(v_2; \mathbf{x}_2)$ with the correspondence point $\mathbf{x} = \boldsymbol{B}_1 \cap \boldsymbol{B}_2$. It is possible to come back to the previous vector scheme, without disturbing generality, by means of substitutions

$$\mathbf{x}_1 \to \mathbf{o}\,, \qquad \mathbf{x} \to \mathbf{h}_1\,, \qquad \mathbf{x}_2 \to \mathbf{f}\,.$$

Also, the scalar condition (4.35) is converted into a vector condition:

$$\mathbf{h}_2 = \lambda\mathbf{A}\mathbf{h}_1\,,$$

where $\mathbf{A} \equiv \mathbf{D}_2\mathbf{F}$, and λ is an arbitrary real parameter. Hence, the following determining relations for vectors $\mathbf{h}_1$ and $\mathbf{h}_2$:

$$\mathbf{h}_1 + \mathbf{h}_2 = \mathbf{f}\,, \qquad \mathbf{h}_2 = \lambda\mathbf{A}\mathbf{h}_1\,. \tag{4.39}$$

Theorem 4.3. *Plane basis* $\mathbf{H} = (\mathbf{h}_1, \mathbf{h}_2)$ *defined by vector conditions* (4.36) *is equivalent to the hyperbolic chord basis.*

Proof. Equations (4.36) can be rewritten in the form of matrix

$$\mathbf{H} = (\mathbf{E} + \lambda\mathbf{A})^{-1}(\mathbf{f}, \lambda\mathbf{A}\mathbf{f})\,. \tag{4.40}$$

In order to complete the solution, the formal parameter λ must be substituted by velocity-related parameters v_1 or v_2. The substitution and subsequent transformations give

$$\mathbf{H} = (\mathbf{V}_1\mathbf{D}_1\mathbf{f}, \mathbf{V}_2\mathbf{D}_2\mathbf{f}) = (\mathbf{V}_1\mathbf{x}_{c1}, \mathbf{V}_2\mathbf{x}_{c2}),$$

i.e. the same chord basis which has been obtained above [see Eqn (4.30)]. ◆

Note 4.2. A peculiar character of this synthesis of geometries is especially well apparent when a basal circle is chosen to serve as a base etalon (Fig. 16c). Such a model depends on relations (4.36) if $\mathbf{A} = \mathbf{J}$. In other words, the condition of linear relation between base vectors is equivalent to the orthogonality condition

$$\mathbf{b}_1 + \mathbf{b}_2 = \mathbf{f}, \qquad \mathbf{b}_2'\mathbf{b}_1 = 0.$$

The 'Euclidean' analogue of the general matrix equation (4.26) is obtained by the choice of a unit metric matrix $\mathbf{M} = \mathbf{E}$. Then, there is basis

$$\mathbf{B} = \cos\alpha\,\mathbf{R}(\alpha) = \cos\alpha(\cos\alpha\,\mathbf{E} + \sin\alpha\,\mathbf{J})$$

instead of (4.20), which contains a pair of basal circles (Fig. 16d). ◆

This concludes the algebraic description and geometric substantiation of the fixed event method.

5. Conclusions

> *Credit must be given first to observation rather than to theories, and to theories only insofar as they are confirmed by the facts observed.*
>
> Aristotle

In this section, we shall discuss in brief the semantic evolution of fundamental notions pertaining to the subject matter of the present review.

5.1 Physical entities

Space, time, and motion are three primary (fundamental) entities of physics, i.e. a science of Nature as it was first established by Aristotle [2]. The comparison of causes and properties of motion of physical bodies also originates in Aristotle's treatise *Physics*. Aristotle introduced the notions of 'force' and 'energy' to distinguish common causes of motion of animate and inanimate objects and coined, in addition, the term 'entelechy' which is currently interpreted as the equivalent of the notion of 'goal-oriented control' [52].

The original definition of physics by Aristotle implied the rational cognition of the world including all natural objects, both animate and inanimate. In the course of time, however, physics concentrated on simpler, primary, mechanical concepts as well as mechanical problems that have taken centuries to be solved and required the efforts of Galileo, Huygens, Newton, Euler, Lagrange, Laplace, and many other scientists. The original cybernetic definition of the essence of life proposed by Aristotle was first disregarded as oriented chiefly to the development of mechanical concepts and then rejected and forgotten among attempts to construct novel definitions proceeding from the mechanistic view of things, i.e. neglecting other entities as 'unnecessary'.

Aristotle's principal contribution to the foundation and progress of physics as a science rests on the conceptual semantic development of practically all basic entities (referents) of the cognition of Nature. Besides the above three entities (space, time, and motion), he included in the list of physical entities place, velocity, acceleration, force, matter, gravity, energy, etc. Also, he subjected all these notions to logical analysis and even derived symbolic formulas for some of them (e.g. velocity).

T Khun [35] advocated interconnection between scientific revolutions and the appearance of new referent notions. According to one of his examples, Galileo introduced into physics the notion of 'velocity', and Newton the notion of 'acceleration'. However, the notion of velocity had actually been introduced by Aristotle, otherwise he would have not been able to explain Zeno's 'Achilles and turtle', 'Arrow', and other paradoxes. Further still the 'Stadium' paradox has a direct bearing on the relativistic theme of 'summation of velocities of relative motions': two groups of horsemen are moving from the opposite directions in front of the stands of a stadium; it is required to find the difference between approach velocities at which the groups are drawing together as estimated by two observers in different states of motion, one being a horseman, the other a spectator at the stands.

Aristotle also developed notions of the position of the point and continuity of space and time (manifest in continuity of mechanical motions), which were important components of his discursive technique. In short, if Khun's criteria are valid, Aristotle initiated the greatest scientific revolution. However, few physicists appear to be aware of the fact and appreciate it, including Khun himself as follows from his comparative analysis of the history of physics [35].

5.2 Time

The very first in-depth and comprehensive semantic analysis of the notion of time was undertaken by Aristotle. His arguments are widely known. Here is an excerpt from his *Physics* [2]:

"Time is most likely to present itself as a motion or a change... The change can be faster or slower, but time cannot since it itself determines what is slow and fast. Fast is what advances far for a short time, slow is what advances little for a long time; meanwhile time is uniform everywhere and throughout. What is moving progresses from something to anything and is described as a continuous quantity: this continuity ensures continuous motion, hence time. The foregoing and forthcoming initially refer to a place, i.e. both are connected with position. Time is a measure of body remaining in the state of motion, it measures motion by means of another restricted motion (the elbow measures the length by determining a certain quantity which is a measure of an arbitrary length). Time is such as motion is."

This quotation describes a method chosen by Aristotle to prove the existence of time. On the one hand, there are many different movements and changes (fast, slow, etc.) at each instant of time. On the other hand, all movements share a common property which should be called *time*. To measure the common characteristic of all these movements, i.e. time, we have to choose a certain *etalon motion* ('clock') and use the notion of, so to say, instrumental time. There are different ways to choose etalon motion. Therefore, instrumental time is such as etalon motion is. In other words, the Aristotelian dependence of instrumental time on the choice of etalon motion contains the modern relativistic time concept.

An updated analysis of the notion of time was undertaken by H Poincaré in the late 19th century [42, 43]. Interestingly, his analysis has much in common with that of Aristotle even though the former contains no allusions to the latter. Instead,

it offers new subjects, e.g. clock synchronization. Comparison of the two texts indicates that the general concept of time underwent little change during the centuries that elapsed from the age of Aristotle to that of Poincaré. The main fact in the evolution of this concept is the appearance of the notion of individual or local time, which gave rise to the clock synchrony problem. Aristotle knew three types of clocks: the sun-dial, the sand-glass, and the water clock (clepsydra), but only the sun-dial was used as a main etalon clock. Therefore, it may be argued that the concept of global single time in the whole Universe is more consistent with Aristotle's genuine thought.

The book by E Taylor and J Wheeler [62] contains a visual representation of the mechanical space-time model in the form of an infinite 3-dimensional cubic lattice made of one meter-long rods and having a clock at each of its nodes. Characteristically, the authors emphasize that the type of the clocks is immaterial. Is it really so? How will it change our understanding of time if sun-dials (or sand-glasses, for that matter) are placed at the nodes of the Taylor – Wheeler lattice? Of course, the authors mean modern mechanical and electronic clocks, or Langevin's clock, when they speak about 'clocks of any type'. We have already considered the consequences of clock choice in the foregoing discussion (see Sections 4.1.1 and 4.1.2). Here, suffice it to repeat the principal conclusion that the transition from mechanical to light ('wave') clock launched the relativistic revolution in the physical worldview.

To sum up, the notion of time has been changing from the age of Aristotle till the present due to the extensive adoption of 'personal chronometers'. The resulting problem of clock synchronization is now dealt with in the framework of the 'world's standard time' concept which reverts our relativistic outlook to the Aristotelian concept of global (absolute) time throughout the Universe. Indeed, a paraphrase of his syllogism (see above) brings us to the following conclusion: if we may use many different clocks at a moment, there must exist a common entity which should be called 'universal time' or simply time.

5.3 Space

Strictly speaking, the notion of a 'relative frame of reference' was first introduced by Aristotle. Although the Aristotelian model of the Universe is essentially geocentric, the role of the local reference system is played by the notion of 'place' [2]:

"Place seems to be something peculiar and difficult to understand... Place has three dimensions: length, width, and depth, i.e. just the same dimensions by which any body is defined... But we do not find any difference between a point and a point place. Place would not be worth studying were it not for the motion with respect to the place. Place is a fixed vessel exactly as the vessel is a movable place. Therefore, if anything is in motion inside something that moves, for instance, a boat in the river, it sooner refers to it as to a vessel. Preferably, place must be fixed; therefore, place is most likely the entire river since as a whole it is stationary. Thus, the first fixed boundary of the enclosure is place. A body outside which there is another body enclosing it is at a certain place... A body without it is not. The Universe is nowhere."

The Aristotelian notion of 'enclosing place or body' is, so to say, a naive analogue of the modern notion of 'reference system', and the rule of 'the first fixed boundary of the enclosure' rightly suggests how to define relative frames of reference, whose 'enclosure sequence' is limited to the Universe (it is exactly for this reason that 'the Universe is nowhere').

The introduction of the notion of velocity was not a central issue in the scientific revolution initiated by Galileo (as he himself noted). But Galileo introduced the instrumental and measuring methodology into physical experiment, discovered quantitative laws of simple mechanical movements, and provided a rationale for the notion of inertial mechanical systems. Galileo was the first to introduce an image of a reference system in uniform motion ('ship') into mechanics in order to demonstrate the impossibility of determining the relative velocity of the ship in mechanical experiments.

Descartes, Newton, Leibnitz, and even Euler also left comments on the notion of 'place'.

Euler [68] wrote: "What is in fact place? This question is not so easy to answer."

The difficulty was due to the fact that Euler was not aware of a 'coordinate system' when he published his book *Mechanics or Science of Motion Presented from the Analytical Viewpoint* in 1736. Strictly speaking, Descartes had introduced a method for plane digitization with the aid of a pair of noncollinear straight lines, but the notion and the term 'Cartesian coordinate system' were proposed by Maclaurin in 1742 (see Ref. [68, p. 11]). As soon as Euler came to know the new notion, he promptly wrote a new version of his *Mechanics* (1765). Later, Lagrange introduced the notion of 'generalized coordinates' in his *Mecanique Analytique* (1788). However, the formulation of vector axiomatics in analytical geometry required many other 'revolutions' to occur (the geometries of Lobachevsky, Riemann, Klein, Weyl, Minkowski, etc.).

Question 5.1. Have these 'geometric revolutions' changed our understanding of space?

The answer is in the affirmative but not without reservation. Indeed, the understanding has changed but partially. On the one hand, a large number of metric geometries brought an end to the monopoly and even dictatorship (after H Weyl [13]) of Euclidean geometry as the sole option available to choose the metric model of physical space. On the other hand, if we are to adhere to the physical, i.e. instrumental (tool-based) and conventional (method-based), view of the nature of metric geometries (as H Poincaré insisted [43]), we should accept the possibility of coexistence of different metric models of the Universe (mechanical, gravitational, electromagnetic, etc.). However, the assumption of such a generalized relativistic view inevitably leads us to the logically justified 'absolute space' concept. This, in turn, removes the artificial opposition between the Newtonian and Einsteinian models of the world. Indeed, applying the above syllogism of Aristotle, we may conclude that if it is possible to simultaneously use many different coordinate systems or frames of reference in the physical description of the Universe, then there is a common entity which should be called 'absolute space' or simply space.

5.4 Principle of presumption of independence

It took physicists rather a long time to digest the idea of space-time unity forwarded by H Minkowski in the early 20th century. In the end, the scientific community fairly well fitted itself into the new situation as indicated by the inclusion of STR in school textbooks. Against such a background, any attempt to revise the fundamentals of STR looks behind the times.

It should be recalled, however, that the history of new geometric concepts was complicated by many centuries of

popular dissatisfaction with Euclid's fifth postulate. And also for centuries Euclidean geometry has been one of the main ingredients of the general school curriculum. More important, it remains such till now. Other examples to the same effect are readily at hand. Therefore, the standing argument most frequently put forward by teachers ('even schoolchildren know this') cannot lay down the law for scientists always calling everything in question.

The history of the fifth Euclidean postulate is interesting and instructive in more than one aspect. When comparing it with the history of the postulate of constant speed of light (PCSL), one important fact should be borne in mind. After the validity of Euclid's fifth postulate had been rejected by Lobachevskian geometry, physicists came to realize that Euclidean geometry was not a unique mathematical metaphor of physical space.

It is symptomatic even if somewhat illogical that, having recognized the nonuniqueness of one geometry, physicists and mathematicians with characteristic perseverance concentrated their efforts on the search for a more general but necessarily unique or unified geometry, field theory, etc. We believe, however, that the genuine cognition of Nature should be sought through pluralism of methods, approaches, and models rather than in pursuit of a unique, solely 'true' model. A physics which embraces an enormous range of problems, from microevents and elementary particles to macroscale events of astrophysics, needs different 'clocks' and 'rulers' at different levels of cognition. There is a greater need for adequate specialized tools than for universal ones.

A specific feature of the Cartesian coordinate system consists in that its abstract realization ensures independent parametrization of different dimensions. It means that not only space and time are introduced *a priori* independently but also all linear subspaces of the space itself are defined in a 'multi-one-dimensional' and linear way. Such a general view of the space and time metric structure can be described as the 'presumption of independence principle' which is geometrically expressed as an independent choice of both the directions of linear coordinate axes and linear scale units for each axis.

We consider upholding presumption of independence of space and time (as opposed to the ideas of 'monolithic unity') to be a paramount aspect of theoretical physics. Indeed, we believe that only this principle provides maximum freedom in the construction of generalized models satisfying one or other additional postulates, e.g. such as PCSL, and in the understanding of limitations imposed by the use of concrete measuring instruments.

In linear algebra, hence in affine geometry, the principal criterion of space (subspace) dimensionality is the number of independent vectors of an appropriate dimension. Whether the space itself is continuous or discrete, finite or infinite is unessential. The libernetic independence criterion determining degrees of freedom for the independent choice of a definite number of space coordinates or parameters of the system is also constructive because it is the most important dimensionality criterion for both spaces and control.

5.5 Organism as a machine

The title of Marey's book [37] suggests the mechanistic character of his scientific methodology. However, it is perhaps more to the point to associate it with machine science [37]:

"Living creatures have been compared with machines throughout the centuries, but only in our time is the importance and relevance of such a comparison fully understandable... The comparison of animals and machines is very useful in more than one aspect... A mechanical engineer can draw useful information from the study of nature, which will many times show him how the most difficult tasks can be performed in a surprisingly simple way."

Aristotle seems to have been the first to understand that regulation (entelechy) is an immanent agency of life [2], which characterizes him as a man of genius. However, this element of his philosophy gained little support, and 'vitalism' remained a matter of controversy and criticism for many centuries after his death. Only a few most creative intellects like R Descartes, who believed that animate bodies are no more than complicated machines [22], later came to understand the Aristotelian concept. This explains why biology, having neither scientific content of its own nor specialized tasks in the cognition of the essence of life, long developed as a descriptive discipline in the spirit of Aristotle's *De Animalibus Historia* [1]. In other words, it largely concentrated on the collection and systematization of new data which was also useful. Moreover, other sciences used biological systems as objects of research which gave rise to interscience disciplines distinguished for a rapid increase in the level of scientific activity, such as biomechanics, biophysics, biochemistry, biomathematics, bionics, etc.

E Schrödinger delivered his famous lectures *What is Life. The Physical Aspect of the Living Cell* in 1943 (see Ref. [67]) shortly before N Wiener's *Cybernetics* [14] was published (1948). Schrödinger's lectures did not directly concern Aristotelian entelechy, nevertheless they greatly promoted further constructive understanding of cybernetic concepts. Our attempts to bring into accord different views of the essence of life and control are summarized in a number of works [50 – 52, 55]. They proceed from the understanding of the organism as a 'constructor' and also distinguish freedoms (degrees of freedom) as basic referents of control. In order to better identify control functions, we proposed that cybernetics should deal with the problems of 'executive power' and libernetics be distinguished as a discipline concerned with 'legislative power'.

It follows from the above that only in the middle of the 20th century, the mathematician N Wiener [14] restored the lost scientific content of biology (making no allusion to Aristotle's ideas).

Why did Aristotle's entelechy sink into oblivion and Wiener's cybernetics revolutionize biology?

We think that Wiener's argumentation proved more convincing as based on the thesis of universal control mechanisms operating in 'the animal and the machine'. In contrast, Aristotle had neither an adequate machine analogue for comparison nor a specimen of a control device or automated system, even though he was the first to introduce the notion of an 'automaton'. In other words, the long history of machine-tool development created prerequisites for the recent progress in biology.

At least five 'machine revolutions' occurred between the age of Aristotle and our time:

(1) hand tools were replaced by machine tools which promoted integration of the production system;

(2) heat machines were instrumental in ensuring the progress of all means of transportation;

(3) electrical machines ensured worldwide electrification;

(4) electronic devices proved indispensable for the progress of means of communication and automation;

(5) modern information technologies support global information networks.

Mechanical computing machines, robots, and other automatically operated devices did not facilitate the understanding of the principles of control; in fact, they hindered it. The understanding of these principles became possible by virtue of the development and introduction of high-level computer programming languages and methods of 'object-oriented programming', which are expected to give way to 'semantically oriented programming'.

Therefore, the afore-cited statement of Marey concerning the practical utility of comparison of living organisms and machines assumes even more importance today than it did a century ago, taking into consideration that any artificial (technical) machine can be shown to have characteristics of its biological analogue. Does the great diversity of such analogies suggest that life cannot be defined in the framework of a single type of machines?

In the course of time, the construction of machines has been changing, thus opening new prospects for comparison with the unaltered structure of living things which contain properties of all artificial mechanisms, both existing and those likely to be created by copying models of biological systems. In this way, man continues to attempt to understand the essence of life through perceiving the principles of why and how machines work in an environment resembling that of living creatures. The synergetic representation of locomotor and other motions is a variant of this machine approach.

5.6 Bioprogramming

In his locomotion studies, Marey used pneumopodographic sensors to record support forces and accelerometers to measure inertial components of forces. However, he focused his attention on kinematic problems related to the formation of step cycles of individual limbs and the phase coordination between cycles of different limbs. In contrast, subsequent studies of Braune and Fischer [73] in the late 19th century were largely devoted to the dynamic reconstruction of an isolated human step. The dynamic approach to the construction of stepping movements has become the most popular one in biomechanical research in the 20th century due to the unprecedented complication of biodynamic features of locomotor systems [10, 15, 25, 47, 76, 82], on the one hand, and the extensive use of Lagrangian formalism for model and theoretical descriptions of limb 'force fields', on the other [8, 21, 82, 83, 86, 92]. At the same time, the second half of the 20th century witnessed an increasing interest in the kinematic aspect of locomotion analysis [7, 15, 45, 61, 75, 77 – 80, 86, 91] with which our own studies are also concerned [3 – 6, 27, 28, 57 – 60].

N A Bernshteĭn, who in many aspects anticipated Wiener's cybernetics in his famous book published in 1947 (see Ref. [10]), proposed a comprehensive rationale of the topological engram as a generalized and kinematic image of integrated movements. For example, when a subject draws geometric figures of different size and shape, the characteristic features he (or she) produces tend to persist regardless of the tool or a limb used for the purpose (or limb and body posture for that matter) as if the brain stores a certain etalon image against which to match a given specimen. Similarly, the elements of letters and words which characterize a person's handwriting reveal a surprising stability of individual invariant traits, which underlies the possibility of graphologic analysis. These simple examples of manual goal-oriented movements are familiar to everybody and therefore elicit no surprise unless one thinks of how the simplicity of such and many other locomotory acts is achieved.

A simple preliminary answer may be found in the hypothesis of a brain kinematic programme planning distal target trajectories, which serve as etalons for dynamic executive programmes or, to put it in different words, programmes of operating control over the targeted accuracy of dynamic performance. We consider such an answer to be right and convincing because modern robotic manipulating tools are operated following the same principles, that is by computers executing object-oriented programmes of three types: for kinematic planning, target correction, and dynamic performance. It should be emphasized, however, that this 'plausible' answer is based on known technical ('machine') solutions which cannot substitute the knowledge of properties and programmes of real neuromotor control. Indeed, the computer robototechnical metaphor of brain regulatory function is needed exactly for the purpose of surveying the boundless extent of mental activity. True, the 'one-finds-whatever-one-looks-for' rule is apt to do a great disservice to a researcher. For example, some searched for Pavlovian reflexes, identifying mental activity as salivation, and did 'observe' them. It is worthwhile to recall that in the recent past, even in the 20th century, such endeavours were considered to be true science and all others pseudoscience. With this in mind, should we not be more cautious in search of new neuroprogramming elements, remembering the difference between the existing electronic computers and the human brain, which is supposed by many to account for the discrepancy between computer models and natural neurophysiological processes?

Not at all. We believe that this work must be intensified rather than curtailed, to reveal more controversies and conflicting phenomena, i.e. to yield negative results. It is readily apparent that the value of the principal achievements of Pavlov and his physiological school lies in the negative findings which provided the basis for a new computer paradigm. On the other hand, although such a slogan as 'the brain is a computer!' and such question as 'can a machine think?' date to the dawn of cybernetics, there has so far been no considerable progress in this field [33, 45, 77, 87 – 89]. As a result, it remains unclear what kind of computational problems the human brain has to deal with and what semantic problems remain beyond the scope of computer systems, just because these problems have never been formalized and written as a programme.

The dynamic variability of walk control contrasting with a far more stable kinematic picture, demonstrated by V S Gurfinkel', S V Fomin, and T K Shtil'kind [21], suggests the independent significance of a kinematic image as a target function of dynamic control. Enhanced efficiency and adaptivity of interactive kinematic control have been confirmed experimentally using a model stepping device [20, 39]. It is therefore not necessary to set off kinematic and dynamic aspects of control since either plays a specific key role in the general task of constructing movements. Indeed, kinematic planning is an indispensable component of sensorimotor targeting ('sensorimotor intellect'), whereas dynamic resources and strategies provide tools to achieve the targeted goals.

The similarity of kinematic walk laws in arthropods and humans, demonstrated in our comparative studies [30, 60], confirms the similarity of kinematic tasks of stepping movements in all walkers, both vertebrate and invertebrate. This, in view of considerable differences in limb construction and motion patterns [15, 34, 76, 81, 82], suggests the necessity of elucidating the neurophysiological mechanisms underlying phylogenetic invariance of kinematic control programmes.

5.7 'Relativistic brain' concept

It has been shown above in Section 4 that the fixed event method best complies with the geochronometric conception of locomotion synergies. The main conclusion from the analysis of the biomechanical nature of stepping locomotor invariants consists in that the motion control should be viewed as the control of events in the space-time continuum. This view can be illustrated by the following theses:

• the task of constructing a target limb motion trajectory is solved by the brain as an integrated spatio-temporal problem;

• the algorithm of constructing a target trajectory is realized in distributed cerebral structures through the use of neural wave processes with the purpose of determining coordinates of support events, e.g. switching from one motion phase to another;

• finite velocities of signal propagation through nerve fibers account for the relativistic chronogeometry of brain control systems; this means that, in the given case, the relativism is of an instrumental measuring nature.

Definitive verification of the 'relativistic brain' concept is the subject matter of future experimental studies including, without doubt, neurophysiological ones. A great deal of preparatory work is needed to initiate such investigations because the protocols of necessary experiments remain unclear. This statement equally refers to such technical problems as

— testing etalon waves and verifying their etalon nature;

— understanding the role of the body map in the solution of movement construction problems;

— obtaining a target trajectory image.

The list of these unresolved problems indicates that the relativistic concept suggests a new language for the description of intracerebral processes and simultaneously requires the development of new experimental techniques.

This means that the practical applicability of biorelativism is a matter of future developments, the prospects of which are currently obscure. Nevertheless, the fundamental significance of such a paradigm is evident. It is conducive to the constructive revision of the general nature of relativism (including its physical sense) on the ground of freer interpretation of chronogeometries as consequences of measuring procedures using waves as etalon processes.

6. Appendix

The definition of geometry as the theory of geometric invariants was first formulated by F Klein [27, 35]. The constructive version of this theory consists in the identification of base invariant systems [42, 44].

6.1 Notation

Formulas, sentences in italics (definitions, lemmas, etc.), figures and tables are consecutively numbered throughout this section; therefore, references separated by large massifs of text are supplemented with the number of the subsection.

Scalars, i.e. real numbers, are denoted by small letters a, b, α, β, etc., and vectors by small bold letters, e.g. $\mathbf{a}$ and $\mathbf{b}$. Second-order vectors (2-vectors) in expanded form are represented as 2-site columns: $\mathbf{a} \equiv (a_1, a_2)'$, $\mathbf{b} \equiv (b_1, b_2)'$. Primed symbols denote transposition (in the present case, for row representation of the column).

Standard vectors: $\mathbf{o} \equiv (0,0)'$, $\mathbf{e}_1 \equiv (1,0)'$, $\mathbf{e}_2 \equiv (0,1)'$, $\mathbf{e} \equiv \mathbf{e}_1 + \mathbf{e}_2 = (1,1)'$.

Basis expansion of a vector: $\mathbf{a} = a_1\mathbf{e}_1 + a_2\mathbf{e}_2$.

Scalar product of vectors (product of a row and a column): $\mathbf{a}'\mathbf{b} \equiv a_1b_1 + a_2b_2$.

Matrices are denoted by bold capital letters $\mathbf{A}$, $\mathbf{B}$, etc.

Special attention should be given to the frequently used short polyvector representation of matrices as a row of columns (vectors). For example, 2-matrices are written in the following way:

$$\mathbf{0} \equiv (\mathbf{o}, \mathbf{o}), \quad \mathbf{A} = (\mathbf{a}_1, \mathbf{a}_2) \equiv \left((a_{11}, a_{21})', (a_{12}, a_{22})'\right),$$

$$\lambda\mathbf{A} = (\lambda\mathbf{a}_1, \lambda\mathbf{a}_2), \quad \mathbf{A} + \mathbf{B} = (\mathbf{a}_1 + \mathbf{b}_1, \mathbf{a}_2 + \mathbf{b}_2),$$

$$\mathbf{AB} = (\mathbf{Ab}_1, \mathbf{Ab}_2), \quad \mathbf{Ab} = b_1\mathbf{a}_1 + b_2\mathbf{a}_2\,.$$

6.2 Algebraic bases

The standard algebraic matrix basis is nilpotent:

$$\mathbf{E}_{ij}\mathbf{E}_{jk} = \mathbf{E}_{ik}, \quad \mathbf{E}_{ij}\mathbf{E}_{mk} = \mathbf{0}\,, \quad j \neq m\,;$$

however, 2-matrices may be represented in the nonstandard matrix basis $\{\mathbf{E}, \mathbf{F}, \mathbf{I}, \mathbf{J}\}$:

$$\mathbf{E}_{11} \equiv (\mathbf{e}_1, \mathbf{o}),\ \mathbf{E}_{12} \equiv (\mathbf{o}, \mathbf{e}_1),\ \mathbf{E}_{21} \equiv (\mathbf{e}_2, \mathbf{o}),\ \mathbf{E}_{22} \equiv (\mathbf{o}, \mathbf{e}_2), \tag{A.1a}$$

$$\mathbf{E} \equiv (\mathbf{e}_1, \mathbf{e}_2),\ \mathbf{F} \equiv (-\mathbf{e}_1, \mathbf{e}_2),\ \mathbf{I} \equiv (\mathbf{e}_2, \mathbf{e}_1),\ \mathbf{J} \equiv (\mathbf{e}_2, -\mathbf{e}_1). \tag{A.1b}$$

Let an arbitrary 2-matrix $\mathbf{A}$ be represented in these bases in the following way

$$\mathbf{A} \equiv a_{11}\mathbf{E}_{11} + a_{12}\mathbf{E}_{12} + a_{21}\mathbf{E}_{21} + a_{22}\mathbf{E}_{22}$$

$$= a_1\mathbf{E} + a_2\mathbf{F} + a_3\mathbf{I} + a_4\mathbf{J};$$

then, the linear connections between scalar components of the two bases are

$$\mathbf{A} \equiv \left((a_{11}, a_{21})',\ (a_{12}, a_{22})'\right)$$

$$= \left((a_1 - a_2, a_3 + a_4)',\ (a_3 - a_4, a_1 + a_2)'\right). \tag{A.2}$$

Matrices of the nonstandard basis (A.1b) are elements of the dihedral group

$$D^4 \cong \{\mathbf{E}, \mathbf{F}, \mathbf{I}, \mathbf{J}, -\mathbf{E}, -\mathbf{F}, -\mathbf{I}, -\mathbf{J} \,|\, \mathbf{F}^2$$

$$= \mathbf{I}^2 = -\mathbf{J}^2 = -\mathbf{FIJ} = \mathbf{E}\}\,.$$

A group of the 8th-order dihedron, D^4, represents all elementary symmetries of the square (bilateral, central, rotation, see below) and is noncommutative:

$$\mathbf{FI} = -\mathbf{IF} = \mathbf{J},\ \mathbf{FJ} = -\mathbf{JF} = \mathbf{I},\ \mathbf{JI} = -\mathbf{IJ} = \mathbf{F}\,.$$

Symmetric and skew-symmetric components of the arbitrary 2-matrix **A** are

$$\mathrm{symm}(\mathbf{A}) \equiv \frac{\mathbf{A}+\mathbf{A}'}{2} = a_1\mathbf{E} + a_2\mathbf{F} + a_3\mathbf{I},$$
$$\mathrm{skew}(\mathbf{A}) \equiv \frac{\mathbf{A}-\mathbf{A}'}{2} = a_4\mathbf{J}\,. \tag{A.3}$$

The nonstandard basis representation of the arbitrary 2-matrix

$$\mathbf{A} = a_1\mathbf{E} + a_2\mathbf{F} + a_3\mathbf{I} + a_4\mathbf{J} \tag{A.4}$$

can be interpreted as a 'dihedral quaternion' or, briefly, 'diquaternion' (another term is 'antiquaternion' [39]), the real matrix **E** is the analogue of the real unit, and matrices **F**, **I**, **J** are real analogues of imaginary units.

Diquaternion is the solution of the quadratic characteristic equation

$$\mathbf{A}^2 - \mathrm{tr}(\mathbf{A})\mathbf{A} + |\mathbf{A}|\mathbf{E} = \mathbf{0}\,, \tag{A.5}$$

containing two scalar coefficients, namely, trace of a matrix and determinant

$$\mathrm{tr}(\mathbf{A}) \equiv a_{11} + a_{22} = 2a_1,$$
$$|\mathbf{A}| = a_{11}a_{22} - a_{12}a_{21} = a_1^2 - a_2^2 - a_3^2 + a_4^2. \tag{A.6}$$

In the dihedral basis, the determinant is equal to the sum of component determinants

$$|\mathbf{A}| \equiv |a_1\mathbf{E}| + |a_2\mathbf{F}| + |a_3\mathbf{I}| + |a_4\mathbf{J}|$$
$$\Leftarrow |\mathbf{E}| = -|\mathbf{F}| = -|\mathbf{I}| = |\mathbf{J}| = 1. \tag{A.7}$$

When distinguishing vector-columns, determinant of 2-matrices is represented by the skew-symmetric bilinear form:

$$|\mathbf{A}| \equiv |\mathbf{a}_1, \mathbf{a}_2| = \mathbf{a}_1'\mathbf{J}\mathbf{a}_2\,. \tag{A.8}$$

Corollary 6.1. A 2-*matrix with zero-trace is quasi-involutive:*

$$\mathrm{tr}(\mathbf{A}) = 0 \Rightarrow \mathbf{A}^2 = -|\mathbf{A}|\mathbf{E} \equiv (a_2^2 + a_3^2 - a_4^2)\mathbf{E}\,. \tag{A.9}$$

The quaternionly conjugate matrix

$$\mathbf{A}^* \equiv a_1\mathbf{E} - a_2\mathbf{F} - a_3\mathbf{I} - a_4\mathbf{J} = \mathrm{tr}(\mathbf{A})\mathbf{E} - \mathbf{A} = |\mathbf{A}|\mathbf{A}^{-1} \tag{A.10}$$

is useful to distinguish 'real' and 'imaginary' components

$$\mathrm{Re}(\mathbf{A}) \equiv \frac{\mathbf{A}+\mathbf{A}^*}{2} = a_1\mathbf{E}\,,$$
$$\mathrm{Im}(\mathbf{A}) \equiv \frac{\mathbf{A}-\mathbf{A}^*}{2} = a_2\mathbf{F} + a_3\mathbf{I} + a_4\mathbf{J}\,. \tag{A.11}$$

Corollary 6.2. *The imaginary part of the diquaternion is quasi-involutive.*

6.3 Congruent matrices

It is assumed default that only 2-matrices are considered. Such a limitation is necessary to use 2-matrices of the dihedral basis without additional reservations.

Matrices **A** and **B** are termed *congruent* if there is such a nondegenerate matrix **X** which satisfies the matrix equation

$$\mathbf{X}'\mathbf{A}\mathbf{X} = \mathbf{B}\,; \tag{A.12}$$

matrix **M** is *autocongruent* if congruent matrices coincide:

$$\mathbf{X}'\mathbf{M}\mathbf{X} = \mathbf{M}\,. \tag{A.13}$$

Lemma 6.1. *Skew-symmetric matrix* **J** *is autocongruent to a multiplier equal to the transforming matrix determinant*: $\mathbf{X}'\mathbf{J}\mathbf{X} = |\mathbf{X}|\mathbf{J}$.

The proof ensues from (A.12) taking into consideration the bilinear form (A.8). ◆

Corollary 6.3.

$$\mathbf{A}^{-1} = \frac{\mathbf{J}'\mathbf{A}'\mathbf{J}}{|\mathbf{A}|} = \frac{\mathbf{A}^*}{|\mathbf{A}|}\,. \tag{A.14}$$

Lemma 6.2. *Solutions of Eqn* (A.13) *give rise to a matrix group of autocongruences.*

The proof is obvious. ◆

Theorem 6.1. *Matrices of a group of autocongruences can be represented as a matrix exponent.*

Proof. Let us assume that matrices **X** of a continuous group of autocongruences are represented as functions of a real group parameter α: $\mathbf{X} \equiv \mathbf{X}(\alpha)$. Differentiation of Eqn (A.13) with respect to the parameter α distinguishes the exponential matrix **N**:

$$\mathbf{N}'\mathbf{M} = -\mathbf{M}\mathbf{N} \Leftarrow \mathbf{N} \equiv \frac{\mathrm{d}\mathbf{X}}{\mathrm{d}\alpha}\,\mathbf{X}^{-1}\,. \tag{A.15}$$

(1) Let matrix **M** be symmetric: $\mathbf{M}' = \mathbf{M}$. In this case, Eqn (A.15) can be rewritten in the following way: $\mathbf{N}'\mathbf{M} = (\mathbf{M}\mathbf{N})' = -\mathbf{M}\mathbf{N}$, i.e. the product **MN** is skew-symmetric. Therefore, it can be substituted by matrix **J** if $|\mathbf{M}| \neq 0$:

$$\mathbf{M}\mathbf{N} = \mathbf{J} \Rightarrow \mathbf{N} = \mathbf{M}^{-1}\mathbf{J}\,. \tag{A.16}$$

Now, in accord with definition (A.15), it is possible to receive for the known constant matrix **N**:

$$\frac{\mathrm{d}\mathbf{X}}{\mathrm{d}\alpha} = \mathbf{N}\mathbf{X} \Rightarrow \mathbf{X}(\alpha) = \mathbf{e}^{\alpha\mathbf{N}}\,. \tag{A.17}$$

(2) Let matrix **M** be skew-symmetric: $\mathbf{M}' = -\mathbf{M}$. Then, it follows from Eqn (A.15) that $(\mathbf{J}\mathbf{N})' = \mathbf{J}\mathbf{N}$ (assuming $\mathbf{M} = \mathbf{J}$), i.e. the product $\mathbf{J}\mathbf{N} \equiv \mathbf{A}$ is a symmetric matrix. Now, using Eqn (A.4): $\mathbf{A} = a_1\mathbf{E} + a_2\mathbf{F} + a_3\mathbf{I}$, we can compute the exponential matrix

$$\mathbf{N} = \mathbf{J}^{-1}\mathbf{A} = -\mathbf{J}\mathbf{A} = n_2\mathbf{F} + n_3\mathbf{I} + n_4\mathbf{J}\,. \tag{A.18}$$

This completes the formal proof of the theorem. ◆

The dihedral basis (A.1b) contains three elementary symmetric matrices:

$$\mathbf{M} = \{\mathbf{E}, \mathbf{F}, \mathbf{I}\} \Rightarrow \mathbf{N} = \{\mathbf{J}, \mathbf{I}, \mathbf{F}\}\,,$$

to which the following canonical rotation formulas correspond:

$$\mathbf{J}^2 = -\mathbf{E} \Rightarrow \mathbf{e}^{\alpha\mathbf{J}} = \cos\alpha\,\mathbf{E} + \sin\alpha\,\mathbf{J} \equiv \mathbf{R}(\alpha)\,, \tag{A.19}$$

$$\mathbf{I}^2 = \mathbf{E} \Rightarrow \mathbf{e}^{\alpha\mathbf{I}} = \cosh\alpha\,\mathbf{E} + \sinh\alpha\,\mathbf{I} \equiv \mathbf{H}(\alpha)\,, \tag{A.20}$$

$$\mathbf{F}^2 = \mathbf{I} \Rightarrow \mathbf{e}^{\alpha\mathbf{F}} = \cosh\alpha\,\mathbf{E} + \sinh\alpha\mathbf{F} \equiv \mathbf{H}(\alpha). \tag{A.21}$$

Corollary 6.4. *The case of* $\mathbf{M} = \mathbf{E}$ *is equivalent to a group of circular rotations* $\mathbf{R}(\alpha)$, *the case of* $\mathbf{M} = \mathbf{F}$ *to a group of canonical hyperbolic rotations* $\mathbf{H}(\alpha)$, *and* $\mathbf{M} = \mathbf{I}$ *to a group of equilateral hyperbolic rotations* $\overline{\mathbf{H}}(\alpha)$.

If $\mathbf{M}$ is an arbitrary symmetric 2-matrix, then $\mathbf{M} = m_1\mathbf{E} + m_2\mathbf{F} + m_3\mathbf{I}$, in compliance with (A.3). Using Eqn (A.14) once again, we find the general exponential matrix

$$\mathbf{M}^{-1} = \frac{m_1\mathbf{E} - m_2\mathbf{F} - m_3\mathbf{I}}{|\mathbf{M}|} \Rightarrow \mathbf{N} = n_2\mathbf{F} + n_3\mathbf{I} + n_4\mathbf{J}\,, \quad (A.22)$$

where $n_2 \equiv m_3/m$, $n_3 \equiv -m_2/m$, $n_4 \equiv m_1/m$, $|\mathbf{M}| = m_1^2 - m_2^2 - m_3^2 \equiv m$.

Corollary 6.5. *In the general case of a symmetric autocongruent 2-matrix* $\mathbf{M}$, *the exponential matrix* $\mathbf{N}$ *of the exponential form* (A.17) *is represented by the imaginary part of diquaternion, which is quasi-involutive* (*see Corollary* 6.2).

It is possible to regard the autocongruent matrix of Eqn (A.13) as normalized (without the loss of generality), i.e. to assume that $|\mathbf{M}| = \pm 1$. Then, it follows from the general definition (taking into account Lemma 6.1) that the square of the exponential matrix becomes

$$\mathbf{N}^2 \equiv \mathbf{M}^{-1}\mathbf{J}\mathbf{M}^{-1}\mathbf{J} = |\mathbf{M}|^{-1}\mathbf{J}^2 = -|\mathbf{M}|^{-1}\mathbf{E}\,. \quad (A.23)$$

Hence, in view of (A.23), two situations are feasible in the general case:

(1) $|\mathbf{M}| = +1 \Rightarrow \mathbf{N}^2 = -\mathbf{E}$ — circular rotation;

(2) $|\mathbf{M}| = -1 \Rightarrow \mathbf{N}^2 = +\mathbf{E}$ — hyperbolic rotation.

6.4 Geometric bases

The Cartesian procedure for coordinatization of a plane (2-dimensional linear manifold $\mathbf{X}^2$) is reduced to distinguishing a starting point $\mathbf{o} \equiv (0, 0)'$ and two axes represented by the straight lines $\boldsymbol{L}_1 \equiv \boldsymbol{L}(\mathbf{o}, \mathbf{e}_1)$ and $\boldsymbol{L}_2 \equiv \boldsymbol{L}(\mathbf{o}, \mathbf{e}_2)$ incidental to the point pairs $\mathbf{o}, \mathbf{e}_1$ and $\mathbf{o}, \mathbf{e}_2$, respectively. Unit vectors $\mathbf{e}_1$ and $\mathbf{e}_2$ are the standards (etalons) of length for the determination (measurement) of arbitrary point coordinates:

$$\mathbf{x} \equiv (x_1, x_2)' = \mathbf{x}_1 + \mathbf{x}_2 = x_1\mathbf{e}_1 + x_2\mathbf{e}_2 \equiv \mathbf{E}\mathbf{x}\,, \quad (A.24)$$

i.e. here the identity matrix $\mathbf{E} \equiv (\mathbf{e}_1, \mathbf{e}_2)$ is a base matrix and the introduced coordinate system $\mathbf{X}^2 \equiv \{\mathbf{x}|\mathbf{o}, \mathbf{E}\}$ is the system of fixed axes (SFA).

The new system of moving axes (SMA) $\mathbf{Y}^2 \equiv \{\mathbf{y}|\,\mathbf{b}_0, \mathbf{B}\}$ is defined with respect to the SFA (Fig. 17a) by introducing a new starting point $\mathbf{b}_0$ and new basis vectors $\mathbf{b}_1, \mathbf{b}_2$ which form the base matrix $\mathbf{B} \equiv (\mathbf{b}_1, \mathbf{b}_2)$. Now, the former vector $\mathbf{x}$ is represented as the sum of new vectors:

$$\mathbf{x} = \mathbf{b}_0 + \mathbf{y}_1 + \mathbf{y}_2 = \mathbf{b}_0 + y_1\mathbf{b}_1 + y_2\mathbf{b}_2 \equiv \mathbf{b}_0 + \mathbf{B}\mathbf{y}\,, \quad (A.25)$$

where $|\mathbf{B}| \neq 0$. The new coordinates y_i are actually the lengths of vectors $\mathbf{y}_i$ in relation to etalons $\mathbf{b}_i$.

When passing into basis $\mathbf{Y}^2$, the new SMA acquires the SFA status, and conversely the old SFA turns into SMA. This is formally described, based on formulas (A.24) and (A.25), by the simple inversion of base matrix $\mathbf{y} = \mathbf{B}^{-1}(\mathbf{x} - \mathbf{b}_0)$. The result is analogous to (A.25):

$$\mathbf{y} = y_1\mathbf{e}_1 + y_2\mathbf{e}_2 \equiv \mathbf{E}\mathbf{y} = \mathbf{a}_0 + x_1\mathbf{a}_1 + x_2\mathbf{a}_2 \equiv \mathbf{a}_0 + \mathbf{A}\mathbf{x}\,, \quad (A.26)$$

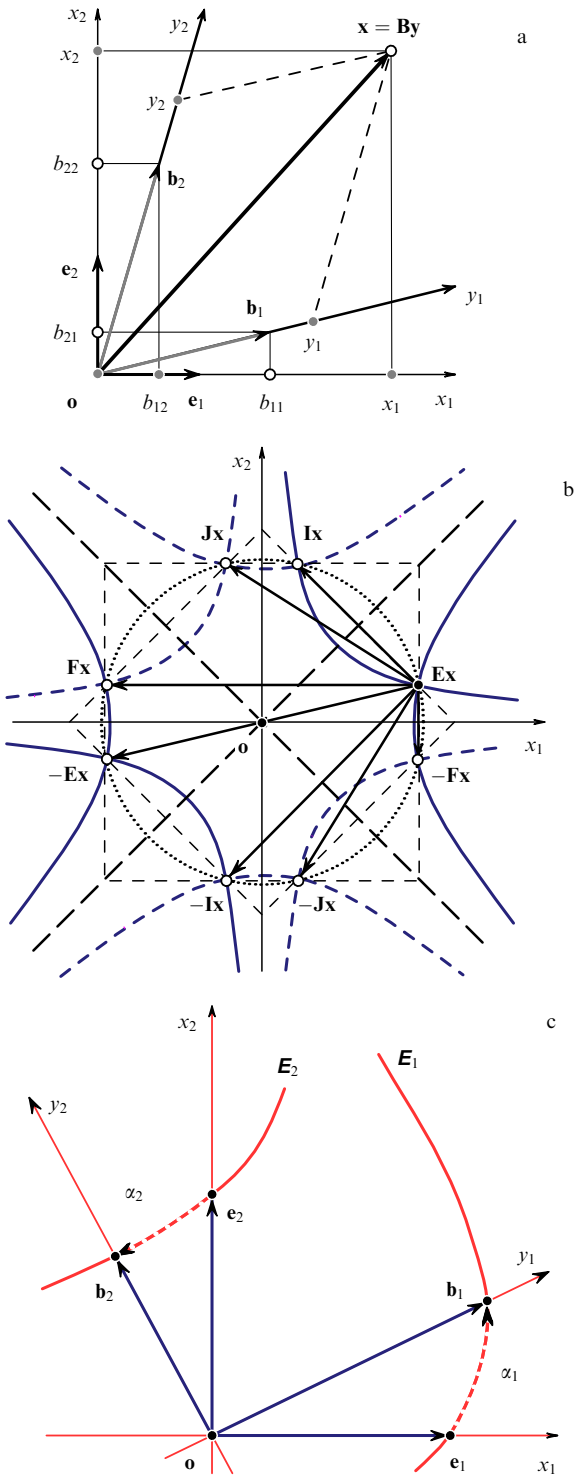

Figure 17. Equivalent points of two coordinate systems (a); symmetries of elementary images of an arbitrary point undergoing the effect of matrix operators of the base dihedral group (b); generalized metaphor of metric plane etalons (c).

where $\mathbf{A} \equiv \mathbf{B}^{-1}$ is the inverse 2-matrix, and $\mathbf{a}_0 \equiv -\mathbf{B}^{-1}\mathbf{b}_0$ is the inverse initial vector.

In the algebraic model of linear space (A.24)–(A.26), the identity matrix $\mathbf{E}$ always represents the observer's intrinsic basis. Therefore, any observer may regard his own basis as a unit $\mathbf{E}$-basis and assume it to be the SFA, while considering nonidentity $\mathbf{B}$ and $\mathbf{A}$ bases to be extraneous and identical to SMA.

6.5 Operator metaphor

The previous base-related interpretation of the vector equality (A.25) is oriented to the 'equivalent points' metaphor.

Definition 6.1. Two points are called *equivalent* if they represent one and the same point of space in different coordinates systems.

Let the SFA and SMA have a common origin, $\mathbf{b}_0 = \mathbf{o}$, and two pairs of equivalent points $\{\mathbf{x}_1, \mathbf{x}_2\} \in \mathbf{X}^2$, $\{\mathbf{y}_1, \mathbf{y}_2\} \in \mathbf{Y}^2$ be given. It is necessary to restore the SMA basis, i.e. to find a matrix $\mathbf{B}$, such that $\mathbf{x}_i = \mathbf{B}\mathbf{y}_i$, $i = 1, 2$.

Matrices of the equivalent pairs, $\mathbf{X} \equiv (\mathbf{x}_1, \mathbf{x}_2)$ and $\mathbf{Y} \equiv (\mathbf{y}_1, \mathbf{y}_2)$, are connected by the base matrix

$$\mathbf{B}\colon\ \mathbf{X} = (\mathbf{x}_1, \mathbf{x}_2) = (\mathbf{B}\mathbf{y}_1, \mathbf{B}\mathbf{y}_2) = \mathbf{B}(\mathbf{y}_1, \mathbf{y}_2) = \mathbf{B}\mathbf{Y}\,, \quad \text{(A.27)}$$

hence, $\mathbf{X} = \mathbf{B}\mathbf{Y}$ and $\mathbf{B} = \mathbf{X}\mathbf{Y}^{-1}$.

A conceptual alternative to the base metaphor is the operator metaphor which implies not only the existence of one and the same space but a single coordinate system as well, namely, the SFA. Then, vectors $\mathbf{x}$ and $\mathbf{y}$ in Eqns (A.25) and (A.26) represent in the general case different points resulting from the action of the operator of direct $\mathbf{A}$ and inverse $\mathbf{B}$ affine transformation:

$$\mathbf{B} \equiv \{\mathbf{b}, \mathbf{B}\}\colon\ \mathbf{x} = \mathbf{b} + \mathbf{B}\mathbf{y} \Leftrightarrow \mathbf{A} \equiv \{\mathbf{a}, \mathbf{A}\}\colon\ \mathbf{y} = \mathbf{a} + \mathbf{A}\mathbf{x}\,. \quad \text{(A.28)}$$

Example. The dihedral group matrices acting as operators on an arbitrary point $\mathbf{x}$ give rise to the vertices of a centrally symmetric octagon (Fig. 17b).

The point of the plane $\mathbf{x} \equiv (x_1, x_2)'$ has two arbitrary coordinates. Therefore, the act of its choice is characterized by two freedoms. We denote this *libernetic* property of the point as $\mathrm{lib}(\mathbf{x}) = 2$ [in the general case of multidimensional spaces, the number of the point's coordinate freedoms is coincident with the space dimensionality, $\mathrm{lib}(\mathbf{x}) = \dim(\mathbf{x})$].

In the case of the operator-based approach, the question arises as to the libernetic resource of an arbitrary transformation, specifically that of the general affine transformation (A.28). This problem is resolved using 'probe figures' containing a fixed set of arbitrary points, $X_m^n \equiv \{\mathbf{x}_1, \ldots, \mathbf{x}_m\}$; the subscript of symbol X_m^n is the number of points (vertices), and the superscript is the space dimensionality, $\mathrm{lib}(X_m^n) = mn$.

Question 6.1. What is the maximum number of points needed to ensure that an arbitrary pair of figures X_m^n and Y_m^n are superposed (congruent) by means of a given transformation?

The answer for linear transformations (A.28) is available from the basic theorem of affine geometry. In the general case $m = n + 1$, because the resources of freedoms of affine transformations and figures are the same:

$$\mathrm{lib}(X_{n+1}^n) = \mathrm{lib}(\mathbf{A}) \equiv \mathrm{lib}(\mathbf{A}) + \mathrm{lib}(\mathbf{a}) = n^2 + n = n(n+1)\,. \quad \text{(A.29)}$$

A particular variant of this general situation is represented by SMA bases (A.25); being geometric objects, they have 3 vertices:

$$\{\mathbf{b}_0, \mathbf{b}_0 + \mathbf{b}_1, \mathbf{b}_0 + \mathbf{b}_2\} = \{\mathbf{x}_1, \mathbf{x}_2, \mathbf{x}_3\} \equiv X_3^2 \Rightarrow \mathrm{lib}(X_3^2) = 6\,. \quad \text{(A.30)}$$

It follows that arbitrary SMA bases are affinely congruent due to the similar parametric freedom resources of both the transformations and bases.

6.6 Free geometries

In the Cartesian method for plane digitalization with the aid of two noncollinear straight lines, the minimal metric rules are used as sufficient for the solution of the plane coordinatization problem. The metric rules are indispensable for any coordinatization. In this sense, there are no nonmetric geometries.

Question 6.2. Does the definition of SFA (A.24) and SMA transformation rules (A.25), (A.26) give rise to a certain geometry?

The answer to this question should be looked for in F Klein's geometry (see Refs [27, 35]) as a theory of geometric invariants. In order to introduce the constructive aspect in the analysis of this theme, assume the following

Definition 6.2. An *invariant* of a transformation (or basis or figure) is designated an additional condition limiting one degree of freedom of this transformation (or basis or figure).

We believe it useful to distinguish between invariants of figures and invariants of transformations, and consider the latter to be invariants of geometries [44].

In his general systematics of geometries, F Klein based his ideas on the group principle and used the criterion of the number of transformation freedoms to rank different geometries.

Group principle. Each geometry is characterized by a certain continuous group and vice versa, the more parametric freedoms a group of transformations has, the higher hierarchic status is ascribed to the corresponding geometry.

Geometric problems related to the analysis of general properties of linear transformations are traditionally considered to be a subject of affine geometry. In the Kleinian interpretation of geometry, the basic referents of such a theory, i.e. its invariants, need to be distinguished.

Let $LG(n, m)$ be the common identifier of a linear group, where n is the space dimensionality, and m is the number of parametric transformation freedoms. General affine transformations preserving the operator structure under the compositions of transformations give rise to a general linear group $LG(n, n^2 + n)$, the unit of which is, as a matter of course, an identical operator $\mathbf{E} = \{\mathbf{o}, \mathbf{E}\}$. The group LG has the maximum number of freedoms intrinsic in linear transformations but has no parametric constraints. In other words, it is a free group and therefore has no invariants, in accord with Definition 6.2.

Corollary 6.6. *Affine geometry as the geometry of a general linear group has no invariants of its own, i.e. it is a free geometry*.

In the forthcoming discussion, we use *centroaffine* transformations as an initial free group; they are defined by all nondegenerate matrices which form a linear group $LG(n, n^2)$.

6.7 General metric metaphor

Metric geometries, such as Euclidean, Galilean, and Minkowskian geometries, are represented in the planimetric version as 1-parametric groups of coordinate transformations, which are in turn subgroups of a general linear group LG. For this reason, metric geometries may be interpreted as subgeometries derived from affine geometry by reducing the parametric freedoms of coordinate transformations or coordinate bases.

In the case of a given affine basis $\mathbf{B} = (\mathbf{b}_1, \mathbf{b}_2)$, we are free to choose etalon vectors $\mathbf{b}_1$ and $\mathbf{b}_2$ arbitrarily and independently.

Let two arbitrary curves $\boldsymbol{E}_1$ and $\boldsymbol{E}_2$ given in the SFA pass through unit points $\mathbf{e}_1$ and $\mathbf{e}_2$ (Fig. 17c). Let the curves $\boldsymbol{E}_1$ and $\boldsymbol{E}_2$ be regarded as etalons of length of all SMA.

What is the outcome of such a global declaration?

Let us also construct in the SFA arbitrary straight lines $\boldsymbol{L}_1 \equiv \boldsymbol{L}(\mathbf{o}, \mathbf{b}_1)$ and $\boldsymbol{L}_2 \equiv \boldsymbol{L}(\mathbf{o}, \mathbf{b}_2)$ intersecting etalons $\boldsymbol{E}_i$ at certain points $\mathbf{b}_i$. Then, vectors $\mathbf{b}_i$ are the base etalons of the new SMA. It is such a linear (affine) parametrization of the straight lines $\boldsymbol{L}_i$ (SMA axes) that gives sense to the global plane metrization with the aid of etalon lines $\boldsymbol{E}_i$, i.e. unit equidistants for a11 conceivable directions of $\boldsymbol{L}_i$ axes.

The new 2-parametric basis $\mathbf{B}(\alpha_1, \alpha_2)$ (Fig. 17c) is defined by vector-functions $\mathbf{b}_i(\alpha_i)$ which are metric invariants (*MI*) of the affine basis:

$$MI_1 : \mathbf{b}_1 = \mathbf{b}_1(\alpha_1), \quad MI_2 : \mathbf{b}_2 = \mathbf{b}_2(\alpha_2) .$$

An additional necessary constraint is $\mathbf{B}(0, 0) = \mathbf{E}$.

In the case of independent changes of angles α_i, the basis axes combine into independent straight line bundles. In order to reduce the independence in the choice of SMA-axes directions, an additional rule of axes correspondence is needed, i.e. a third nonmetric invariant which can be opportunely referred to as *orientational invariant* (*OI*):

$$OI : \mathbf{b}_1 \to \mathbf{b}_2 \Rightarrow \varphi(\alpha_1, \alpha_2) = \text{const} .$$

Thus, the reduction of affine geometry (AG) to metric geometry (MG) is secured by virtue of the base invariant system (BIS):

$$\text{BIS} \sim \{MI_1, MI_2, OI\} : \text{AG} \to \text{MG} ; \tag{A.31}$$

free affine geometry loses three freedoms out of the four, while metric geometry acquires one freedom per rotation.

6.8 Geometries of symmetric quadratic forms

The description of 'solid body' rotation in Euclidean geometry is based on the requirement of quadratic form invariance for the equivalent points $\mathbf{x}$ and $\mathbf{y}$:

$$x_1^2 + x_2^2 = y_1^2 + y_2^2 \Leftrightarrow \mathbf{x}'\mathbf{x} = \mathbf{y}'\mathbf{B}'\mathbf{B}\mathbf{y} = \mathbf{y}'\mathbf{y} ,$$

which [see (A.13)] is equivalent to a property of autocongruence intrinsic in the identity matrix $\mathbf{E}$:

$$\mathbf{B}'\mathbf{E}\mathbf{B} = \mathbf{E} ; \tag{A.32}$$

matrices $\mathbf{B}$ as solutions of this generating equation provide the necessary orthogonal bases which form their own orthogonal group.

In Minkowskian geometry, the invariant quadratic form is represented by the difference (but not the sum) of the squares of coordinates of the equivalent points $\mathbf{x}$ and $\mathbf{y}$:

$$-x_1^2 + x_2^2 = -y_1^2 + y_2^2 \Leftrightarrow \mathbf{x}'\mathbf{F}\mathbf{x} = \mathbf{y}'\mathbf{B}'\mathbf{F}\mathbf{B}\mathbf{y} = \mathbf{y}'\mathbf{F}\mathbf{y} ,$$

therefore, the matrix generating equation contains the metric matrix $\mathbf{F}$:

$$\mathbf{B}'\mathbf{F}\mathbf{B} = \mathbf{F} . \tag{A.33}$$

The invariance condition of the general quadratic form with an arbitrary symmetric (nonsingular) metric matrix $\mathbf{M}$ leads to the matrix equation

$$\mathbf{B}'\mathbf{M}\mathbf{B} = \mathbf{M} . \tag{A.34}$$

The properties of bases $\mathbf{B}$ in this equation have been described earlier (Theorem 6.1, Corollaries 6.4 and 6.5).

Traditional definitions of metric geometries are restricted to the postulates of invariant properties of a scalar vector product, but it is the matrix forms (A.34) that specify the entire base invariant system:

$$\mathbf{B}'\mathbf{M}\mathbf{B} \equiv \left((\mathbf{b}_1'\mathbf{M}\mathbf{b}_1, \mathbf{b}_2'\mathbf{M}\mathbf{b}_1)', \ (\mathbf{b}_1'\mathbf{M}\mathbf{b}_2, \mathbf{b}_2'\mathbf{M}\mathbf{b}_2)'\right) = \mathbf{M} .$$

Here, diagonal scalar equalities represent metric invariants, and nondiagonal ones the orientational invariant. This means that the invariant quadratic form method corresponds to the generalized metric model of BIS (A.30).

It follows from (A.32) that for *Euclidean geometry* (EG)

$$\text{SBI}_{\mathbf{M}=\mathbf{E}} \sim \{\mathbf{b}_1'\mathbf{b}_1 = \mathbf{b}_2'\mathbf{b}_2 = 1, \ \mathbf{b}_1'\mathbf{b}_2 = 0\} , \tag{A.35}$$

i.e. etalons $\boldsymbol{E}_1$ and $\boldsymbol{E}_2$ of the base vectors coincide with one and the same unit circle (Fig. 18a). This suggests an angle between coordinate axes and allows the geometric content of *OI* to be expressed in the following way: the angle between the axes is always the same and right, $\alpha_2 - \alpha_1 = \pi/2$. In case of an elliptical rotation (Fig. 18b), the etalons $\boldsymbol{E}_1$ and $\boldsymbol{E}_2$ are represented by different ellipses but the angles are determined using a common unit circle.

It follows from (A.33) for *Minkowskian geometry* (MG) that

$$\text{SBI}_{\mathbf{M}=\mathbf{F}} \sim \{\mathbf{b}_1'\mathbf{F}\mathbf{b}_1 = -1, \ \mathbf{b}_2'\mathbf{F}\mathbf{b}_2 = 1, \ \mathbf{b}_1'\mathbf{F}\mathbf{b}_2 = 0\} . \tag{A.36}$$

Here, the etalons $\boldsymbol{E}_1$ and $\boldsymbol{E}_2$ are different branches of the hyperbola, having common diagonal asymptotes $x_2 = \pm x_1$ (Fig. 18c). This geometry does not imply an angle between coordinate axes, but the angles α_1 and α_2 of SMA axes with respect to different SFA axes can be measured and compared in terms of size. Then, the geometric content of the *OI* is reduced to the statement of equality of angles: $\alpha_2 = \alpha_1$. In other words, the equality of angles reflects the vector equality $\mathbf{b}_2 \equiv \mathbf{I}\mathbf{b}_1$, i.e. diagonal symmetry of SMA axes.

In Corollary 6.4, a third geometry model $\mathbf{M} = \mathbf{I}$ is also distinguished, the etalons of which are equilateral hyperbolas (Fig. 18d) (their asymptotes coincide with the axes of coordinates). In terms of metric invariant properties, this model looks 'exotic':

$$\text{SBI}_{\mathbf{M}=\mathbf{I}} \sim \{\mathbf{b}_1'\mathbf{I}\mathbf{b}_1 = \mathbf{b}_2'\mathbf{I}\mathbf{b}_2 = 0, \ \mathbf{b}_1'\mathbf{I}\mathbf{b}_2 = 1\}, \tag{A.37}$$

that is the notion of length is interpreted here differently from the way it is in cases (A.35) and (A.36).

6.9 Linear rotations

If the curved etalons in the description of the general metric metaphor are substituted by straight lines, then the SMA base vectors

$$\mathbf{b}_1(\alpha_1) \equiv \mathbf{e}_1 + \alpha_1\mathbf{c}_1, \ \mathbf{b}_2(\alpha_2) \equiv \mathbf{e}_2 + \alpha_2\mathbf{c}_2$$

will make linear rotations. The choice of the group principle of additive parametrization:

$$\mathbf{B}(\alpha_1)\mathbf{B}(\alpha_2) = \mathbf{B}(\alpha_1 + \alpha_2)$$

for the extension of a definition of matrix $\mathbf{B}(\alpha)$, where $\boldsymbol{\alpha} \equiv (\alpha_1, \alpha_2)'$, leads to an 1-parametric group of linear

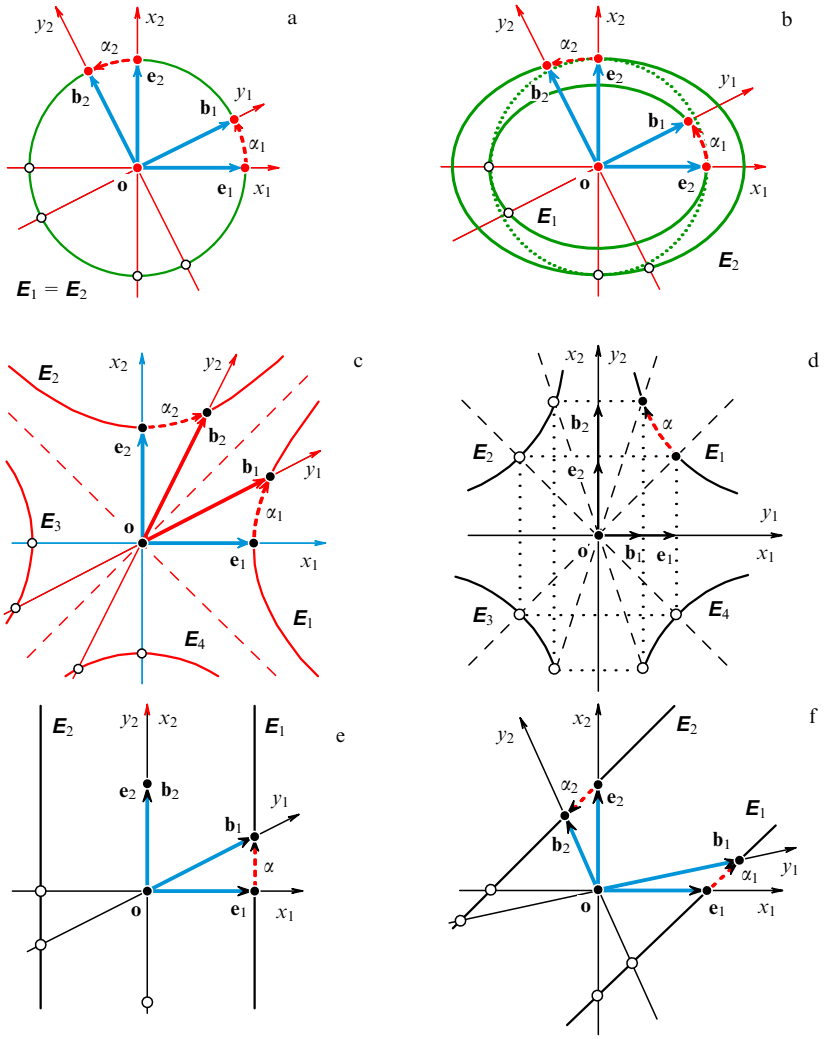

Figure 18. Examples of representation of typical metric geometries through base etalons.

rotations

$$\mathbf{B} = \mathbf{E} + \alpha\mathbf{N} = \mathbf{e}^{\alpha\mathbf{N}}\,, \tag{A.38}$$

where the structural matrix $\mathbf{N} \equiv (\mathbf{e}_1 + c\mathbf{e}_2,\ -c^{-1}\mathbf{e}_1 - \mathbf{e}_2)$ is nilpotent:

$$\mathrm{tr}(\mathbf{N}) = 0,\ |\mathbf{N}| = 0 \Rightarrow \mathbf{N}^2 = \mathbf{0},\ |\mathbf{B}| = \mathbf{e}^{\mathrm{tr}(\alpha\mathbf{N})} = 1\,.$$

The following expression holds for *linear rotation geometry* (LRG) ($c = 1$, Fig. 18f):

$$\mathrm{SBI}_{\mathrm{LRG}} \sim \left\{ b_{11} - \frac{b_{21}}{c} = 1,\ cb_{12} - b_{22} = -1,\ \frac{c}{v_1} + \frac{v_2}{c} = 2 \right\}. \tag{A.39}$$

Theorem 6.2. *Galilean geometry is a limiting variant of linear rotation geometry as* $c \to \infty$.

Proof. In order to effect a linear rotation, the linear α-parametrization needs to be first substituted by projective v-parametrization:

$$v_1 \equiv \frac{b_{21}}{b_{11}} = \frac{c}{1 + \alpha_1^{-1}}\,,\quad v_2 \equiv \frac{b_{22}}{b_{12}} = c(1 + \alpha_2^{-1})\,.$$

The base matrix (A.38) retains its structure and becomes parametrically nonlinear but after the limiting transition the basis is linearly dependent on the parameter:

$$\mathbf{B}(v; c) = \mathbf{E} + \left(\frac{v}{c - v}\right)\mathbf{N}\Big|_{c\to\infty} \to \mathbf{B}(v) = \mathbf{E} + v\mathbf{N} \equiv \mathbf{e}^{v\mathbf{N}}\,, \tag{A.40}$$

where $v \equiv v_1$, and $\mathbf{N} \equiv \mathbf{E}_{21} \equiv (\mathbf{I} + \mathbf{J})/\mathbf{2}$ is the new structural matrix. Now, it follows that $\boldsymbol{E}_1$: $\mathbf{b}_1(v) \equiv \mathbf{e}_1 + v\mathbf{e}_2$ is the vertical straight line (Fig.18e) and $\boldsymbol{E}_2$: $\mathbf{b}_2 \equiv \mathbf{e}_2$, which proves the theorem. ◆

6.10 Numerical models of geometries

Some authors tried to find a relationship between complex or other 2-site algebraic numbers (binions) and metric geometries (see, for example, Refs [39, 60]). An adequate geometric interpretation of binions is possible using real matrix representations which allow numbers to be determined through the employment of the corresponding invariant system, i.e. in the same way as geometries.

A system of two invariants is needed for the transition from a 4-parametric affine group to a 2-parametric binion group. Therefore, binion geometries are two-invariant geometries. The general matrix representation of a binion

$$\mathbf{X} = x_1\mathbf{E} + x_2\mathbf{N} \tag{A.41}$$

contains a structural matrix $\mathbf{N}$ of the 'imaginary' part, the extension of a definition of which is implicitly given by the conditions

$$\mathrm{tr}(\mathbf{N}) = 0\,,\ \ \mathbf{N}^2 \in \{-\mathbf{E}, \mathbf{0}, \mathbf{E}\}\,,$$

where variant $\mathbf{N}^2 = -\mathbf{E}$ corresponds to *complex numbers* (CN), variant $\mathbf{N}^2 = \mathbf{0}$ to dual numbers or *nil-numbers* (NN), and variant $\mathbf{N}^2 = \mathbf{E}$ to *double numbers* (DN).

Simple explicit matrices $\mathbf{N}$ for CN and DN ensue from the dihedral basis (A.1b), and for NN from the Galilean geometry basis (A.40) (see Table 7).

Table 7. Structural matrices of binions.

Number	$\mathbf{N}$	$\mathbf{N}^2$	$\lvert\mathbf{N}\rvert$	$\lvert\mathbf{X}\rvert$
CN	$\mathbf{J}$	$-\mathbf{E}$	1	$x_1^2 + x_2^2$
NN	$\mathbf{E}_{21}$	$\mathbf{0}$	0	x_1^2
DN	$\mathbf{F}, \mathbf{I}$	$\mathbf{E}$	-1	$x_1^2 - x_2^2$

If pairs of binion invariants are determined by comparing the general base matrix $\mathbf{B} = (\mathbf{b}_1, \mathbf{b}_2)$ with matrix (A.41), the reduction of the common basis $\{I_1, I_2\}\!:\mathbf{B} \to \mathbf{X}$ can be expressed by a single vector condition

$$\mathbf{b}_2 = \mathbf{N}\mathbf{b}_1\!: \quad \mathbf{B} = (\mathbf{b}_1, \mathbf{b}_2) = (\mathbf{b}, \mathbf{N}\mathbf{b})\,. \tag{A.42}$$

CN invariants can be represented by scalar products:

$$\{I_1, I_2\} \sim \{\mathbf{b}_2'\mathbf{b}_2 = \mathbf{b}_1'\mathbf{b}_1, \mathbf{b}_1'\mathbf{b}_2 = 0\}\,, \tag{A.43}$$

where I_1 is the equality condition for the Euclidean lengths of basis vectors, and I_2 is the condition of Euclidean basis vector orthogonality. It follows from the polar representation $\mathbf{B} = \rho(\cos\alpha\,\mathbf{E} + \sin\alpha\,\mathbf{J})$ that a third invariant is necessary to obtain Euclidean geometry:

$$I_3\!: \quad |\mathbf{B}| = 1\,, \tag{A.44}$$

which extends the definition of metric etalons to a unit circle.

For DN, there are analogous invariants

$$\{I_1, I_2\} \sim \{\mathbf{b}_2'\mathbf{F}\mathbf{b}_2 = \mathbf{b}_1'\mathbf{F}\mathbf{b}_1, \mathbf{b}_1'\mathbf{F}\mathbf{b}_2 = 0\} \tag{A.45}$$

instead of (A.43), where I_1 is the equality condition for the basis vector lengths in Minkowski metrics, and I_2 is the basis vector orthogonality condition in the same metrics. It follows from DN hyperbolic parametrization

$$\mathbf{B} = \rho\big(\cosh\alpha\,\mathbf{E} + \sinh\alpha\,\mathbf{I}\big)$$

that a third variant is needed to reduce DN geometry to Minkowskian geometry, namely, the unimodularity condition (A.44).

NN geometry arises from affine geometry by virtue of two invariants, and its unimodular version is equivalent to Galilean geometry:

$$\{I_1, I_2, I_3\} \sim \{\mathbf{b}_1 = \mathbf{e}_1 + \alpha\mathbf{e}_2,\ \mathbf{b}_2 = \mathbf{e}_2,\ |\mathbf{B}| = 1\}\,.$$

Numerical models of geometries (NMG) suggest a similarity of invariant specification schemes by which Euclidean, Minkowskian, and Galilean geometries are distinguished from affine geometry. In these models, the first invariant is termed *metric* (*MI*), the second *orientational* (*OI*), and the third *unimodular* (*UI*).

Thus, we have proved the following:

Theorem 6.3. *The BIS of numerical models of geometries is different from the BIS of the general metric metaphor* (A.31):

$$\mathrm{SBI}_{\mathrm{NMG}} \sim \{I_1, I_2, I_3\} \sim \{MI, OI, UI\}\,. \tag{A.46}$$

If binion groups (algebras) are interpreted as subgroups (subalgebras) of the diquaternion group (algebra):

$$\mathbf{A} = a_1\mathbf{E} + a_2\mathbf{F} + a_3\mathbf{I} + a_4\mathbf{J}\,,$$

it is possible to indicate two-invariant algebraic systems by means of which the necessary reduction is achieved: quaternion $\to$ binion or $\mathbf{A} \to \mathbf{X}$, with $\mathbf{X}$ having the form of (A.41). For example, the following pairs of conditions correspond to different variants of the choice of matrix $\mathbf{N}$ from Table 7:

$$\mathrm{CN}: a_2 = a_3 = 0\,, \quad \mathrm{NN}: a_2 = a_3 + a_4 = 0\,,$$
$$\mathrm{DN}: a_2 = a_4 = 0 \vee a_3 = a_4 = 0\,.$$

CN and DN geometries are constructed in different group bases of matrices $\{\mathbf{E}, \mathbf{I}\}$ and $\{\mathbf{E}, \mathbf{J}\}$. Matrices $\{\mathbf{E}, \mathbf{I}\}$ form a cyclic group $C^2 \cong \{\mathbf{E}, \mathbf{I}\} \cong \{\mathbf{E}, -\mathbf{E}\}$ or a group of involutions.

DN algebra is defined in the dihedral group basis

$$D^2 \cong \{\mathbf{E}, \mathbf{I}\} \times \{\mathbf{E}, -\mathbf{E}\} \cong \{\mathbf{E}, \mathbf{I}, -\mathbf{E}, -\mathbf{I}\}\,.$$

CN algebra is defined in the group basis of the 4-order cyclic group

$$C^4 \cong \{\mathbf{E}, \mathbf{J}, -\mathbf{E}, -\mathbf{J}\} \cong \{\mathbf{E}, \mathbf{J}, \mathbf{J}^2, \mathbf{J}^3\}\,.$$

There are only two nonisomorphic groups (cyclic C^4 and dihedral D^2) [40] among abstract 4-order groups.

Corollary 6.7. *CN and DN geometries as well as Euclidean and Minkowskian geometries have nonisomorphic group bases.*

The NN basis is not a group basis, and the nilpotent matrix $\mathbf{N}$, $\mathbf{N}^2 = \mathbf{0}$ cannot be an element of the discrete multiplicative group, whereas an algebra constructed in the nilpotent basis is a continuous group. A similar situation occurs for the choice of the standard nilpotent matrix basis (A.1a).

6.11 Polar coordinates models

The exponential formulas (A.20), i.e. matrix analogues of the known Euler scalar formula for complex numbers, introduce polar representations of base and other matrices, because the distinguished scalar parameter α is geometrically interpreted as the rotational transformation angle. Exponential representations of rotations are canonical polar forms which ensure additivity of angles in rotation compositions:

$$\mathbf{B}(\alpha_1)\mathbf{B}(\alpha_2) = \mathbf{B}(\alpha_1 + \alpha_2)\,.$$

Let us consider another models of polar representations.

In the transition from the Cartesian coordinates of point $\mathbf{x} \equiv (x_1, x_2)'$ to the polar coordinates $\mathbf{x} \equiv \rho\mathbf{a}(\alpha)$, the role of standards (etalons) of length ρ and protractors of angle α is played by various straight and curved lines. Standards of length can simultaneously serve as protractors, especially in

Euclidean, Minkowskian, and Galilean geometries (Fig. 18a, c, e). Conversely, lengths and angles can be measured using different etalons. In the definition of elliptical rotations (Fig. 18b), etalons of length are different ellipses, while protractors are a common unit circle.

Figure 19a demonstrated three variants of the choice of etalon straight lines:

$$\boldsymbol{L}_1 \equiv \boldsymbol{L}(\mathbf{e}_1, \mathbf{e})\,, \quad \boldsymbol{L}_2 \equiv \boldsymbol{L}(\mathbf{e}_2, \mathbf{e})\,, \quad \boldsymbol{L}_3 \equiv \boldsymbol{L}(\mathbf{e}_1, \mathbf{e}_2)\,,$$

which yield three linear models of polar coordinates (PC):

$$\mathbf{x} = \rho_1(1, \alpha_1)' \Leftarrow \rho_1 \equiv x_1,\ \alpha_1 \equiv \frac{x_2}{x_1}\,, \tag{A.47}$$

$$\mathbf{x} = \rho_2(\alpha_2, 1)' \Leftarrow \rho_2 \equiv x_2,\ \alpha_2 \equiv \frac{x_1}{x_2}\,, \tag{A.48}$$

$$\mathbf{x} = \rho(1-\lambda, \lambda)' \Leftarrow \rho \equiv \mathbf{e}'\mathbf{x},\ \lambda \equiv \frac{x_2}{\rho}\,. \tag{A.49}$$

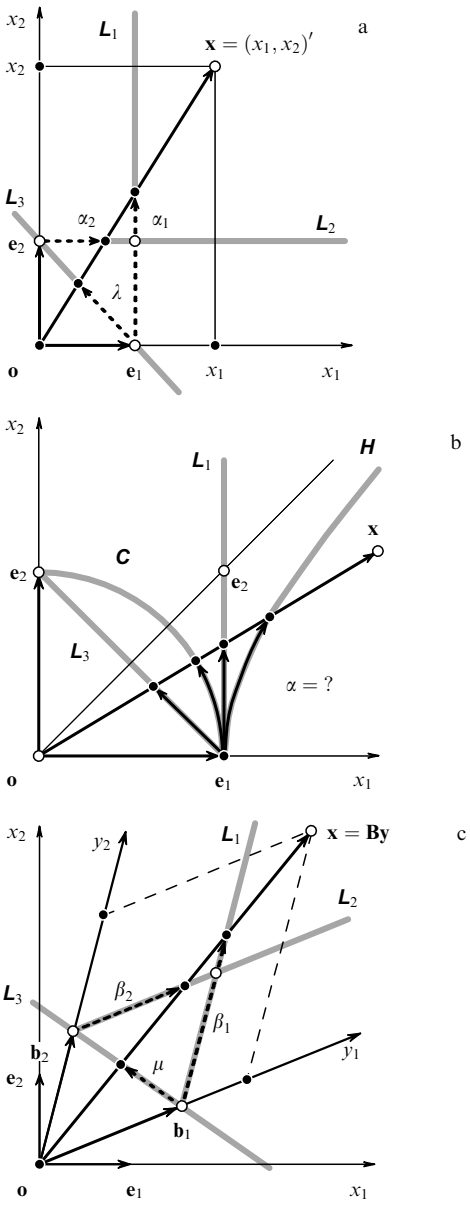

Figure 19. Angular measures of linear and nonlinear etalons.

Intrinsic angular measures of these etalons are related in a linear-fractional way:

$$\lambda = \frac{\alpha_1}{1+\alpha_1} = \frac{1}{1+\alpha_2} \Leftrightarrow \alpha_1 = \frac{1}{\alpha_2} = \frac{\lambda}{1-\lambda}\,. \tag{A.50}$$

These relations can be used to transfer (map) angular parametrizations from one etalon to another. The mapping $\lambda \to \alpha \equiv \alpha_1$ results in projective α-parametrization, instead of affine λ-parametrization (A.49):

$$\mathbf{x} \equiv \rho\,\mathbf{a}(\alpha) = \rho\big(\mathrm{cl}(\alpha), \mathrm{sl}\,(\alpha)\big)' \Leftarrow \rho \equiv \mathbf{e}'\mathbf{x},\ \mathrm{tl}\,(\alpha) \equiv \frac{x_2}{x_1}\,; \tag{A.51}$$

here, linear cosine and sine functions

$$\mathrm{cl}\,(\alpha) \equiv \frac{1}{1+\alpha},\quad \mathrm{sl}\,(\alpha) \equiv \frac{\alpha}{1+\alpha},\quad \mathrm{cl}\,(\alpha) + \mathrm{sl}\,(\alpha) = 1\,,$$

and a linear tangent function

$$\mathrm{tl}\,(\alpha) \equiv \frac{\mathrm{sl}\,(\alpha)}{\mathrm{cl}\,(\alpha)} = \alpha$$

were introduced.

In the polar descriptions of linear (A.51), circular, and hyperbolic rotations

$$\mathbf{x} = \rho\big(\cos\alpha, \sin\alpha\big)' \Leftarrow \rho^2 \equiv \mathbf{x}'\mathbf{E}\mathbf{x}, \tan\alpha \equiv \frac{x_2}{x_1}\,, \tag{A.52}$$

$$\mathbf{x} = \rho\big(\cosh\alpha, \sinh\alpha\big)' \Leftarrow \rho^2 \equiv \mathbf{x}'\,\mathbf{F}\mathbf{x}, \tanh\alpha \equiv \frac{x_2}{x_1} \tag{A.53}$$

there is a standard tendency to prefer the projective parameter (Cartesian coordinate ratio x_2/x_1) as a primary angular measure providing the basis on which to determine various functions of angle α for etalons of different form (Fig.19b).

Note 6.1. The definition of the Euclidean angle as the Euclidean arc length of a circle, using the differential quadratic form $\mathrm{d}\alpha^2 = \mathrm{d}\mathbf{x}'\mathbf{E}\,\mathrm{d}\mathbf{x}$, gives rise to the angle trigonometric functions. This method is employed in differential geometry for the natural parametrization of arbitrary continuous lines. Hyperbolic etalons of Minkowskian geometry are also amenable to natural parametrization, but hyperbolic functions of an angle need parametrization based on the hyperbolic quadratic form $\mathrm{d}\alpha^2 = \mathrm{d}\mathbf{x}'\mathbf{F}\,\mathrm{d}\mathbf{x}$.

6.12 Linear-fractional transformations

Let **x** and **y** be the equivalent points of the SFA and SMA. The affine relation between the Cartesian coordinates of these points undergoes transformation to a linear-fractional relation between their angles:

$$\mathbf{x} = \mathbf{B}\mathbf{y} \Rightarrow \alpha = \frac{b_{11}\beta + b_{12}}{b_{21}\beta + b_{22}} \equiv \mathrm{fr}(\beta; \mathbf{B})\,; \tag{A.54}$$

here, $\alpha \equiv x_1/x_2 \equiv \alpha_2$, $\beta \equiv y_1/y_2 \equiv \beta_2$ (Fig.19a,b), and $\mathrm{fr}(\beta; \mathbf{B})$ is the common identifier of the linear-fractional transformation (LFT) associated with matrix **B** of the affine linear transformation (ALT).

The transition ALT $\to$ LFT occurs with the explicit loss of base transformation dimensionality. That is to say, vector transformation is replaced by scalar transformation with the implicit loss of one parametric freedom hidden in the possibility to reduce the common multiplier of the numerator and denominator.

The inverse transition LFT $\to$ ALT:

$$\alpha \equiv \frac{x_1}{x_2} \to \mathbf{x} \equiv (x_1, x_2)', \quad \beta \equiv \frac{y_1}{y_2} \to \mathbf{y} \equiv (y_1, y_2)' \qquad \text{(A.55)}$$

is performed by introducing a common undetermined scalar multiplier necessary to restore ALT parametric freedoms:

$$\beta = \mathrm{fr}(\alpha; \mathbf{A}) \to \mathbf{y} = \rho \mathbf{A}\mathbf{x} \vee \alpha = \mathrm{fr}(\beta; \mathbf{B}) \to \mathbf{x} = \sigma \mathbf{B}\mathbf{y}\,, \qquad \text{(A.56)}$$

where $\mathbf{B} = \mathbf{A}^{-1}$, and $\sigma = \rho^{-1}$. Transformations (A.55) are normally referred to as *the transition from the nonuniform coordinates of a straight line to the uniform coordinates of a plane* [65].

The arbitrary LFT (A.54) with a nondegenerate 2-matrix of coefficients $\mathbf{B}$, $|\mathbf{B}| \neq 0$ form a 3-parametric projective group $PG(1,3)$ with respect to the operation of composition $\mathrm{fr}(\mathrm{fr}(\beta; \mathbf{B}_1); \mathbf{B}_2) = \mathrm{fr}(\beta; \mathbf{B}_2\mathbf{B}_1)$ equivalent to the product of matrices, i.e. a group operation of the affine group. Major variants of matrix transformations in LFT formulas are summarized in Table 8.

Table 8. Main LFT formulas.

1	$\beta = \mathrm{fr}(\alpha; \mathbf{E})$	$\beta = \alpha$
2	$\beta = \mathrm{fr}(\alpha; \mathbf{A})$	$\alpha = \mathrm{fr}(\beta; \mathbf{A}^{-1})$
3	$\beta = \mathrm{fr}(\alpha; \mathbf{A}_1), \gamma = \mathrm{fr}(\beta; \mathbf{A}_2)$	$\gamma = \mathrm{fr}(\alpha; \mathbf{A}_2\mathbf{A}_1)$
5	$\mathrm{fr}(\alpha; \mathbf{A}_1) = \mathrm{fr}(\beta; \mathbf{A}_2)$	$\beta = \mathrm{fr}(\alpha; \mathbf{A}_2^{-1}\mathbf{A}_1)$
6	$\beta^{-1} = \mathrm{fr}(\alpha^{-1}, \mathbf{A})$	$\beta = \mathrm{fr}(\alpha; \mathbf{IAI})$
7	$\beta = \mathrm{fr}(d_1\alpha/d_2; \mathbf{A})$	$\beta = \mathrm{fr}(\alpha; \mathbf{AD})$
8	$\beta = (d_1/d_2)\mathrm{fr}(\alpha; \mathbf{A})$	$\beta = \mathrm{fr}(\alpha; \mathbf{DA})$

The formulas are arranged on numbered lines, with 1 being identical transformation, 2 — inverse transformation, 3 — composition, etc. In formulas 7 and 8, the matrix $\mathbf{D} = \mathrm{diag}(d_1, d_2)$.

Explicit reconstruction of an LFT 3-parametric matrix is possible by means of the scalar projective basis.

In an SFA (Fig. 19a), three points $\{\mathbf{e}_1, \mathbf{e}/2, \mathbf{e}_2\} \in \boldsymbol{L}_3 \equiv \boldsymbol{L}(\mathbf{e}_1, \mathbf{e}_2)$ (see (A.50)) correspond to the following triples of angular parameters:

$$\lambda = \left\{0, \frac{1}{2}, 1\right\} \to \alpha_1 = \{0, 1, \infty\} \to \alpha_2 = \{\infty, 1, 0\}\,.$$

In the SMA (Fig. 19c), three equivalent points $\{\mathbf{b}_1, \mathbf{b}/2, \mathbf{b}_2 \,|\, \mathbf{b} \equiv \mathbf{b}_1 + \mathbf{b}_2\} \in \boldsymbol{L}_3 \equiv \boldsymbol{L}(\mathbf{b}_1, \mathbf{b}_2)$ correspond to the same values of equivalent angular parameters:

$$\mu = \left\{0, \frac{1}{2}, 1\right\} \to \beta_1 = \{0, 1, \infty\} \to \beta_2 = \{\infty, 1, 0\}\,.$$

The substitution of base values $\beta = \{0, 1, \infty\}$ into LFT (A.54) yields

$$\beta = \frac{(\alpha_1 - \alpha_\infty)/(\alpha_1 - \alpha_0)}{(\alpha - \alpha_\infty)/(\alpha - \alpha_0)}\,. \qquad \text{(A.57)}$$

Here, $\alpha_1 \equiv \mathrm{fr}(1; \mathbf{B})$, etc., that is coefficient matrix $\mathbf{A} \equiv \mathbf{B}^{-1}$ of the 3-parametric base LFT $\beta \equiv \mathrm{fr}(\alpha; \mathbf{A})$ can be represented as a product of two matrices:

$$\mathbf{A} \equiv \mathrm{diag}(\alpha_1 - \alpha_\infty, \alpha_1 - \alpha_0)(\mathbf{e}, -\alpha_0\mathbf{e}_1 - \alpha_\infty\mathbf{e}_2)\,, \qquad \text{(A.58)}$$

$$|\mathbf{A}| = (\alpha_1 - \alpha_0)(\alpha_1 - \alpha_\infty)(\alpha_0 - \alpha_\infty)\,.$$

The inverse LFT is defined in the same way.

6.13 Projective invariant

The projective invariant (wurf) of four angles $\{\alpha_1, \alpha_2, \alpha_3, \alpha_4\}$ is traditionally represented in the form of a double ratio of four differences:

$$\mathrm{w}(\alpha_1, \alpha_2, \alpha_3, \alpha_4) \equiv \frac{(\alpha_1 - \alpha_3)/(\alpha_1 - \alpha_4)}{(\alpha_2 - \alpha_3)/(\alpha_2 - \alpha_4)}\,. \qquad \text{(A.59)}$$

The wurf is interesting in that its value is an LFT invariant:

$$\alpha = \mathrm{fr}(\beta; \mathbf{B}) \Rightarrow \mathrm{w}(\alpha_1, \alpha_2, \alpha_3, \alpha_4) = \mathrm{w}(\beta_1, \beta_2, \beta_3, \beta_4)\,.$$

The comparison of formulas (A.59) and (A.57) reveals the connection

$$\beta = \mathrm{w}(\alpha, \alpha_1, \alpha_0, \alpha_\infty)\,. \qquad \text{(A.60)}$$

This means that the base LFT is a function and can be represented as a wurf. The inverse representation of the wurf in the form of LFT is also possible:

$$\mathrm{w}(\alpha_1, \alpha_2, \alpha_3, \alpha_4) = \frac{d_1}{d_2} \Rightarrow \alpha_2 = \mathrm{fr}(\alpha_1; \mathbf{A})\,,$$

where $\mathbf{A} = \mathbf{X}^{-1}\mathbf{D}^{-1}\mathbf{X}$ and $\mathbf{X} \equiv -\mathbf{F} + (x_4^{-1}\,\mathbf{e}_2, -x_3\mathbf{e}_1)$, $\mathbf{D} \equiv \mathrm{diag}\,(d_1, d_2)$.

For the systematics of invariants of plane geometries, the wurf may be represented profitably in a bilinear form:

$$\frac{y_1}{y_2} = \mathrm{fr}\left(\frac{x_1}{x_2}; \mathbf{A}\right) \Rightarrow \mathbf{y}'\mathbf{M}\mathbf{x} = 0,\ \mathbf{M} = \mathbf{J}\mathbf{A}\,. \qquad \text{(A.61)}$$

The bilinear condition $\mathbf{y}'\mathbf{J}\mathbf{A}\mathbf{x} = 0$ at $\mathbf{A} = \mathbf{J}$ corresponds to Euclidean orthogonality of vectors $\mathbf{y}$ and $\mathbf{x}$. Hence, if $\mathbf{A}$ is an arbitrary LFT matrix, condition (A.61) may be interpreted as a projective orthogonality condition.

6.14 Unimodular invariant

Because unimodular matrices constitute a group, it is appropriate to speak about unimodular geometry in accordance with the Klein group principle. The plane variant of such geometry is of special interest. It follows from Lemma 6.1 that

$$|\mathbf{B}| = 1 \Leftrightarrow \mathbf{B}'\mathbf{J}\mathbf{B} = \mathbf{J}\,, \qquad \text{(A.62)}$$

i.e. unimodular planimetry is equivalent to symplectic planimetry which is generated by the invariant skew-symmetric form [13, 20].

According to Theorem 6.1 or formulas (A.17) and (A.18) for that matter, one has

$$\mathbf{B}(\alpha) = \mathbf{e}^{\alpha\mathbf{N}} = b_1\mathbf{E} + b_2\mathbf{N} \Leftarrow \mathbf{N} = n_2\mathbf{F} + n_3\mathbf{I} + n_4\mathbf{J}\,. \qquad \text{(A.63)}$$

The functional aspect of scalar components b_1 and b_2 of the binion form (A.63) depends on the determinant of the structural matrix $\mathbf{N}$, since $\mathbf{N}^2 = -|\mathbf{N}|\mathbf{E}$, where $|\mathbf{N}| = -n_2^2 - n_3^2 + n_4^2$. Three values of this determinant $|\mathbf{N}| = \{1, 0, -1\}$ correspond to the geometry with three types of rotation, i.e. elliptical, linear, and hyperbolic. If the determinant is fixed, the structural matrix $\mathbf{N}$ has two free parameters which can be represented as angles α_1 and α_2 of the trigonometric and hyperbolic functions listed in Table 9.

Now, metric Euclidean (EG), Galilean (GG), and Minkowskian (MG) geometries can be interpreted now as

Table 9. Components of a symplectic basis.

$\lvert\mathbf{N}\rvert$	$\mathbf{N}^2$	b_1	b_2	n_2	n_3	n_4
1	$-\mathbf{E}$	$\cos\alpha$	$\sin\alpha$	$\sinh\alpha_1\cos\alpha_2$	$\sinh\alpha_1\sin\alpha_2$	$\sinh\alpha_1$
0	$\mathbf{0}$	1	α	$\alpha_1\cos\alpha_2$	$\alpha_1\sin\alpha_2$	α_1
-1	$\mathbf{E}$	$\cosh\alpha$	$\sinh\alpha$	$\cos\alpha_1$	$\sin\alpha_1\cosh\alpha_2$	$\sin\alpha_1\sinh\alpha_2$

concrete cases of symplectic planimetry:

$$\mathrm{EG}\colon\ |\mathbf{N}|=1,\ \alpha_1=0;\quad \mathrm{GG}\colon |\mathbf{N}|=0,\ \alpha_1=1,\ \alpha_2=\frac{\pi}{2};$$

$$\mathrm{MG}: |\mathbf{N}|=-1,\ \alpha_1=0\,. \qquad \text{(A.64)}$$

In summary, the initial postulate of unimodular base 2-matrix is fairly constructive for analytic specification of symplectic planimetry models, because it additionally takes into consideration the properties of autocongruence of a skew-symmetric 2-matrix.

References

1. Aristotle *De Animalibus Historia* (Lipsiae: B.G. Teubneri, 1907) [Translated into Russian (Moscow: ITs RGGU, 1996)]
2. Aristotle *Opera* 3 (Berolini: G. Reimerum, 1831) [Translated into Russian (Moscow: Mysl', 1981)]
3. Artem'eva E N, Smolyaninov V V *Biomekhanika* **24** 70 (1992)
4. Artem'eva E N, Smolyaninov V V *Biofizika* **38** (4) 714 (1993)
5. Artem'eva E N et al., in *Mozzhechok i Struktury Stvola Mozga* (Cerebellum and Cerebral Trunk Structures) (Erevan: Gitugyun, NAN RA, 1995) p. 14
6. Artem'eva E N et al. *Med. Biomekhanika* **3** 26 (1986)
7. Arshavskiĭ Yu I et al. *Biofizika* **10** (3) 665 (1965)
8. Beletskiĭ V V *Dvunogaya Khod'ba* (Bipedal Walk) (Moscow: Nauka, 1984)
9. Bellman R *Introduction to Matrix Analysis* (New York: McGraw-Hill, 1960) [Translated into Russian (Moscow: Nauka, 1969)]
10. Bernshteĭn N A *Ocherki po Fiziologii Dvizheniĭ i Fiziologii Aktivnosti* (Essays on Physiology of Motion and Physiology of Activity) (Moscow: Medgiz, 1966)
11. Burke W *Spacetime, Geometry, Cosmology* (Mill Valley, Calif.: University Science Books, 1980) [Translated into Russian (Moscow: Mir, 1985)]
12. Bondi H *Assumption and Myth in Physical Theory* (Cambridge: Cambridge University Press, 1967) [Translated into Russian (Moscow: Mir, 1972)]
13. Weyl H *The Classical Groups. Their Invariants and Representations* (Princeton: Princeton University Press, 1939) [Translated into Russian (Moscow: IL, 1947)]
14. Wiener N *Cybernetics* (New York: J. Wiley, 1948) [Translated into Russian (Moscow: Sov. radio, 1968)]
15. Gambaryan P P *Beg Mlekopitayushchikh* (Running in Mammals) (Leningrad: Nauka, 1972)
16. Gel'fand I M, Tsetlin M L *Dokl. Akad. Nauk SSSR* **131** (6) 1242 (1960)
17. Gel'fand I M et al., in *Modeli Strukturno-Funktsional'noĭ Organizatsii Nekotorykh Biologicheskikh Sistem* (Models of Structural and Functional Organization of Certain Biological Systems) (Moscow: Nauka, 1966) p. 264
18. Ginzburg V L *O Teorii Otnositel'nosti* (On the Theory of Relativity) (Moscow: Nauka, 1979)
19. Goubaux A, Barrier G *The Exterior of the Horse* (Philadelphia: J.B. Lippincott Co., 1892) [Translated into Russian (Orel, 1901)]
20. Gurfinkel' V S et al., in *Issledovaniya Robototekhnicheskikh Sistem* (Studies on Robototechnical Systems) (Moscow: Nauka, 1980) p. 15
21. Gurfinkel' V S, Fomin S V, Shtil'kind T K *Biofizika* **15** 380 (1970)
22. Descartes R *Discours de la Methode Pour bien Conduire sa Raison et Chercher la Verite Dans les Sciences. Plus le Dioptrique, les Meteores et la Geometrie* (Paris: J. Vrin, 1930) [Translated into Russian (Moscow: AN SSSR, 1953)]
23. Dubrovin B A, Novikov S P, Fomenko A T *Sovremennaya Geometriya* (Modern Geometry) (Moscow: Nauka, 1986) [Translated into English (New York: Springer-Verlag, 1992)]
24. Dieudonne J *Algebra Lineaire et Geometrie Elementaire* (Paris: Hermann, 1968) [Translated into Russian (Moscow: Nauka, 1972)]
25. Zatsiorskiĭ V M, Aruin A S, Seluyanov V N *Biomekhanika Dvigatel'nogo Apparata Cheloveka* (Biomechanics of Human Locomotor System) (Moscow: Fizkul'tura i sport, 1981)
26. Karpovich A L, Smolyaninov V V *Zh. Evolutsion. Biokhim. Fiziol.* **10** (5) 480 (1974)
27. Karpovich A L, Smolyaninov V V *Fiziol. Cheloveka* **1** (1) 167 (1975)
28. Karpovich A L, Smolyaninov V V, in *Biomekhanika* (Trudy Rizhskogo NII Travmatologii i Ortopedii) Vol. 13 (Riga, 1975) p. 672
29. Karpovich A L, Smolyaninov V V *Zh. Evolutsion. Biokhim. Fiziol.* **13** (1) 31 (1977)
30. Karpovich A L, Smolyaninov V V, in *Lokomotsiya Zhivotnykh i Biomekhanika Oporno-Dvigatel'nogo Apparata* (Animal Locomotion and Biomechanics of the Locomotor System) (Kiev: Naukova Dumka, 1979) p. 182
31. Klein F *Elementarmathematik vom höheren Standpunkte aus* Bd. 1 *Arithmetik, Algebra, Analyse*; Bd. 2 *Geometrie* (Berlin: Springer, 1968) [Translated into Russian (Moscow: Nauka, 1987)]
32. Clifford W C *Common Sense of the Exact Sciences* (New York: D. Appleton and Co., 1888) [Translated into Russian (Petrograd, 1922)]
33. Crick F, in *The Brain* (New York: Scientific American, 1979) [Translated into Russian (Moscow: Mir, 1982) p. 256]
34. Kublanov M G, Smolyaninov V V, in *Intellektual'nye Protsessy i Ikh Modelirovanie* (Intellectual Processes and Their Modelling) (Moscow: Nauka, 1992) p. 117
35. Kuhn T S *The Structure of Scientific Revolutions* (Chicago: Univ. of Chicago Press, 1970) [Translated into Russian (Moscow: Progress, 1975)]
36. Lanczos C *The Variational Principles of Mechanics* (Toronto: Univ. of Toronto Press, 1949) [Translated into Russian (Moscow: Mir, 1965)]
37. Marey E *Mechanics of Animal Organism* (New York, 1874) [Translated into Russian (St.-Petersburg: Znanie, 1875)]
38. Marder L *Time and the Space Traveller* (London: Butterworths, 1971) [Translated into Russian (Moscow: Mir, 1974)]
39. *Nekotorye Voprosy Mekhaniki Robotov i Biomekhaniki* (Current Problems of Robotomechanics and Biomechanics) (Moscow: MGU, 1978)
40. Norden A P (Ed.) *Ob Osnovaniyakh Geometrii* (Fundamentals of Geometry) (Moscow: Gostekhizdat, 1956)]
41. Pauli W *The Theory of Relativity* (New York: Dover Publ., 1981) [Translated into Russian (Moscow: Nauka, 1983)]
42. Tyapkin A A (Compil.) *Printsip Otnositel'nosti* (Principle of Relativity) (Moscow: Atomizdat, 1973)
43. Poincaré H *O Nauke* (About Science) (Ed. L S Pontryagin) (Moscow: Nauka, 1983)
44. Rozenfel'd B A *Neevklidovy Geometrii* (Non-Euclidean Geometries) (Moscow: GITTL, 1955)
45. Szentagothai J, Arbib M *Conceptual Models of Neural Organization* (Boston: The MIT Press, 1974) [Translated into Russian (Moscow: Mir, 1976)]
46. Skornyakov L A *Elementy Algebry* (Elements of Algebra) (Moscow: Nauka, 1980)
47. Skvortsov D V *Klinicheskiĭ Analiz Dvizheniĭ. Analiz Pokhodki* (Clinical Analysis of Movements. Analysis of Gaits) (Moscow: MBN, 1996)
48. Smolyaninov V V, in *Matematicheskaya Teoriya Biologicheskikh Protsessov. Tezisy Dokladov 1-ĭ Konf., Kaliningrad, 1976* (Mathematical Theory of Biological Processes. Proc. 1st Conf. held in Kaliningrad, 1976) (Exec. Ed. A K Prits) (Kaliningrad, 1976) p. 276
49. Smolyaninov V V "Lokomotornaya teoriya otnositel'nosti" (Locomotor theory of relativity) Preprint IPPI AN SSSR (Moscow: IPPI AN SSSR, 1984)
50. Smolyaninov V V "Strukturnye i funktsional'nye invarianty raspredelennykh biologicheskikh sistem" (Structural and functional invariants of distributed biological systems) Preprint NTsBI AN SSSR (Pushchino: NTsBI AN SSSR, 1985)

51. Smolyaninov V V, in *Intellektual'nye Protsessy i Ikh Modelirovanie* (Intellectual Processes and Their Modelling) (Moscow: Nauka, 1992) p. 66
52. Smolyaninov V V *Biol. Zh. Armenii* **8** 712 (1990)
53. Smolyaninov V V, in *Mozzhechok i Struktury Stvola Mozga* (Cerebellum and Cerebral Trunk Structures) (Erevan: Gitugyun, NAN RA, 1995) p. 378
54. Smolyaninov V V *Dokl. Ross. Akad. Nauk* **341** (4) 478 (1995)
55. Smolyaninov V V *Biol. Membrany* **14** (6) 574 (1997)
56. Smolyaninov V V, Karpovich A L *Zh. Evoluts. Biokhim. Fiziol.* **8** (5) 523 (1972)
57. Smolyaninov V V, Karpovich A L *Biofizika* **20** (3) 527 (1975)
58. Smolyaninov V V, Karpovich A L *Biofizika* **20** (4) 709 (1975)
59. Smolyaninov V V, Karpovich A L *Biofizika* **20** (5) 925 (1975)
60. Smolyaninov V V, Karpovich A L, in *Lokomotsiya Zhivotnykh i Biomekhanika Oporno-Dvigatel'nogo Apparata* (Animal Locomotion and Biomechanics of the Locomotor System) (Kiev: Naukova Dumka, 1979) p. 176
61. Sukhanov V B *Obshchaya Sistema Simmetrichnoĭ Lokomotsii Nazemnykh Pozvonochnykh* (General System of Symmetric Locomotion in Terrestrial Vertebrates) (Leningrad: Nauka, 1968)
62. Taylor E, Wheeler J *Spacetime Physics* (San Francisco: Freeman, 1966) [Translated into Russian (Moscow: Mir, 1969, 1971)]
63. Fedoseev P N et al. (Eds) *Filosofskie Problemy Sovremennogo Estestvoznaniya. Trudy Vsesoyuznogo Soveshchaniya po Filosofskim Voprosam Estestvoznaniya* (Current Philosophical Problems of Natural Sciences. Proc. All-Union Workshop on Philosophical Problems in Natural Sciences) (Moscow: Izd. AN SSSR, 1959)
64. Hinde R *Animal Behaviour. A Synthesis of Ethology and Comparative Psychology* 2nd ed. (New York: McGraw-Hill, 1970) [Translated into Russian (Moscow: Mir, 1975)]
65. Chetverukhin N F *Proektivnaya Geometriya* 8th ed. (Projective Geometry) (Moscow: Prosveshchenie, 1969)
66. Schmidt-Nielsen K *Scaling: Why Is Animal Size So Important?* (Cambridge: University Press, 1984) [Translated into Russian (Moscow: Mir, 1987)]
67. Schrödinger E *What Is Life. The Physical Aspect of the Living Cell* (Cambridge: Univ. Press, 1967) [Translated into Russian (Moscow: Atomizdat, 1972)]
68. Euler L *Osnovy Dinamiki Tochki* (Principles of Point Dynamics) (Moscow-Leningrad: GRTTL, 1938)
69. Einstein A *Fizika i Real'nost'* (Physics and Reality) (Moscow: Nauka, 1965)
70. Yaglom I M *Printsip Otnositel'nosti Galileya i Neevklidova Geometriya* (Galilean Principle of Relativity and Non-Euclidean Geometry) (Series in Mathematical Circle Library, Vol. 11) (Moscow: Nauka, 1969)
71. Braitenberg V *Prog. Brain Res.* **25** 334 (1967)
72. Borelli J A *De Motu Animalum* (Lugduni Batavorum, 1680)
73. Braune W, Fischer O *Sachsischen Gesellschaft der Wissenschaften* **26** 561 (1889)
74. Das P, McCollum G *Neuroscience* **25** 1023 (1988)
75. Delcomyn F *J. Exp. Biol.* **54** 443 (1971)
76. Gray J *Animal Locomotion* (New York: W W Norton and Co., 1968)
77. Grillner S, in *Handbook of Physiology* (1982) p. 1179
78. Grillner S et al. *Brain Res.* **165** 177 (1979)
79. Halbertsma J *Acta Physiol. Scand., Suppl.* **521** 75 (1983)
80. Hughes G M *J. Exp. Biol.* **34** 306 (1957)
81. Kuznetsov A N *J. Theor. Biol.* **172** 95 (1995)
82. Lewandowski A A *Acta Ornithol.* **16** 365 (1978)
83. Mena D, Mansour J M, Simon S R *J. Biomechanics* **14** 823 (1981)
84. Mochon S, McMahon T A *J. Biomechanics* **13** 49 (1980)
85. Muybridge E *Animal Locomotion* 2nd ed. (Philadelphia, 1887; New York: Animal in motion, 1957).
86. *Neural Control of Locomotion* (Advances in Behavioral Biology, Vol. 18) (New York: Plenum Press, 1976)
87. *Neurobiological Basis of Human Locomotion* (Tokyo: Japan Scientific Societies Press, 1991)
88. Pellionisz A, Llinas R *Neuroscience* **16** (2) 245 (1985)
89. Rohrle H et al. *J. Biomechanics* **17** 409 (1984)
90. Weber W, Weber E *Mechanik der Menschlichen Gewerkzeuge* (Göttingen, 1836)
91. Wilson D M *Ann. Rev. Entomol.* **11** 103 (1966)
92. Winter D A *Biomechanics of Human Movement* (New York: John Wiley and Sons, 1979)